4-2011

The OptiFilt Approach to Biopharmaceutical Filter Testing: Scale-Up to Tangential Flow Filtration with Fouling

Elizabeth Blake
University of Pennsylvania

Janielle Johnson
University of Pennsylvania

Nikhil Shankar
University of Pennsylvania

The OptiFilt Approach to Biopharmaceutical Filter Testing: Scale-Up to Tangential Flow Filtration with Fouling

Abstract
Ultrafiltration (UF) membranes are required in the biopharmaceutical industry to concentrate or purify the final biologic product, thereby ensuring patient safety and fulfilling regulatory requirements. It is crucial that biotechnology clients select the optimal operating parameters for each filtration step. Unsuccessful filtrations might fail to purify a near-finished drug product, thereby wasting product and incurring financial loss. In less extreme cases, failure to optimize filtration steps will lead to slowed filtration steps, potentially causing bottlenecks and reduced throughput. Overall, efficient, effective filtration is crucial to the financial success of biopharmaceutical companies.

Generally, these companies pre-test filtration processes using commercially available filter test rigs. Although commonly used, these filters are geometrically and mechanically simplistic and therefore provide an incomplete picture of filter behavior. Results from these simple filters do not appropriately represent the behavior of complex industrial filters. As a consequence, filtration tests are inherently flawed and industrial processes are not optimized.

OptiFilt will solve this problem by providing more accurate filtration analysis services to biotechnology client companies. Using proprietary computational models and experimental analysis, OptiFilt will determine unknown hindered convective and diffusive coefficients of client-supplied test UF material. OptiFilt scientists will determine the unknown properties by fitting the parameters to a MATLAB model for dead-end flow with fouling. The results from this MATLAB model will be supplied to a tangential flow filtration COMSOL model which more appropriately describes industrial filter behavior. Overall, this process will provide more accurate predictions of filter behavior, thereby allowing our clients to more effectively optimize their filter operating parameters.

We project that OptiFilt filtration analysis services will help our clients reduce filtration time and increase throughput by 50%. As a result, clients will enjoy increased profitability. OptiFilt, then, will provide biotechnology clients with a crucial advantage in these competitive times.

OptiFilt will function as a start-up company, beginning its R&D stage in 2012 and seeking investments in 2012 and 2013. Financial analyses have confirmed that this is a profitable and relatively secure venture, even in the case of events which could adversely affect the business.

April 12, 2011

Elizabeth Blake, Jennielle Jobson, Nikhil Shankar

The OptiFilt Approach to Biopharmaceutical Filter Testing: Scale-Up to Tangential Flow Filtration with Fouling

Faculty Advisor: Dr. Matthew J. Lazzara

Professor Leonard A. Fabiano

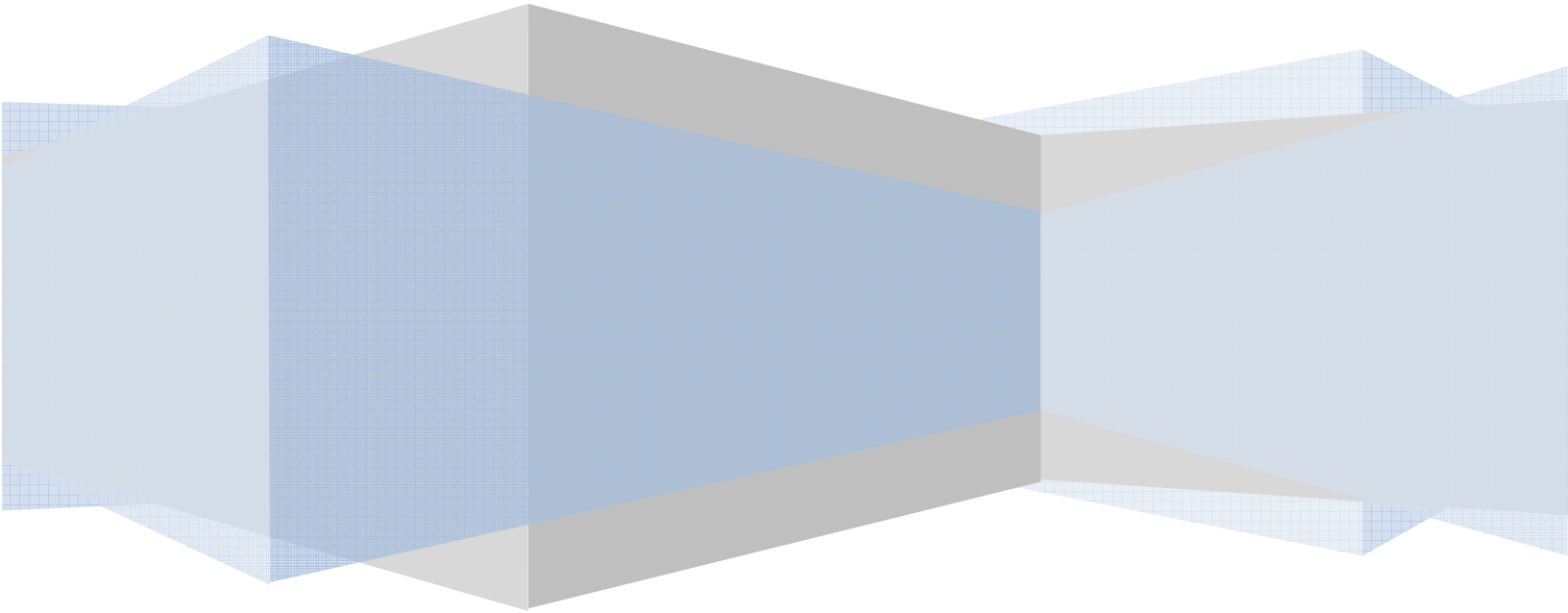

April 12, 2011

Department of Chemical and Biomolecular Engineering
School of Engineering and Applied Science
University of Pennsylvania
220 South 34th Street
Philadelphia, PA 19104

Dear Dr. Lazzara, Dr. Seider, and Professor Fabiano:

We are pleased to present our completed Senior Design report: *The OptiFilt Approach to Biopharmaceutical Filter Testing: Scale-up for Tangential Flow Filtration with Fouling.* This project solves a problem commonly seen by present-day biopharmaceutical companies. As explained in our Abstract, it is crucial that companies effectively optimize operating conditions for industrial filter cartridges.

However, currently in industry, there is a disconnect between instruments used for testing and the industrial filters used in scaled-up bioprocesses. Generally, industrial filters have tangential flow filtration, complex geometries, and membrane fouling. In contrast, available test rigs generally assume normal flow filtration; simple, dead-end geometries; and minimal membrane fouling. For these reasons, test rigs do not appropriately represent industrial filter behavior.

Our project provides a more thorough approach to filter testing by using two models of filter behavior: a simple, dead-end flow model in MATLAB and a more complex tangential flow model in COMSOL. For a client-supplied test ultrafiltration (UF) filter, a modified test-rig instrument will be used to collect real-time concentration data in the retentate and in the filtrate. These data will be imported to our MATLAB model. Using this model, MATLAB will compute the particular hindered convective and diffusive coefficients describing the test filters. These parameters will then be supplied to the COMSOL model, which will predict filtration results in an industrial filter. More accurate predictions will allow clients to optimize operating conditions—such as applied transmembrane pressure or fluid flow rate—in order to cut filtration time and increase throughput.

The OptiFilt service is unlike any analysis available to biotechnology companies today. We are confident that the Company will attract clients by providing superior analyses and helping clients increase throughput and profitability. Additionally, although this project focuses on UF, the concept is applicable to viral, sterile, and depth filtration processes as well—all potential targets for OptiFilt. Financial analyses confirm that even in worst-case scenarios, our business model is relatively low-risk, and in all except a few worst-case scenarios, OptiFilt stock issuances offer a very lucrative investment opportunity.

Sincerely,

_____

Elizabeth Blake

_____

Jennielle Jobson

_____

Nikhil Shankar

Table of Contents

Abstract

Ultrafiltration (UF) membranes are required in the biopharmaceutical industry to concentrate or purify the final biologic product, thereby ensuring patient safety and fulfilling regulatory requirements. It is crucial that biotechnology clients select the optimal operating parameters for each filtration step. Unsuccessful filtrations might fail to purify a near-finished drug product, thereby wasting product and incurring financial loss. In less extreme cases, failure to optimize filtration steps will lead to slowed filtration steps, potentially causing bottlenecks and reduced throughput. Overall, efficient, effective filtration is crucial to the financial success of biopharmaceutical companies.

Generally, these companies pre-test filtration processes using commercially available filter test rigs. Although commonly used, these filters are geometrically and mechanically simplistic and therefore provide an incomplete picture of filter behavior. Results from these simple filters do not appropriately represent the behavior of complex industrial filters. As a consequence, filtration tests are inherently flawed and industrial processes are not optimized.

OptiFilt will solve this problem by providing more accurate filtration analysis services to biotechnology client companies. Using proprietary computational models and experimental analysis, OptiFilt will determine unknown hindered convective and diffusive coefficients of client-supplied test UF material. OptiFilt scientists will determine the unknown properties by fitting the parameters to a MATLAB model for dead-end flow with fouling. The results from this MATLAB model will be supplied to a tangential flow filtration COMSOL model which more appropriately describes industrial filter behavior. Overall, this process will provide more accurate predictions of filter behavior, thereby allowing our clients to more effectively optimize their filter operating parameters.

We project that OptiFilt filtration analysis services will help our clients reduce filtration time and increase throughput by 50%. As a result, clients will enjoy increased profitability. OptiFilt, then, will provide biotechnology clients with a crucial advantage in these competitive times.

OptiFilt will function as a start-up company, beginning its R&D stage in 2012 and seeking investments in 2012 and 2013. Financial analyses have confirmed that this is a profitable and relatively secure venture, even in the case of events which could adversely affect the business.

Chapter 1:

Introduction

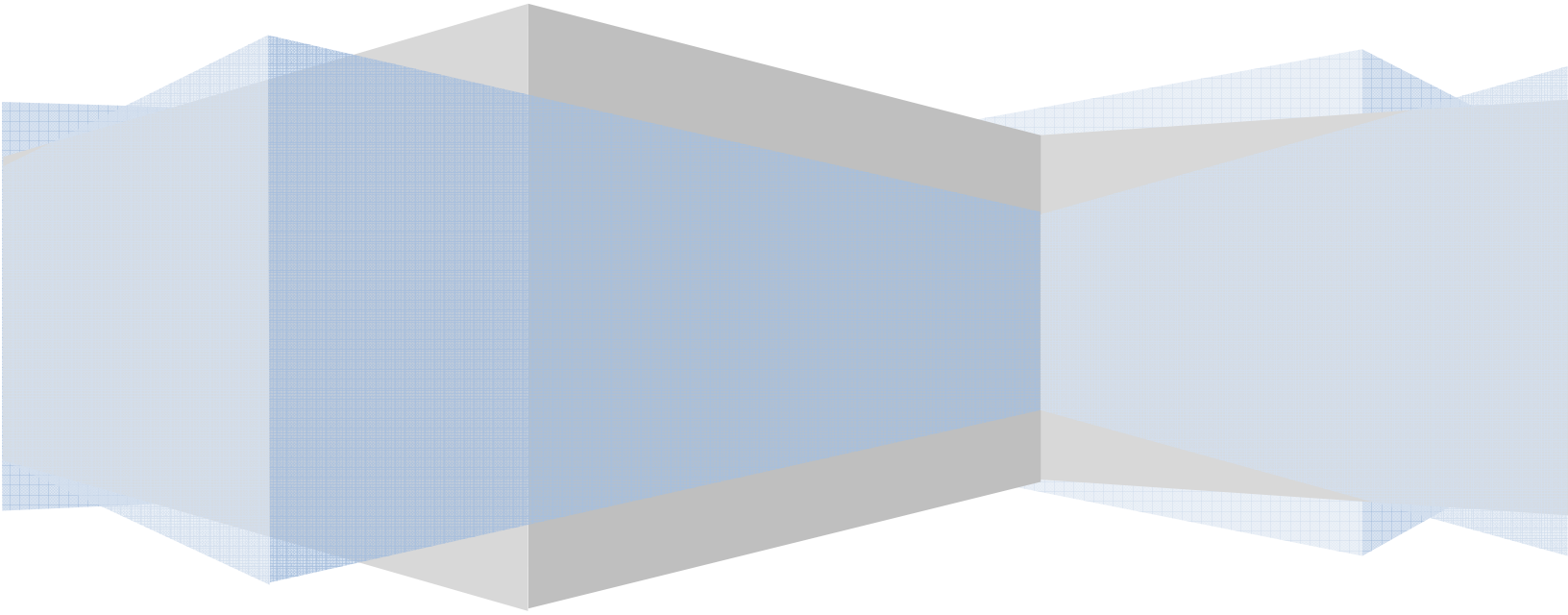

I. Filtration and Bioprocesses

Membranes and filters play a key role in the production of small-molecule drugs and biologics.[1] The U.S. Food and Drug Administration (FDA), along with its international counterparts, strictly regulates what quantities and types of impurities are permissible in final drugs and biologic products (the Code of Federal Regulations governing drug impurities are included in the Appendix). The filtration process itself is also tightly controlled. All manufacturing processes must be pre-approved to maximize quality and minimize risks and hazards; any deviations from pre-approved processes, including the re-filtering of impure or poorly separated materials is dangerous and often illegal. As such, the ability to predict filtration conditions is an important step in any biopharmaceutical process. Given the context of this project, this section will focus on the production of biologic drugs rather than small organic molecules.

A representative process flow diagram for biologics manufacturing is shown in Figure 1-1. Filtration is used at several points in downstream biopharmaceutical manufacturing[2] to remove impurities from the final protein product. The type of filter used depends not only on the product, but also on the impurity of interest. As Figure1-1shows, soon after drugs are produced (via fermentation or other biochemical steps), they undergo centrifugation to remove the largest process impurities. Centrifugation is followed by the first filtration step, depth filtration (sometimes called pre-filtration). Depth filtration consists of several filters in series in which most biomass and cellular debris is removed. Removing these larger particles prior to finer filtration steps prevents unnecessary damage to finer filters further in the downstream process.

[1] Biologic drugs are those with large, generally protein, active ingredients which are derived from biochemical or biological processes. In contrast, small molecule drugs are derived purely from chemical processes.
[2] In pharmaceutics, a 'downstream' process refers to that portion of the larger manufacturing process which occurs after the drug (or biologic) is produced (the 'upstream' process) biochemically. 'Downstream' goals include separation, purification, and packaging of the final drug product.

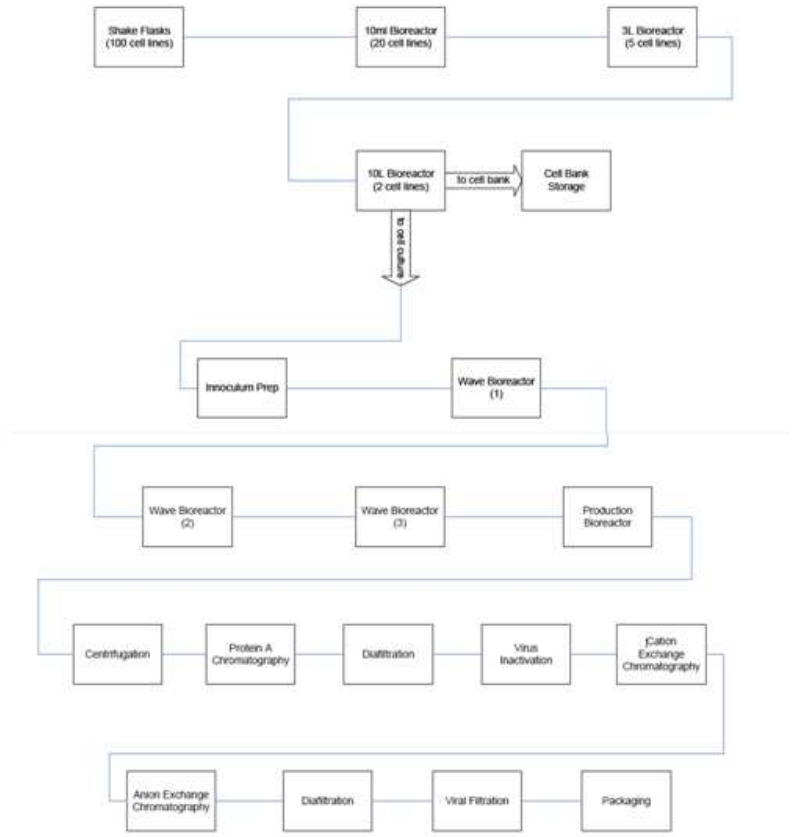

Figure 1 - 1 Representative biologic production process [1-1].

Following depth filtration, undesired proteins are removed from the stream via chromatography. The product stream is sent through a polish filter to remove any bacteria introduced to the process during chromatography. A second series of depth filters follows polish filtration. In this case, the depth filters' pore size is small enough to restrict the flow of the protein product through the membrane; the goal in this step is to remove impurities which are *smaller* than the drug product (media components from fermentation, acetic acid, buffers, etc.). The next steps in this representative process include virus inactivation and ion chromatography. The latter, like filtration, helps to remove impurities from the process stream.

Chromatography is followed by sterile filtration. As the name implies, sterile filtration ensures the sterility of the final protein product by removing any remaining bacteria. This

representative protein product stream undergoes multiple rounds of sterile filtration, which can be separated by holding periods depending on the product, its impurities, and the scheduling requirements. Viral filtration is subsequently performed to remove any remaining viruses from the product stream. Again, multiple rounds of viral filtrations often take place.

Ultrafiltration (UF) is used throughout the process to concentrate the product stream and further isolate the protein product. For example, this representative process employs UF between sterile and viral filtration steps to increase the efficiency of steps further downstream. This type of filtration is also used in the final purification and isolation steps; the goal in these final steps is to achieve as pure and concentrated a protein product as possible.

In UF steps, an applied pressure forces the product stream against a semipermeable membrane, thereby removing water and small molecules and concentrating the larger protein molecules. This type of filtration is the focus of this project.

II. Types of Filters and Filtration

Even a single chemical process, such as the representative bioprocess shown in Figure 1-2, contains variety of filters and filtration types. When describing a filtration process, a key defining characteristic is the type of flow involved. The simplest flow set up is normal or dead-end flow, in which fluid flows perpendicular to the membrane surface. Because all fluid is flowing normal to the membrane, dead-end flow is the most likely to cause a buildup of solute caking on the membrane surface.

In contrast, in cross-flow filtration, fluid flows parallel to the membrane surface. In this case, parallel-flowing fluid is able to wash away a portion of the solute cake as it builds; in this way, cross-flow filtration results in significantly less solute caking than does dead-end flow. The

caking of solute or impurities on the membrane surface almost always leads to reduced throughput through the membrane, in addition to premature filter wear. Therefore, cross-flow filtration is often favorable in industry because is lessens the effects of caking on the filtration process.

This project primarily concerns UF membranes, although the basic framework is applicable to a wide range of viral, sterile, and depth filters as well. Generally, for UF membranes, target solutes range in diameter from 0.001 to 0.1 μm, or have molecular weight cut-offs[3] (MWCO) on the order of 1,000 to 10,000 Da. In an UF process such as the ones studied in this project, the membrane pores are small enough so that the target protein product cannot pass through the membrane. As solvent and smaller impurities pass into the filtrate, the target protein is concentrated on the retentate side of the membrane.

In industrial-scale bioprocesses, UF steps usually take place after sterile, viral, and microfiltration steps take place. The earlier steps in the process help remove large impurities which would lead to premature fouling if introduced to an UF process. As explained previously, sterile and viral filters remove bacteria and viruses, respectively, from the product process stream. As opposed to UF processes, in which the product to be purified remains on the retentate side of the membrane, sterile and viral filters contain pores which are large enough to allow the target product to pass through the membrane. Instead, large impurities (bacteria and biomass for sterile filters, or viruses for viral filters) are held on the retentate side.

Microfiltration functions similarly. In microfiltration processes, pores are large enough to allow the target product to pass through the membrane. However, these pores are small enough to prevent the passage of larger particles such as fat globules, cell debris, and colloids. Here, the size cutoff ranges from 0.04 to 10 μm, significantly larger than that for UF. Again, a

[3] The MWCO of a filter is the largest possible molecular weight which can pass through that filter.

microfiltration step is generally included prior to UF steps in order to prevent premature fouling and wear of UF membranes.

III. Relevant Industrial Applications

In the biopharmaceutical industry, UF devices come in a variety of geometries and materials. Generally, for the aforementioned reasons, these devices employ a cross-flow configuration rather than normal flow, and their geometries are designed such that the filter maximizes filter surface area, and therefore process throughput, without requiring an unreasonably large total filter volume. In other words, industrial filters' geometries pack a large membrane surface area into a relatively small total volume. As a consequence, geometries are complex and difficult to model with normal-flow assumptions. Typical UF devices used in the biopharmaceutical industry are illustrated in Figure 8-2.

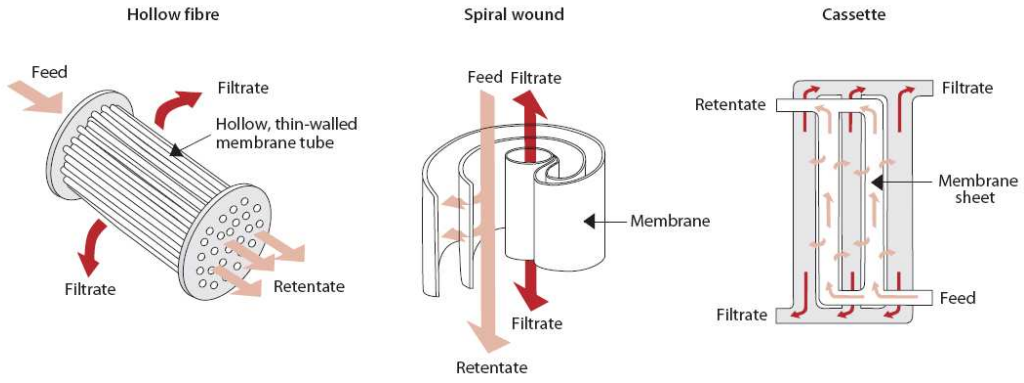

Figure 1 - 2 Typical UF devices used in the biopharmaceutical industry [1-2].

IV. Key Parameters and Equations

Figure 1-3 shows a typical normal-flow UF process in cross-section. Although this image shows fluid flowing from left to right, of course, vertical and other orientations are common as

well. Here, an applied transmembrane pressure ΔP_{TM} forces solvent, which contains the orange solute molecules shown, through the membrane of thickness δ. In this case, the molecular weight cutoff (MWCO) of the membrane is large enough to allow the passage of solute molecules into the filtrate side of the membrane.

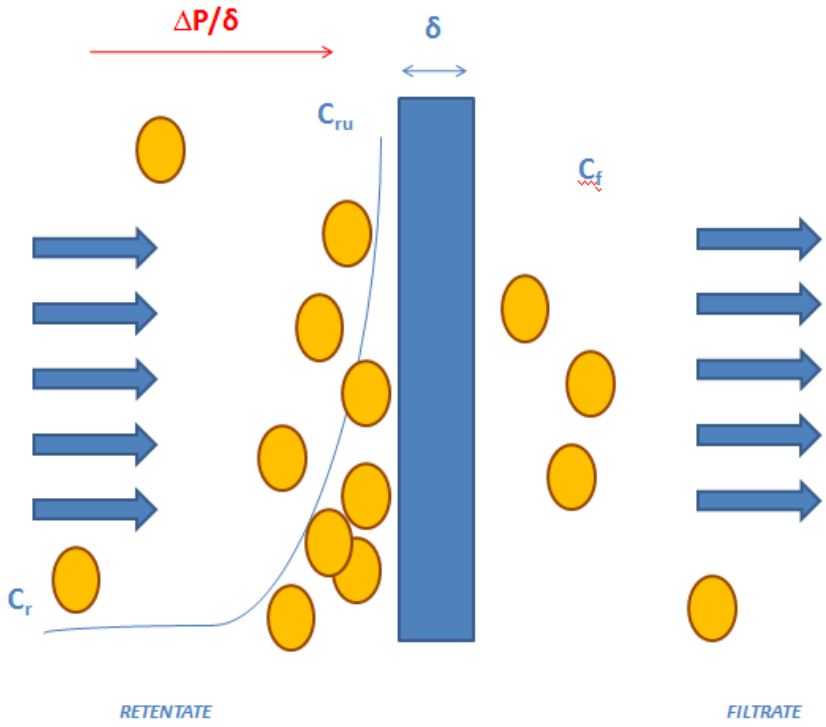

Figure 1 - 3 Pseudo-steady state concentration profile for a normal-flow UF process.

As solute particles flow to the filtrate side, the solute concentration in the filtrate (C_f), begins to build. The solute concentration in the retentate changes as is dictated by a) the mass transfer out of the retentate side, and b) the loss of solvent volume on the retentate side, V_r. Note that we have two possible solute concentration values on this side of the membrane. As flow runs against the membrane surface, a portion of solute particles flow through the membrane, while others are retained at the membrane surface. These retained solute particles lead to a buildup of solute close to the membrane. As a result, the concentration on the retentate side of the membrane is higher closer to the membrane surface. Although there is an experimentally

measurable or apparent $C_{r,}$ there is a higher concentration at the upstream surface of the memrane, the upstream or intrinsic $C_{r,u.}$ This phenomenon is referred to as *concentration polarization.*

The dimensionless sieving coefficients describe membrane behavior by comparing the concentrations on either side of the membrane. Because retentate-side concentration has two possible values, there are two possible values for the sieving coefficient. First, the measurable or apparent sieving coefficient is an experimentally-determinable value which compares C_f to $C_{r.}$ The apparent sieving coefficient is given

$$\theta' = \frac{C_f}{C_r} \text{ , (1-1)}$$

In contrast, the intrinsic sieving coefficient compares C_f to $C_{r,u,}$ and therefore cannot be determined directly from experimental data. The sieving coefficient is given

$$\theta = \frac{C_f}{C_{r,u}} \text{ , (1-2)}$$

Because θ cannot be determined experimentally, we must compute it from experimentally-determined θ' values. To relate these two variables, we use the equation

$$\theta = \frac{\theta'}{(1-\theta')\left(e^{v_f/k_c}\right)+\theta'} \text{ , (1-3)}$$

where v_f and k_c are the fluid velocity through the membrane and the mass transfer coefficient of the system, respectively. The mass transfer coefficient is computed as

$$k_c = 2.33\mu^{1/6}D^{1/3}, \text{(1-4)}$$

where μ and D are the viscosity of the solvent and the diffusivity of the solute, respectively. In contrast, in our models, v_f changes with time and is described by

$$v_f = L_p(\Delta P - \sigma\Delta\pi) \text{ , (1-5)}$$

where L_p is the hydraulic permeability constant; σ is the osmotic reflective coefficient, and $\Delta\pi$ is the osmotic pressure across the membrane. The hydraulic permeability constant is essentially a measure of how able solvent is to pass through the membrane. In our simplest models, we have assumed that L_p is constant; however, as the membrane cakes, this actually decrease for the composite membrane.

The osmotic pressure drop changes with time with or without membrane caking. As C_f builds relative to $C_{r,u,}$ the osmotic pressure builds in the direction opposite that of the applied pressure (toward the retentate), in an 'attempt' to reestablish equal concentrations of solute on either side of the membrane. Experimental data have shown numerous relations between $\Delta\pi$, $C_{f,}$ and $C_{r,u;}$ these relations are specific to the solute and solvents used. In our models, we have assumed

$$\Delta\pi = 23.487 \exp\left(0.0116 C_r \theta' \left(\frac{1}{\theta} - 1\right)\right), \text{(1-6)}$$

to accurately determine osmotic pressure.

OptiFilt relies on a few other relationships to describe the behavior of UF membranes. First, an overall material balance restricts $C_{f,}$ $C_{r,}$ and V_r such that

$$\frac{dC_r}{dt} = \left(\frac{1}{V_r}\right)\left(\theta' C_r v_f A_c - C_r \frac{dV_r}{dt}\right), \text{(1-7)}$$

By the same idea, the total rate of volume change in the retentate is determined by the fluid velocity through the membrane, such that

$$\frac{dV_r}{dt} = -A_c v_f, \text{(1-8)}$$

Finally, the structure of the Company's filtration analysis service requires that we determine θ and θ' mathematically as well as experimentally. To this end, we compute θ from known physical properties of the membrane, using the relation

$$\theta = \frac{\Phi K_c}{1-(1-\Phi K_c)\exp(-Pe)}, \quad (1\text{-}9)$$

where Φ is the partition coefficient across the membrane, K_c is the convective coefficient of the membrane, and Pe is a dimensionless number described by

$$Pe = \frac{(\Phi K_c)v_f \delta}{(\Phi K_d)\mathcal{D}}. \quad (1\text{-}10)$$

where K_d is the diffusive coefficient of the membrane studied.

IV. Membrane Fouling

Previously described models assume no membrane caking or fouling; that is, they assume that any buildup of solute particles on the membrane surface have a negligible impact on fluid velocity and hydraulic permeability. In reality, this is never the case. As filtration proceeds, solute builds up either on the membrane surface or within the membrane pores. These phenomena effectively reduce the pore size of the membrane, thereby slowing fluid flow and the filtration process.

A variety of models describe the membrane fouling. As is discussed in further detail in Chapter 5, the cake-adsorption model was selected in this project because it most appropriately describes fouling in biopharmaceutical filters. Mathematically, this model uses experimental data to fit a relation between the hydraulic permeability and time. The changing hydraulic permeability slows fluid flow and, when introduced to the existing models, provides a more accurate picture of membrane behavior in real systems. The equations and parameters used for this model are detailed in Chapter 4.

Chapter 2:

The OptiFilt Approach

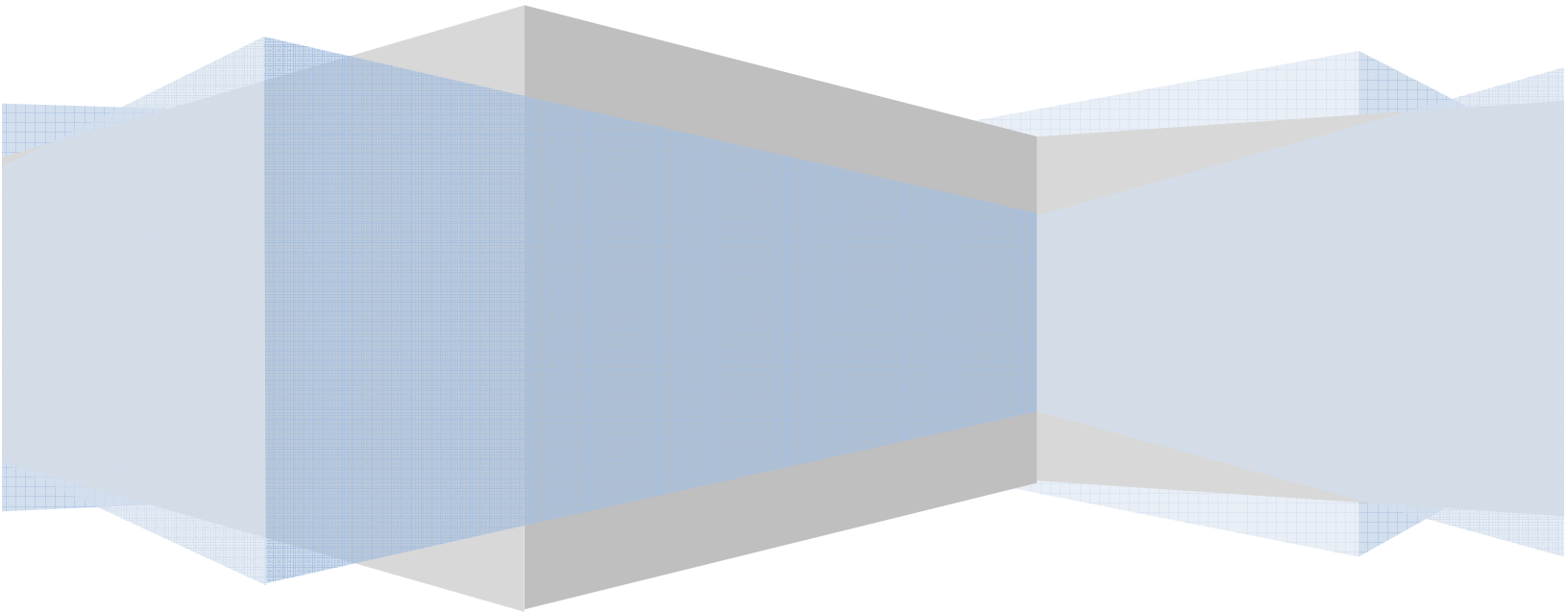

I. Market Analysis

Therapeutic monoclonal antibodies command a market of more than $30 billion annually. Much research has been invested in the development of therapeutic monoclonal antibodies for the treatment of various cancers, autoimmune diseases, inflammatory conditions, and infectious diseases that are characterized by elevated expression of a target protein at a cell surface. The proven safety of and efficacy of mAbs as a drug class has driven faster developmental and regulatory timelines and the search for more efficient pipeline of the drugs from their discovery to the market [3-1]. Within the past twenty years, the United States Food and Drug Administration has approved numerous monoclonal antibodies for therapeutic use (as shown in Figure 3-1) and hundreds are currently undergoing clinical trials [3-2]. Thus, on an industrial scale, there is a large market for the efficient production of therapeutic mAbs that can meet the level of purity required by FDA regulations. The high demand for mAbs has focused attention on the need for advanced purification techniques and systems to increase the speed, robustness, and scalabilty of the downstream processes required for mAb manufacturing. The driving force behind mAb process technology development is improved productivity – achieved by enhancing the ease of operation, reproducibility, quality control, and process validation.

Therapeutic mAbs are also among the most expensive drugs to produce. Due to a large potential market consisting of over 500,000 patients, expensive large-scale production capacity is required in order to produce 10–100 kg/year of each mAb. The high cost of manufacture is further reflected in the cost of treatment; the annual cost per patient can reach $35,000 for antibodies treating cancer conditions due to their use for chronic conditions and their relatively low potency resulting in the need for high doses (grams per patient per year rather than milligrams) [3-3]. The large financial burden associated with the manufacture of mAbs negatively affects the ability of pharmaceutical companies to manufacture mAbs at the necessary scale to meet the demand. This problem came to

Antibody	Trade Name	Company	Target	Type	Year Approved	Therapeutic Indication
Muromonab – CD3	Orthoclone OKT3	Centocor (Johnson & Johnson)	CD3	Murine	1989	Transplant Rejection
Abciximab	ReoPro	Centocor (Johnson & Johnson)	GPIIb/IIIa	Chimeric	1994	High Risk Angioplasty
Rituximab	Rituxan	Genentech	CD20	Chimeric	1997	Non-Hodgkin's Lymphoma Chronic lymphocytic Leukemia Rheumatoid Arthritis
Daclizumab	Zenapax	Roche	CD25	Humanized	1997	Transplant Rejection
Trastuzumab	Herceptin	Genentech	HER-2	Humanized	1998	Breast Cancer Metastatic Gastric or Gastroesophagel Junction Adenocarcinoma
Infliximab	remicade	Centocor (Johnson & Johnson)	TNFα	Chimeric	1998	Transplant Rejection
Basiliximab	Simulect	Novartis	CD25	Chimeric	1998	Transplant Rejection
Palivizumab	Synagis	Medimmune	RSV F protein	Humanized	1998	Respiratory Syncytial Virus
Alemtuzumab	Campath	Genzyme	CD52	Humanized	2001	B-cell chronic lymphocytic leukemia
Adalimumab	Humira	Abbot	TNFα	Human	2002	Rheumatoid Arthritis Juvenile Idiopathic Arthritis Psoriatic Arthritis Ankylosing Spondylitis Crohn's Disease Plaque Psoriasis
Ibritumomab Tiuxetan	Zevalin	Biogen Idec	CD20		2002	Non-Hodgkin's Lymphoma
Tositumomab and Iodine 131	Bexxar	Corixa, GlaxoSmithKline	CD20	Murine	2003	Non-Hodgkin's Lymphoma
Omalizumab	Xolair	Genentech, Novartis	IgE	Humanized	2003	Asthma
Bevacizumab	Avastin	Genentech	VEGF	Humanized	2003	Metastatic Colorectal Cancer Non-Small Cell Lung Cancer Metastatic Breast Cancer Metatastic Renal Cell Carcinoma
Cetuximab	Erbitux	Imclone, Merck	EGFR	Chimeric	2004	Head and Neck Cancer Colorectal Cancer
Natalizumab	Tysabri	Biogen Idec	VLA-4	Humanized	2004	Multiple Sclerosis Crohn's Disease
Ranibizumab	Lucentis	Genentech	VEGF-A	Humanized Antibody Fragment	2006	Neovascular Age-Related Macular Degeneration
Panitumumab	Vectibix	Amgen	EGFR	Human	2006	Metastatic Colorectal Carcinoma
Eculizumab	Soliris	Alexion Pharmaceuticals	Complement C5	Humanized	2007	Paroxysmal Nocturnal Hemoglobinuria
Certolizumab	Cimzia	UCB	TNFα	Humanized Antibody Fragment	2008	Chrohn's Disease Rheumatoid Arthritis
Ofatumumab	Arzerra	Genmab, GlaxoSmithKline	CD20	Human	2009	Chronic lymphocytic Leukemia
CanaKinumab	Ilaris	Novartis	IL - 1β	Human	2009	Cryopyrin-associated Periodic Syndromes
Golimumab	Simponi	Centocor (Johnson & Johnson)	TNFα	Human	2009	Rheumatoid Arthritis Psoriatic Arthritis Ankylosing Spondylitis
Ustekinumab	Stelara	Centocor (Johnson & Johnson)	IL - 11 IL - 23	Human	2009	Plaque Psoriasis
Tocilizumab	Actemra	Roche	IL - 6	Humanized	2010	Rheumatoid Arthritis
Denosumab	Prolia Xgeva	Amgen	RANKL	Human	2010	Postmenopausal Osteoporosis Prevention of SREs

Figure 3-1: Therapeutic monoclonal antibodies approved by the FDA. [3-2]

mainstream attention in 2000 when demand for the antibody Enbrel® exceeded capacity because its manufacturer, Immunex, did not have the money to build a large enough scale facility to manufacture the drug in sufficiently large quantities [3-4]. These concerns have increased the pressure to drive down manufacturing costs of mAbs by an order of magnitude from $1000's per grams to $100's per gram [3-3].

The pharmaceutical industry is volatile and high-risk as companies invest billions of dollars into finding the next billion-dollar drug. Most FDA-approved mAbs are produced in a batch/fed batch culture of mammalian cells followed by purification steps using chromatography with intermediate sterile, viral, and ultrafiltration steps in order to remove cell debris, bacteria, viruses, and other contaminants [3-3]. One way to decrease the financial burden of mAb manufacturing is to optimize these filtration steps in order to conserve the antibodies, increase throughput, lower pressure drops, and decrease operation time and its associated energy and labor costs. However, the high cost of manufacturing monoclonal antibodies prevents the use of industrial scale equipment to optimize the filtration process [3-5]. Thus, it is necessary to develop small scale filtration processes which can reliably predict manufacturing scale performance, requiring the use of smaller quantities of mAbs and thereby reducing the cost of production and process characterization [3-6].

Consequently, OptiFilt has a great opportunity to provide in-house testing of filtration processes. Although such testing services already exist, OptiFilt would be the first to provide important features such as high throughput, parallel testing, real-time data collection, and information on the fouling mechanism of the membrane all within the same system. It is this abundance of features and the resulting convenience that make our testing services more attractive. Our potential clients include smaller manufacturers of mAbs which may not have employed a filtration scientist, but wish to optimize their filtration process to reduce their operating costs. Furthermore, these clients may not currently employ a person with experience using software to model membrane filtration processes. The cost to hire someone with such expertise or to train a current employee may be too much for a small manufacturer.

II. Competitive Analysis

a. SciLog

SciLog manufactures and sells the FilterTec Plus 3-Filter Testing Station, which provides parallel testing, real-time monitoring, and an automated software interface to perform filterability studies on up to three filters simultaneously. As shown in Figure 3-7, the sample solution being studied is pumped through a test filter at constant pressure, typically between 10-20 psi. Using an electronic scale, the cumulative solution weight (or volume) exiting the dead-end filtration device is recorded as a function of time [3-8]. A single run typically takes about ten minutes [3-9].

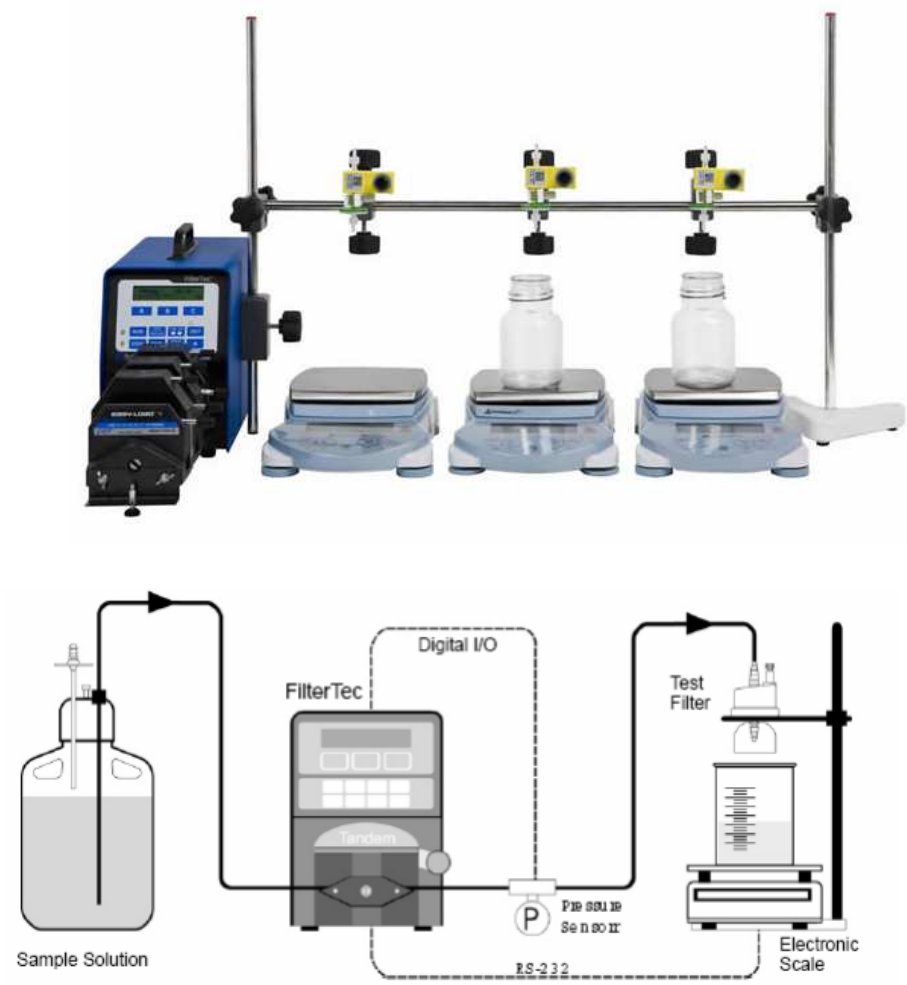

Figure 3-2: Sci Log Filter Tec Plus 3-Filter testing Station [3-8] [3-9]

Assuming a fouling mechanism of a gradual “pore plugging” model, a linear plot of the time divided by the cumulative solution weight versus the time is obtained. The inverse of the slope of this line is Vmax, the maximum amount of fluid that will pass through the filter before it is completely plugged [3-7]. The system also monitors the pressure, feed rate, and collection rate of the operation of the filters, allowing the user to determine the optimal parameters to give the highest Vmax value for a given filter and mAb solution.The solution is distributed through the system using the FilterTec Smart Pump, which maintains the selected backpressure at a constant value by modulating the pump output. Built –in alarms can also be programmed for each run, allowing walk-away operation and thereby increasig productivity. TheFilterTec Plus is compatible with a wide variety of 47mm disk test filters. Its operation also offers much flexibilty – the system can be run at constant pressure or pump rate, in serial or parallel configuration, or with a programmable continuous changing of pump rate or pressure with time [3-10]. Sci Log also provides an automated software interface with the test rig, Sci Doc, which is implemented within Microsoft Excel and allows real-time process analysis with graphing of data and documentation of process parameters (see Figure 3-2).

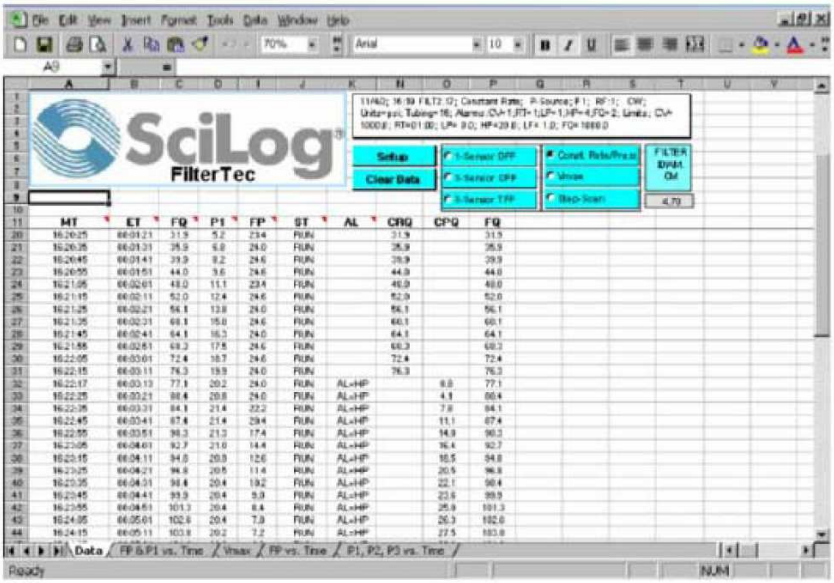

Figure 3-3: SciDoc , the software asscociated with the FilterTec Plus Multi-filter Capacity testing System [3-9]

Easily fit on a laboratory bench, the FilterTec Plus testing station costs $16, 795 and requires no other purchases besides test filters.

b. Millipore

Millipore Corporation provides Vmax Filtration System Optimization, a client service that performs Vmax testing for the design and optimization of filtration systems used in the production of pharmaceutical fluid (Figure 3-4). Requiring only small volume of process fluid, the Vmax test can be performed in about an hour and meaningful results can be gained after only 10 minutes , ensuring its cost-effectiveness while maintaining its accuracy for scale-up to the industrial level.

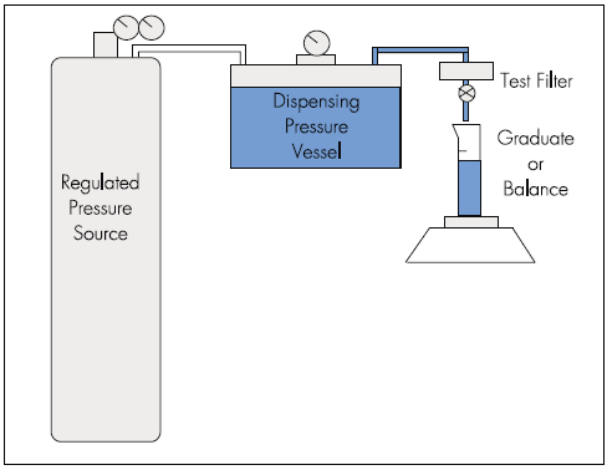

Figure 3-4: Millipore Vmax Testing setup [2-7]

The versatility of the service is an important factor – Millipore Validation Specialists are trained to analyze entire filter trains using this technology. As previously explained, the cumulative volume is recorded as a function of time at a specified differential pressure (usually 5-10 psi) and used to calculate the value of Vmax by assuming fouling on the membrane occurs through the gradual pore blocking mechanism typically exhibited during the filtration of biological fluids [3-11]. Vmax testing can accurately predict throughput for dead-end filters in less than ten minutes (Figure 3-5). Millipore will evaluate filters of various media compositions and pore sizes with a wide range of process fluids

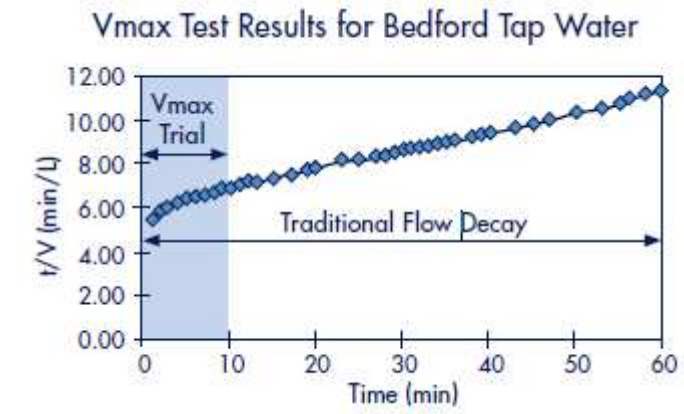

Figure 3-5: Vmax Filtration System Optimization offered by Millipore. Notice the time saved by Millipore's proprietary technique. [3-12]

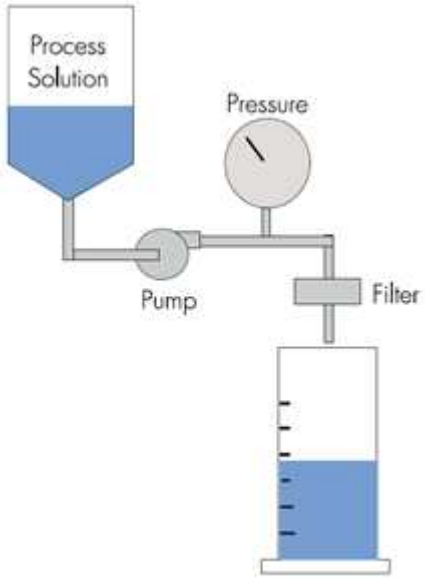

Figure 3-6: Millipore Pmax testing Setup [3-12]

Millipore has also developed Pmax, a sizing technique for filters operated at a constant flux (see Figure 3-6). The filter resistance to flow - the pressure across the membrane as a function of throughput – is plotted versus the throughput of the filter. From this function, the filter sizing is then calculated within the Pmax sizing spreadsheet. This method is independent of the fouling model. However, it requires longer testing times and larger sample volumes than Vmax testing [3-11].

To collect and analyze the results of Vmax and Pmax testing, Millipore has developed proprietary Vmax software (Figure 3-7). This software enables the validation specialists to recommended filter sizing, filter configuration, and operating conditions for optimization of the entire filter train.

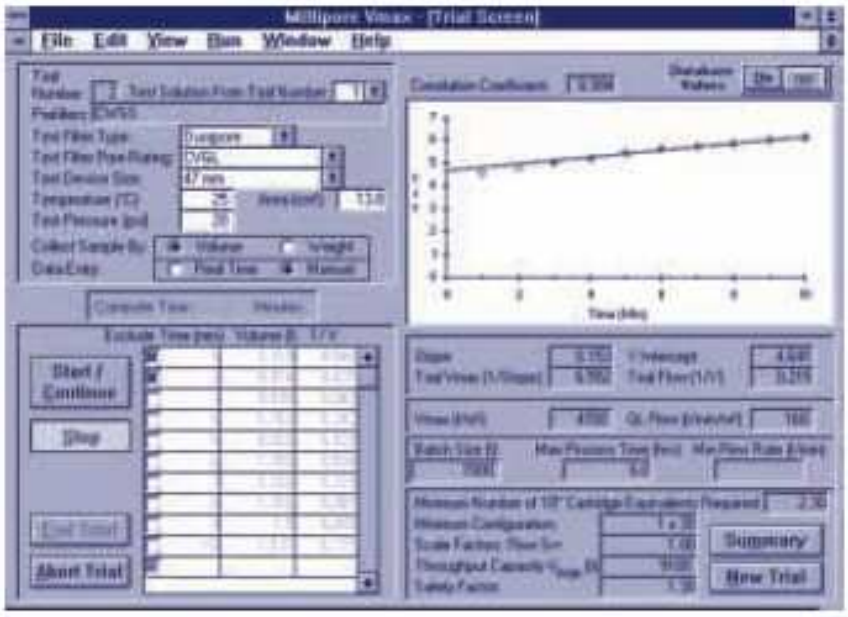

Figure 3-7: Software associated with millipore's optimization package. [3-12]

For new processes, Millipore offers its validation and optimization services free of charge for the first time. For the optimization of validation testing of existing processes, the prices vary depending on the size of the process, the cost of travel to the site, the time required to optimize the service, and the level of service need. This typically costs $1,000 to $1,500 per day depending on the level of service needs. For example, consultation or training could be less costly than troubleshooting and programming. At a large scale, 3-5 days would be needed depending on the complexity of the system, for a site test, adding up to about $7,500 to optimize an entire filtration process.

c. OptiFilt – Overview of Science and Software

As previously mentioned, OptiFilt will provide filtration testing services using laboratory scale dead-end filters to client companies and recommend optimal operating conditions for scale-up to other filter

geometries used at the industrial scale. For the purposes of illustration, this report will focus on scale up to a tangential flow ultrafiltration membrane module. Using the FilterTec Plus Multi-capacity Testing Station as a base, the testing rig will monitor conditions such as pressure, filtrate and permeate volume, filtrate and permeate velocity as a function of time. Refractometers will measure the index of refraction of the filtrate and permeate, which can then be used to calculate the bulk concentration of the filtrate and permeate of each filter as a function of time. In order to determine the operating parameters for optimal performance of the filter, parameters such as the pH, solute concentration, and applied pressure will be varied and tested in parallel to conserve sample. Chapter 7 includes a more detailed explanation of this instrumentation. The data collected will then be imported and analyzed using a one-dimensional model of the mass transfer involved in dead-end membrane filtration which is implemented in MATLAB.

i. MATLAB Model

Briefly, parameters such as the initial sample volume, initial sample concentration, mass transfer coefficient, initial hydraulic permeability, and the cross-sectional area of the membrane will be inputted into the model. The model with then solve a differential-algebraic system of equations describing the mass transfer across the dead-end filter , and produce plots showing how the concentration and volume of the filtrate and volume, the osmotic pressure across the membrane, and other parameters change as a function of time. Chapter 3 will discuss the mass transfer equations for the normal flow filter in more detail. Most importantly, the MATLAB model utilizes simulated annealing, which fits an estimate of the unknown intrinsic properties of the membrane to the data. Chapter 5 will discuss the MATLAB model and simulated annealing in further depth. The determined values for the intrinsic properties will then be used to model the industrial crossflow filter in COMSOL.

ii. COMSOL Model

A finite element solver, COMSOL Multiphysics was used to simulate the mass transfer and fluid mechanics with the industrial filter. A simplified two-dimensional model of tangential flow filtration was drawn within its interface. The Navier-Stokes Equation modeled the flow of the mAb solution within the

channel of the filter, the Brinkman Equations modeled its flow within the membrane, and a species balance modeled the convection and diffusion of the mAbs within both the channel and membrane. The appropriate boundary conditions were then set – operation by a constant applied pressure was assumed and the flux through the membrane was calculated using the intrinsic properties of the membrane determined using MATLAB. Chapter 6 will further discuss the COMSOL model.

d. Pricing Analysis

As Chapter 8 will further explain, OptiFilt plans to charge $150,000 to perform filterability trials for client biotechnology companies. This price is much more expensive than the cost of purchasing a FilterTec Plus 3-Filter Testing Station directly from Sci Log or utilizing Millipore's testing services. Although each utilizex Vmax testing, the service provided by OptiFilt is superior to that of Millipore and Sci Log for several different reasons. Our testing rig is able to test membranes in parallel, allowing us to provide our clients with results more quickly. Furthermore, our testing rig includes refractometers to provide information on the concentrations of the filtrate and permeate during filtration. Vmax testing, on the other hand, only predicts the total throughput of the filter. Furthermore, the MATLAB model will take in account numerous modes of membrane fouling, while Vmax testing is only applicable when fouling occurs according to the gradual pore-plugging model. In addtion, although Millipore and Sci Log offer their product and serives for much cheaper, the service provided by Optifilt is more useful because it is able to scale up to any geometry. Whereas a company that utilizes different filtration processes would have to buy multiple test rigs from Sci Log or utilize Millipore's service multiple times for different geometries, the MATLAB model can be easily scaled up to the chosen geometry drawn within the COMSOL interface. In addition, many industrial filters are operate at flows within the transitional regime. The COMSOL model is able to accurately model complex flow characteristics both at steady-state and transiently.

Our decision to provide testing services rather than to sell the testing rig has two main advantages for the survival of our company and the convenience of our client. For our company's benefit, providing a service ensures us a stream of recurring revenue as biotechnology companies will have to request and pay for our service when developing a new process or streamlining an older one. If we chose to sell the test rigs, demand could decrease as the market becomes saturated with our equipment. From the perspective of our prospective clients, although they would be paying more money by using our service multiple times rather than purchasing the filter station for themselves, they would access the expertise of a company that focuses completely on membrane filtration. Furthermore, because a biotechnology company would likely work to optimize a process a few times per year, they avoid having the filter station taking up space within their facility and remaining unused for most of the year.

Chapter 3:

Concept Stage

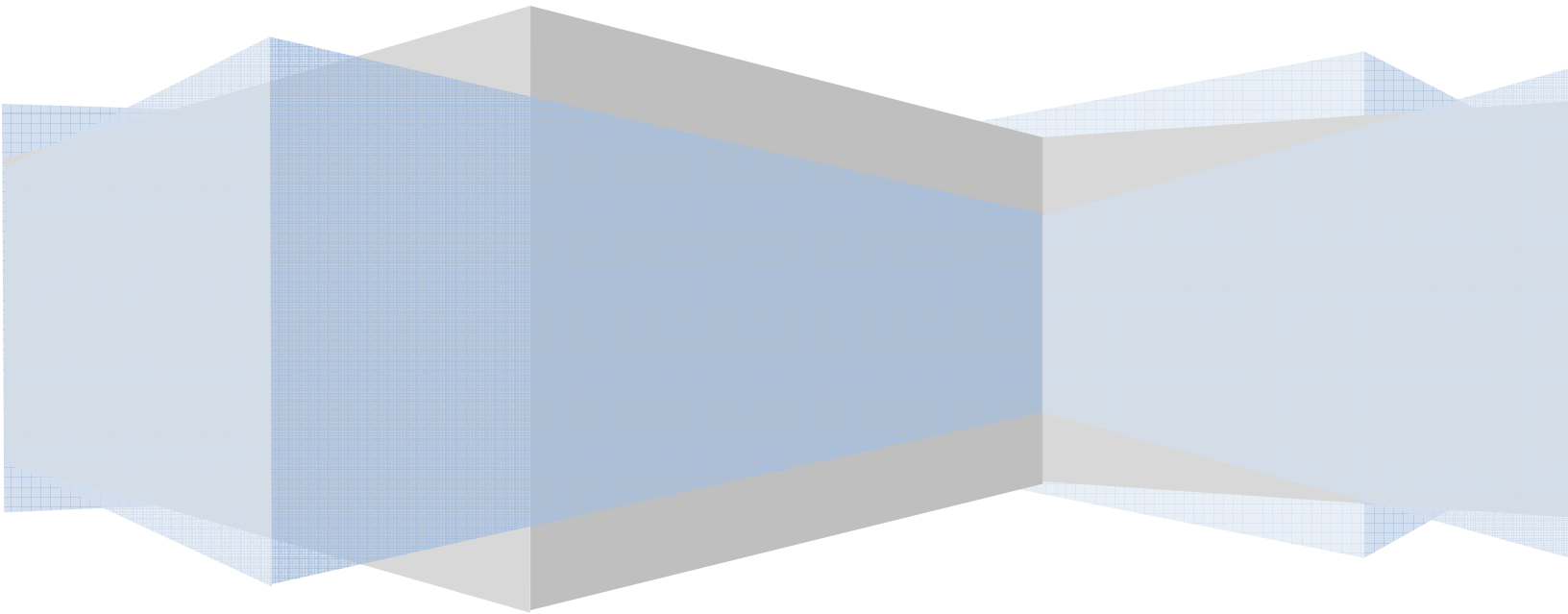

I. The OptiFilt Approach

OptiFilt aims to deliver high-throughput testing of membrane filtration conditions in parallel in order to improve the ability to identify optimal operating parameters for the ultrafiltration of mAb solutions at a laboratory scale for use in increasing the efficiency of the production of mAbs at the industrial scale. This project consists of four main goals: designing the instrumentation and physical specifications of the testing rigs and determining its cost, developing software that can accurately model mass transfer properties of the normal flow filtration setup within MATLAB, modeling the mass transfer and fluid mechanics of the filtration with the tangential flow setup, and providing a feasible plan for a start-up company which receives samples of mAb solutions from clients and identifies conditions for efficient filtration.

a. Project Charter

Project Name	The OptiFilt Approach
Project Champion	Dr. Matthew Lazzara
Project Leaders	Elizabeth Blake, Jennielle Jobson, Nikhil Shankar
Specific Goals	Design a high-throughput dead-end ultrafiltration system and the software necessary to test filtration conditions in parallel to identify optimal operating parameters for the tangential flow filtration of mAbs
Project Scope	In Scope: • Design of the test rig and its equipment • Develop analytic models to characterize laboratory-scale dead-end filtration in MATLAB and industrial-scale cross-flow ultrafiltration in COMSOL • Provide in-house testing of filtration processes using protein solutions and membranes provided by clients • Develop a working business model • Test rig must utilize parallel testing of membrane in real time Out of Scope: • Expansion of testing to sterile and viral filtration membranes • Detailed instrumentation of the test rig • Integration of the filtration process into manufacturing process of mAbs
Deliverables	• Market assessment and competition analysis • Technical feasibility assessment • Financial and sensitivity analyses over the course of 8 years • Manufacturing capability assessment • Product life-cycle assessment
Timeline	• Construction of the test rig, process development, and implementation of the analytical models within 12 months • Scale-up operations within 2 years • Full scale production in years 4-7 • Continue with the company, liquidate assets, or sell the company after the conclusion of the eight year

Table 2.1 OptiFilt's Project Charter

b. Technology Readiness Assessment

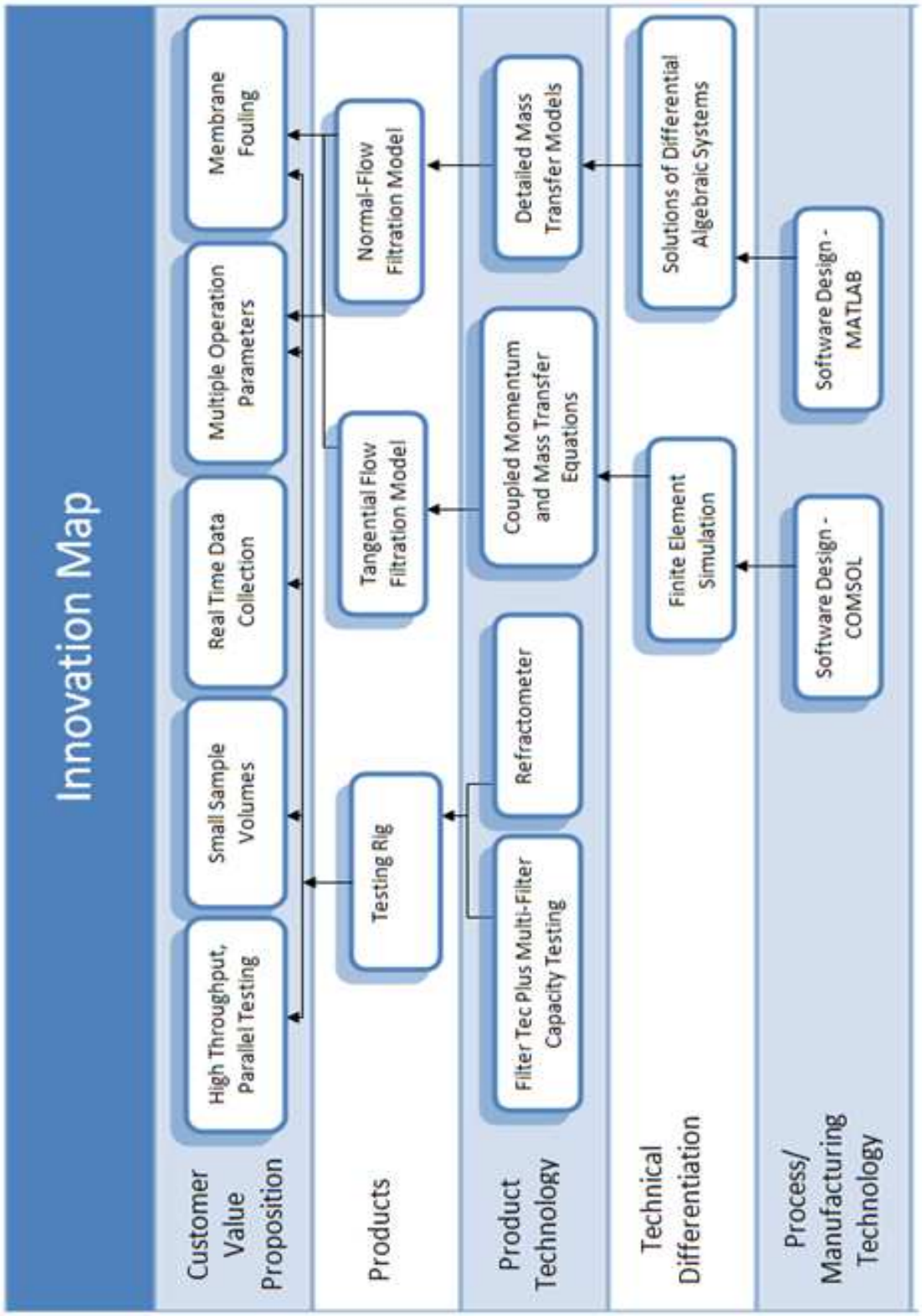

Chapter 4:

Dynamic, Dead-End Flow Test Rig Models

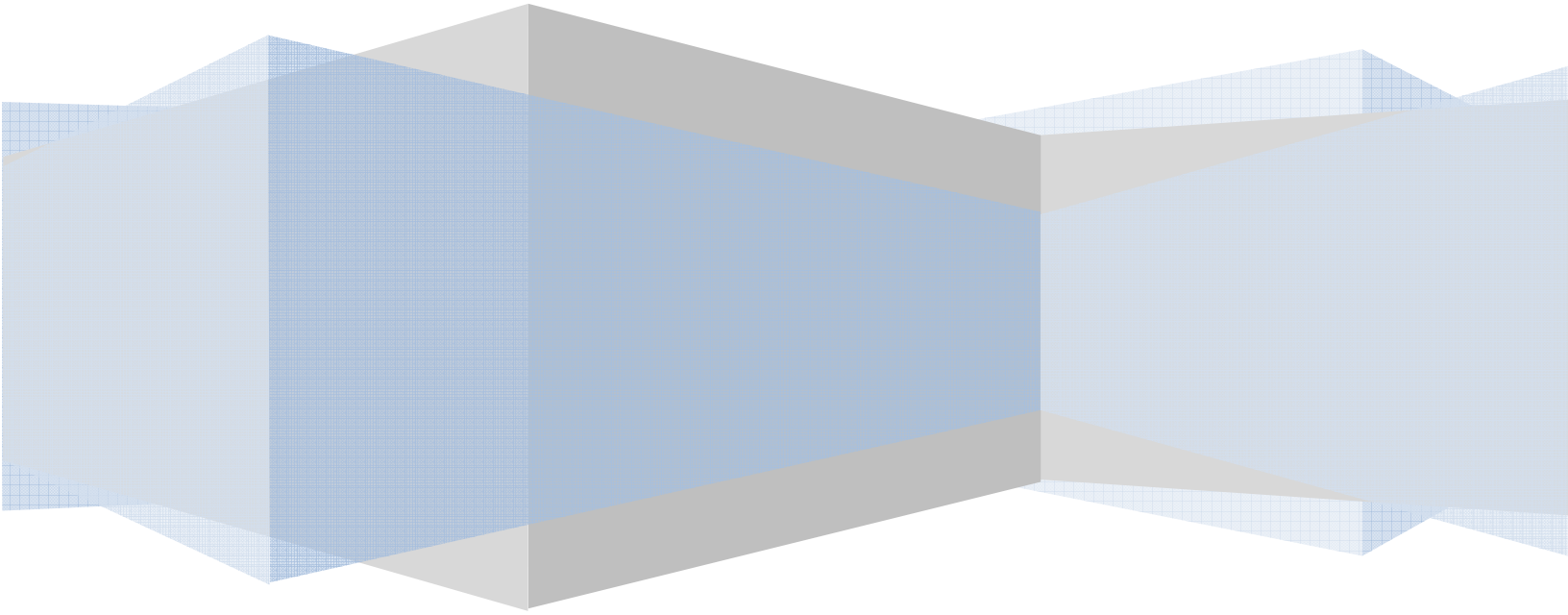

I. Assumptions of the Test Rig Model

The test rig is intended to improve UF performance on an industrial scale, and to lessen the chance of UF failure and associated financial burden. As such, the model needs to emulate reality as closely as possible to be generally applicable, while still remaining highly customizable to the demands of the company.

A set of interdependent differential and algebraic equations were derived to define the time-dependent behavior of flux, θ, and θ'. These were solved simultaneously in MATLAB R2010a both in the complete absence of fouling and the presence of cake-adsorption fouling. While the standard (pore-plugging) model is generally sufficiently accurate [4-2], the cake-adsorption model is considered the most relevant for to mAb filtration fouling [4-1] and is therefore used in this model. Should a company prefer another type of fouling evolution, the modifications are quite simple. However, some other fouling models result in decreasing pore radius, or increasing membrane thickness, and the model operator should take care to consider that these values are now variable. In the cake-adsorption fouling model for mAb, resistance builds up because of topical cake formation of (relatively) small thicknesses, compared to the filter [4-8]. When cake fouling appreciably affects membrane thickness, flux decreases markedly, the membrane rapidly approaches capacity, and the filter is washed. Therefore, membrane thickness is assumed constant during the span of functional operation. Nevertheless, it would technically be an improvement to this model if membrane thickness were recorded as variable. The cake-adsorption model also assumes that caked foulants are incompressible, though this is not always true. In the case of mAb deposition, however, and for most other proteins, this is a safe assumption [4-1].

It was decided that the UF model would run under constant trans-membrane pressure (pressure), rather than constant flow rate (flux), as the former is the most common type of laboratory filtration performed today [4-3]. If filtration is indeed desired at constant flux, the model can be adjusted to accommodate the change by replacing the flux relationship with one of pressure and by changing the empirical equations for fouling into their new constant-flux form. The most recently developed fouling models were designed to be able to predict the membrane capacity in one mode of operation when data from the other mode was fit to the correlation [4-8]. This has not always been the case; the two modes of operation have long been considered vastly different, and only in 2006 were hybrid fouling models created. Today, fortunately, changing from constant flux to constant pressure operation, upon request by the company, is straightforward.

The extent of CP is reflected in the model by the difference between θ and θ'. The model equations used as correlations for θ and θ' are standard in membrane science; the true sieving coefficient is a function of the products ΦK_c and ΦK_d, and apparent sieving coefficient is a function of the true one. These algebraic relationships are always true [4-7].

The sieving coefficients are also dependent on k_c. Many different theoretical equations and correlations exist for the specific k_c of various materials and flows. Thus, an appropriate estimation for k_c should be obtained and entered into the model prior to simulation. This model uses the k_c correlation for the general case of a CSTR that provides ideal mixing, or constant C_∞, and whose base is replaced by a standard UF membrane [4-7]. This approximation vastly simplifies calculation. This k_c equation (a function of μ and $\mathcal{D}$) is generally valid for most solutions but it would be ideal to use a more specific correlation if one is known.

Electrostatic effects are highly dependent on solution composition, and are not the dominant contribution to flux decay in membrane dynamics [4-10]. Most solutions do have charged species, but if molar concentrations are high, these effects are overwhelmed. It is possible, of course, that a certain protein (e.g. albumin) or membrane polymer possesses enough charge at particular solution conditions to significantly affect fouling beyond that predicted by classic pore or thickness adsorption. In this case, repulsion or attraction yields decay in flux that, nevertheless, may still be properly fit to a K_c and K_d pair. If electrostatic effects are suspected, either upon inspection of the protein to separate or because of optimization failure, the technician may utilize an available approximation to the Poisson-Boltzmann equation, or other available theoretical model [4-10], to consider them in this model [4-11].

$\Delta\pi$ always acts in opposition to the driving pressure applied to the UF system, and increasingly slows filtration over time. While $\Delta\pi$ is a colligative property, equations that properly predict its magnitude vary significantly based on the type of protein in the system, temperature, charge, and other properties. For a specific solution to be filtered, the natural osmotic pressure across a semipermeable membrane should be determined by experiment (or extracted from literature), fit to equation, and entered into the model. For this model, the $\Delta\pi$ correlation was found experimentally for constant solution pH and substance charge [4-9] and the resulting equation was used to model osmotic effects in the simulation. It is never desirable to use the Morse correlation for dilute solutions to approximate $\Delta\pi$, as the osmotic effects in relevant concentration regimes are not linear.

The remaining variables (viscosity, diffusivity, membrane length and cross-sectional area, applied pressure, osmotic reflection coefficient, starting permeability, initial volumes and concentrations) are case-dependent and can freely be adjusted based on a company's

specifications. These are all held constant. The model operator should find accurate values (usually readily tabulated in literature) to eliminate constants as any potential source of error. A restriction with this model is its limitation to only one dominant solute in the sample. The model will accommodate as many solutes as desired, as long as there are no solute-solute interactions, and as long as any solute beyond the first contributes negligibly to the gel-based CP at the membrane boundary.

Once the general model successfully predicted results for a sample set of mAb filtration data, the code was overhauled to function as an optimization algorithm. The new model accepts empirical results (which should be collected from a bench-scale experiment) detailing the behavior of θ and θ' over time. Then, using a simulated annealing (SA) algorithm, the model performs a two-parameter fit, selecting the optimal ΦK_c and ΦK_d that yield results that minimize the sum of squares of the residuals (SSR) between data and simulation. In trial runs, this method of optimization took between 3 seconds and 7 minutes on an Intel Core i5 CPU, depending on the proximity of the initial guess to the true global minimum. Thus, this method, while potentially fairly lengthy, is quite exhaustive and thorough. If no global minimum is found, or if the minimum is too large, the model operator should try other suspected fouling models to see if fit can be improved. ΦK_c and ΦK_d are strong decaying exponential functions of membrane radius, so a fouling model that assumes material deposition within pores would not fit a constant ΦK_c and ΦK_d. Rather, the SA algorithm would fit constants in a generic function $\Phi K_c = \exp(Ar)$ and $\Phi K_d = \exp(Br)$, where r is pore radius and A and B are presumably negative [4-7]. If all suspected fouling models also fail, the technician should consider electrostatic effects, or consider introducing a minute time delay to account for this model's intrinsic assumption of instant reaction to filtrate conditions at the retentate-membrane boundary.

SA relies on several variables which must be carefully selected by the technician, specifically: the lower and upper bound of search space, maximum error tolerance, and temperature (step size) profile. In recent years, adaptive simulated annealing (ASA) has gained popularity as an algorithm which self-modifies these parameters as optimization progresses. In this manner, ASA allows far more leniency in parameter selection. However, these parameters can quite easily be determined by the technician prior to running a simulation for a company. Additionally, while ASA is a more automated process, it results in longer processing times. There is therefore no particular need to modify the model to use ASA instead of SA. Both algorithms always require that the technician provide an initial starting point.

UF is a highly scalable process, but the geometry of flow is extraordinarily different between the testing-rig and industrial-rig scale. A given UF membrane is fully defined by K_c and K_d, the particular hindered convective and diffusive coefficients of that filter [4-6]. (Models for Φ are readily available, and once the products ΦK_c and ΦK_d are found by SA, K_c and K_d can easily be extracted.) However, the MATLAB model functions over the breadth of very simple, dead-end flow, and a basic square membrane. In an industrial setting, companies typically prefer crossflow over dead-end flow, as less fouling occurs and the membrane can easily be washed after use [4-5], and utilize more complicated geometry, such as cylindrical tubes. Crossflow and more complex geometries create more difficult flow conditions, introducing internal eddies, dead flow, and position-dependent Reynolds number regimes. Therefore, for the purpose of accurate scalability, the optimal K_c and K_d from the MATLAB model are imported into COMSOL, where the desired flow geometry is emulated. In COMSOL, boundary conditions of the UF membranes are well-defined by these fit parameters. Time- and space- dependent flow and concentration patterns can then be extracted from the simulation results, and analyzed by a technician. If the

profiles are undesirable, or fouling is extensive, filtration variables (e.g. pressure, membrane MWCO) and/or geometry can be freely adjusted, and new results obtained.

II. Model without fouling

The first model was designed under the highly simplified assumption of no fouling. This model is defined by a differential algebraic equation (DAE) system, consisting of two ODEs and five algebraic relationships, which were derived, drawn from literature, or fit from experimental data. The equations are described below.

$$\frac{dV_r}{dt} = -A_c v_f \text{ for } V_r \geq 0, \text{ (1-8)}$$

$$\frac{dC_r}{dt} = \left(\frac{1}{V_r}\right)(\theta' C_r v_f A_c - C_r \frac{dV_r}{dt}) \text{ for } C_r \geq 0, \text{ (4-1)}$$

In these equations, V_r is retentate volume, A_c is cross-sectional area, v_f is filtration velocity, C_r is retentate concentration, and θ' is the apparent sieving coefficient. Recall that Equation 1-8 implies that loss of volume in the retentate side of the testing rig is based solely on filtrate flux, which is a realistic statement. Equation 4-1 is a mass balance.

$$v_f = L_p(\Delta P_{TM} - \sigma\Delta\pi) \text{ for } v_f \geq 0, \text{ (1-5)}$$

Here, L_p is the hydraulic permeability, ΔP_{TM} is pressure, σ is the osmotic reflection coefficient, and $\Delta\pi$ is the osmotic pressure. Pressure is the driving force for membrane filtration, and flux is directly proportional to the net pressure [4-12], where the constant of proportionality is L_p. Because of the tendency for $C_{r,u}$ to increase over time (due to CP), the trans-membrane

concentration gradient and osmotic pressure will increase over the course of filtration. This opposes flow. σ is a factor that corrects for real-world deviation from the ideal semi-permeable membrane. Though assumed constant in this model, σ may be variable, in which case it is exclusively a function of θ (which is itself a function of $C_{r,u}$) because such boundary concentration buildup has the potential to alter the membrane's ability to effectively exclude solute. One reference uses $\sigma = 1 - \theta$, which can be inserted into the model with fouling for trials where θ is on the order of 10^{-1} or greater [4-7].

$$\mathrm{Pe} = \frac{(\Phi K_c) v_f \delta}{(\Phi K_d)\mathcal{D}} \text{ for } \mathrm{Pe} \geq 0, \text{ (1-10)}$$

Φ is the partition coefficient, δ is membrane thickness, $\mathcal{D}$ is diffusivity, and K_c and K_d are, respectively, defining convective and diffusive coefficients of the membrane. The Peclét number, Pe, is the dimensionless ratio of the convective elements of flow to the diffusive elements of flow. It is an integral aspect of CP and general membrane dynamics. No sufficiently accurate models exist for the products ΦK_c and ΦK_d for most membrane materials (though there are models for straight-pore membranes) [4-7], which necessitates the optimization-based nature of this model.

$$\theta = \frac{\Phi K_c}{1-(1-\Phi K_c)\exp(-\mathrm{Pe})}, \text{ for } 0 \leq \theta \leq 1, \text{ (1-9)}$$

$$\theta' = \frac{\theta \exp\left({}^{V_f}/_{k_c}\right)}{1-\theta+\theta \exp\left({}^{V_f}/_{k_c}\right)} \text{ for } 0 \leq \theta' \leq 1, \text{ (4-2)}$$

Equations 1-9 and 4-2 define θ and θ′ according to accepted models [4-7].

$$\Delta\pi = 23.487 \exp\left(0.0116 C_r \theta' \left(\frac{1}{\theta} - 1\right)\right),$$

$$24 \text{ mm Hg} \leq \Delta\pi \leq 3840 \text{ mm Hg} \text{ (1-6)}$$

The osmotic pressure equation above is empirically defined as a best-fit equation to experimental pressure measurements from [4-9].

This model utilizes a simultaneous equation solver to produce time-dependent results. MATLAB offers a multistep solver function called `ode15s`, designed for stiff ODE solutions and general DAEs, which uses the numerical differentiation formulae as algorithms. DAE solvers, `ode15s` included, require both initial conditions for the ODEs and good guesses for the algebraic equations. If these guesses are inadequate, or mathematically inconsistent, the solver simply terminates. A consistent set of initial guesses can be approximated by the model technician, or the function `fmincon` can be used. `fmincon` minimizes the normalized sum of the five algebraic equations above given filtration conditions set by the company.

a. Results

Model results for a standard run (with realistic values for all relevant constants, provided below) are shown below in Figure 4-1(a) through (g). Hydraulic permeability values were identified from Biomax UF membrane product sheets as approximately 3 LMH/psi, or 1.612 x

10^{-8} m/s mm Hg [4-13]; remaining constants are from Millipore product sheets detailing appropriate usage of the company's UF membranes [4-14].

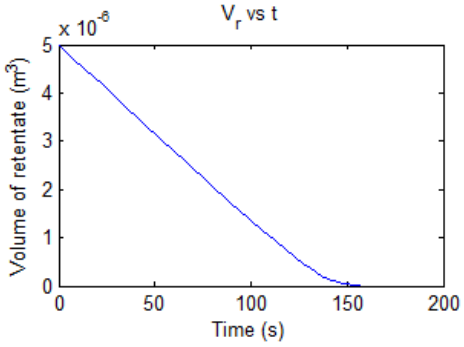

(a)

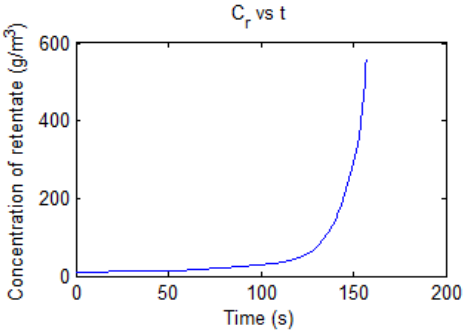

(b)

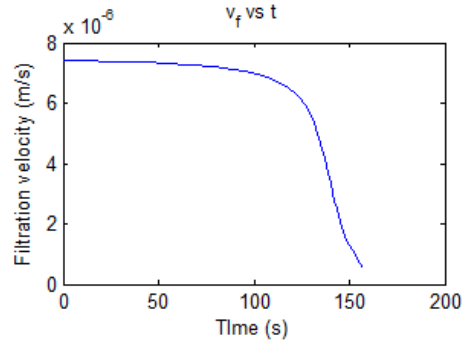

(c)

The results from the no-fouling model can be divided into two regimes: where osmotic effects are negligible, and where they are significant.

Figure 4-1(a) shows how the volume of 5 mL filtrate decreases linearly for the first part of the simulation, which, upon inspection of Equation 1-8, must be caused by a constant or near-constant filtration flux. As Figure 4-1(c) shows, this is indeed the case, up until approximately 120 seconds. Therefore, $0 \leq t \leq \sim 120$ sec is mostly *pressure-dependent*, in that mainly the applied trans-membrane pressure affects results. During this time span, $\Delta\pi$ increases to 30 mm Hg, but while the applied ΔP_{TM} during this trial was 100 mm Hg, trans-membrane pressure still dominates. Figures 4-1(d) and (e) show how θ and θ' increase relatively slowly in this first regime. In the absence of osmotic effects and fouling, the membrane is functionally a much more permeable membrane, both to solute and solvent. While solute flows through the membrane at a steady pace, solvent

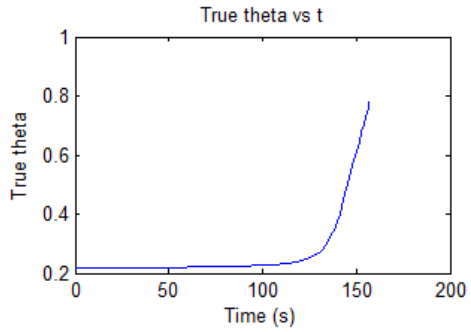

(d)

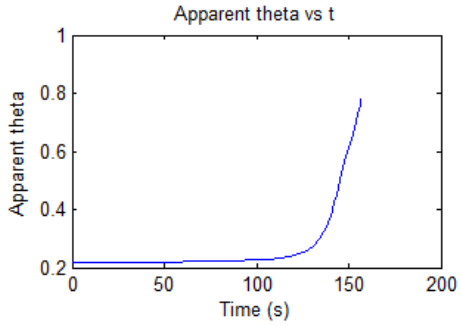

(e)

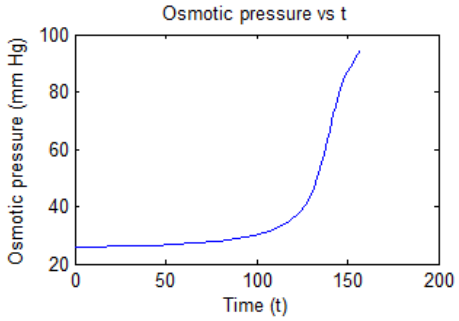

(f)

does so as well, and though filtration is occurring (and mass is transferring), concentrations change only gradually. Then, since $\theta = \frac{C_f}{C_{r,u}}$ and $\theta' = \frac{C_f}{C_r}$, both exhibit little change.

Following this, $C_{r,u}$ at the membrane boundary continues to increase until osmotic effects become significant, and the system also becomes *concentration-dependent*. In this regime, in spite of increasing osmotic flow, CP increases as the simulation continues due to practical limitations of mass flow within the membrane. Particles cannot flow through the pores instantly, causing mass buildup. Additionally, because of the significant osmotic pressure, some solvent flows back through the membrane from the filtrate to the retentate, dramatically concentrating filtrate product and decreasing net pressure and velocity. Though both θ and θ' now quickly increase, θ' does so faster than θ,

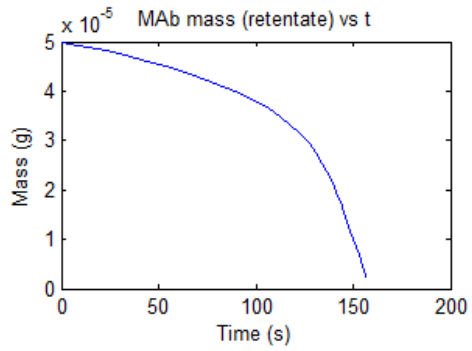

(g)

Fig 4-1: Membrane and flow dynamics in the fouling-free model. MATLAB stops the trial at 158 seconds.

Constants used as real-world approximations

μ = 10 cP	ΔP_{TM} =100 mm Hg
L_p =1.612x10E-8 m/s mm Hg	σ = 1
$\mathcal{D}$ =10E-8 m^2/s	A_c = 5 cm^2
ΦK_c=0.01	ΦK_d=0.02
L = 1 mm	

implying the presence of CP in the model. As flux is lessened, filtrate volume decreases more gradually, tending to zero asymptotically. In the presence of very limited volume, the remaining mAb mass becomes very highly concentrated (as shown in Figure 4-1(b)). Figure 4-1(g) shows, however, that the remaining mass of mAb on the retentate side of the membrane is decreasing, as expected. Figure 4-1(g) also shows that mass is filtered at a faster rate when filtration becomes concentration-dependent, which is due primarily to the very high $C_{r,u}$ associated with this regime. Therefore, although solvent flow decreases, solute transfer increases and the majority of filtration occurs near the end of the trial. As OptiFilt trials aim for minimal transfer of product mass through the UF membrane, significant undesired activity occurs in the concentration-dependent regime in this idealized, fouling-free model. If this behavior was actually observed in real experimental runs, companies would run UF purification only to the second regime, and then cease trials to prevent product loss.

Filtration nears completion when osmotic pressure approaches applied pressure, as all filtration activity stops as flux nears zero. There is consistently a minute amount of mass remaining on the retentate side after the simulation stops.

b. Limiting cases

To ensure that the model predicted trends that agreed closely with reality, the limiting cases of θ and $\theta' \approx 0$ (complete impermeability to solute) and θ and $\theta' \approx 1$ (complete permeability to solute) were tested. It is important to recall that constant sieving coefficients do not imply constant concentrations, only constant concentration ratios.

For $\theta = 0.01$ and $\theta' = 0.02$, one expects that because of the minimally permeable membrane, mAb proteins will filter through the membrane only until the osmotic pressure equals the applied pressure, at which point filtration (but not transport) will stop. One also expects that overall mass transfer will be small. This bounded model is fundamentally different from the previous model because it restricts the behavior of $C_{r,u}$, and limits the degree of CP that can exist. In limiting $C_{r,u}$, osmotic pressure increases proportionally to the degree of filtration, and only gradually approaches applied pressure. As discussed earlier, $C_{r,u}$ increases exponentially in the normal model because of increasing C_r and ever-flowing forward filtration rate. These conditions create a type of feedback loop which leads to the unexpected result of faster mass filtration at longer times. As $C_{r,u}$ is not permitted this exponential growth when so bounded by θ and θ', the behavior of osmotic pressure should be much more controlled, and exponential increases in concentration should not be seen at long times. Rather, all concentrations are expected constant prior to model termination.

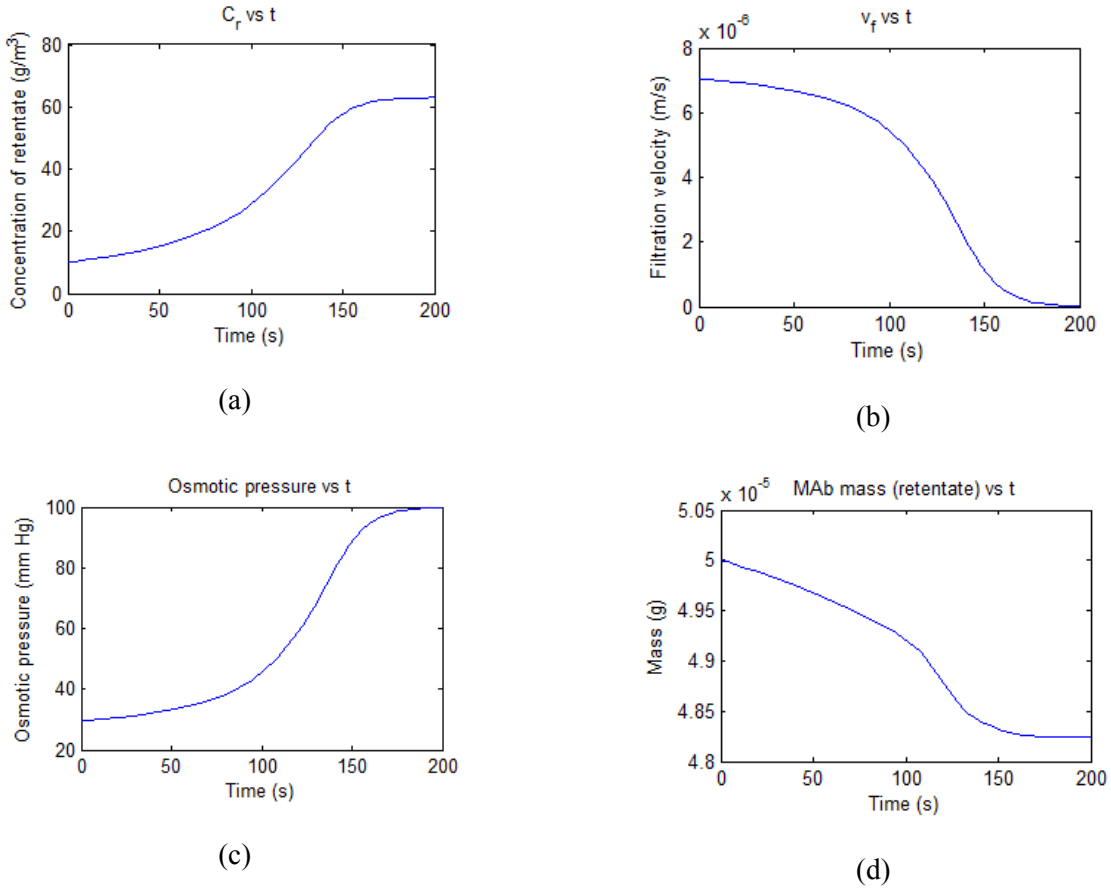

Fig 4-2: Membrane and flow dynamics in the fouling-free model under the constraints of θ = 0.01 and θ′ = 0.02, otherwise same constants as above. Notice the presence of a third regime where filtration slows down again, beginning at t = 145 s.

Figures 4-2(a) through (d) show the results of a simulation under these constraints. Beyond the prior two regimes discussed in the unconstrained model, there now exists a final third regime in which filtration slows and the feedback loop is broken by θ and θ′ constraints. As expected, overall mass transfer is small, with only 1.7 μg passing through the membrane. Because volume is non-zero at long times (since slowing effects of the third regime stop the feedback before $V_r = 0$), final retentate concentration increases from 10 g/m^3 to 64 g/m^3, instead of tending to infinity as before. Finally, of special note is the behavior of osmotic pressure and velocity, which more clearly support the existence of a third regime. While flux and Δπ approached final values quickly in Figures 4-1(c) and (f), their graphs here have a point of

inflexion where function slope begins to tend gradually to zero as the variables tend toward zero flux and 100 mm Hg, respectively. Therefore, the results for an impermeable membrane seem to agree with expected membrane behavior under this condition.

For $\theta = 0.98$ and $\theta' = 0.99$, the maximally permeable membrane, solute and solvent particles flow freely through the membrane at all times and at all filtrate and retentate concentrations. Since particles flow through the pores so quickly, slower flux on the retentate side (causing CP) is minimal. Thus, the membrane is scarcely an impediment to mass transfer at all. As $C_{r,u}$ never increases to critically large values, simulation results under this constraint should solely emulate the behavior of the pressure-dependent first regime.

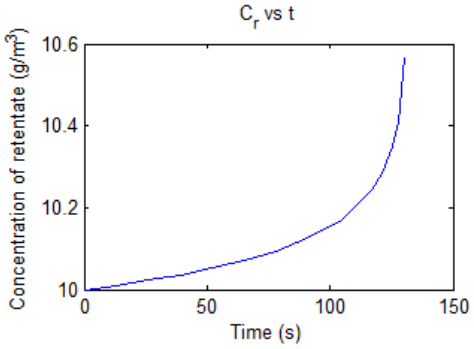

(a)

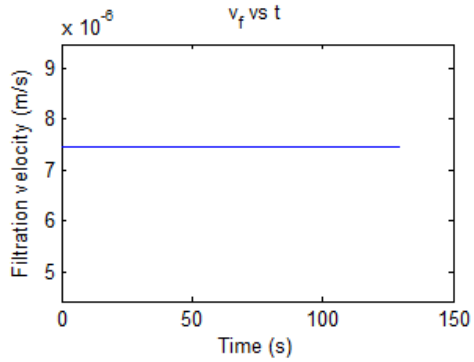

(b)

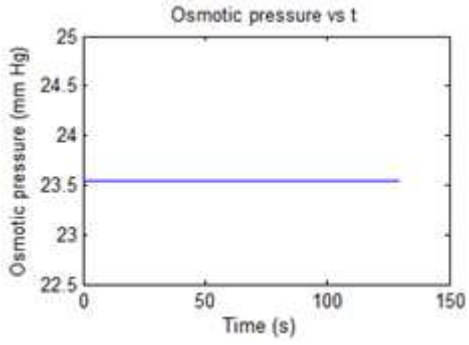

(c)

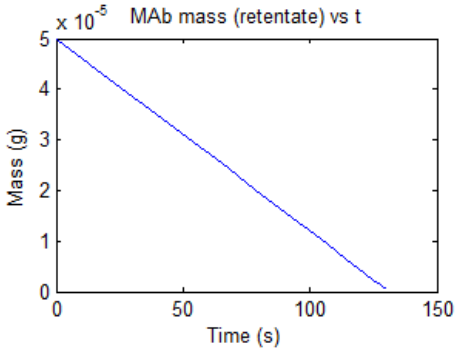

(d)

Fig 4-3: Membrane and flow dynamics in the fouling-free model under the constraints of $\theta = 0.98$ and $\theta' = 0.99$, otherwise same constants as above. Functional response is constant throughout; one regime only.

Figures 4-3(a) through (d) show the simulation results under these conditions. Figure 4-3(d) shows the expected constant rate of decrease of retentate mass, in agreement with the constant rate of decrease of retentate volume (not shown). Note from Figure 4-3(b) and (c) that filtrate velocity and osmotic pressure are functionally constant throughout the entire trial, as observed in the pressure-dependent region of the normal model. Figure 4-3(a) shows a small increase in concentration, from 10 g/m^3 to 10.58 g/m^3, because the membrane was modeled as *nearly* perfectly permeable, with $\theta \neq 1$. (This was done to avoid computational discontinuities associated with extreme values.) All of the results from this scenario fundamentally emulate the responses of the variables in the first regime of the unbounded model, as predicted, and it can be said with some certainty that the model without fouling is successful at predicting fouling-free membrane dynamics.

III. Model with fouling

To add fouling, the foregoing equations were reused, and Equation 4-3, defined below, was added to the model. Fouling models define the dimensionless ratio of current flux to maximum (initial) flux in constant-pressure operation, or alternatively, define the ratio of current pressure to initial pressure in constant-flow operation. For either type of operation, the fouling equations can be manipulated to express fouling as a ratio of current L_p to initial L_p. This can then be inserted into the model quite easily. Fouling will always lead to decreasing hydraulic permeability over time, though this rate of decrease is a function of many variables, and the type of fouling model chosen has significant effects on the model results [4-8].

$$L_p = \frac{L_{p,0}(\Delta P_{TM} - \sigma\Delta\pi_0)}{((1-K_a t)^{-4} + K_c v_f V_f)(\Delta P_{TM} - \sigma\Delta\pi)},\ L_p \geq 0 \quad (4\text{-}3)$$

For 1.0 kg/m^3 BSA trials, varying pressure to 2, 5, 10, and 20 psi, through 0.2 μm track-etched polycarbonate membrane, K_a and K_c were selected at 5.03 x 10^6 s/m^2 and 3.36 x 10^{-4} s^{-1}, respectively. Analogous values for K_a and K_c in the case of mAb filtration were not available in literature, and so were tentatively approximated as above in the design of this model. [4-8]

In Equation 4-3, $L_{p,0}$ is initial hydraulic permeability, $\Delta\pi_0$ is initial osmotic pressure, and t is time. Equation 4-3 is for the cake-adsorption model, with K_a and K_c fit to the type of solution being filtered. To properly utilize any fouling model, a technician must first find acceptable values for these parameters. Doing so is straightforward. While holding all other variables constant, the technician should record four or five time-dependent profiles of flux (taken over a range of pressures) from experimental trials. Osmotic contributions to each case should be predicted by Equation 1-6 or similar correlation, to isolate the effect of decreasing permeability on flux. Then, using simulated annealing in a manner not unlike how the algorithm is used to extract ΦK_c and ΦK_d, K_a and K_c should be selected as the pair that minimizes the SSR between equation ($\frac{J}{J_0} = f(\Delta P_{TM})$, as above) and reality [4-8]. Other fouling models like intermediate-adsorption or complete-adsorption have at most two fit parameters, with some having only one [4-8]. Following determination of constants, Equation 4-3 may be inserted into the model with fouling, which is then capable of predicting membrane behavior of any variable at any provided trans-membrane pressure.

The late-stage increased rate of filtration found in the first model was valid for a non-fouling, ideal case, and is therefore unlikely in actual filtration systems. However, under certain conditions and assumptions of fouling, the simulation terminates before system variables are equilibrated due to $V_r = 0$. In early termination, it is possible for fouling to not sufficiently

impede the natural $C_{r,u}$ buildup, in which case the idealized filtration behavior may occur. In normal cases, fouling plays too great a role in flux decay for the aforementioned feedback loop to occur, and late-stage filtration is slow, not fast. Knowledge of the filtration conditions that cause either behavior and/or allow equilibration of concentrations is, of course, valuable to the customer company.

e. Results using identical conditions as in the fouling-free model

To run the simulation and obtain results, a similar `ode15s` and `fmincon` solution was used. To ensure that the effects of fouling on all variables could be readily identified, all simulation conditions were kept identical to the non-fouling model (though this resulted in the model terminating before equilibration, i.e., zero flux). No other changes were made, for the purpose of obtaining comparable results.

Figures 5-4(a) through (h) show the results from the model with fouling. Here, there are no clear "regimes" of operation, as the trends of system variables change dramatically with small changes in constants (which can be seen by comparing Figure 5-4 to Figure 5-5).

Fouling causes V_r to decrease non-linearly with time throughout the range of time constraints, as expected, due to the decreasing hydraulic permeability caused by the cake-adsorption fouling effects, shown in Figure 5-4(h). Under the conditions of this trial, V_r does equal zero at long times, effectively ending the simulation. For various permutations of constants (permeability, pressure) and initial conditions, one often finds that the model terminates simulation with a more plausible non-zero final retentate volume, as shown in Figure 5-5 (with

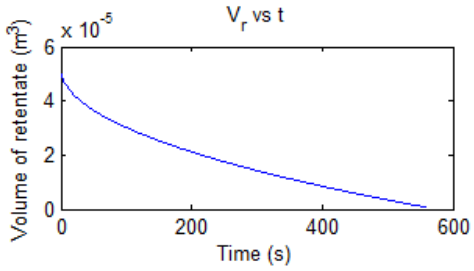

(a)

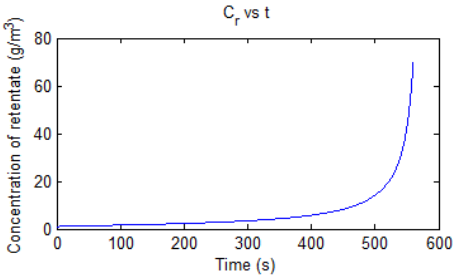

(b)

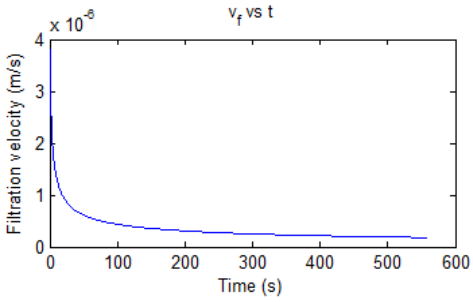

(c)

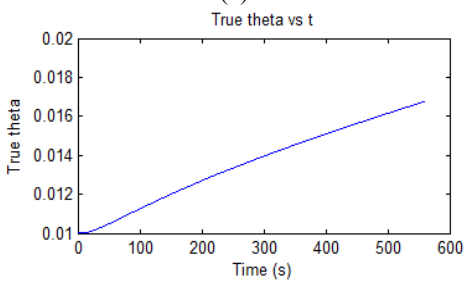

(d)

constants and ICs shown). For instance, if initial V_r is increased in the trial of Figure 5-4, hydraulic permeability decreases too quickly for all of the volume in the retentate to be filtered. Osmotic pressure is consistently increasing, so there comes a time when $\Delta\pi = \Delta P_{TM}$ and remaining volume on the filtrate-side is simply under no net driving force for fluid filtration.

When using this model, it is also important to take into account the variability of δ and/or r, if the selected fouling model and operation conditions appreciably affect these terms over the trial. This is easily done by adding another equation defining the nature of pore decrease or thickness increase, with such equations being pulled from supplementary information about the fouling model. For mAb fouling modeled by the cake-adsorption fouling model, δ and r do not change appreciably, so such equations were not used in this model.

With fouling, filtration took approximately three times as long to complete, with "completion" defined as the time when either V_r or v_f decreased to 0.5% of its initial value, whichever occurred first.

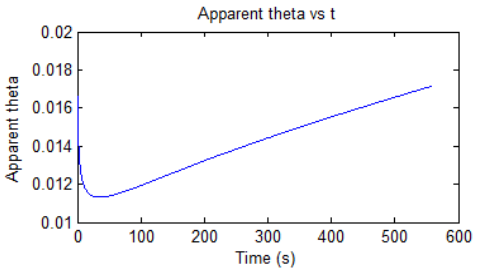

(e)

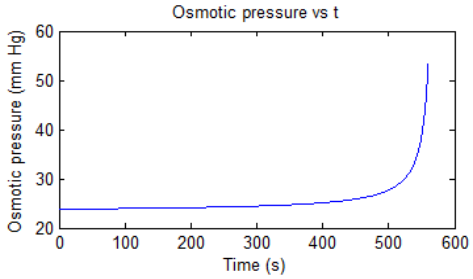

(f)

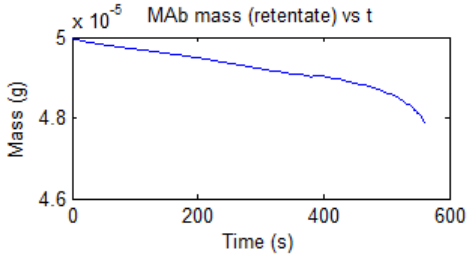

(g)

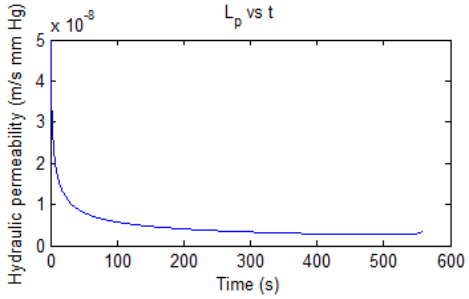

(h)

Fig 5-4: Membrane and flow dynamics in the complete model. MATLAB stops the trial at 541 seconds, compared to 158 seconds in the fouling-free model.

Constants used as real-world approximations

μ = 10 cP	ΔP_{TM} =100 mm Hg
σ = 1	$\mathcal{D}$ =10E-8 m^2/s

Additionally, overall mass transfer was greatly decreased, with only 2 μg of mAb successfully passing through to filtrate (compared with nearly 48 μg in the fouling-free model). Furthermore, θ and θ′ are significantly smaller than they were in the absence of fouling, suggesting that only minor filtration has occurred.

Osmotic pressure increases at long times to approach applied pressure, but the simulation ends before $\Delta\pi = \Delta P_{TM}$, as shown in Figure 5-4(f). Both θ and θ′ increase as the simulation progresses, implying the presence of increasing amounts of mAb mass in the filtrate as time goes on. These trends are entirely expected [5-6]. Companies must provide a threshold for acceptable amount of product loss in the filtrate, and a guideline as to what degree of concentration they desire in retentate product.

f. Results using conditions that permit equilibration

To obtain a more complete analysis of the membrane, conditions were varied so that the simulation would terminate only after reaching equilibrium (i.e., after satisfying the v_f criterion for completion, such that net flow is nearly zero). These trial results are not directly analogous to the results from the fouling-free model, but they are more realistic, in that they are expected to be observed in practice.

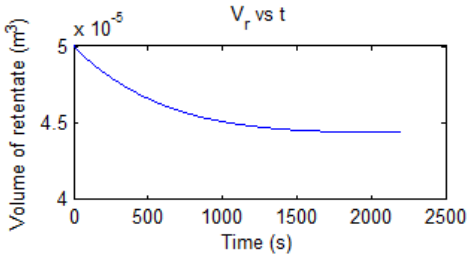

(a)

Figure 4-5 shows the behavior of several variables when the model reaches zero net pressure. The major and most significant change is for L_p, which is decreased by two orders of magnitude. These

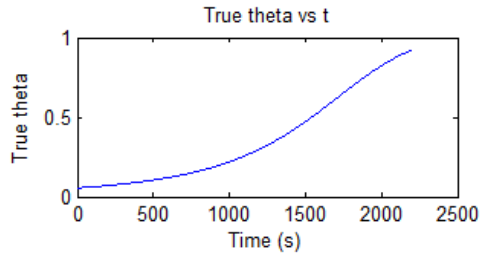

(b)

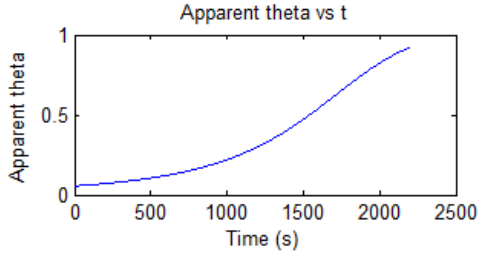

(c)

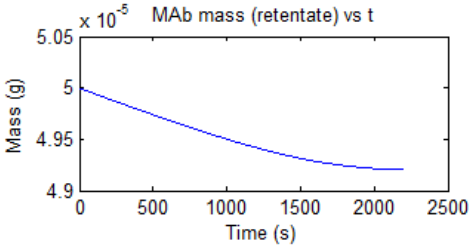

(d)

Fig 4-5: Membrane and flow dynamics in the complete model, with lower permeability than in Fig 4-4.

Constants used as real-world approximations

μ = 10 cP	ΔP_{TM} =100 mm Hg
σ = 1	$\mathcal{D}$ =1.12E-8 m^2/s
A_c = 5 cm^2	ΦK_c=0.01
ΦK_d=0.02	L = 1 mm
L_p = 4.48E-10m/s mm Hg	

conditions lead to much longer simulation time scales, of about 45 min. In this case, the simulation ends because of v_f approaching zero, not V_r doing so as in Figure 4-4. V_r now terminates at about 88% of its initial value.

Non-zero steady-state V_r is expected (and required) in real filtration since solutes of greater molecular weight than the MWCO will remain on the retentate side [4-3] and because cross-flow filtration, which is preferred over dead-end flow, physically requires the presence of some volume for flow. For these reasons, zero V_r is simply nonphysical.

One also notes that over the scope of this trial, θ and θ' are generally larger than they were in Figure 4-4. This tremendous improvement in apparent membrane permeability when shifting L_p in a direction that should lead to poorer throughput clearly suggests that the previous trial terminated before the system reached equilibrium. Since permeability never reaches zero (only approaches it), there is consistently an available avenue for equilibrating concentrations. It therefore seems appropriate to redefine "completion" as the time for v_f to

decrease to 0.5% of its initial value, where systems that exhibit the V_r condition are nonphysical, and modified to exclusively satisfy the v_f criterion.

In further support of this constraint for the model, Figure 4-5(d) shows the rate of mass transfer. Instead of faster filtration at longer times, mAb transfers quickly early on and more slowly as fouling increases and permeability decays. This behavior is observed in physical models and indicates promising model results.

g. Limiting cases

The limiting cases of near-zero and near-unity θ and θ′ were analyzed in the model with fouling as well. The results again suggest internal consistency.

For θ and θ′ ≈ 0, plots for V_r, v_f, and L_p should be comparable to those of Figure 4-5. In the case of no fouling, this limit resulted in large values of Δπ which eventually approached ΔP_{TM} and stopped flux. However, for these parameters, and with fouling, the minimally permeable membrane no longer relies on osmotic pressure to implicitly define the time span of a trial. For both free and restricted θ and θ′, the system still undergoes the same degree of fouling, and in the latter case, this fouling replaces osmotic pressure as the principal retarding force of the model. Therefore, the plot of Δπ is expected to vary only slightly from initial values, reflecting slight CP. Finally, mAb filtrate mass should be minimal, since the membrane is nearly impermeable.

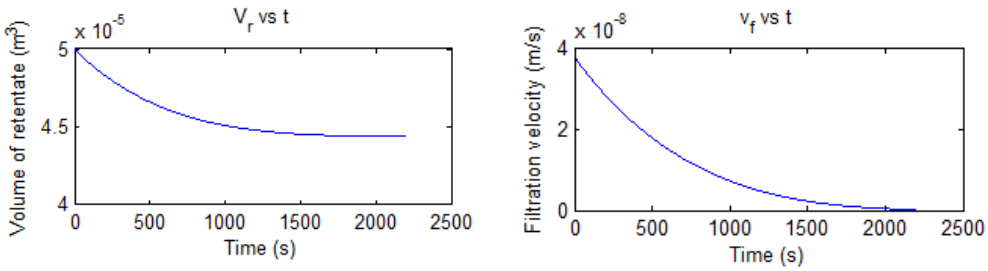

(a) (b)

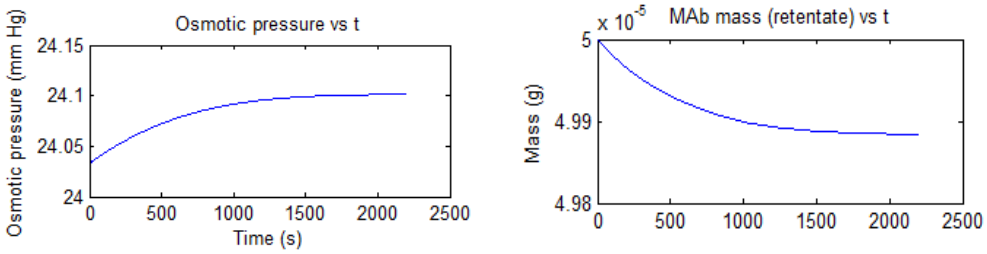

(c) (d)

Fig 4-6: Membrane and flow dynamics in the complete model under the constraints of $\theta = 0.01$ and $\theta' = 0.02$, otherwise same constants as above.

Figure 4-6(a) through (d) show this predicted behavior. V_r is unaffected by this change, as is v_f, osmotic pressure increases only minimally, and a mere 0.12 μg of mAb is filtered.

At the other extreme, θ and θ' near unity, predicted trends again vary from those expected for the fouling-free model; and once again, this is because L_p is unaffected by θ and θ'. Since osmotic pressure does not change in the perfectly permeable membrane (see Figure 4-3(c)), only hydraulic permeability affects the decrease in flux. Therefore, V_r and v_f should be the same as before, osmotic pressure should remain constant, and the decrease in retentate mass should be larger than in the unconstrained case.

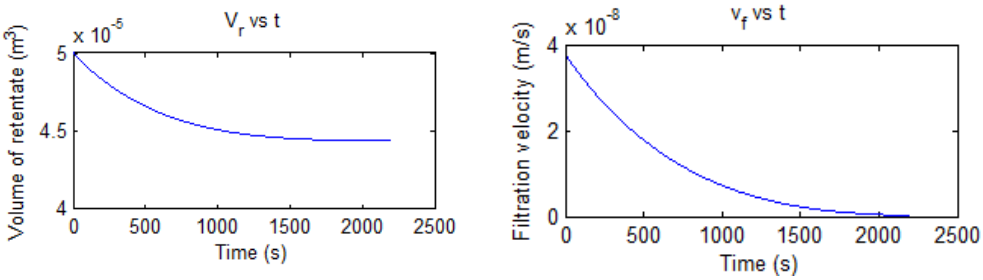

(a) (b)

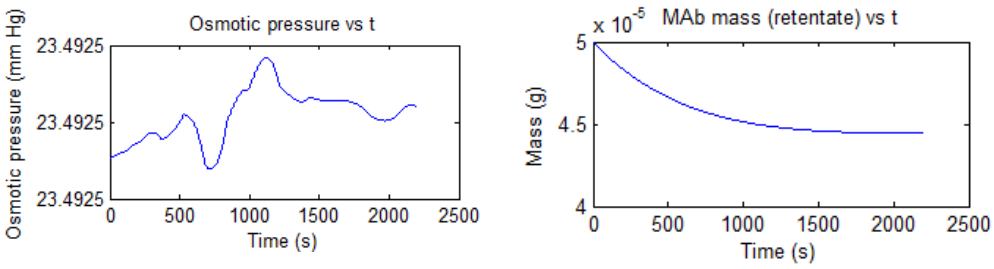

(c) (d)

Fig 4-7: Membrane and flow dynamics in the complete model under the constraints of $\theta = 0.98$ and $\theta' = 0.99$, otherwise same constants as above. Results as expected.

Potentially useful for a customer is the knowledge of theoretical minimum and maximum filtrate mass. Given conditions set by the company or determined by the model technician, θ and θ' can be set to a very small value, and then a very large one, to determine the range of possible extents of filtration (with the lower bound typically being zero, if θ and θ' are sufficiently small). For instance, under these conditions, the impermeable membrane, unconstrained membrane, and fully permeable membrane predict 0.12 µg, 0.8 µg, and 5.2 µg of mAb filtrate, respectively. If the minimum of 0.12 µg (Figure 4-7(d)) is an unacceptable loss of product, optimization for those conditions can be skipped, and a new set of conditions chosen, to save time and effort.

The results from these limiting-cases tests confirm that the model with fouling appears to be a fully functional extension of the previous, valid, fouling-free model.

III. Simulated Annealing

In the previous results, approximations were made for ΦK_c and ΦK_d, in which K_c and K_d are fundamental properties of a membrane that do not change with flow geometry or composition, or membrane size or orientation [4-6]. A key element of scalability, in addition to determining the scale-up factor, is identifying these parameters for the specific membrane in use.

Membranes are imperfect, in that pores may be of slightly varying radii or that pores may be unevenly distributed throughout the membrane. UF membranes are rated on their capacity and MWCO, not on their degree of physical ideality. Therefore, determining K_c and K_d is extraordinarily difficult from first principles, as any equation would need incorporate factors that account for uneven pore radii, etc. Alternatively, it is simpler to collect real experimental data, insert the conditions of that trial into a model, and have the model vary the terms ΦK_c and ΦK_d until a suitable fit is achieved, whereupon these products can be divided by Φ which is determined from models [4-6]. SA is an excellent optimizing algorithm for this purpose, and more time-effective than exhaustive brute-force, though the latter method may be used if the absolute best solution is desired. Using SA, the previous model with fouling was reversed in function, such that it now accepts data and outputs parameters, rather than the other way around.

θ and θ' are used because they encapsulate the important experimental results. θ and θ' describe fundamental information about CP, membrane capacity, and the time-dependent C_f and C_r profiles. In addition, the sieving coefficients are dimensionless, so results are widely applicable to a variety of feed concentrations. Knowing θ' behavior for a given membrane and solution, and knowing C_{f0}, allows predictions of concentration in the retentate and filtrate. For flow conditions, notice from Equations 4-5 and 4-6 that only ΦK_c and ΦK_d are undefined and unknown. Once ΦK_c and ΦK_d are found, then, θ and θ' can be predicted.

SA was coded in this model to simultaneously optimize θ and θ', with SSR deviations for both functions weighted equally in calculating overall fit-experiment discrepancy.

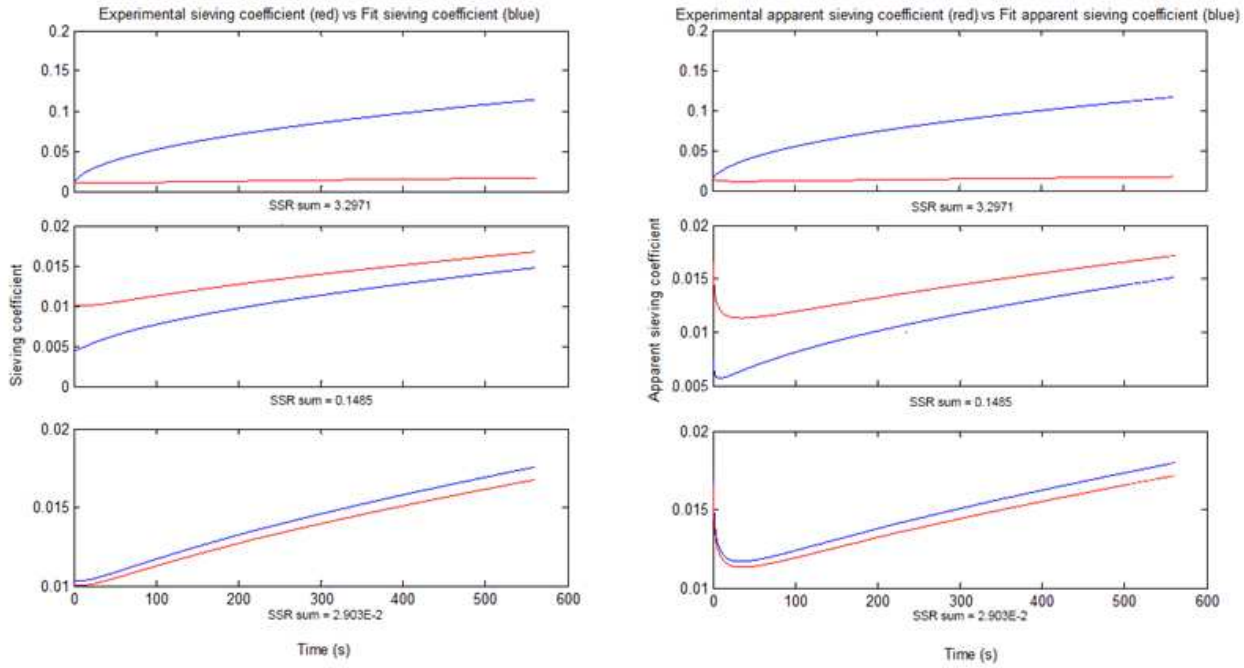

Fig 4-8: Optimization using SA. Notice that as SSR sum decreases, fit between curves becomes closer, simply from observation. SA was arbitrarily set to terminate when SSR $\leq 10^{-10}$, though ΦK_c and ΦK_d fits reasonably well at SSR on the order of 10^{-5}.

Figure 4-8 shows the results from a test run. The experimental sieving coefficient data was pulled from the complete model with fouling, with $\Phi K_c = 0.01$ and $\Phi K_d = 0.02$, and this data was simply imported into the SA model to test code fidelity. A search space was defined with lower bound of [0, 0], with no higher bound, though the model technician must provide an initial guess of appropriate magnitude, and if optimization fails, modify the temperature (step-size) schedule to that smaller magnitude.

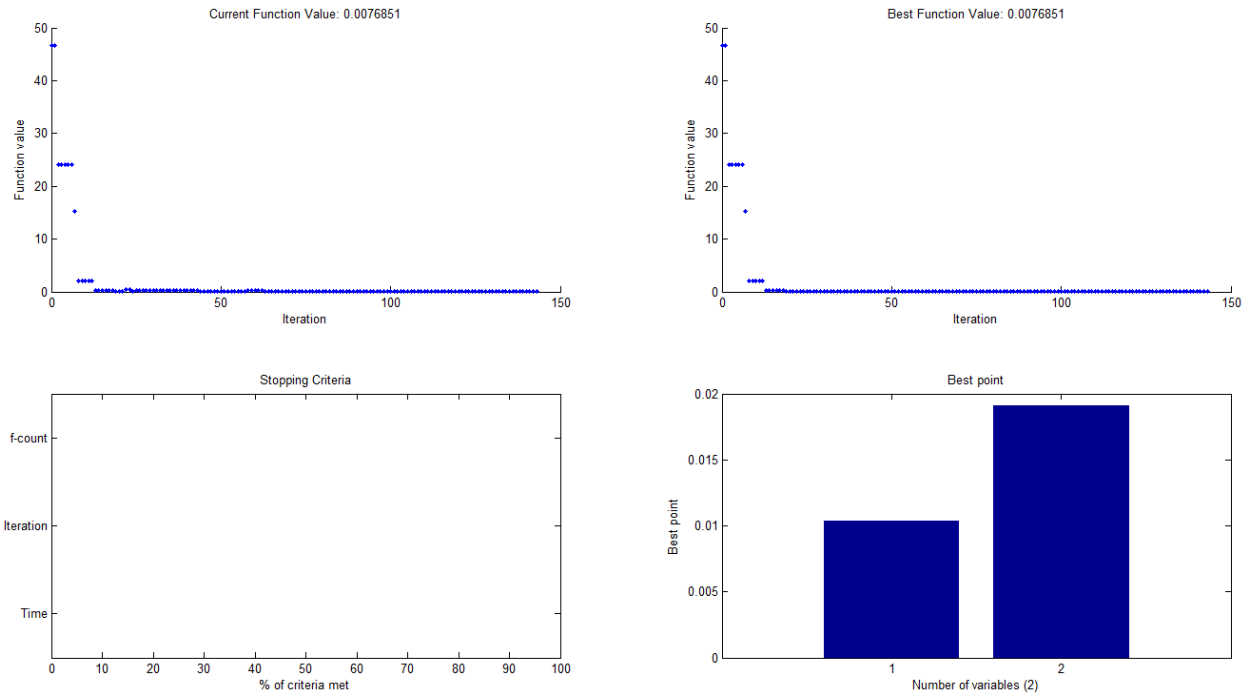

Fig 4-9: Optimization using SA. Process run time was 330 seconds.

Figure 4-9 shows the process of simulated annealing. Optimization was manually stopped after about 5 minutes to show the progress of the algorithm; it self-terminates with SSR $\leq 10^{-10}$ after a much longer length of time, on the order of hours. Figure 4-9 details the same kind of test fit shown in Figure 4-8, in that the correct ΦK_c and ΦK_d are 0.01 and 0.02. SA iteratively solves the DAE system to find $\Phi K_c = 0.0103$ (variable #1 above) and $\Phi K_d = 0.0191$ (variable #2) after this length of time, and finds ΦK_c and ΦK_d to a much higher degree of accuracy if allowed to self-terminate.

The SA model should be used to fit variables to experimental data, not to simulated data as done above. In addition to this (successful) test of code fidelity, physical trials should be performed to confirm the accuracy of this model. This model should only be used commercially if and when it is successful in performing experimental fit.

a. Optimal control code

SA ultimately finds K_c and K_d that fit experimental data. The alternative, which is arguably much more powerful, is to provide *desired* θ and θ′ profiles and have the model optimize all filtration conditions – membrane length and cross-sectional area, trans-membrane pressure, initial conditions, choice of solvent, flow geometry, and type of fouling – to find the cheapest and/or fastest conditions that still, within tolerance, satisfy the θ and θ′ goals. All optimized variables will be subject to practical constraints and other constraints provided by the customer. Models that perform such multivariable optimization contain "optimal control code", and can be highly complex. Such control code would require a dynamic transfer of information between MATLAB and COMSOL, and could be mediated by specifically designed packages like MUSCOD-II [4-4] which would employ optimization techniques beyond SA, if necessary. In such optimal control code, error to minimize is still the SSR between fit and goal for θ and θ′, but sources contributing to that error cannot be equally weighted, and the search space and temperature profiles are markedly different among all variables.

OptiFilt aims to produce θ and θ′ profiles for provided conditions, and reliably predict membrane behavior on an industrial scale. OptiFilt has not yet developed optimal control code for companies with more freedom in membrane design, and less in the degree of product filtration, though this may be feasible in the future. Though this is potentially more computationally intensive, optimal control code is not inherently more difficult to code, merely more time-consuming.

IV. Conclusions

The model described and developed in this section was shown to provide results (see Figures 4-1, 2, 3, 5, 6, 7) which agreed with behavior that would be expected from an

experimental system. This does not definitively prove the accuracy of the model, but acts in strong support of its general applicability. This complete model with fouling should be able to predict θ and θ' profiles for any conditions with a single dominant solute, and without significant electrostatic dipoles.

Use of the model requires several steps prior to SA optimization, in which parameters are determined by independent experiment. To begin, the technician must empirically derive a correlation for the osmotic pressure of the protein to filter. The technician then selects the most appropriate fouling model based on literature. If not available, he should obtain flux profiles at different pressures to test each of the four hybrid models (cake-adsorption, intermediate-adsorption, complete-adsorption and adsorption) detailed in [4-8]. Controlling for osmotic effects by using the $\Delta\pi$ correlation, the technician should then attempt to fit each fouling model to the flux results to find the minimum possible SSR among all models. If this SSR is also acceptably small, the technician should select this fouling model and the associated fit parameters; if SSR is still large, electrostatic effects may be present, in which case approximate solutions to the Poisson-Boltzmann equation should be used. Remaining system conditions should be specified by the company or chosen by the technician. The model can now be used. θ and θ' profiles should be recorded for a wide range of pressures, and for each case, the technician should record fit values of ΦK_c and ΦK_d (or of constants in the radius-dependent exponential decay of ΦK_c or ΦK_d). Φ is then determined by appropriate model [4-6] and K_c and K_d determined for each trial. If standard deviation is relatively small among obtained values, K_c and K_d should then be definitively taken as an arithmetic average of all trials. These values are imported into COMSOL where various permutations of geometry and flow conditions can be tested for the company.

This process is lengthy, but the potential payoff is in most cases excellent, as detailed in the economic analysis of Chapter 7. The technician can complete his report by providing information on the effect of various variables on membrane performance. This effect, after all, cannot be deduced from simple inspection of the system. DAE systems are remarkably sensitive to perturbations of initial conditions or associated constants. Small changes may lead to an unexpectedly large system response. This model should be very helpful in predicting these effects, for the purpose of optimizing overall membrane performance according to company constraints.

Chapter 5:

Industrial Filter Model

Finite Element Method

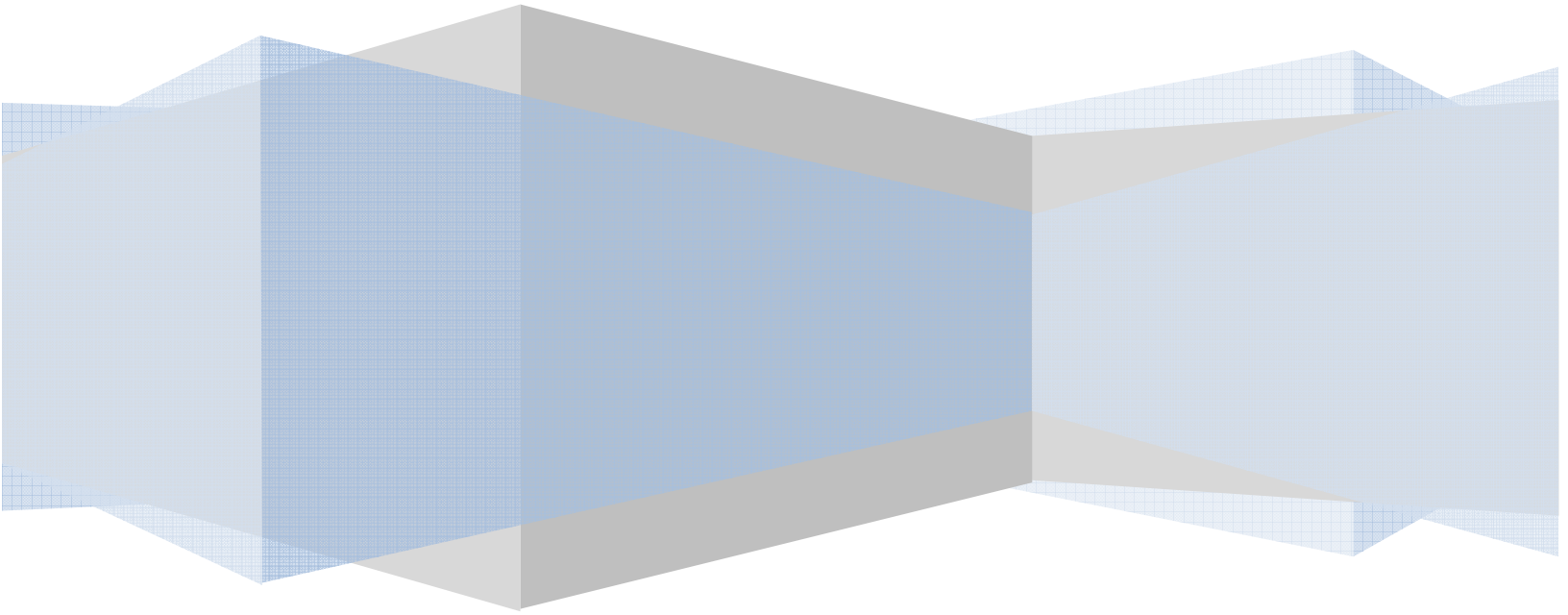

I. Invalid Assumptions from Test Rig Model

On the industrial scale, companies typically use tangential flow rather than normal flow filters to minimize fouling. Due to the use of tangential flow, several of the assumptions made when modeling the laboratory scale filter are no longer applicable to the model of the industrial filter. Because fluid flows through the channel in a direction tangential to that of the flow through the membrane, the model of the industrial filter must account for at least two dimensions. In addition, industrial filters typically utilize complicated geometry, such as hollow fiber and spiral wound membrane modules, introducing the possibility of turbulent flow. Consequently, an overall mass balance over the filter is no longer sufficient to model the UF membrane. Due to this complexity, COMSOL Multiphysics, a finite element solver and simulation package, was used to model the industrial UF membrane.

II. Rationale for Using COMSOL

The finite element method (FEM) approach implemented in COMSOL Multiphysics was used to model simplified two-dimensional tangential flow filter. FEMs are a numerical technique designed to find approximate solutions general partial differential equations (PDE) as well as of integral equations [5-1]. The FEM approach works to either eliminate the differential equation completely for steady state problems or render the PDE into an approximating system of ordinary differential equations, which are then numerically integrated using standard techniques such as Euler's method or the Runge-Kutta methods. FEMs are useful for complex geometries or varying domains because they rely on “mesh discretization” of a continuous domain into a set of discrete subdomains of a simple sample. Called elements, these subdomains are typically triangles for 2D geometries and tetrahedrons for 3D geometries. Because modeling the tangential flow filter involves the coupling of four PDEs (Navier-Stokes,

Brinkman, and two convection-diffusion equations), arriving at an analytical solution is not feasible. Consequently, the finite element method was used to simulate the filter instead.

III. Equations and Assumptions

As explained in Chapter 4, the Navier-Stokes, Brinkman, and Convection-Diffusion equations are coupled together within COMSOL to calculate the velocity, pressure, and concentration field throughout the entire filter. It was assumed that the filter was infinite in the z-direction and that the gradients of the pressure, velocity, and concentration of the protein were negligible in that direction. With these assumptions, the geometry of a tangential flow filter was simplified to two dimensions. This geometry was approximated to be equivalent to that of parallel plates, with the bottom plate semi-permeable to fluid flow. The problem was also assumed to be at steady state, bringing the times derivatives in all the equation to zero.

Within industry, TFF processes are typically operated at pressures high enough to bring the flow within the filter to the translational regime. This creates unpredictable flow patterns, such as eddies, which work to decrease fouling and concentration polarization at the membrane by inducing greater mixing within the filter. However, for simplification, flow through the channel was assumed to be laminar. The following equations were used to calculate the maximum velocity and Reynolds number for flow between parallel plates:

$$u_{max} = \frac{1}{2\eta}\frac{dP}{dx}(-h^2) \quad (5\text{-}1)$$

$$Re = \frac{puy}{\eta} \quad (5\text{-}2)$$

where h is half of the distance between the plates.

Industrial filters are typically operated at a pressure drop of 10 psi between the inlet and outlet. For this pressure drop, Equations 5-1 and 5-2 were solved simultaneously to find the length of the filter

that would ensure that the Reynolds number remains below 2000 to keep the flow from entering the transitional regime. It could then be assumed that the Navier-Stokes equation could adequately describe the flow within a channel of the calculated dimensions. Furthermore, we assumed that the mAb solution was dilute enough to be incompressible and that its density was equal to that of water. The viscosity of mAb solutions has been found to increase as the concentration of the solution increases [5-2]. However, for the purposes of simplification, the viscosity of the fluid within the filter is assumed to be independent of its concentration. The body force on the fluid was also considered to be zero. With these simplifications, the Navier-Stoke s equations become:

$$\nabla \cdot [-\eta(\nabla \boldsymbol{u} + (\nabla \boldsymbol{u})^T) + p\boldsymbol{I}] = -\rho(\boldsymbol{u} \cdot \nabla)\boldsymbol{u} \quad (5\text{-}3)$$

$$\nabla \cdot \boldsymbol{u} = 0 \quad (5\text{-}4)$$

In addition to the same assumptions made for the Navier-Stokes equations, the dilatational viscosity and source term were also considered to be zero. The Brinkman equations could then be simplified to:

$$\frac{\rho}{\varepsilon}\frac{\partial \mathbf{u}}{\partial t} + \nabla \cdot \left[-\frac{\eta}{\varepsilon}\left(\nabla \mathbf{u} + (\nabla \mathbf{u})^{T}\right) + p\mathbf{I}\right] = -\frac{\eta}{k}\mathbf{u} \quad (5\text{-}5)$$

$$\nabla \cdot \boldsymbol{u} = 0 \quad (5\text{-}6)$$

The diffusion coefficient in the convection-diffusion equation was assumed to be isotropic (uniform in all directions). At steady state, the convection-diffusion equation simplified to:

$$\nabla \cdot [-D\nabla c + c\boldsymbol{u}] = 0 \quad (5\text{-}6)$$

Although these assumptions are made for the simple illustration of the utility of the model, more realistic assumptions can be made according to the needs of our clients. Transitional and turbulent flow can be simulated within COMSOL using the K-ε and K-ω turbulence models. Expressions for thermophysical properties, such as the viscosity and density, can also be entered directly into the COMSOL user interface and applied to the selected subdomains if they are not truly constant.

IV. Geometry and Boundary Conditions

As shown in Figure 5-1, both flat sheet and plate and frame membrane modules are composed of flat sheet membranes attached to rectangular channels. In order to simplify the model for the purposes of illustration, a single channel was simulated with rectangular coordinates was simulated within the COMSOL interface.

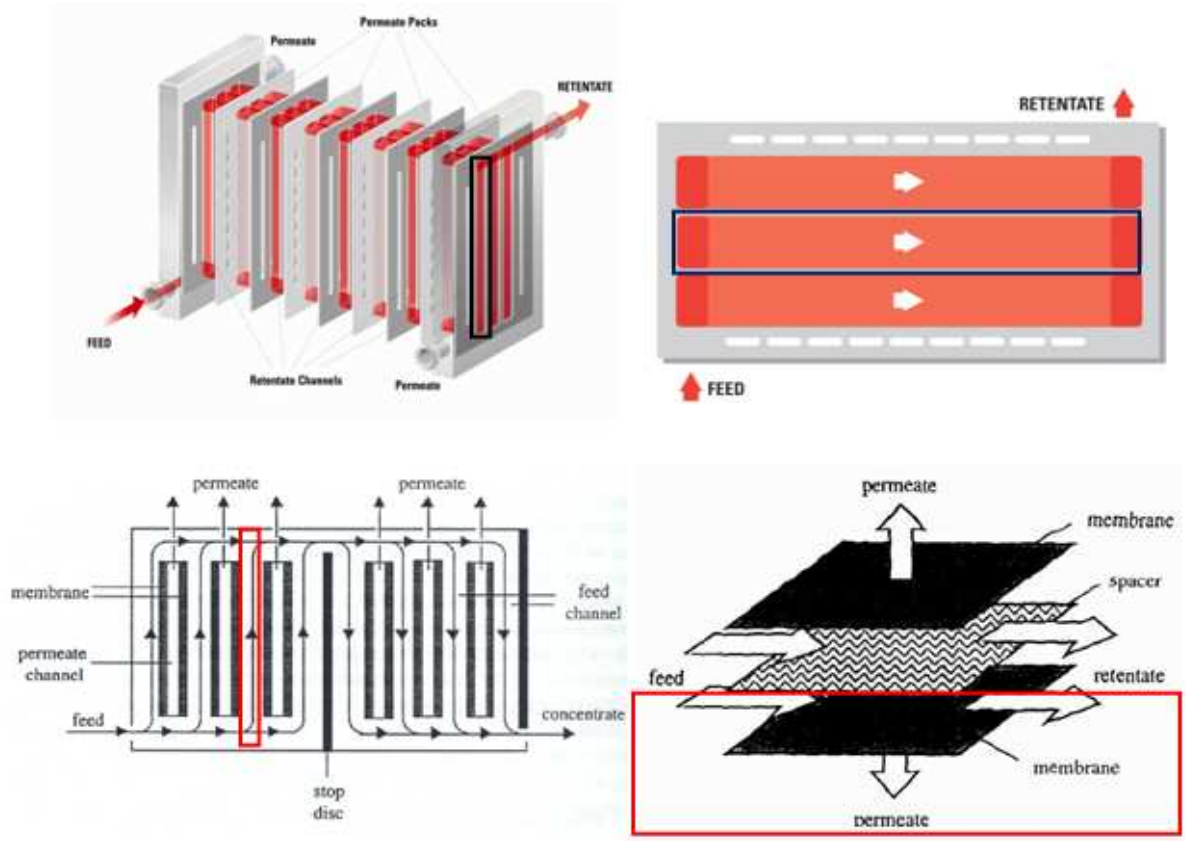

Figure 5-1: Top – OPTISEP Flat Sheet Membrane Module from SmartFlow Technologies and a cross-sectional view of its rectangular channels [5-3]. Bottom – A typical plate and frame membrane module and a cross-sectional view of its rectangular channels [5-4].

Figure 5-2 shows the geometry of the model simulated within COMSOL and its boundary conditions. It consists of a rectangular channel with a membrane attached to one of its boundaries. The

channel has a height of 1 mm and a width of 16 mm. The membrane has a height of 0.125 mm. The Navier-Stokes is applied to the channel and the Brinkman equations to the membrane. The flow through the channel is driven by the pressure drop of 4 Pa between the inlet (boundary 1) and outlet of the channel (boundary 7). There are no slip conditions at boundaries 2, 6, and 8, which state that there are no velocity components perpendicular to these boundaries:

$$\boldsymbol{u} \cdot \boldsymbol{n} = 0 \quad (5\text{-}7)$$

Here, **n** is a unit vector that has a direction perpendicular or normal to a boundary. An outlet pressure of 0 Pa is specified at boundary 4. The Brinkman and Navier-Stokes equations are coupled at their common boundary, boundary 3. Here, the boundary condition is continuity:

$$\boldsymbol{n}(n_1(\nabla \boldsymbol{u_1} + (\boldsymbol{\nabla u}_1)^T - p_1\boldsymbol{I} - n_2(\nabla \mathbf{u}_2 + (\nabla \mathbf{u_2})^{\mathrm{T}} + \mathrm{p}_2\mathbf{I}) = 0 \quad (5\text{-}8)$$

This condition specifies that the pressure and the velocity components on either side of boundary 4 which are perpendicular to the boundary are equal. The viscosity of the solution was set to 10^{-3} Pa·s, the density to 1000 kg/m^3, the permeability to 10^{-10} m^2, and the porosity to 0.1. From the boundary conditions and constants, the fluid mechanics of the entire filter is fully specified and can be solved for the velocity and pressure field.

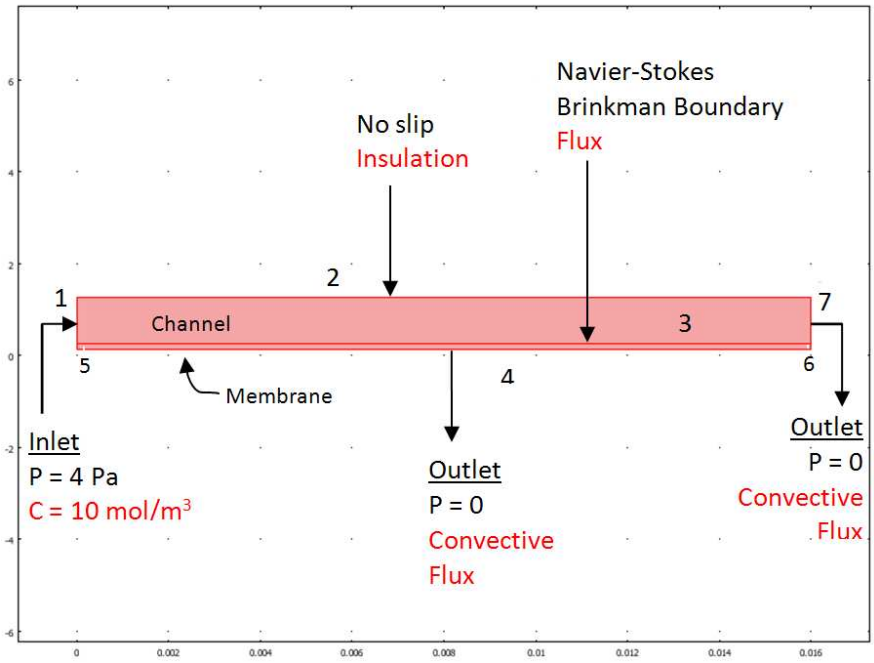

Figure 6-2: Depiction of the modeling geometry with its associated boundary conditions – The boundary conditions for the Navier-Stokes and Brinkman equations are outline in black. The boundary conditions of the two convection-diffusion equations are shown in red.

Because the concentration across the boundary between the channel and membrane is discontinuous, two convection-diffusion equations were necessary to accurately model the concentrations across the entire filter. The inlet concentration was specified to be 10 mol/m^3 at boundary 1. Because they are walls, the boundary conditions at boundaries 2, 5, and 6 were set to be insulated:

$$\nabla \cdot [-D\nabla c + c\boldsymbol{u}] = \boldsymbol{N} \quad (5\text{-}9)$$

$$\boldsymbol{n} \cdot \boldsymbol{N} = 0 \quad (5\text{-}9)$$

Here, **N** denotes the vector of the total flux. This condition sets the total flux perperdicular to the the boundary to a value of zero. At boundaries 4 and 7, because there is no longer any impediment to the transport of protein, the convective contribution to the mass transport is assumed to be much larger than the diffusive contribution:

$$\boldsymbol{n} \cdot (-D \cdot \nabla c) = 0 \quad (5\text{-}10)$$

Consequently, the diffusive flux can be considered to be negligible at these boundaries. The two convection-diffusion equations are coupled together at the interface between the channel and the membrane, boundary 3. Here, the concentration in the channel in channel is related to the concentration in the membrane by the partition coeffiecient, K:

$$K = \frac{c_m}{c_c} \quad (5\text{-}11)$$

c_m is the concentration of the protein within the membrane and c_c is the concentration of the protein within the channel. In addition, at boundary 3, the total flux of the protein exiting the channel must be equal to the total flux entering the membrane . However, the COMSOL interface does not allow these boundary conditions to be specified at the same boundary simultaneously: defining the concentrations according to the partition coefficient K destroys the continuity of the flux. Instead, the stiff spring method (applicable to PDEs for which the solution changes rapidly) is used to define continuous flux conditions that also force the concentrations to the desired values [5-5]:

$$(-D_c \nabla c_c + \mathrm{c_c}\boldsymbol{u}) \cdot \boldsymbol{n} = M(c_m - Kc_c) \quad (5\text{-}12)$$

$$(-D_m \nabla c_m + \mathrm{c_m}\boldsymbol{u}) \cdot \boldsymbol{n} = M(Kc_c - c_m) \quad (6\text{-}13)$$

D_c and D_m denote the diffusion coefficients of the mAb within the channel and the membrane, respectively. M is a (nonphysical) velocity. Equation 5-12 is applied at boundary 3 for the convection-diffusion equation applied to the channel and equation 5-13 is applied at boundary 3 for the convection-diffusion equation applied to the membrane. If both sides of equations 5-12 and 5-13 are divided by M, in the limit of large values of M, the left hand sides of the equations go to zero:

$$\lim_{M\to\infty} \frac{(-D_c \nabla c_c + \mathrm{c_c}\boldsymbol{u}) \cdot \boldsymbol{n}}{M} = (c_m - Kc_c) = 0 \quad (5\text{-}14)$$

$$\lim_{M\to\infty} \frac{(-D_m \nabla c_m + \mathrm{c_m}\boldsymbol{u}) \cdot \boldsymbol{n}}{M} = (Kc_c - c_m) = 0 \quad (5\text{-}15)$$

This satisfies equation 5-11. Furthermore, the concentration differences on the right hand sides of equations 5-12 and 5-13 are the same, but reversed compared to each other. This means that the normal component of the flux exiting one boundary enters the other boundary, giving a continuous flux across the interfaces. The diffusion coeffiencts within the membrane and the channel were set 10^{-9} m^2/s, the partition coefficient was set to 0.1, and the stiff spring velocity was set to 10,000 m/s.

The two convection-diffusion equations were coupled to the Navier-Stokes and Brinkman equations through their convective terms. For the channel, the velocity vector of the convection term was set to be equal to that of the velocity field calculated by the Navier-Stokes equation. Similarly, within the membrane, the velocity vector of the convection term was set to be equal to that of the velocity field calculated by the Brinkman equations. Most importantly, we can account for the mass transfer properties of the membrane, k_c and k_d, by multiplying these values by u and v (the velocity in the x- and y-directions) within the domain of the membrane. These k_c and k_d values will be calculated from the one-dimensional MATLAB model using simulated annealing. Using FEM, COMSOL approximated the velocity, pressure, and concentration fields for the entire model.

V. Results

The results of the COMSOL model are shown below. Figure 6-3 shows a surface and arrow plot of the velocity field within the channel and membrane. The velocity of the fluid within the channel reaches a maximum value of 57 mm/s at about 1 mm into the channel. The velocity of the fluid decreases along the length of the channel as fluid exits through the membrane. The arrow plot shows that the velocity profile is parabolic over the length of the entire filter.

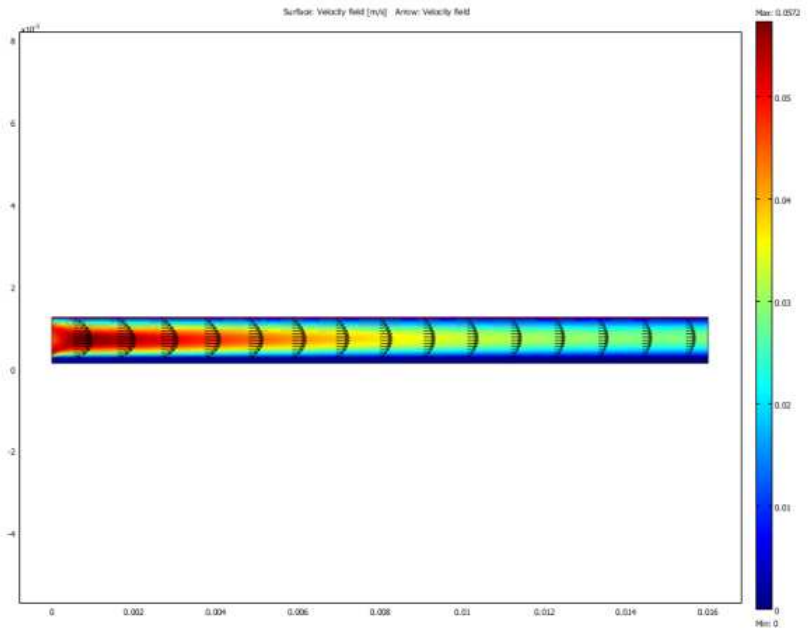

Figure 5-3: Surface and Arrow Plot of the Velocity Profile within the channel and membrane

Figure 6-4 (a) shows the velocity profile at various cross-sections along the length of the filter. The green line is the velocity profile of the cross-section at the inlet of the channel and orange line is the velocity profile of the cross-section at the outlet. At the inlet, the flow is not yet parabolic as it has not completed its adjustment to the no slip condition at the top wall and the membrane boundary at the bottom wall. After the hydrodynamic entry length, the velocity profile becomes parabolic and remains so for the entire length of the filter. In the limit of low membrane permeability to water, the flow within the TFF channel can simplified to that of flow between two parallel plates. Consequently, the fluid within the channel exhibits a parabolic velocity profile similar to the velocity profile of flow between flat plates. However, unlike flow between flat plates, as the position within the filter increases in the x-direction, the velocity of the mAb solution decreases as some of the fluid exits through the membrane and its volume decreases even though the cross-sectional velocity profile remains parabolic. At the height of the channel, the velocity is zero at all cross-sections along the filter. This indicates that the no slip condition is indeed being fulfilled at boundary 4. However, at the Navier-Stokes and Brinkman boundary, the velocity reaches a nonzero value and remains constant at this value across the membrane. This nonzero value

decreases with the in the x-direction of the filter as less fluid is passing through the membrane further into the filter.

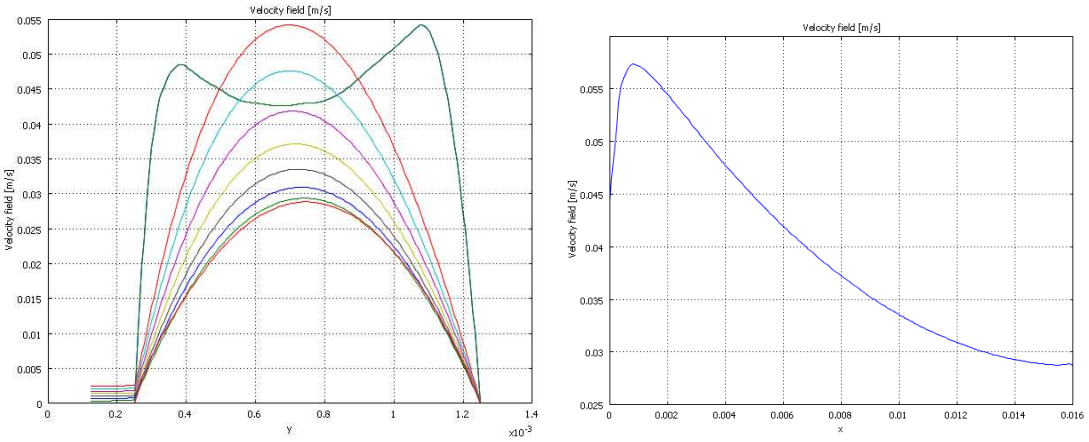

Figure 6-4: a) Cross-sectional velocity profile along the length of the filter. b) Line plot of the velocity profile along the length of the channel

A line plot of the velocity profile along the length of the channel can be seen in Figure 5-4 (b). Within the hydrodynamic entry length, the velocity of the fluid rapidly increases to its maximum value. Once fully-developed, the velocity decreases with the length of the filter as the water passes through the membrane and the volume of fluid decreases. The rate of the decrease in the velocity profile decreases towards the end of the channel. This occurs because the pressure drop decreases along the length of the filter. At a given point along the length of the filter, the average transmembrane pressure drop is related to the pressure drop across the length of the channel by the following equation:

$$TMP = \frac{p - p_{out}}{2} \quad (5\text{-}16)$$

P denotes the pressure at the point along the length of the filter and p_{out} is the outlet pressure. Therefore, because the pressure drops along the length of the filter, the difference between p and p_{out} also decreases, giving a lower TMP. As a result, there is less pressure forcing fluid through the membrane as you move further along the channel in the x-direction, causing the flux of water through the membrane to decrease and the velocity to decrease along the change at a slower rate.

Figure 5-5(a) shows a surface plot of the pressure field across the entire filter. Figure 5-5(b) shows a line plot of the pressure along the length of the channel at the centerline of the channel's height. The pressure drop across the channel decreases linearly across the length of the channel, which is to be expected because the behavior of the flow within the channel should approach that of flow between parallel plates in the limit of low water permeability.

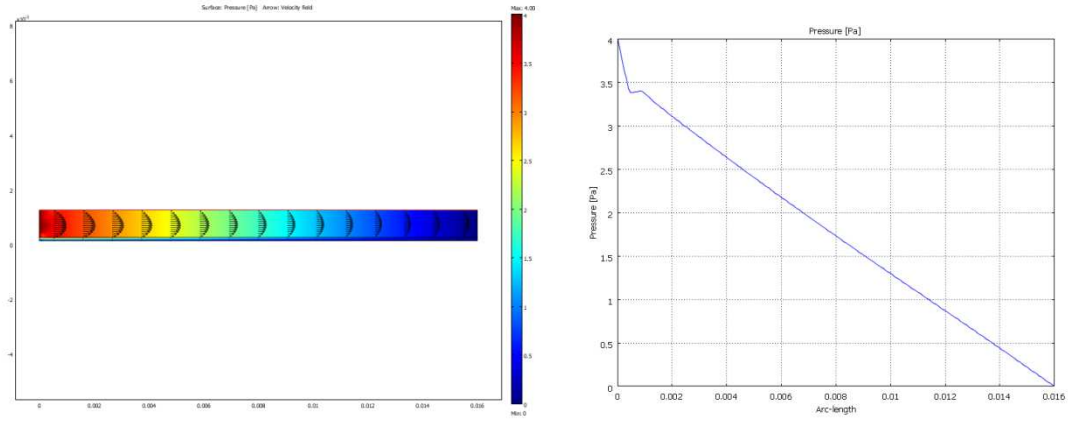

Figure 5-5: a) Surface plot of the pressure profile within the filter. b) Line plot of the pressure profile along the length of the channel

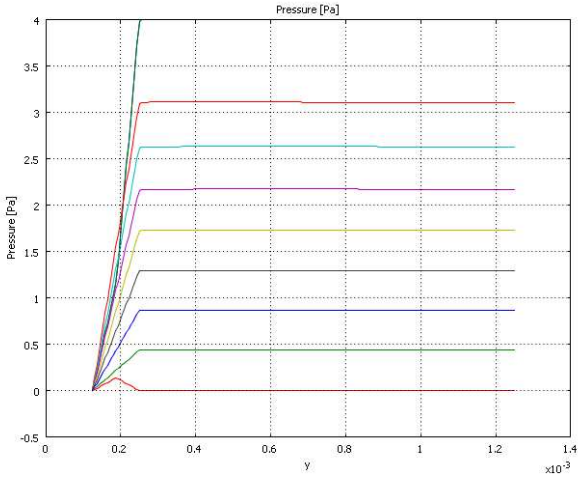

Figure 5-6: Cross-sectional pressure profile along the length of the filter

Figure 5-6 shows series of line plots of the pressure profile at different cross-sections along the length of the filter. For each cross-section, the pressure is constant across the channel and then decreases

linearly across the membrane. The TMP decreases with increasing length in the x-direction as expected from Figure 5-4 (b).

As shown in Figure 5-7 (a), the concentration of the mAbs within the channel increases from 10 mol/m^3 at the inlet to about 19 mol/m^3 at the outlet. The concentration within the center of the channel is not influenced by the filtration process until about halfway into the channel. The developing diffusion layer before the membrane can also be clearly seen. The concentration reaches a maximum of 24 mol/m^3, but decreases due to the increased effect of the diffusion of the protein throughout membrane as the velocity of the fluid decreases, reducing the convective contribution to the total flux. The concentration within the membrane also increases along its length as a small portion of the mAbs partition into the domain.

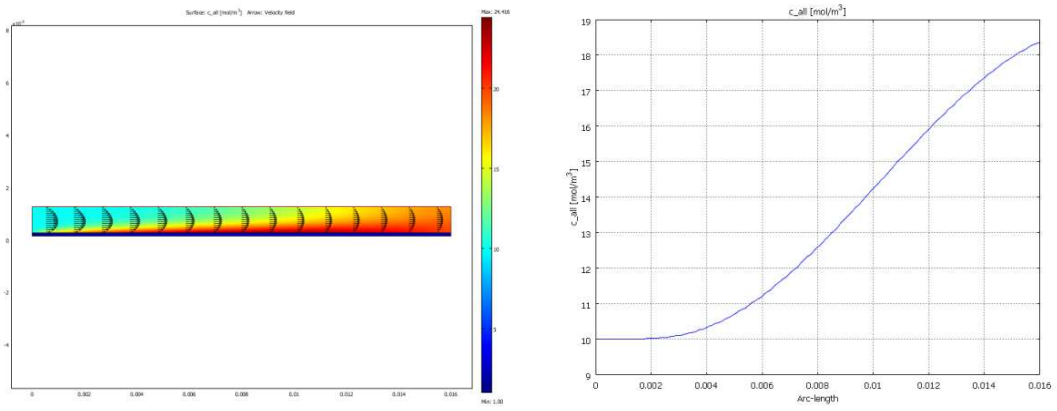

Figure 5-6: a) Surface Plot of the Concentration Field. b) Line plot of the concentration across the length of the channel

Figure 5-7 (b) shows the increase in the concentration of the mAbs within the channel along the length of the channel along the centerline of the channel. The concentration increases from 10 mol/m^3 to about 18.5 mol/m^3. From about 2 to 12 mm into the channel, the concentration increases linearly in the x-direction. However, the rate of increase begins to reach a steady state value close to 19 mol/m^3 from 12-16 mm into the channel. The TMP decreases along the length of the channel causing the flux rate of water through the membrane to also decrease. As the water exits the channel through the membrane at a slower rate, the total volume of fluid begins to decrease more slowly. As a result, the rate at which the mAbs within the channel concentrates also begins to decrease. The concentration within the center of the

channel is not influenced by the filtration process until about halfway into the channel. The developing diffusion layer before the membrane can also be clearly seen.

Figure 5-8 (a) shows how the concentration varies in the x-direction at boundary 4. At the boundary between the channel and membrane, the concentration is immediately affected by the permeation of water through the membrane, rising quickly. However, less than 2 mm into the filter, the rate of increase in the concentration at the boundary begins to slow and then the concentration at the boundary actually begins to decrease 8 mm into the filter, before the fluid exits that channel at a concentration of 20 mol/m^3. As previously stated, this occurs because the diffusive contribution to the total flux of the mAbs becomes more significant as the velocity of the fluid decreases within the channel. Consequently, as you move through the channel in the x-direction, a greater percentage of the channel experiences an increase in the concentration as the mAbs begin to spread throughout the channel and the diffusive layer increases.

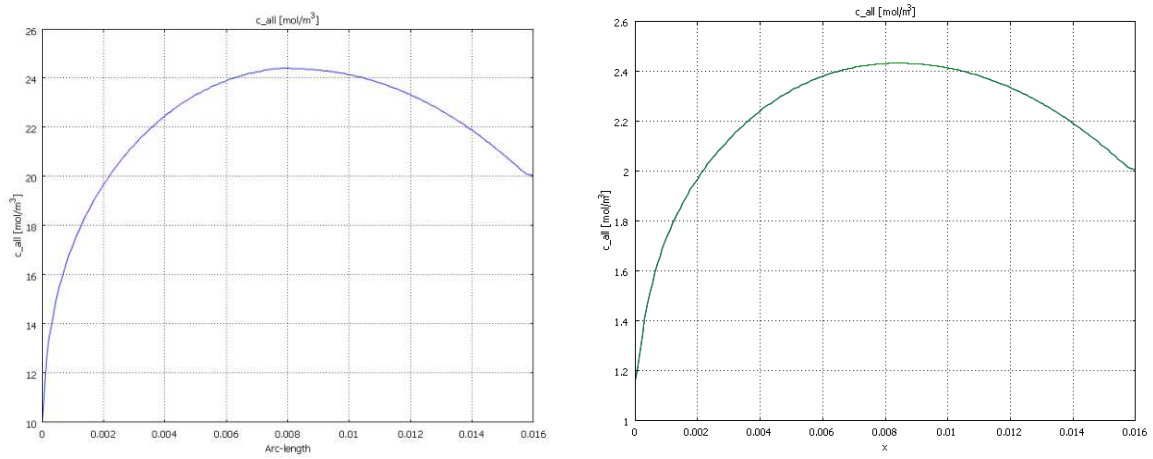

Figure 5- 7: a) Line plot of the concentration at the channel-membrane boundary across the length of the membrane. b) Line plot of the concentration at the outlet boundary of the membrane

Similarly, Figure 5-8 (b) shows how the concentration varies in the x-direction at boundary 3. Figure 5-8 (b) looks exactly the same as Figure 5-8 (a); however, the values of the concentrations are 10 times smaller. This occurs because the flux into the membrane is equal to the flux out of the channel at boundary 3 and the partition coefficient is 0.1. Thus, at every point along the boundary between the

membrane and the channel, any changes in concentration in the channel are reflected in the concentration in the membrane. Moreover, because the mAbs and water move at the same velocity and in the same directions once in the membrane (there is no internal partition) and because the membrane is so thin, the concentration immediately diffuses through the membrane in the y-direction and does not change. This means that the concentration of the fluid at the outlet of the membrane is the same as that directing over the membrane and we can be confident that the stiff spring method adequately specified the continuous flux and concentration boundary conditions.

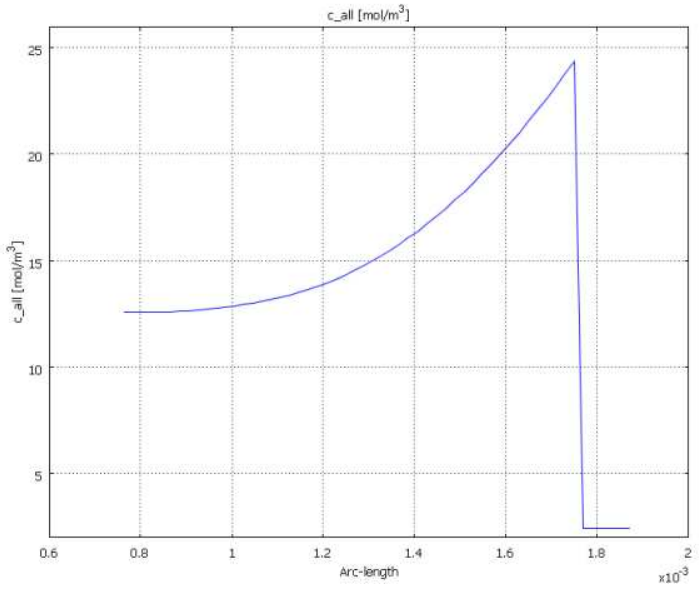

Figure 5-8: Concentration Polarization across the Membrane

Figure 5-9 shows a line plot of the concentration at a representative cross-section of the filter. As seen in normal flow filtration, the presence of the membrane causes the concentration to increase rapidly directly before the membrane, followed by a discontinuous drop in concentration. Here, the bulk concentration in the channel is about 12 mol/m^3, the concentration in the channel directly before the membrane is 24 mol/m^3, and the concentration within the membrane is 1 mol/m^3. Thus, at this cross-section, $\theta = 0.04$ and $\theta' = 0.083$. Within COMSOL, average values of the bulk concentration within the retentate, and concentration within the retentate at the membrane, and the concentration of the filtrate were calculated by the integrating the values of the concentrations over their respective boundaries.

Integrating over boundary 4, the average concentration within the filtrate was calculated to be 0.035374 mol/m^2. Integrating over boundary 3, the average concentration within the retentate at the membrane was calculated to be 0.353744 mol/m^2. Integrating over boundary 1, the average concentration of the feed was calculated to be 0.01 mol/m^2. Using these values, the θ and θ' of the system are 0.1 and 3.54, respectively. Consequently, whereas empirical data is usually necessary to determine θ and θ', our company can determine that directly from the industrial model.

VI. Limiting Cases

In order to illustrate the flexibility and accuracy of the COMSOL model, several limiting cases will be discussed in the following section. First, the model was tested in the limit of a completely impermeable membrane to the mAb solute molecules, but permeable to water through the use of an insulation condition at boundary 3. This sets the normal flux through the membrane and, as a result, the concentration within the membrane to zero. The velocity and pressure field are not affected by this change and, as such, are not reproduced. However, as shown in Figures 5-10 (a) and (b), the outlet concentrations increased by about three moles compared to the previously specified flux, which makes sense because no protein is being transported the membrane.

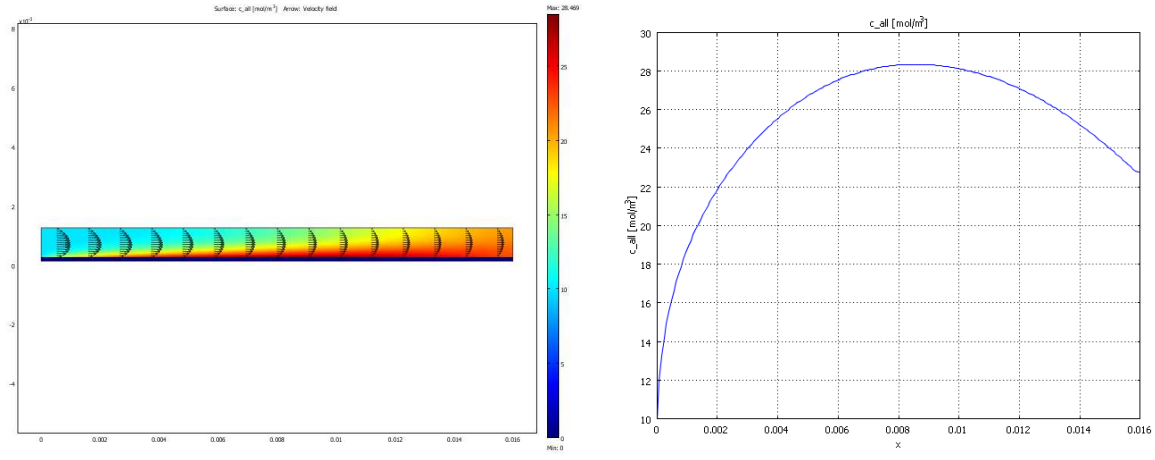

Figure 5-9: Surface Plot of Concentration and Velocity

Figure 5-11 shows the surface plot of the concentration for a membrane that is completely permeable to mAbs. This was achieved by setting the partition coefficient equal to a value of one. Because the protein is not being partitioned between the channel and the membrane, the protein is able to move throughout the entire filter freely. As a result, the concentration within the entire filter is zero.

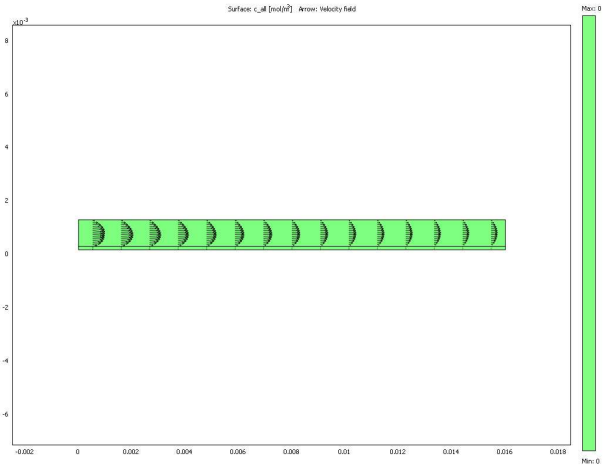

Figure 5-10: The surface concentration for a completely permeable membrane.

In order to investigate the effect of the diffusion coefficient on the surface concentration, it was increased by a factor of 100. Figures 6-12 (a) and (b)

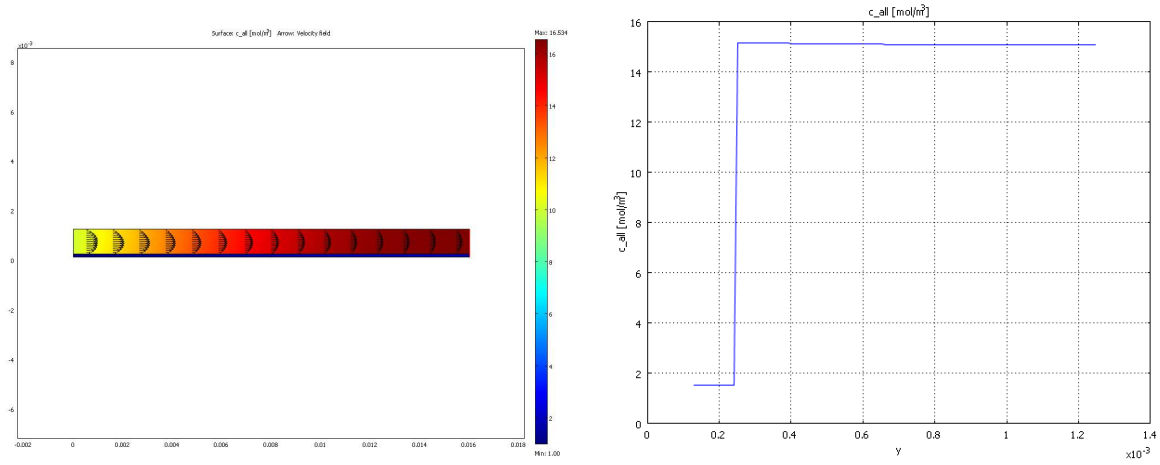

Figure 5-11: a) The surface concentration of a species with a much higher diffusion coefficient. b) Line plot of the cross-sectional concentration of a species with a much higher diffusion coefficient

Figure 5-12 (a) shows that for a species with a higher diffusion coefficient, the increase in concentration due to the loss of fluid spread through the system much more quickly. The effect of the

filtration process affected the concentration of the species at the height of the column directly at the inlet of the channel. Similarly, because the transport due to diffusion was so high compared to the x-direction, there was no a gradient in the concentration across the height of the filter. Consequently, as shown in figure 5-12 (b), there was no longer any concentration polarization due to a greater diffusive flux. However, the concentration increased to a smaller value – only 16 mol/m^3 – by the outlet compared to the model with a smaller diffusion coefficient. This stems from the fact that the diffusive flux contributes to the flux out of the channel. As the diffusion coefficient increases, the flux out of the channel also increases, decreasing the concentration of mAbs within the channel.

Increasing the permeability by a factor of 10 changes the fluid mechanics of the model, which in turn affects the concentration field. Increasing the flow through the membrane disrupts the previously parabolic velocity profile. Instead, the parabola begins to lean toward the membrane as more of the fluid streamlines pass through the membrane. Consequently, the velocity in the x-direction decreases by a larger amount across the length of the filter but remains at a higher value that the velocity in the previous filter. This occurs because the TMP doesn't have to be as high to push fluid though a more permeable membrane, increasing the overall velocity of the fluid compared to flow through a filter with a less permeable membrane.

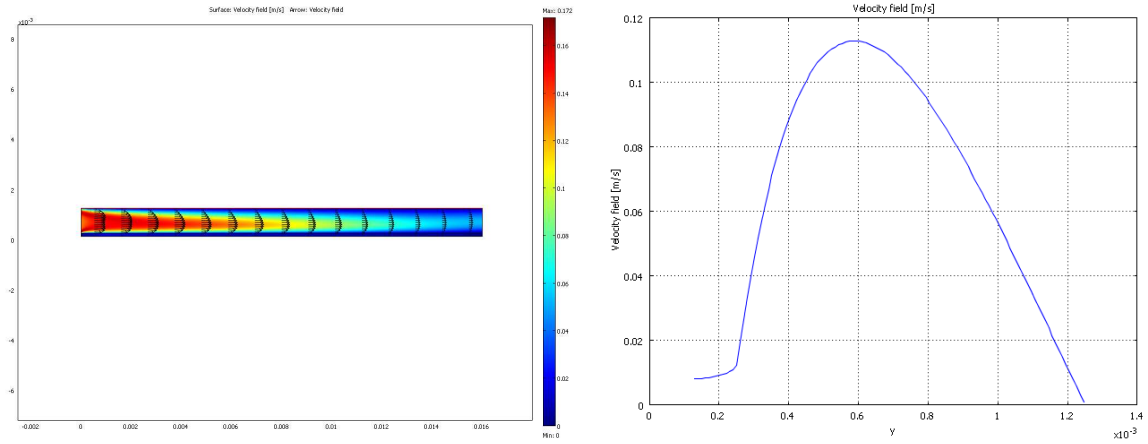

Figure 5-12: a) Velocity field and b) cross-sectional velocity for a membrane with a higher hydraulic permeability

As more fluid passes through the filter, the channel can no longer be modeled as fluid flow through parallel plates. Figures 5-14 (a) and (b) show that the pressure drop across the length of the channel is no longer linear. In fact, there is a steep drop in pressure within the initial 5% of the channel. This is probably due to the hydrodynamic entry length of the channel. After this, the pressure increases once again and then decreases once again in a nonlinear manner.

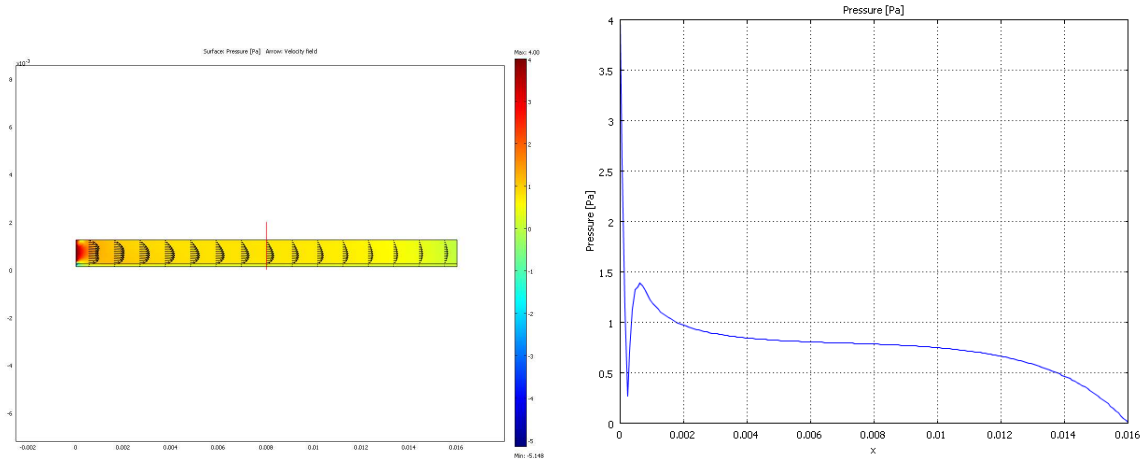

Figure 5-13: a) Surface Pressure and b) pressure drop across the length of a membrane with a lower permeability

As expected, Figures 5-15 (a) and (b) shows that the concentration increases to a higher value as the permeability increases. Resulting from an increased loss of fluid, the concentration increases to about 35 mol/m^3 at the outlet, after reach a maximum concentration of about 60 mol/m^3. Because the velocity of the fluid is higher compared to the less permeable case, the diffusive contribution to the total flux is lower. This causes there to be less diffusive spreading of the concentration with the channel and the concentration at the centerline of the channel is only influenced by the filtration process towards the outlet of the channel.

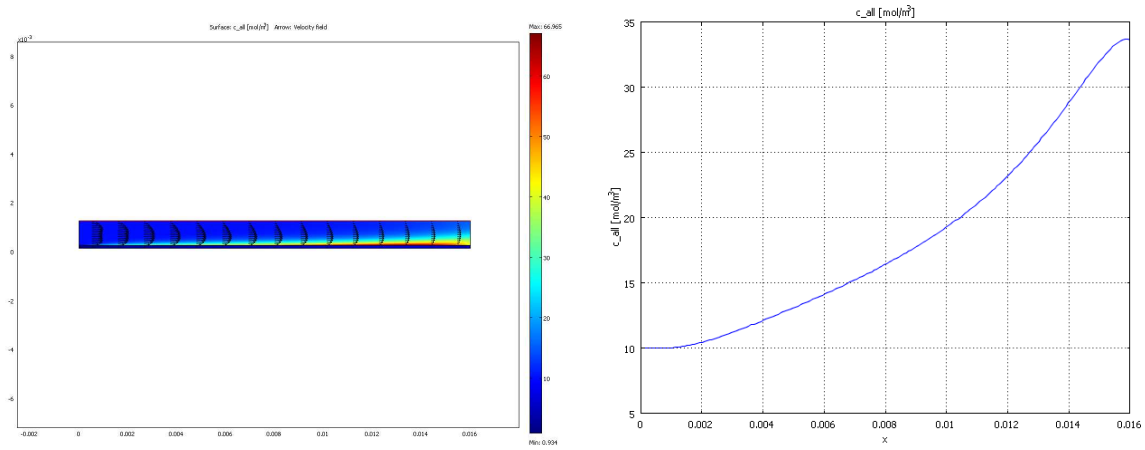

Figure 5-14: a) Surface Concentration. b) Line plot of the concentration across the length of the membrane with a lower permeability

As demonstrated here, using the COMSOL model, OptiFilt will be able to quickly and easily analyze the effects of varying different parameters affecting the efficiency of TFF. Although this was demonstrated for a simplified geometry and governing equations, these results are applicable to a wide range of other geometries, including those involving radial symmetry, and to complicated mechanics, such turbulent or Forchheimer flow.

Chapter 6:

Equipment and Instrumentation

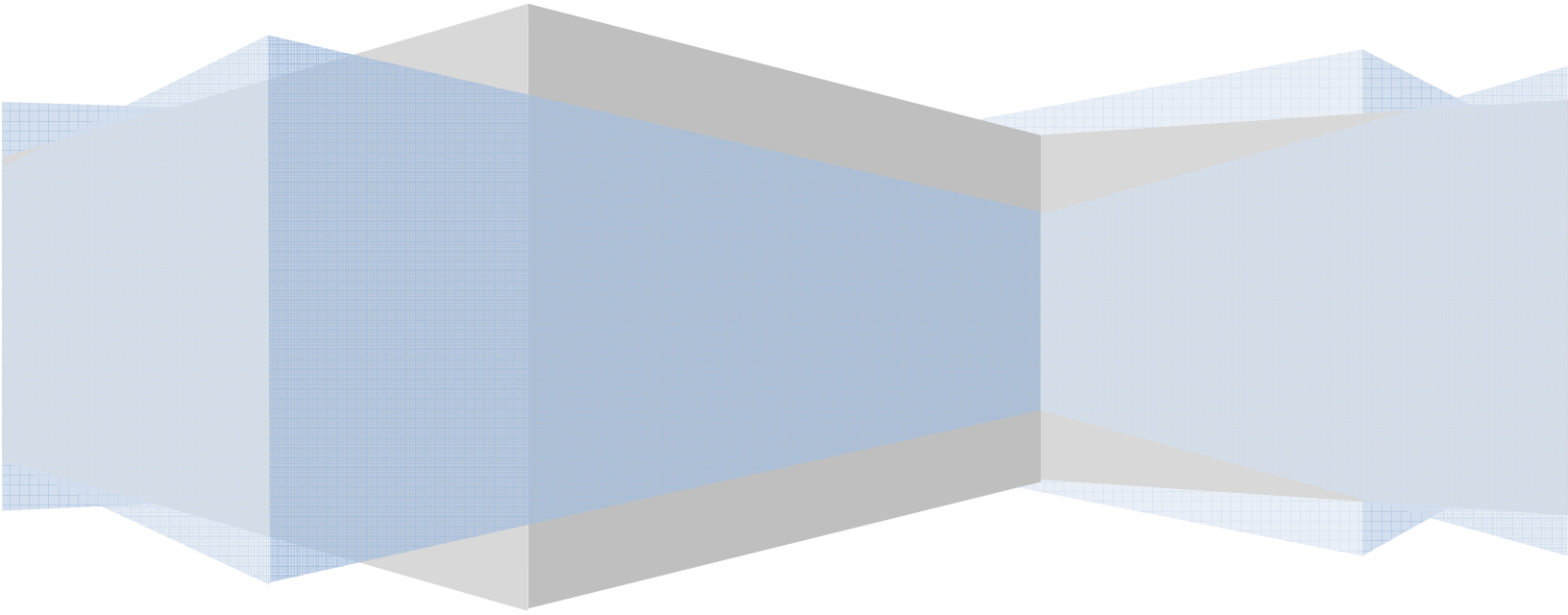

I. Test Rig Overview

As explained in Chapter 4, normal-flow fouling models compute K_c and K_d for client UF membranes by comparing experimental sieving coefficient data to that predicted by our proprietary MATLAB model. As such, the test rig equipment will need to collect C_f and C_r in real time; in this way, OptiFilt scientists will compute experimental □ and □' values for use in our computational models.

We have elected to purchase a simplified filter test rig, such as those commonly used by biotechnology clients today, and additional monitors which can be attached to the filters such that they will provide in-line, real-time measurements of C_f and C_r. We have selected refractometers to monitor these concentrations. The Pharma Refractometer PR-23-AC, purchased for $18,760 each from K-Patents, can be used in-line with a slow fluid stream and is appropriate for large biologic solutes (full product specifications are included in the Appendix).

We have selected this refractometer because it is accurate within a refractive index corresponding to 0.1% of the solute weight, thereby providing as accurate a measurement as possible of the protein concentration on either side of the test filter. It also meets pharmaceutical industry guidelines including the Food and Drug Administration's Code of Federal Regulations (CFR) and Good Manufacturing Practices (GMP).

For the test rig, we have selected the Filter Tec Plus Multi-Filter Capacity Testing system, purchased for $16, 795 each from SciLog Bioprocessing Systems (specifications are included in the Appendix). These systems can perform three normal-flow filtrations at once, at either constant fluid velocity or constant applied pressure, and parameters can vary from one filtration to another. Because we want to perform more than three filtration test at a time, we will purchase three of these systems and perform nine filtrations at once. In this way, our tests will

collect as much data as possible and our analyses will be more thorough than if three tests had been conducted.

Two refractometers are needed per individual test filter used—one for the filtrate side, and one for the retentate side. This means that a total of 18 refractometers are required for the OptiFilt filtration analysis system—six per three-filter Filter Tec testing system. Intuitively, this quantity of filters seems excessive; however, given the price we will charge per analysis, as well as the minimal inventory and rental costs we will incur, a relatively large investment in quality refractometers is reasonable (see Chapter 7: Financial Analysis).

Figure 6-1 illustrates a rough prototype of a single three-filter test rig. The protein solution to be filtered, which will be supplied by the client, will run through each of three individual filters. As filtration proceeds, refractometers will continuously measure the protein concentration in the filtrate and retentate side of the membranes. These real-time data will be supplied to workstations where experimental apparent sieving coefficients will be computed.

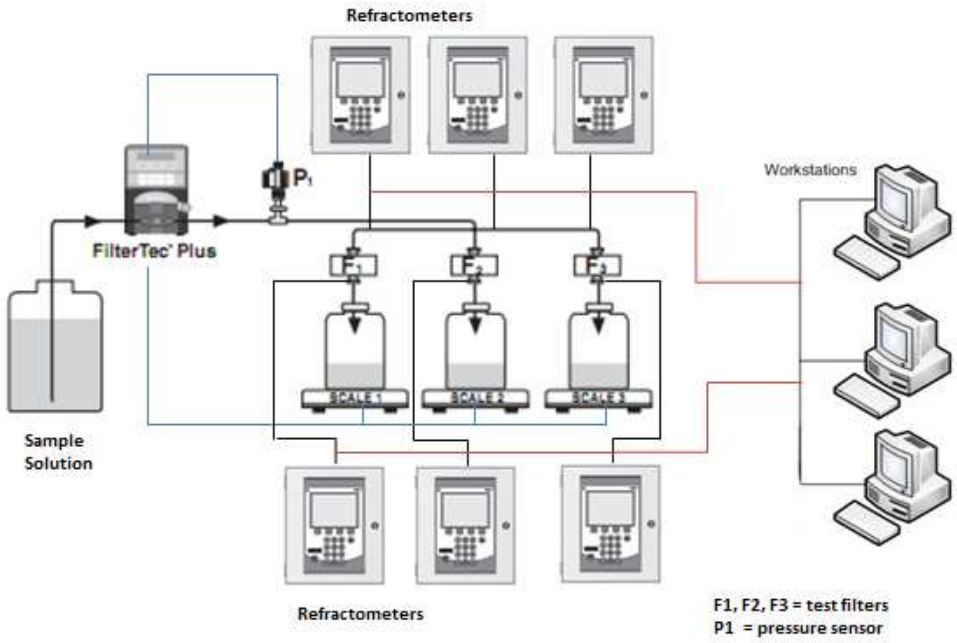

Figure 6-1: Prototype for a single three-filter test rig. Refractometers will collect concentration data in real time.

As explained previously, experimental apparent sieving coefficient will be used to calculate the intrinsic experimental sieving coefficient for the filtration process studied. These data will then be compared to proprietary MATLAB models; this comparison will allow OptiFilt scientists to determine K_c and K_d for the specific membrane used. Finally, these K_c and K_d values will be supplied to proprietary COMSOL models, which will predict industrial-scale filtration results for the filter, solution, and operating parameters used.

All computational aspects of the analysis will be performed on Inspiron 560s Desktop computers, purchased for $798 each from Dell. These computers were selected because they appropriately balanced cost and superior processing capabilities, which will be necessarily in order to efficiently run the MATLAB and COMSOL models.[4] Two PowerConnect 6224 Switches were purchased for $1,300 each from Dell to ensure that data can be properly shared across OptiFilt computers. In this way, physical filtration tests and computational analyses can be performed simultaneously, thereby increasing service throughput.

II. Test Filters

For all analyses performed, the filters themselves, like the protein solutions to be separated, will be supplied by clients. Generally, filter manufacturers produce small-scale test filters for this purpose; these filters are made of the same material as their industrial-scale counterparts. Obviously, these test filters will be UF membranes, because the proprietary MATLAB and COMSOL models described previously most appropriately apply to UF behavior. The Filter Tec Plus Multi-Filter Capacity Testing system can accommodate test filters ranging from 8.0 to 15.0 cm in diameter (as seen in the Appendix); these values are typical for test filters currently on the market.

[4] We have elected to purchase one desktop computer per OptiFilt employee. This means that seven computers will be purchased in the R&D stage, and three additional computers in the following year (see: Chapter 8, Financial Analysis).

III. Cleaning and Maintenance

In between runs, the test rig will be disinfected with 91% isopropyl alcohol, which can be purchased inexpensively from local retail pharmacies. WFI will be used to wash out the system following disinfection. To ensure that no remaining water will affect subsequent filtration tests, three Miniature Dessicant Air Dryers (one for each test rig system) will be purchased from Twin Tower Engineering for $599 each. Rigs will be dried thoroughly prior to each new filtration analysis begins. Throughout testing, pH will be maintained at levels appropriate for the protein products of interest. For the purpose of cost projections and financial analyses, we have selected a representative buffer kit to be kept in OptiFilt inventory. The kits, purchased from Invitrogen for $152 each, will contain 100 ml samples of buffer solution.

Biohazard waste will be stored in 1-gallon biohazard boxes, purchased form Stericycle for $152 each. Waste will be treated and removed monthly by Clean Harbors. Waste treatment services will be performed monthly at a cost of $800 per month.

IV. Space and Other Requirements

As previously explained, the Filter Tec Plus Multi-Filter Capacity Testing system is a bench-scale apparatus. All physical experiments and data collection will require no more space than the average desk. Of course, OptiFilt will require also space for its Dell desktop computers, as well as space in which scientists, computer scientists, and technicians can perform filtration analyses. The Company will also require a (likely adjacent) office space which management and sales representatives will use as their 'home base.' We estimate that the total space required will be 1,500 square feet.

In the (albeit small) laboratory space, care will be taken to maintain steady room temperatures and low humidity levels. We have provided for enough space to carefully store

disinfectants, WFIs, buffers, and other inventory items, as well as the client-supplied samples and test filters. Because of these requirements, we have estimated the rental cost of our laboratory space to be slightly higher than average Cambridge, MA rents (see: Chapter 7, Financial Analysis).

Chapter 7:

Financial Analysis

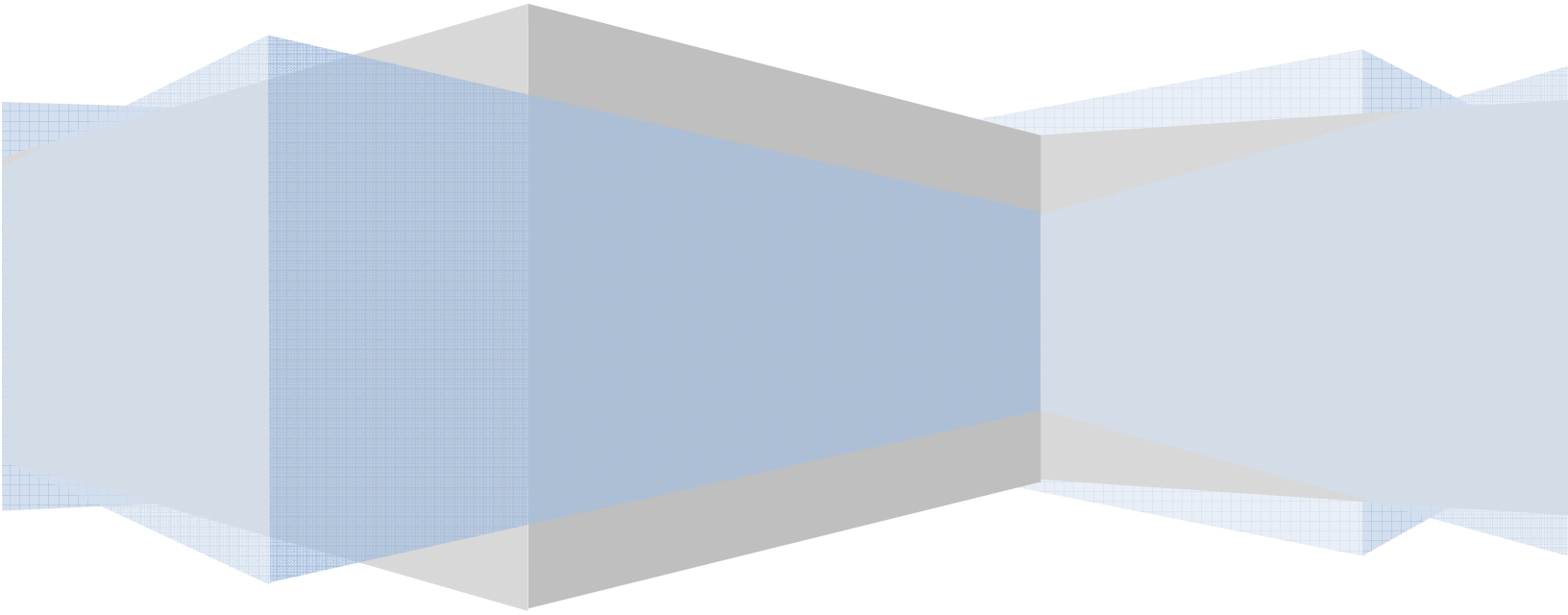

I. Market Analysis

As stated previously, OptiFilt will have a service-based, rather than product-based, business model: the Company will provide filtration testing and analysis services on a fee-per-service basis. A service-based model has a number of advantages over a product-based model (in which OptiFilt would sell its test rig instrumentation rather than actual analyses), including: a) clients will receive more rigorous analyses, conducted by scientists for whom filtration is a full-time job, and b) this service-based model will provide a recurring revenue stream as clients re-seek analysis services.

Before forecasting the Company's profitability, it is crucial to ensure that there exists a significant, well-funded and stable client base. In this case, OptiFilt's target clients are biotechnology companies which manufacture therapeutic proteins. Generally, these companies are producing proteins a) for immediate human or veterinary use, or b) for clinical trials of drugs seeking FDA approval. Regardless of their end-products, all client companies intend to maximize product throughput and minimize process time and consequently, operating costs.

OptiFilt has a large and growing group of potential clients. In the United States alone, there were 1,452 biotechnology companies in 2006, 336 of which were publicly traded [7-1]. In New England, in which OptiFilt will be located, there were 60 publicly traded biotechnology companies at this time [7-2]. Assuming that the portion of public companies is evenly distributed across the country, approximately 260 biotechnology companies (private or public) existed in New England as of 2006.

These biotechnology companies are increasingly profitable and well-funded. Between 1994 and 2006, the total number of U.S. biotechnology companies increased only 11%, from 1,311 to 1,452. In the same time period, however, total industry revenues skyrocketed from $11.2 billion

to $53.5 billion—a 378% increase. Furthermore, although investment in the industry dipped in the early 2000s, it has increased significantly since the 1990s. In 2007, total biotechnology financing was $24.8 billion—a 359% increase since 1998 [7-3].Existing biotechnology companies are becoming more profitable as they produce more new drugs and/or enjoy larger profit margins on existing products [7-4].

OptiFilt's success requires not only that client companies exist and are well-funded, but also that these companies are active, consistently developing new products or continuing to produce approved products. Despite significant R&D costs, the industry continues to be prolific. As of 2010, over 600 biologic drugs were in development by United States biotechnology companies [7-5], and over 200 therapeutic proteins and vaccines had been developed by these companies already [7-6]—in addition to hundreds of diagnostic, agricultural, and environmental products. Of the 600 products in development, 400 are in clinical trials [7-7]. There is also a growing market for biosimilars, or generic biologic drug products intended to mimic the therapeutic result of their brand-name counterparts. The biosimilars market is projected to reach $10 billion by 2017 [7-8].

Given the trends of the past decades, as well as the large number of biologic drugs currently in development, it is clear that the biotechnology industry fulfills OptiFilt's requirement of a sizable, well-funded, and stable client base. Even so, changes in the client industry are possible and could affect OptiFilt's future success. These changes are discussed in detail later in the following chapter (see Chapter 9: Scenario and Sensitivity Analyses).

II. Projected Quantities Sold

The first step in our financial analysis is to estimate how many services OptiFilt will provide at full capacity. The quantity of services sold will be restricted by the smaller of two potential limiting factors: a) OptiFilt's manufacturing capabilities, or b) projected demand for filtration analysis services by biotechnology clients.

It is the most logical to estimate client demand prior to estimating OptiFilt's capabilities. If client demand is low, there will be no need to project capabilities with doubled equipment, night shift workers, and other strategies meant to increase the supply of filtration analysis services.

Client demand is primarily dependent upon a) the number of biotechnology companies in the U.S. and in New England, b) how frequently these companies design new bioprocesses or reevaluate existing processes, and c) what portion of the existing biotechnology market OptiFilt successfully attracts.

As stated previously, there were 1,452 U.S. biotechnology companies as of 2006. Approximately 260 of these companies were located in New England. Due to the relatively slow growth rate in number of companies over the past two decades, as well as the recent macroeconomic recession, we will conservatively assume that an equal number of companies exist today.

It was also stated previously that as of 2006, there were over 200 therapeutic biologics available on the U.S. market, 400 biologics in clinical trials, and 600 biologics in any stage of development. Again, OptiFilt's analysis services will help client companies to reduce filtration time and consequently increase throughput. Biotechnology clients will therefore only be interested in these services if they are producing large quantities of biologic products. For this reason, we will consider relevant drug products to be those biologics which are either a)

currently produced for patient use, or b) currently undergoing clinical trials. For our purposes, then,

$$200\ marketed\ products + 400\ clinical\ trial\ products = 600\ 'relevant products,' \quad (7\text{-}1)$$

where 'relevant products' are those biologic drugs whose manufacturing processes may be improved by OptiFilt's services.

Intuitively, it seems unreasonable that there exist fewer biologic drug products in development than there are biotechnology companies. However, 'biotechnology companies' includes those companies involved in blood and plasma, diagnostic services, genetically modified foods, and other non-drug activities. Although some of these 'non-drug' companies do produce relevant protein products, it is clear from the company-product discrepancy that a large portion of total biotechnology companies are not relevant to OptiFilt. For this reason, we will base our quantity analysis on the number of 'relevant products' in the U.S., rather than the number of biotechnology companies.

Any biotechnologically-produced active ingredient will be produced and sold in a variety of formulations; these formulations have different dosages and inactive ingredients. Despite this fact, we are interested in improving the downstream manufacturing process of the active ingredient only; OptiFilt cannot help clients assemble their final drug products. For this reason, we make the conservative assumption here that each of the 600 relevant products has only one corresponding manufacturing process. Under these assumptions, 600 processes exist today which could benefit from OptiFilt's filtration analysis services.

To approximate future demand, we must estimate a) at what rate companies reevaluate existing processes, and b) at what rate the number of relevant processes will change. On the first point, by the suggestion of our advisor, Dr. Matthew Lazzara, we will assume that a

biotechnology client company will re-evaluate existing manufacturing processes each year. On the second, we note that biotechnology R&D processes are very slow, taking 10-15 years on average [7-9], and that only 132 new biologics were approved between 2000 and 2003 [7-10] despite the industry's highest-ever level of financing in 2000 [7-11]. Additionally, although the biosimilars market is expected to grow in the next decade, especially given its new FDA approval pathway created by the Patient Protection and Affordable Care Act of 2010, production of these drugs is nearly as slow as that of their brand-name counterparts. Unlike small-molecule generics, biosimilars can take up to a decade to develop [7-12]. The time required for new biologics to be produced, then, exceeds the period of study for this profitability analysis. For this reason, we conservatively assume here that the rate at which new 'relevant processes' are developed is equal to the rate at which current processes are discontinued. Hence the total number of relevant processes will be 600 for each year in this study.

OptiFilt's success hinges upon what portion of these relevant processes' parent companies will seek our filtration analysis services. Obviously, fraction depends not only on the quality of our service, but on how successfully we market the Company and seek new clients. Again, we assume there are 1,452 biotechnology companies in the U.S., 260 of which are in New England. Assuming that 'releveant processes' are evenly distributed across all biotechnology companies[5], approximately 18% of relevant processes (107 processes) will be New England-based.

When projecting our success rate in attracting clients, we note three observations. First, nearly all relevant processes already involve some type of filter integrity testing; our success hinges not on introducing a new step in the bioprocess, but on replacing clients' existing filter

[5] We are maintaining our assumption here that a large portion of these biotechnology companies have no relevant processes at all.

testing strategies. Second, in an attempt to cut costs and process times, U.S. biopharmaceutical companies are increasingly outsourcing parts of their research and manufacturing processes to small, specialized companies like OptiFilt. In fact, outsource spending in the industry grew 15% from 2001 to 2008 [7-13].

Finally, because OptiFilt's Cambridge, MA location is also a biotechnology hub, it makes sense for us to focus much of our marketing and sales efforts locally. In this way, we will access a large number of potential clients with minimal time and expense. A consequence of this strategy is that our success in attracting New England clients will be higher than that for other U.S. potential clients. For these reasons, we project that by the time we reach full capacity, we will have successfully attracted 35% of New England 'relevant processes' as clients and 20% of non-New England 'relevant processes' as clients. This means that at this time, the total demand for OptiFilt's services will be

$$0.35 \times 107 + 0.20 \times (600 - 107) \cong 136\ services/yr. \quad (7\text{-}2)$$

Of course, OptiFilt's success is contingent upon the accuracy of our projections here. Failure to attract this portion of potential clients will reduce company profits and investors' returns. This issue is discussed in the following chapter.

Before assuming that OptiFilt will provide 136 filtration analyses per year, we must confirm that this quantity is within our capabilitites at full-capacity. In an attempt to minimize equipment costs (see: Chapter 6), we will purchase only enough equipment to perform one filtration analysis at once. Each analysis takes a total of 12.8 hours and is comprised of the steps shown in Table 7-1. However, OptiFilt employees will be able to provide services at a rate greater than one service per 12.8 hours, because a) the longest step, *Code*, can be performed overnight without supervision, and b) only the *Prep, Run,* and *Clean* steps require the test rig

instrumentation. As a consequence, multiple samples can be analyzed at once, provided that the samples' *Prep, Run,* and/or *Clean* steps do not overlap.

Step	***Description***	***Time (hr)***
Prep	Set up test rig with client filters and samples	0.5
Run	Run test filtration and collect data	3.3
Code	Run MATLAB and COMSOL analyses	5.0
Analyze	Analyze COMSOL results and predict optimal filtration conditions	3.0
Clean	Clean and dry test rig	1.0
	Total	12.8

Table 7 - 1 Time requirements for one OptiFilt filtration analysis service.

A sample process schedule is given in Figure 1. Under this schedule, one sample (Sample 1) begins at t=0 hours on the first day. It is run through the test rig instrumentation, after which the rig is cleaned and a second sample is introduced at t=3.8 hours (because we have used generous time requirements in Table1, we are assuming that there is no lag or break time between steps). Sample 2's *Prep, Run,* and *Clean* steps are completed at t=9.6 hours. Simultaneously with Sample 2's test rig steps, the data from Sample 1's *Run* steps are run through MATLAB and COMSOL analyses, which are completed at t=8.8 hours on Day 1. If we assume a ten-hour workday, then by the end of Day 1, we will have COMSOL and MATLAB results for Sample 1 (from *Code*), and raw experimental data (from *Run*) for Sample 2.

As mentioned previously, the *Code* step can be run overnight without supervision. In this example, Sample 2 will undergo this step in the evening between Days 1 and 2. At the beginning of Day 2, then, both samples' analyses are only missing the final *Analysis* step. These steps take three hours each and are performed in succession, completing the analyses at t=6 on Day 2.

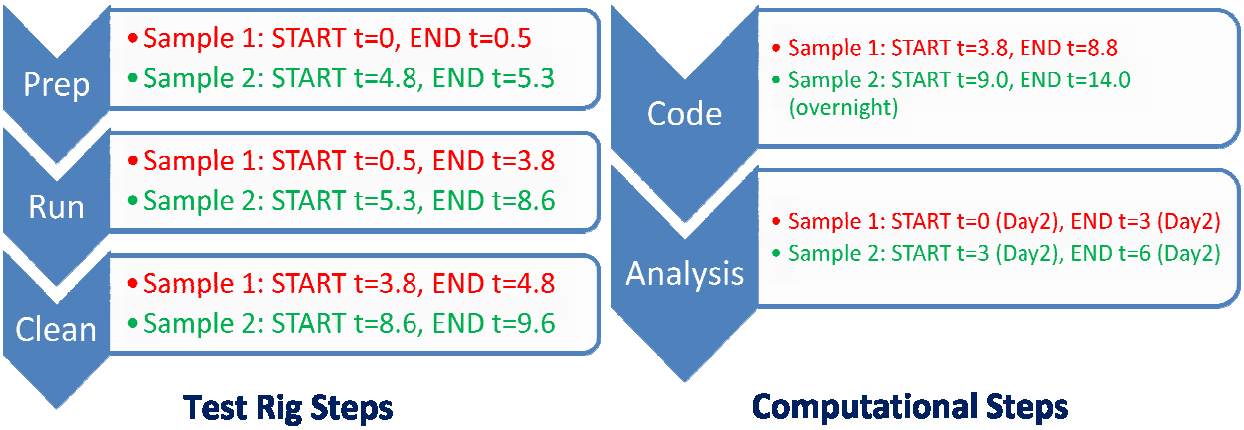

Figure 7 - 1 Proposed schedule for two OptiFilt filtration analysis services.

This example illustrates that with a ten-hour workday, OptiFilt will be able to perform two filtration analysis services in approximately 1.6 working days. Assuming that the Company operates 52 weeks out of the year, 5 days per week, the Company will have a total of 260 days in which to perform filtration analyses. In this timespan, OptiFilt will be able to perform a maximum of

(7-3)

which is much greater than the projected demand for these services. Consequently, client demand, not OptiFilt's capabilities, will be the limiting factor in determining what the quntity of services sold. For the remainder of this profitability analysis, we will assume that the Company will provide 136 services per year. The remainder of available operating time will be used for marketing, sales, and R&D as the company expands into new services (see: Chapter 9, Scenario and Sensitivity Analyses).

III. Pricing

When determining a price for one filtration analysis service, we are primarily concerned with how biotechnology companies value the service; in other words, we must estimate the price these clients are willing to pay. It is also important to determine which prices allow OptiFilt to remain profitable given its costs. However, this point will be ignored in this section, because a) if OptiFilt's price requirement is higher than what clients are willing to pay, clients will not purchase any services, and b) if OptiFilt's price requirement is lower than what clients are willing to pay, OptiFilt management would be foolish to price the service lower than what is warranted by client demand. By this logic, biotechnology clients' willingness to pay should be the sole determiner of OptiFilt's pricing strategy.

Clients' willingness to pay for filtration analysis services is determined by a number of factors. First, we consider clients' existing alternatives to OptiFilt's services. Next, we consider the advantages we can offer over these alternatives. Finally, we look at clients' typical budgets for outsourcing parts of their manufacturing processes to companies like OptiFilt.

Nearly all 'relevant processes' include some type of bench-scale filter testing. Generally, these tests are performed in-house using diagnostic instruments such as the FilterTec Plus Multi-Filter Capacity Testing rig, which OptiFilt will use in its analyses (see Chapter 7: Instrumentation). This particular system costs $17,808[6] and measures three filtrations in parallel; typically, similar instruments are priced within the $10,000 to $30,000 range [7-14].[7] These rigs are re-usable.

[6] The test rig itself costs $16,795; necessary accessories (sensors and software) bring the total system cost to $17,808. OptiFilt will not require these accessories because we will use refractometers to collect concentration data.
[7] Additional costs of in-house filter testing include the costs of test filters; however, these filters will be supplied by the clients in OptiFilt's analyses, and so they are ignored here.

Performing these tests in-house generally does not require large blocks of time; in the representative biopharmaceutical manufacturing process described earlier in this report, these tests took 15 minutes and were performed prior to each batch [7-15]. However, these tests cannot provide the detailed analysis that OptiFilt can provide its clients. The FilterTec System, for example, can measure filtrate weight and processed volume; however, it does not provide real-time data on solute concentration (and, consequently, intrinsic or apparent sieving coefficients)—thereby providing an incomplete picture of mass transfer conditions at the filter surface. By determining ΦK_c and ΦK_d values for a client-supplied filter material, OptiFilt will provide information about each filter which an in-house test cannot possibly provide.

Furthermore, these in-house tests generally have no realistic scale-up component; rather, they assume that test rig results accurately model industrial filter cartridges. As discussed earlier in this report, industrial filters involve complex geometries and fluid mechanics, and therefore are governed by a different mathematical model than are the test rig results. By taking a more realistic approach to this scale-up, OptiFilt will more accurately predict filtration results in industrial filter cartridges.

Finally, whereas in-house testing is typically performed by a technician with many competing laboratory duties, OptiFilt's analyses will be performed by scientists whose focus is filtration. We project that this expertise will translate superior data analysis and more innovative, successful solutions for our clients.

OptiFilt's analysis services will allow client companies to reduce filtration time and consequently increase product throughput. We project that our analysis will help clients reduce filtration times by 50%. Using the previously-defined representative mAb process as a benchmark, we then estimate that *OptiFilt Ultra* will save clients 727.5 minutes per batch,

increasing product throughput by 2.69 kg mAb per year. This additional production will add over $3,000,000 to clients' profits each year (see Table 7-2).

Old Process	**Total Processing Time**	**984**	**hours**
	UF Processing Time	1440	minutes
	Filter Integrity Testing Time	15	minutes
	Total 'Relevant' Time per Process	1455	minutes
	Potential Time Savings per Batch	**727.5**	**minutes**
New Process	New Capacity	39.6	batches/yr
	Old Capacity	39	batches/yr
	Net Gain	0.6	batches/yr
	Addl. Yearly Production	2.69	kg mAb/yr
	Addl. Yearly Revenues	**$ 3,030,241**	**$/yr**

Table 7 - 2 Potential time savings and additional yearly revenues for a typical biotechnology client using *OptiFilt* services.

The final piece of the pricing puzzle involves estimating client companies' budgets for outsourcing. According to PhRMA, it costs $1.2 billion to develop a biologic product from drug discovery through FDA approval [7-16]. As biopharmaceutical companies are pressured to cut costs, increasing portions of these R&D budgets are spent on outsourced services. For example, of the $51.8 billion spent on biopharmaceutical R&D in the U.S. in 2005, $6.6 billion on contract clinical trials services alone [7-17]. It is clear that potential biotechnology client companies recognize outsourcing as a means to increase productivity and cut costs, and therefore are likely willing to invest in contract services like those offered by OptiFilt.

Given the potential savings provided by our filtration analysis services, as well as client companies' large budgets for outsourced services, we find it reasonable to price our service at $150,000 per analysis. This price conservatively estimates what clients are willing to save, as it less than 50% of potential savings and 0.04% of the total cost to bring a biologic drug to market.

IV. Revenue Projections

For the purposes of this profitability analysis, we have split the study period into four stages: 1) R&D, 2) Scale-up, 3) Full Capacity, and 4) Terminal. The R&D stage is a 1-year period in which OptiFilt will finalize the test rig instrumentation and analysis procedure, and Company management will seek and obtain initial clients. The next three years comprise a Scale-up stage in which the Company increases its client base and builds capacity. For the purposes of this analysis, we assume that OptiFilt will add 25% of its full capacity each year until full capacity is reached. The following three years comprise the Full Capacity stage, in which OptiFilt is providing the full 136 services per year, but continues its R&D efforts in order to remain competitive. At the final Terminal stage, all initial investments have been recovered. At this point, management will either a) continue OptiFilt's operations, b) sell the Company, c) liquidate assets and dissolve the Company. A timeline of the study period is shown in Table 7-3.

Year	**2012**	**2013**	**2014**	**2015**	**2016**	**2017**	**2018**	**2019**
Stage Name	R&D	Scale-up	Scale-up	Scale-up	Full Capacity	Full Capacity	Full Capacity	Terminal
Design Capacity	0%	25%	50%	75%	100%	100%	100%	100%
Revenue	-	$5,101,875	$10,203,750	$15,305,625	$20,407,500	$20,407,500	$20,407,500	$20,407,500

Table 7 - 3 Revenue projections by stage.

V. Equipment and Recurring Costs

In order to project future profits, we must determine the Company's expenses at each year in the period of interest. OptiFilt's costs fall into five catetories: equipment, inventory, labor, rental, and sales and research costs. Equipment costs are one-time costs associated with the purchase of test rig instruments, as well as computers and software licenses. The majority of these costs are incurred at the beginning of the R&D period (2012), but three additional computers are

purchased in the following year as scale-up takes place and additional personnel are hired. Equipment costs are detailed in Table 7-4.

Equipment Costs				
R&D Stage:				
Item	*Cost*	*Qty*	*Tot. Cost*	Vendor
Filter Tec Plus Multi-Filter Capacity Testing	$ 16,795	3	$ 50,385	SciLog Bioprocessing Systems
COMSOL Multiphysics Named Single User License	$ 9,995	2	$ 19,990	COMSOL
MATLAB License	$ 2,100	2	$ 4,200	MathWorks
Microsoft Office Home & Business 2010	$ 280	1	$ 280	Microsoft
Inspiron 560s Desktop	$ 798	7	$ 5,586	Dell
PowerConnect 6224 Switch	$ 1,300	2	$ 2,600	Dell
Pharma Refractometer PR-23-AC	$ 18,760	6	$ 112,560	K-Patents
Miniature Desiccant Air Dryer	$ 599	3	$ 1,797	Twin Tower Engineering
Start of Sales Stage:				
Item	*Cost*	*Qty*	*Tot. Cost*	Vendor
Inspiron 560s Desktop	$ 798	3	$ 2,394	Dell

Table 7 - 4 Equipment costs.

Inventory costs are recurring costs associated with the purchase of non-durable goods, such as WFI, buffers, and disinfectant. Inventory costs are variable costs; that is, they increase with production. However, inventory costs are very small relative to the other four cost categories. For this reason, we can make the approximation that there are only two levels of inventory costs: the total cost at the R&D stage, and the total cost at the Scale-up, Full Capacity, and Terminal stages, which require approximately three times the materials that are required during 2012. (For simplicity, we here refer to the three later stages of the study period as the Sales stage). We are ignoring here the fact that capacity increases gradually throughout the Scale-up stage, and so inventory costs will actually increase throughout the Sales stage. Table 7-5 lists inventory costs for the R&D and Sales stages.

Inventory Costs					
R&D Stage:					
Item	*Cost*	*Units*	*Qty*	*Units*	*Total Cost*
WFI	$ 110.50	per 5 L bottle	12	bottles	$ 1,326.00
91% isopropyl alcohol	$ 2.99	per 32 oz. bottle	4	bottles	$ 11.96
Biohazard Box	$ 37.50	per box	4	boxes	$ 150.00
Buffer Kit	$ 152.00	per kit (100 ml samples)	1	kits	$ 152.00
Sales Stage:					
Item	*Cost*	*Units*	*Qty*	*Units*	*Total Cost*
WFI	$ 110.50	per 5 L bottle	36	bottles	$ 3,978.00
91% isopropyl alcohol	$ 2.99	per 32 oz. bottle	12	bottles	$ 35.88
Biohazard Box	$ 37.50	per box	12	boxes	$ 450.00
Buffer Kit	$ 152.00	per kit (100 ml samples)	3	kits	$ 456.00

Table 7 - 5 Inventory costs.

Labor costs are salaries paid to management, sales representatives, scientists, and technicians. During the first year of operation, OptiFilt will have a CEO (who will also serve as a sales representative), two senior scientists, two laboratory technicians, one computer scientist, and one filtration expert (a chemical engineer whose specialty is filtration and mass transfer). All employees' salaries are based on the average salaries for comparable positions in the Boston metropolitan area, as published by the U.S. Bureau of Labor Statistics[8]. Because top-notch scientists will be key to the OptiFilt's success, we have elected to pay our senior scientists and filtration expert at the higher end of this salary range. At the beginning of the Sales stage (2013), one additional filtration expert will be hired, as well as two sales representatives. Salaries paid in each stage are outlined in Table 7-6.

[8] We have elected to pay full salaries to management and senior scientists during the R&D stage rather than issue these personnel equity in OptiFilt. Doing so allows OptiFilt to offer the maximum equity share possible to angel investors in the R&D stage, thereby allowing us to attract as much funding as possible in these early stages.

Labor Costs			
R&D Stage:			
Personnel	*Salary*	*Qty*	*Tot. Cost*
CEO (also Sales)	$ 177,980	1	$ 177,980
Senior Scientists	$ 100,000	2	$ 200,000
Laboratory Technician	$ 60,000	2	$ 120,000
Computer Scientist	$ 89,070	1	$ 89,070
Filtration Expert	$ 100,000	1	$ 100,000
Sales Stage:			
Personnel	*Salary*	*Qty*	*Tot. Cost*
CEO	$ 177,980	1	$ 177,980
Senior Scientist	$ 100,000	2	$ 100,000
Laboratory Technician	$ 60,000	2	$ 60,000
Computer Scientists	$ 89,070	1	$ 89,070
Sales Representatives	$ 130,000	2	$ 130,000
Filtration Expert	$ 100,000	2	$ 100,000

Table 7 - 6 Labor costs.

Rental costs consist of rent and utilities for OptiFilt's Cambridge, MA office/lab space. These costs consist of a) the cost of physical space, b) utilities costs, which include electricity, Internet, and phone services, c) maintenance costs, and d) waste management services, which will be provided monthly by Clean Harbors Environmental Services. We assume here that all rental costs are constant throughout all stages of the study period. Table 7-7 lists these costs. Rent and utilities costs were estimated based upon average rental costs in the Cambridge area, and waste management costs are based upon Clean Harbor's monthly fees.

Rental Costs				
Space	*Cost/Sq. Ft/mo.*	*Sq. Ft*	*mo.yr*	*Tot.Cost*
Laboratory/Office	$ 20	1000	12	$ 240,000
Item	*Cost/mo.*	*mo./yr*	*Tot. Cost*	
Utilities	$ 6,000	12	$ 72,000	
Maintainence	$ 1,000	12	$ 12,000	
Waste Management	$ 800	12	$ 9,600	

Table 7 - 7 Rental costs.

Finally, sales and research costs are those costs associated with a) attracting new clients and b) updating our technology in order to remain competitive. Because these costs are an investment in the Company's future, we estimate sales and R&D costs to comprise 3% and 15%,

respectively, of OptiFilt's gross sales in the following fiscal year, which is comparable to sales budgets for other biotechnology startups [7-18]. Based on the revenue projections shown in Table 7-3, Sales and R&D costs are projected in Table 7-8.

Year	**2012**	**2013**	**2014**	**2015**	**2016**	**2017**	**2018**	**2019**
Stage Name	R&D	Scale-up	Scale-up	Scale-up	Full Capacity	Full Capacity	Full Capacity	Terminal
Design Capacity	0%	25%	50%	75%	100%	100%	100%	100%
Revenue	-	$5,101,875	$10,203,750	$15,305,625	$20,407,500	$20,407,500	$20,407,500	$20,407,500
Sales Costs	$153,056	$306,113	$459,169	$612,225	$612,225	$612,225	$612,225	$408,150
R&D Costs	$765,281	$1,530,563	$2,295,844	$3,061,125	$3,061,125	$3,061,125	$3,061,125	$2,040,750

Table 7 - 8 Sales and R&D costs.

VI. PPE and Depreciation

Depreciation and Property, Plant, and Equipment (PPE) changes must be computed in order to project OptiFilt's free cash flows. As is typical for the comparable equipment purchases, a 5-year MACRS depreciation schedule was used to maximize tax reductions early in the period of study. Depreciation for all equipment purchased is detailed in Table 7-9; PPE changes and the final net PPE for each fiscal year are also shown.

MACRS Tax Schedule	**20.00%**	**32.00%**	**19.20%**	**11.52%**	**11.52%**	**5.76%**		
Year	2012	2013	2014	2015	2016	2017	2018	2019
R&D Stage								
Equipment Total	$ 197,398							
Depreciation		$ (39,480)	$ (63,167)	$ (37,900)	$ (22,740)	$ (22,740)	$ (11,370)	
All Later Stages								
Equipment Total		$ 2,394						
Depreciation			$ (479)	$ (766)	$ (460)	$ (276)	$ (276)	$ (138)
Initial Net PPE	-	$ 197,398	$ 160,312	$ 96,666	$ 58,000	$ 34,800	$ 11,784	$ 138
Purchased (Sold)	$ 197,398	$ 2,394	-	-	-	-	-	-
Less: Total Dpcn	-	$ (39,480)	$ (63,646)	$ (38,666)	$ (23,200)	$ (23,016)	$ (11,646)	$ (138)
Final Net PPE	$ 197,398	$ 160,312	$ 96,666	$ 58,000	$ 34,800	$ 11,784	$ 138	$ (0)

Table 7 - 9 Depreciation schedule and net PPE.

VII. Income Statement

Table 7-10 shows a projected income statement for OptiFilt for the period of interest. Here, the 'cost of sales' includes any costs directly related to providing the filtration analysis services. These figures include equipment costs, inventory costs, and rental costs. In contrast, 'operating costs' include any costs that are not directly related to providing filtration analysis services; rather, these costs are incurred in selling, general, and administrative (SG&A) activities of OptiFilt. Operating costs include labor, sales, and R&D costs.

For each year in the study period, gross profit is calculated as the total revenue less the cost of sales. For the purpose of determining taxes, OptiFilt's pre-tax income equals this gross profit, less operating costs and depreciation. We have assumed here that federal, state, and local taxes combined will equal 40% of OptiFilt's pre-tax income. Net income, then, is the remaining 60% of pre-tax income after taxes have been paid.

Net income is negative in the study period's first year; consequently, by these accounting methods, OptiFilt receives a positive tax shied[9] from the government in this year. Although tax shields are not always provided in cases like this, we will assume here that OptiFilt will receive a tax shield when these negative earnings occur.

[9] A tax shield is essentially a 'negative tax'—in this example, the government pays OptiFilt its negative taxes as calculated on its income sheet, rather than OptiFilt paying taxes to the government.

	R&D			*Sales*				
Year	2012	2013	2014	2015	2016	2017	2018	2019
Revenue	-	$ 5,101,875	$ 10,203,750	$ 15,305,625	$ 20,407,500	$ 20,407,500	$ 20,407,500	$ 20,407,500
Cost of Sales	$ (688,638)	$ (496,914)	$ (494,520)	$ (494,520)	$ (494,520)	$ (494,520)	$ (494,520)	$ (494,520)
Gross Profit	$ (688,638)	$ 4,604,961	$ 9,709,230	$ 14,811,105	$ 19,912,980	$ 19,912,980	$ 19,912,980	$ 19,912,980
Operating Costs, SG&A	$ (1,605,388)	$ (2,493,725)	$ (3,412,063)	$ (4,330,400)	$ (4,330,400)	$ (4,330,400)	$ (4,330,400)	$ (4,330,400)
Depreciation	-	$ (39,480)	$ (63,646)	$ (38,666)	$ (23,200)	$ (23,016)	$ (11,646)	$ (138)
Pre-Tax Income	$ (2,294,025)	$ 2,071,757	$ 6,233,521	$ 10,442,039	$ 15,559,380	$ 15,559,564	$ 15,570,934	$ 15,582,442
Taxes (40%)	$ 917,610	$ (828,703)	$ (2,493,409)	$ (4,176,815)	$ (6,223,752)	$ (6,223,826)	$ (6,228,374)	$ (6,232,977)
Net Income	$ (1,376,415)	$ 1,243,054	$ 3,740,113	$ 6,265,223	$ 9,335,628	$ 9,335,738	$ 9,342,561	$ 9,349,465
Capacity	0%	25%	50%	75%	100%	100%	100%	100%
Margins								
Gross Margin	0.00%	90.26%	95.15%	96.77%	97.58%	97.58%	97.58%	97.58%
Profit Margin	0.00%	24.36%	36.65%	40.93%	45.75%	45.75%	45.78%	45.81%

Table 7 - 10 Projected income statement for OptiFilt.

IX. Working Capital

In order to correctly analyze free cash flow and investors' returns, we must adjust OptiFilt's income statement for cash items. Of primary interest here is working capital, the amount of capital OptiFilt will need to have on hand for its daily operations. Essentially, working capital is the portion of profits which is kept on hand as cash in order for the Company to operate.

We have assumed four types of working capital to be relevant here. First, accounts receivable (A/R) are those payments OptiFilt is owed by clients but has yet to receive. If we assume that clients will be required to pay within 30 days of contracting our services,

$$\frac{A}{R} = \frac{Revenue\ (\$)}{yr} \times \frac{1\ yr}{365\ days} \times 30\ days. \quad (7\text{-}4)$$

The higher A/R are, the more cash is owed OptiFilt; conversely, this implies that OptiFilt has less cash on hand. Therefore a positive A/R represents a decrease in working capital.

Second, inventory consists of the non-durable goods OptiFilt must purchase to provide filtration analysis services. As discussed previously, these items include WFI, buffers, and disinfectants. If we assume that inventory items are purchased every 30 days,

$$Inventory = \frac{Inventory\ Costs\ (\$)}{yr} \times \frac{1\ yr}{365\ days} \times 30\ days. \quad (7\text{-}5)$$

Higher inventory implies that OptiFilt has spent cash to purchase these items. Therefore, an increase in inventory represents a decrease in working capital.

Third, accounts payable (A/P) are bills owed by OptiFilt which have not yet been paid. These bills include rental, sales, and research costs. Assuming that OptiFilt pays its bills every 30 days,

$$\frac{A}{P} = \frac{(Rent + Sales\ Costs + R\&D\ Costs)(\$)}{yr} \times \frac{1\ yr}{365\ days} \times 30\ days. \quad (7\text{-}6)$$

Higher A/P implies that OptiFilt is holding more cash as it waits to pay its monthly bills. Therefore, an increase in A/P effectively increases working capital available to the Company.

Finally, cash reserves (C/R) consist of the cash kept on hand to pay salaries in the near future. Assuming that salary for one fiscal quarter (three months) is kept on hand,

$$C/R = \frac{Salary\ (\$)}{yr} \times \frac{1\ yr}{12\ mo.} \times 3\ mo. \quad (7\text{-}7)$$

An increase in C/R implies that OptiFilt is setting aside a larger portion of its cash to pay future salaries; reserving capital in this way effectively reduces working capital. Therefore, an increase in C/R represents a decrease in working capital.

Table 7-11 lists the change in each working capital component at each point in the study period, as well as the total working capital change. It is this total change which will allow us to determine free cash flows from OptiFilt's net income.

Year	**2012**	**2013**	**2014**	**2015**	**2016**	**2017**	**2018**	**2019**
Item								
A/R	-	$ 419,332	$ 838,664	$ 1,257,997	$ 1,677,329	$ 1,677,329	$ 1,677,329	$1,677,329
Inventory	$ 135	$ 404	$ 404	$ 404	$ 404	$ 404	$ 404	$ 404
A/P	$ 40,241	$ 40,241	$ 40,241	$ 40,241	$ 40,241	$ 40,241	$ 40,241	$ 40,241
Cash Reserve	$ 171,763	$ 164,263	$ 164,263	$ 164,263	$ 164,263	$ 164,263	$ 164,263	$ 164,263
WC Change								
(+)/- A/R	-	$ (419,332)	$ (419,332)	$ (419,332)	$ (419,332)	-	-	-
(+)/- Inventory	$ (135)	$ (270)	-	-	-	-	-	-
(-)/+ A/P	$ 40,241	-	-	-	-	-	-	-
(+)/- C/R	$ (171,763)	$ 7,500	-	-	-	-	-	-
Total WC Change	$ (131,656)	$ (412,102)	$ (419,332)	$ (419,332)	$ (419,332)	-	-	-

Table 7 - 11 Working capital changes by year.

X. Free Cash Flow

Unlike net income, free cash flows represent the actual cash received by those holding equity in OptiFilt. As mentioned previously, net income must be adjusted for cash items, such as working capital, in order to determine free cash flows. In this analysis, free cash flows are calculated as

$$free\ cash\ flows = (net\ income) + (\Delta\ working\ capital)$$
$$+ (\Delta PPE) + (equity\ issuances) \quad (7\text{-}8)$$

and are shown in Table 7-12 for each year in the study period.

As shown in Table 7-12, OptiFilt will issue stock twice in the study period: in 2012 and 2013. The earlier investors, hereafter referred to as 'research stage' investors, are angel investors who will provide the capital required for the costs of beginning the Company's R&D stage. Based on the costs incurred in this first stage of operation (see: Equipment and Recurring Costs), research stage investors will provide approximately $970,341 at EOY 2011. Because these investors are providing capital with minimal evidence of future sales, they will be granted a higher rate of return granted that the Company is successful.

In the following year, $1,000,000 in capital will be provided by a second group of investors, hereafter referred to as 'sales stage' investors. Sales stage investors are venture capitalists who will invest in OptiFilt upon evidence of a stronger, more versatile service prototype and client contracts. The $1,000,000 investment is again based upon equipment and operating costs, and will allow OptiFilt to operate until profits can cover all operating costs

Year	**2012**	**2013**	**2014**	**2015**	**2016**	**2017**	**2018**	**2019**
Net Income	$ (1,376,415)	$ 1,243,054	$ 3,740,113	$ 6,265,223	$ 9,335,628	$ 9,335,738	$ 9,342,561	$ 9,349,465
Cash Flow Statement								
Cash From Operating Activities								
Plus: Depreciation	-	$ 39,480	$ 63,646	$ 38,666	$ 23,200	$ 23,016	$ 11,646	$ 138
WC Change								
(+)/- A/R	-	$ (419,332)	$ (419,332)	$ (419,332)	$ (419,332)	-	-	-
(+)/- Inventory	$ (135)	$ (270)	-	-	-	-	-	-
(+)/- A/P	$ 40,241	-	-	-	-	-	-	-
(+)/- C/R	$ (171,763)	$ 7,500	-	-	-	-	-	-
Total WC Change	$ (131,656)	$ (412,102)	$ (419,332)	$ (419,332)	$ (419,332)	-	-	-
Cash From Investing Activities								
(Purchase)/Selling of Equipment	$ (197,398)	$ (2,394)	-	-	-	-	-	-
Cash From Financing Activities								
Issuance of Common Stock	$ 970,341	$ 1,000,000	-	-	-	-	-	-
Free Cash Flow	$ (735,129)	$ 1,868,038	$ 3,384,427	$ 5,884,557	$ 8,939,496	$ 9,358,754	$ 9,354,206	$ 9,349,603

Table 7 - 12 Projected free cash flows.

XII. Terminal Value

Net present value and rate of return analyses require that we project a theoretical terminal value for OptiFilt. The terminal value estimates the present value of all cash flows continuing past the study period (assuming that Company management decides to move forward with its operations rather than liquidate or sell the company). Terminal values are calculated using the perpetuity growth model, which assumes a constant growth rate *g* for OptiFilt moving forward and a discount rate *r*. OptiFilt's terminal value was determined using the formula

$$Terminal\ Value = Free\ Cash\ Flow\ \times \frac{(1+g)}{(r-g)}, \quad (7\text{-}9)$$

where *r* is the discount rate. We have assumed a discount rate of 25%, which is comparable to rates used in other biotechnology startups [7-19], and a conservative growth rate of 2%. For comparison, we have calculated the terminal value of OptiFilt at 25% and 30%; these results are shown in Tables 7-13 and 7-14, respectively.

XIII. NPV Valuation

The terminal value of OptiFilt is represented as the free cash flow value for the year following the end of the study period. This value allows us to create a more complete picture of OptiFilt's valuation by considering growth and profits that extend past the year 2019.

One method of valuing OptiFilt requires determining its net present value (NPV), or the present value of all future cash flows. The NPV is calculated by discounting the free cash flows at each year (including the terminal value) to their present value, and then summing these discounted cash flows to find the NPV. Obviously, the NPV is very sensitive to the discount rate used. As explained previously, we used a 25% discount rate for these analyses; these results are

shown in Table 7-13. For comparison, we also include an NPV analysis using a discount rate of 30%; these results are shown in Table 7-14.

It is important to note that in both Tables 7-13 and 7-14, the 2012 discount rate is 50% rather than 25 or 30%. This rate is higher because research stage (2011) investors, as noted previously, are making a riskier investment than sales stage investors. Consequently, research stage investors require a higher rate of return on their capital. The discount rate chosen for 2012 is comparable to similar discount rates for early-stage investments in biotechnology startups [7-20].

Also included in the NPV calculation are the present values of all investments made in OptiFilt. Under OptiFilt's planned financial structure, stock issuances sell partial ownership in the Company to angel and venture capital investors; therefore, the NPV decreases with stock issuances made. Research and sales stage investments are discounted to the year 2012 and included as negative values in the total NPV.

Year	**2011**	**2012**	**2013**	**2014**	**2015**	**2016**	**2017**	**2018**	**2019**	**Terminal Value**
T	0	1	2	3	4	5	6	7	8	9
Free Cash Flow	-	$ (735,129)	$ 1,868,038	$ 3,384,427	$ 5,884,557	$ 8,939,496	$ 9,358,754	$ 9,354,206	$ 9,349,603	$ 43,773,142
Discount Rate	0%	50%	25%	25%	25%	25%	25%	25%	25%	25%
PV	-	$ (490,086)	$ 1,195,544	$ 1,732,827	$ 2,410,315	$ 2,929,294	$ 2,453,341	$ 1,961,719	$ 1,568,603	$ 5,875,132
Investments	$ (970,341)	$ (1,000,000)								
Discount Rate	0%	25%								
PV	$ (970,341)	$ (800,000)								
NPV	$ 17,866,348									
Growth Rate	3%									

Table 7 - 13 NPV Analysis at 25% discount rate.

Year		**2011**	**2012**	**2013**	**2014**	**2015**	**2016**	**2017**	**2018**	**2019**	**Terminal Value**
T		0	1	2	3	4	5	6	7	8	9
Free Cash Flow		-	$ (735,129)	$ 1,868,038	$ 3,384,427	$ 5,884,557	$ 8,939,496	$ 9,358,754	$ 9,354,206	$ 9,349,603	$ 35,667,005
Discount Rate		0%	50%	30%	30%	30%	30%	30%	30%	30%	30%
PV		-	$ (490,086)	$ 1,105,348	$ 1,540,476	$ 2,060,347	$ 2,407,666	$ 1,938,911	$ 1,490,745	$ 1,146,163	$ 3,363,384
Investments	$ (970,341)		$ (1,000,000)								
Discount Rate	0%		30%								
PV	$ (970,341)		$ (769,231)								
NPV	$ 12,823,384										
Growth Rate		3%									

Table 7 - 14 NPV Analysis at 30% discount rate.

XIV. Financing

As mentioned previously, OptiFilt will obtain capital through two stock issuances: a 'research stage' issuance of $970, 341 at EOY 2011, and a 'sales stage' issuance of $1,000,000 at EOY 2012. Both investments will provide capital necessary to purchase equipment and inventory and pay rental fees, salaries, and sales and research expenses.

Research stage investors are angel group investors or early-stage venture capitalists. These investors will provide capital to OptiFilt with minimal evidence of future success; consequently, they are undertaking a relatively risky endeavor. To compensate investors for their risk, research stage investors will receive a higher rate of return than sales stage investors, assuming that OptiFilt is successful. Sales stage investors are venture capitalists who will provide the Company capital after the development of a strong service prototype and preliminary client list.

In determining the portion of OptiFilt owned by each stage of investors, we discount the sales stage investment to the present year. To account for the risk inherent in research stage investments, a discount rate of 50% was here; this valuable is comparable to other biotechnology startup rates [7-21]. Percentage ownership by each group of investors is outlined in Table 7-15.

	Investment	Discount Rate	FV Investment	Percentage
RSCH Stage Investors	$ 970,341	50%	$ 646,894	39.3%
Sales Stage Investors	$ 1,000,000		$ 1,000,000	60.7%
Total			$ 1,646,894	100.0%

Table 7 - 15 Percentage ownership by investor group.

Using these equity shares, we can estimate the dollar amount owned by each investor group at each year in the study period. For each group, this value equals OptiFilt's NPV at a particular year, multiplied by the fraction of the Company that is owned by that group. These equity percentages are outlined in Table 7-16.

Year	***2012***	***2013***	***2014***	***2015***	***2016***	***2017***	***2018***	***2019***	***Terminal***
Scientists	0.0%	0.0%	0.0%	0.0%	0.0%	0.0%	0.0%	0.0%	0.0%
RSCH Stage Investors	100.0%	39.3%	39.3%	39.3%	39.3%	39.3%	39.3%	39.3%	39.3%
Sales Stage Investors	0.0%	60.7%	60.7%	60.7%	60.7%	60.7%	60.7%	60.7%	60.7%
Total	100.0%	100.0%	100.0%	100.0%	100.0%	100.0%	100.0%	100.0%	100.0%
NPV @ 25%	$ (1,460,427)	$ (1,064,882)	$ 667,944	$ 3,078,259	$ 6,007,553	$ 8,460,894	$ 10,422,613	$ 11,991,217	$ 17,866,348
				Share Values v. Time					
Scientists	-	-	-	-	-	-	-	-	-
RSCH Stage Investors	$ (1,460,427)	$ (418,282)	$ 262,366	$ 1,209,129	$ 2,359,745	$ 3,323,408	$ 4,093,965	$ 4,710,106	$ 7,017,836
Sales Stage Investors	-	$ (646,601)	$ 405,578	$ 1,869,130	$ 3,647,808	$ 5,137,486	$ 6,328,649	$ 7,281,110	$ 10,848,512
Total	$ (1,460,427)	$ (1,064,882)	$ 667,944	$ 3,078,259	$ 6,007,553	$ 8,460,894	$ 10,422,613	$ 11,991,217	$ 17,866,348

Table 7 - 16 Equity percentages by investor group.

Investors' rates of return are determined via modified internal rate of return (MIRR) analysis. Although the internal rate of return (IRR) method is traditionally used to determine investors' returns, an IRR approach is inappropriate in this case. An IRR analysis assumes that all positive cash flows are reinvested at the IRR being calculated. In contrast, OptiFilt will not reinvest its positive cash flows; it only has two investment stages (at EOY 2011 and 2012). Therefore, an IRR analysis would exaggerate investors' returns in this case.

An MIRR analysis more conservatively determines OptiFilt's investors' returns. In order to calculate the MIRR, we must define a reinvestment rate, or the rate of return OptiFilt owners receive on positive cash flows, and a finance rate, or the rate that OptiFilt will owe its creditors in the event that negative cash flows are generated. We have assumed a reinvestment rate of 0.15%, which as of April 1, 2011 was the current yield on a six month United States Treasury bill [7-22]; we assumed that our finance rate equals the prime loan interest rate of 3.25% [7-23].[10]

Table 7-17 details this MIRR analysis for OptiFilt. According to the previously calculated equity percentages, free cash flows for each year in the study period are appropriated to research and sales stage investor groups. The MIRR(…) function in Microsoft Excel was then used to determine the MIRR each investor groups' MIRRs. We project that research stage investors will receive an MIRR of 41%, while sales stage investors will receive 56%.

Finally, a pro forma income statement is shown in Table 7-18, which includes the previously computed free cash flows, NPV, and MIRRs. Also included are the projected terminal values of OptiFilt for discount rates of 25 and 30%.

[10] The reinvestment rate chosen here is the risk-free rate, or the rate of return on an investment with negligible risk. Obviously, biotechnology startups like OptiFilt are inherently riskier than U.S. Treasury bills, and so a higher reinvestment rate is possible here. We have elected to remain conservative in our profitability analysis and use the risk-free rate regardless of the riskiness of this venture.

Year		***2012***	***2013***	***2014***	***2015***	***2016***	***2017***	***2018***	***2019***	***Terminal***
Free Cash Flows		$ (735,129)	$ 1,868,038	$ 3,384,427	$ 5,884,557	$ 8,939,496	$ 9,358,754	$ 9,354,206	$ 9,349,603	$ 43,773,142
Equity Percentage										
RSCH Stage Investors		100.0%	39.3%	39.3%	39.3%	39.3%	39.3%	39.3%	39.3%	39.3%
Sales Stage Investors		0.0%	60.7%	60.7%	60.7%	60.7%	60.7%	60.7%	60.7%	60.7%
	Investment					*Divided Free Cash Flows*				
Cash Flows										
RSCH Stage	$ (970,341)	$ (735,129)	$ 733,758	$ 1,329,391	$ 2,311,433	$ 3,511,401	$ 3,676,085	$ 3,674,298	$ 3,672,490	$ 17,193,931
Sales Stage	$ (1,000,000)	-	$ 1,134,279	$ 2,055,036	$ 3,573,125	$ 5,428,094	$ 5,682,670	$ 5,679,908	$ 5,677,113	$ 26,579,212
RSCH Stage MIRR	41%									
Sales Stage MIRR	56%									
Finance Rate	3.25%									
Reinvestment Rate	0.50%									
Terminal Value (25%)	$ 43,773,142									
Terminal Value (30%)	$ 35,667,005									

Table 7 - 17 MIRR Analysis at 25% discount rate, 3.25% finance rate, and 0.50% reinvestment rat

Year	2012	2013	2014	2015	2016	2017	2018	2019
Income Statement								
Revenue	-	$ 5,101,875	$ 10,203,750	$ 15,305,625	$ 20,407,500	$ 20,407,500	$ 20,407,500	$ 20,407,500
Cost of Sales	$ (688,638)	$ (496,914)	$ (494,520)	$ (494,520)	$ (494,520)	$ (494,520)	$ (494,520)	$ (494,520)
Operating Costs, SG&A	$ (1,605,388)	$ (2,493,725)	$ (3,412,063)	$ (4,330,400)	$ (4,330,400)	$ (4,330,400)	$ (4,330,400)	$ (4,330,400)
Depreciation	-	$ (39,480)	$ (63,646)	$ (38,666)	$ (23,200)	$ (23,016)	$ (11,646)	$ (138)
Pre-Tax Income	$ (2,294,025)	$ 2,071,757	$ 6,233,21	$ 10,442,039	$ 15,559,380	$ 15,559,564	$ 15,570,934	$ 15,582,442
Taxes (40%)	$ 917,610	$ (828,703)	$ (2,493,409)	$ (4,176,815)	$ (6,223,752)	$ (6,223,826)	$ (6,228,374)	$ (6,232,977)
Net Income								
Cash Flow Statement								
Cash from Operating Activities								
Plus: Depreciation	-	$ 39,480	$ 63,646	$ 38,666	$ 23,200	$ 23,016	$ 11,646	$ 138
WC Change								
(+)/- A/R	-	$ (419,332)	$ (419,332)	$ (419,332)	$ (419,332)	-	-	-
(+)/- Inventory	$ (135)	$ (270)	-	-	-	-	-	-
(+)/- A/P	$ 40,241	-	-	-	-	-	-	-
(+)/- C/R	$ (171,763)	$ 7,500	-	-	-	-	-	-
Total WC Change	$ (131,656)	$ (412,102)	$ (419,332)	$ (419,332)	$ (419,332)	-	-	-
Cash From Investing Activities								
(Purchase)/Selling of Equipment	$ (197,398)	$ (2,394)	-	-	-	-	-	-
Cash From Financing Activities								
Issuance of Common Stock	$ 970,341	$ 1,000,000	-	-	-	-	-	-
Free Cash Flow	$ (735,129)	$ 1,868,038	$ 3,384,427	$ 5,884,557	$ 8,939,496	$ 9,358,754	$ 9,354,206	$ 9,349,603
% Design Capacity	0%	25%	50%	75%	100%	100%	100%	100%
	Investment				*Divided Free Cash Flows*			
RSCH Stage Investors (39.3% Equity)	$ (970,341)	$ (735,129)	$ 733,758	$ 1,329,391	$ 2,311,433	$ 3,511,401	$ 3,676,085	$ 3,674,298
Sales Stage Investors (60.7% Equity)	$ (1,000,000)	-	$ 1,134,279	$ 2,055,036	$ 3,573,125	$ 5,428,094	$ 5,682,670	$ 5,679,908
NPV at 25%	$ 17,866,348							
NPV at 30%	$ 12,823,384							

Table 7 - 18 Projected pro forma for OptiFilt.

Chapter 8:

Scenario and Sensitivity Analyses

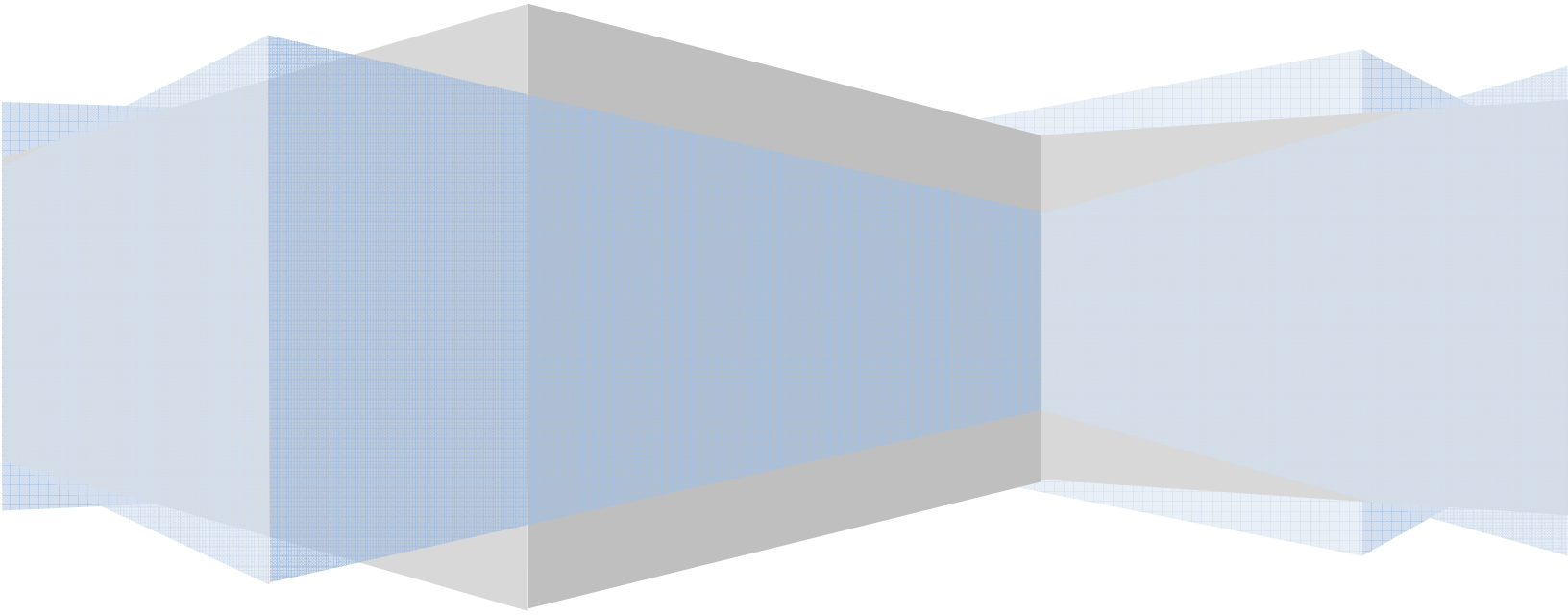

I. Scenario Analysis

Previous financial analyses have made a number of assumptions about OptiFilt's operations, sales, and market. Inaccuracies in these assumptions will in turn lead to faulty NPV and MIRR projections. In an attempt to avoid these errors, we will present financial projections for several possible scenarios. These scenarios range from the optimistic 'best-case' possibilities to the pessimistic 'worst-case possibilities.' Scenarios studied are summarized in Table 8-1.

R&D	R1	R&D Stage takes one year.
	R2	R&D Stage takes two years.
Quantities Sold	Q1	Capacity builds in 25% increments to 185 services/yr.
	Q2	Capacity builds in 25% increments to 136 services/yr, as planned.
	Q3	Capacity builds in 25% increments to 101 services/yr.
Competition	C1	Company maintains market superiority throughout the study period, as planned.
	C2	Successful competitors arise at the terminal stage; Company forced to halve prices.
	C3	Successful competitors knock out the Company at the terminal stage; sales reach zero.
Growth	G1	Company grows at 3% annually, as planned.
	G2	Company size remains constant after the end of the study period.
	G3	Company is dissolved or sold at the end of the study period.

Table 8 - 1 Scenarios considered.

Scenarios of interest fall into four categories: R&D, quantities sold, competition, and company growth. First, previous analyses have assumed that the R&D stage take only one year, 2012, after which OptiFilt will begin providing services to clients. It is possible that scientists will need more than one year to develop perfect the ComanyX filtration analysis service. This scenario, labeled R2 in Table 8-1, accounts for the possibility of the R&D stage taking two years rather than one. In this case, sales would begin in the year 2014 rather than 2013.

Second, in determining the quantity of services sold at full capacity, we have assumed that we attract 35% of all New England 'relevant process' clients (see: Chapter 7, Financial Analysis) and 20% of all 'relevant process' clients elsewhere in the U.S. It is possible that the Company sales team will be more or less successful in attracting clients. Scenarios Q1 through

Q3 range from the most optimistic to the most pessimistic of these possibilities. In case Q1, OptiFilt management is able to attract 35% of New England processes and also 30% of non-New England processes; full capacity in this case is 185 services per year. Case Q2 is the base case assumed in previous analyses. Finally, case Q3 assumes that management attracts only 25% of New England clients, and 15% of non-New England Clients; full capacity in this case is 101 services per year.[11]

Third, previous analyses have assumed that the Company will sell at the same price after the study period ends. It is possible that competitors will arise, thereby either a) forcing OptiFilt to lower its price per service, or b) force OptiFilt out of business altogether. Cases C1 through C3 cover these scenarios. Case C1 is the case previously assumed, in which minimal competition arises and OptiFilt is able to maintain its setpoint prices. In case C2, competitors successfully enter the filtration analysis market, and OptiFilt is forced to halve its prices at the terminal stage. Case C3 is the worst-case scenario, in which competitors drive OptiFilt out of the market altogether, and sales stop at the terminal stage.

Finally, previously calculated terminal values are dependent upon the assumed growth rate past the study period. Case G1 in Table 8-1 is the base case previously assumed, in which OptiFilt grows at a rate of 5% after the study period ends. Case G2 assumes a zero percent growth rate; that is, OptiFilt achieves essentially the same cash flows after the study period ends. In case G3, the Company is dissolved or sold at the end of the study period. Note that cases C3 and G3 are essentially the same; for this reason, only case C3 will be included in subsequent analyses.

[11] In the base case analyses performed previously (see: Quantities Sold), OptiFilt had the means to produce more than twice the analyses that client demand warranted. For this reason, scenarios Q1 through Q3 are all possible given the speed at which the Company can provide filtration analysis services.

Profitability analyses were performed for every combination of the previously defined scenarios. NPVs were determined at discount rates of 25 and 30%, and the MIRR was determined for research and sales stage investors. Results are summarized in Table 8-2.

						MIRR	
R&D	Quantity	Competition	Growth	NPV (25%)	NPV (30%)	RSCH Stage	Sales Stage
R1	Q1	C1	G1	$ 25,516,587	$ 18,507,527	44.19%	62.13%
			G2	$ 24,330,397	$ 17,919,001	43.06%	60.84%
		C2	G1	$ 18,888,595	$ 14,492,171	37.02%	53.99%
			G2	$ 18,464,244	$ 14,281,630	36.42%	53.31%
		C3	G1	$ 12,260,604	$ 10,476,816	11.51%	10.63%
			G2	$ 12,598,090	$ 10,644,259	12.71%	12.08%
	Q2	C1	G1	$ 17,858,534	$ 12,817,578	40.72%	56.34%
			G2	$ 17,003,270	$ 12,393,241	39.61%	55.09%
		C2	G1	$ 12,986,064	$ 9,865,749	33.54%	48.29%
			G2	$ 12,690,854	$ 9,719,281	32.97%	47.64%
		C3	G1	$ 8,113,595	$ 6,913,920	10.05%	9.32%
			G2	$ 8,378,439	$ 7,045,322	11.19%	10.73%
	Q3	C1	G1	$ 12,388,496	$ 8,753,329	37.03%	50.80%
			G2	$ 11,769,608	$ 8,446,269	35.95%	49.60%
		C2	G1	$ 8,769,971	$ 6,561,162	29.81%	42.78%
			G2	$ 8,567,005	$ 6,460,461	29.27%	42.18%
		C3	G1	$ 5,151,446	$ 4,368,995	8.32%	7.76%
			G2	$ 5,364,402	$ 4,474,653	9.40%	9.11%
R2	Q1	C1	G1	$ 20,764,974	$ 14,215,614	34.89%	63.73%
			G2	$ 19,510,223	$ 13,593,073	33.70%	62.27%
		C2	G1	$ 14,136,982	$ 10,200,259	27.72%	54.96%
			G2	$ 13,644,070	$ 9,955,702	27.00%	54.08%
		C3	G1	$ 7,508,990	$ 6,184,903	8.62%	10.60%
			G2	$ 7,777,916	$ 6,318,330	9.52%	12.04%
	Q2	C1	G1	$ 14,373,920	$ 9,673,285	31.22%	57.89%
			G2	$ 13,468,256	$ 9,223,942	30.06%	56.49%
		C2	G1	$ 9,501,450	$ 6,721,457	24.07%	49.23%
			G2	$ 9,155,840	$ 6,549,983	23.38%	48.39%
		C3	G1	$ 4,628,981	$ 3,769,628	6.67%	9.11%
			G2	$ 4,843,425	$ 3,876,024	7.51%	10.50%
	Q3	C1	G1	$ 9,808,882	$ 6,428,765	27.43%	52.33%
			G2	$ 9,152,565	$ 6,103,135	26.31%	50.97%
		C2	G1	$ 6,190,356	$ 4,236,598	20.26%	43.69%
			G2	$ 5,949,963	$ 4,117,327	19.61%	42.91%
		C3	G1	$ 2,571,831	$ 2,044,431	4.47%	7.35%
			G2	$ 2,747,360	$ 2,131,519	5.24%	8.69%

Table 8 - 2 NPV and MIRR calculations for the 36 scenarios considered.

The resultant best-case, mid-range, and worst-case NPV and MIRR results are shown in Table 8-3. The best-case values are an average of the three most optimistic projections for NPV

and MIRR; similarly, the worst-case values are an average of the three most pessimistic projections.

	Best-Case	Mid-Range	Worst-Case
NPV (25%)	$ 23,537,319	$ 10,789,245	$ 3,316,057
NPV (30%)	$ 16,880,714	$ 7,437,517	$ 2,648,526
MIRR - RSCH	40.71%	31.69%	5.46%
MIRR - Sales	62.24%	50.97%	8.38%

Table 8 - 3 Best-case, mid-range, and worst-case NPV and MIRR results.

As stated previously, it is a Company goal to compensate investors for their risk by achieving MIRRs of at least 50% for research stage investors, and 30% for sales stage investors (see: Chapter 7, Financial Analysis). As indicated in Table 8-3, this goal is achieved in all but the worst-case scenario. Pro forma for each of the 36 scenarios studied are included in the Appendix.

II. Sensitivity Analyses

The aforementioned scenarios study the potential impact of incorrectly forecasted R&D time, quantities sold, competition, or growth. However, all these cases assume a target price of $150,000 per filtration analysis service. Furthermore, the cases assume a study period (and company life) of eight years, ending in 2019. It is possible that competition will arise and challenge OptiFilt earlier than cases C1 through C3, summarized previously, predict. In this case, OptiFilt may dissolve or be sold earlier than 2019. Sensitivity analyses were performed to determine the impact of a) price point and b) company life on the profitability of the Company.

For the price sensitivity analysis, we determined NPV (at a 25% discount rate) and MIRR analyses at ten potential prices for a single filtration analysis service. These analyses were performed for the best-case, mid-range, and worst-case scenarios determined in the previous section. We have included the base price chosen previously (see: Pricing), as well as prices

above and below that value. Results are shown in Table 8-4, along with breakeven prices for the best-case, mid-range, and worst-case scenarios.

	NPV (25%)			MIRR - Research Stage			MIRR - Sales Stage		
Price/Service	Best	Mid-Range	Worst	Best	Mid-Range	Worst	Best	Mid-Range	Worst
$ 150,000	$23,537,319	$ 11,769,608	$ 2,747,360	0.43%	35.95%	5.24%	62.24%	49.60%	8.69%
$ 140,000	$ 23,268,308	$ 11,189,764	$ 2,344,117	43.09%	35.83%	4.67%	60.42%	49.19%	8.22%
$ 130,000	$ 22,206,219	$ 10,609,921	$ 1,940,874	43.12%	35.70%	4.04%	59.98%	48.76%	7.69%
$ 120,000	$ 21,144,130	$ 10,030,078	$ 1,537,631	43.15%	35.56%	3.33%	59.54%	48.33%	7.09%
$ 110,000	$ 20,082,041	$ 9,450,235	$ 1,134,388	43.19%	35.42%	2.54%	59.08%	47.89%	6.42%
$ 100,000	$ 19,019,952	$ 8,870,391	$ 731,145	43.23%	35.28%	1.64%	58.62%	47.43%	5.64%
$ 90,000	$ 17,957,863	$ 8,290,548	$ 327,902	43.27%	35.12%	0.60%	58.14%	46.96%	4.72%
$ 80,000	$ 16,895,773	$ 7,710,705	$ (75,341)	43.31%	34.96%	-0.61%	57.66%	46.48%	3.64%
$ 70,000	$ 15,833,684	$ 7,130,862	$ (478,584)	43.35%	34.79%	-2.04%	57.15%	45.99%	2.33%
$ 60,000	$ 14,771,595	$ 6,551,019	$ (881,827)	43.40%	34.61%	-3.80%	56.64%	45.49%	0.70%
$ 50,000	$ 13,709,506	$ 5,971,175	$ (1,285,070)	43.45%	34.43%	-6.03%	56.11%	44.97%	-1.41%
Breakeven Price	< $50,000	< $50,000	$ 81,868						

Table 8 - 4 Price sensitivity analysis for best-case, mid-range, and worst-case scenarios.

For the mid-range scenario, OptiFilt's breakeven price was lower than the $50,000 lower limit, well below our previously determined $150,000 price point. For the worst-case scenario, OptiFilt breaks even at a price of $81,868, which is still comfortably below the previously determined price point. These results confirm that OptiFilt can comfortably charge clients $150,000 per filtration analysis service—this value is well above the value required for the Company to remain profitable. Additionally, at this price point, our MIRR goals are achieved for each investor group. From a demand viewpoint, this value is also reasonable considering the added profits clients will enjoy as a result of our services (see: Chapter 7, Financial Analysis).

At the same time, however, the Company might consider lowering its price point in an attempt to expand its consumer base or remain profitable in the midst of competitors. Because OptiFilt's price point is comfortably above breakeven points for even the worst-case scenario, these results confirm that the Company can elect to reduce its price point and remain profitable, given that the new price point is far enough from the break-even point to maintain acceptable profits.

With $150,000 confirmed as the price for one filtration analysis service, we examine the effects of a shortened company life. As explained previously, unforeseen competition can rise quickly and force OptiFilt out of business before the end of the previously established study period, 2019. Such rapid innovation from competitors is unlikely because the OptiFilt computational models will be proprietary and therefore protected by intellectual property laws. Even so, given the rapid growth and innovation present in the U.S. biotechnology industry, it is prudent to prepare for a potential early termination of company life.

NPV and MIRR analyses were performed using a service price of $150,000 for three early termination scenarios: these cases have OptiFilt dissolving after two, four, and six years of sales (at EOY 2014, 2016, and 2018, respectively). For comparison, the base case (in which the terminal stage begins at EOY 2019 is also included. Results are shown in Table 8.5. In each early termination scenario, the scale-up schedule was kept constant; that is, if the company dissolves at EOY 2014, 2014 capacity is the same as in the base case.

		NPV (25%)			***MIRR - Research Stage***			***MIRR - Sales Stage***		
	Years of Sales	*Best*	*Mid-Range*	*Worst*	*Best*	*Mid-Range*	*Worst*	*Best*	*Mid-Range*	*Worst*
	2	$ 4,812,652	$ 1,113,974	$ (3,388,171)	16.14%	6.67%	-15.91%	30.40%	17.15%	-14.48%
	4	$ 5,339,538	$ 1,401,625	$ 1,102,187	2.56%	-0.46%	0.46%	1.59%	-1.16%	3.45%
	6	$ 12,598,090	$ 5,364,402	-	12.71%	9.40%	-	12.08%	9.11%	-
	Base Case	$ 23,537,319	$ 10,789,245	$ 3,316,057	40.71%	31.69%	5.46%	62.24%	50.97%	8.38%
Breakeven		< 2 years	< 2 years	3 years						

Table 8 - 5 Early termination effects. Note that the worst-case scenario has a maximum company life of five years, and so the six-year case does not apply in this scenario.

For the mid-range case, the Company breaks even within the first two years of sales, assuming that capacities in each year are the same as those projected in the base case. After two years of sales at most, OptiFilt can dissolve without losing investors' money.[12] The Company, then, only needs to operate into 2014 to prevent a loss on initial investments. For this reason, the

[12] Although no money is lost at the breakeven point, neither group of investors will receive their desired rates of return. Even so, this analysis is a 'worst-case' safeguard against loss rather than a profitability analysis. The goal here is to determine the vulnerability of the Company to financial loss.

early termination analysis assures us that OptiFilt is generally well-protected against this type of financial loss, assuming that the Company operates at least as favorably as the mid-range scenario predicts.

In the event of worst-case operations, the Company will need to operate for approximately three years in order to avoid losing investors' money. Again, because OptiFilt's models are proprietary, it will be very difficult for competitors to force OptiFilt out of business within this short period of time. For this reason, it is unlikely even in this worst case that OptiFilt will be dissolved before the breakeven point and lose investors' money. The Company is very well-protected against loss.

III. Conclusions

These profitability, scenario, and sensitivity analyses provide strong evidence that OptiFilt will be financially successful and stable, even in the event of various unlikely but disadvantageous scenarios. As such, the Company presents a lucrative and responsible investment opportunity for both angel investors and venture capitalists. In the vast majority of scenarios studied, investors receive returns comparable to or greater than those seen elsewhere in the biotechnology industry. Furthermore, early termination analyses have shown that financial loss is very unlikely even in the worst of scenarios.

Despite our confidence in OptiFilt and the care with which we conducted these analyses, it is important to note that this study is not perfect. An infinite number of factors can impact OptiFilt's profitability moving forward, many of which are external and out of the Company's control. Like all financial opportunities, investment in OptiFilt inherently contains some risk. The most probable and relevant of these risks were included in the foregoing analysis.

Chapter 9:

Conclusions & Acknowledgements

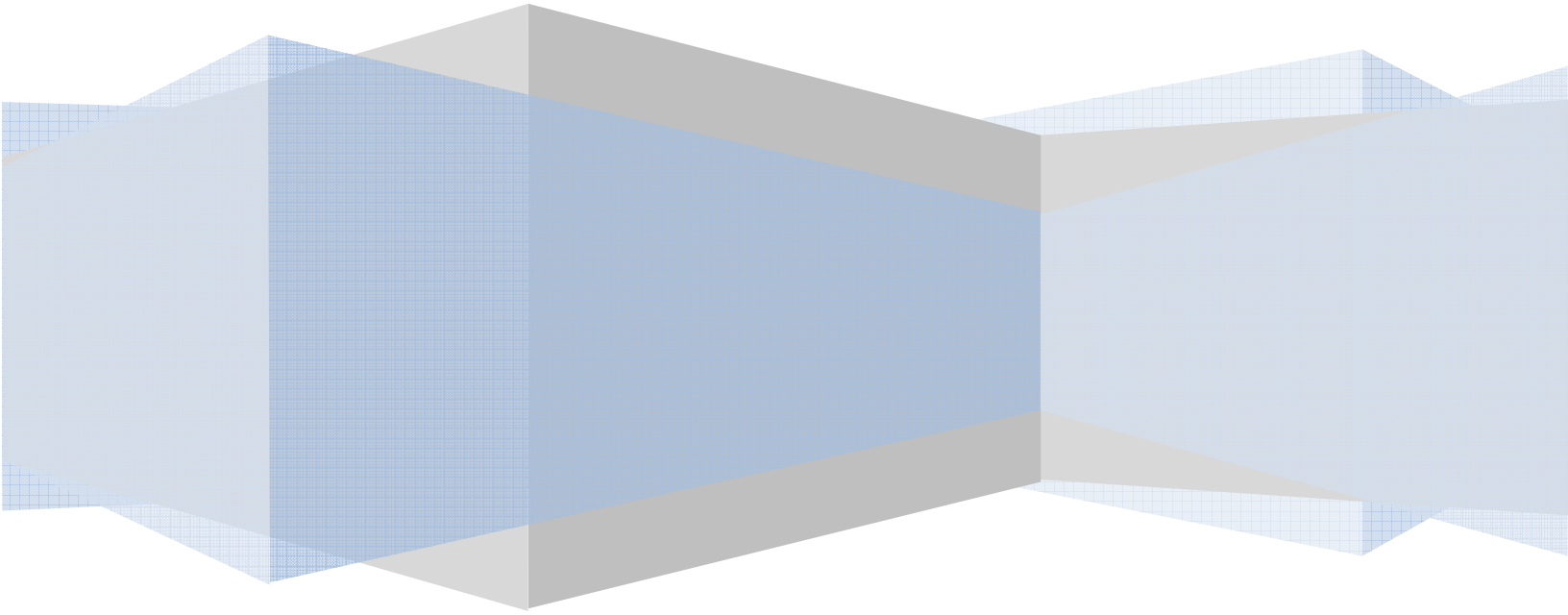

Conclusions

The goal of this project was to create a high-throughput system for testing new membranes that was both highly scalable and accurate. To accomplish this purpose, OptiFilt plans to use a mix of bench-side experimentation and semi-empirical models designed in MATLAB and COMSOL. Biopharmaceutical companies would be able to utilize OptiFilt's service to optimize the performance of their membrane-based separation and purification processes, which, depending on the protein of interest, can cost companies millions of dollars per year. We have shown our break-even price to be approximately $50,000, with a suggested selling point of $150,000, which nets OptiFilt a positive NPV valuation. Companies will profit by saving product that would otherwise be lost in the waste filtrate of a purification process.

It was shown that OptiFilt's current MATLAB and COMSOL models are internally consistent, satisfying multiple tests in which the models produced the expected real-world behavior. The MATLAB model obtained different K_c and K_d values when excluding fouling, and when using one of the four types of accepted fouling models today. Changing other filtration conditions also allows OptiFilt to characterize the membrane differently. When these coefficients of membrane behavior are integrated into the COMSOL model, complex flow geometries and concentration profiles are obtained, all of which are heavily dependent on K_c and K_d. In the future, a complete bench to MATLAB to COMSOL analysis may be performed for the purpose of impressing interested companies.

Competitors in this industry include Sci Log, Fluid Components, and Millipore, all of which offer a more rigid service, with decreased customizability, at a cheaper price. While OptiFilt will charge more, OptiFilt offers multiple models of fouling, full concentration profiles through time, and is fully tuned for scaling. Furthermore, OptiFilt will train technicians to

perform pressure correlations and fouling model analyses, thereby condensing the lengthy process of filtration optimization into one convenient service. Other services lack scalability, in that a customer of Sci Log would have to purchase multiple FilterTec Plus systems for several desired geometries. Furthermore, companies typically pay for only the products, and must train their own personnel to operate them. OptiFilt will be entirely self-contained, and a purchase will behave as a full subscription to the service for as long as it takes to optimize the purification.

If the current UF-based optimization is popular and successful, OptiFilt will expand to sterile, viral, and depth filtration in the coming years, thereby increasing its consumer base. Sterile and viral filtration are not fundamentally different from ultrafiltration; associated filters simply have pore sizes of different magnitudes. OptiFilt will be able to create MATLAB and COMSOL models for these purposes as well.

OptiFilt technology will significantly improve the performance of downstream purification in a multitude of biopharmaceutical processes. In so doing, companies will improve their product yields, thereby increasing general access to potentially life-saving drugs. Furthermore, by eliminating the difficulties of one step in the long sequence of drug discovery, synthesis, and purification, OptiFilt will expedite innovation and drug design. We strongly believe that this technology will not only prove to be a profitable endeavor, but will also greatly aid in the availability of crucial pharmaceuticals throughout the world.

Acknowledgments

We would be remiss if we did not thank those who helped us as we pursued this project. First and foremost, we would like to thank Dr. Matthew J. Lazzara for his guidance, advice, and patience throughout the semester. Dr. Lazzara's expertise and coaching was crucial to our understanding of the subject matter and our completion of this report.

We would also like to thank Calixte Monast for his MATLAB tutorials. Calixte's help was indispensible as we added simulated annealing to our MATLAB models and created as elegant a code as possible.

We also greatly appreciate all the industrial consultants with whom we met each week throughout the semester. Mr. Steven M. Tieri of DuPont was particularly helpful as we discussed test rig instrumentation and selected equipment.

Finally, we would like to thank Professors Leonard A. Fabiano and Warren D. Seider for devoting their time to guiding us through the design process. Professors Fabiano and Seider thoroughly taught us the principles of design.

Appendices

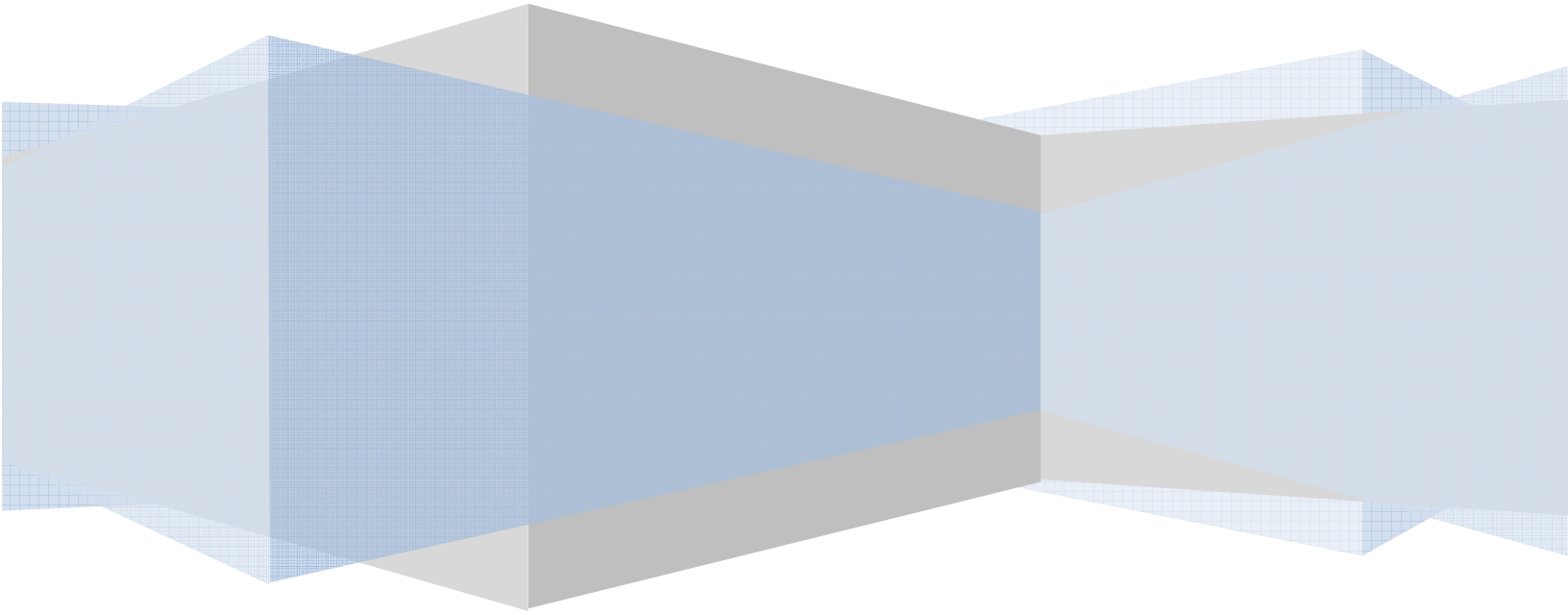

Appendix A: FDA Biologic Impurity Guidelines

[Code of Federal Regulations]
[Title 21, Volume 7]
[Revised as of April 1, 2010]
[CITE: 21CFR610.13]

TITLE 21--FOOD AND DRUGS
CHAPTER I--FOOD AND DRUG ADMINISTRATION
DEPARTMENT OF HEALTH AND HUMAN SERVICES
SUBCHAPTER F--BIOLOGICS

PART 610 -- GENERAL BIOLOGICAL PRODUCTS STANDARDS

Subpart B--General Provisions

Sec. 610.13 Purity.

Products shall be free of extraneous material except that which is unavoidable in the manufacturing process described in the approved biologics license application. In addition, products shall be tested as provided in paragraphs (a) and (b) of this section.

(a)(1)*Test for residual moisture.* Each lot of dried product shall be tested for residual moisture and shall meet and not exceed established limits as specified by an approved method on file in the biologics license application. The test for residual moisture may be exempted by the Director, Center for Biologics Evaluation and Research or the Director, Center for Drug Evaluation and Research, when deemed not necessary for the continued safety, purity, and potency of the product.

(2)*Records.* Appropriate records for residual moisture under paragraph (a)(1) of this section shall be prepared and maintained as required by the applicable provisions of 211.188 and 211.194 of this chapter.

(b)*Test for pyrogenic substances.* Each lot of final containers of any product intended for use by injection shall be tested for pyrogenic substances by intravenous injection into rabbits as provided in paragraphs (b) (1) and (2) of this section:*Provided,* That notwithstanding any other provision of Subchapter F of this chapter, the test for pyrogenic substances is not required for the following products: Products containing formed blood elements; Cryoprecipitate; Plasma; Source Plasma; Normal Horse Serum; bacterial, viral, and rickettsial vaccines and antigens; toxoids; toxins; allergenic extracts; venoms; diagnostic substances and trivalent organic arsenicals.

(1)*Test dose.* The test dose for each rabbit shall be at least 3 milliliters per kilogram of body weight of the rabbit and also shall be at least

equivalent proportionately, on a body weight basis, to the maximum single human dose recommended, but need not exceed 10 milliliters per kilogram of body weight of the rabbit, except that: (i) Regardless of the human dose recommended, the test dose per kilogram of body weight of each rabbit shall be at least 1 milliliter for immune globulins derived from human blood; (ii) for Streptokinase, the test dose shall be at least equivalent proportionately, on a body weight basis, to the maximum single human dose recommended.

(2)*Test procedure, results, and interpretation; standards to be met.* The test for pyrogenic substances shall be performed according to the requirements specified in United States Pharmacopeia XX.

(3)*Retest.* If the lot fails to meet the test requirements prescribed in paragraph (b)(2) of this section, the test may be repeated once using five other rabbits. The temperature rises recorded for all eight rabbits used in testing shall be included in determining whether the requirements are met. The lot meets the requirements for absence of pyrogens if not more than three of the eight rabbits show individual rises in temperature of 0.6 deg. C or more, and if the sum of the eight individual maximum temperature rises does not exceed 3.7 deg. C.

[38 FR 32056, Nov. 20, 1973, as amended at 40 FR 29710, July 15, 1975; 41 FR 10429, Mar. 11, 1976; 41 FR 41424, Sept. 22, 1976; 44 FR 40289, July 10, 1979; 46 FR 62845, Dec. 29, 1981; 49 FR 15187, Apr. 18, 1984; 50 FR 4134, Jan. 29, 1985; 55 FR 28381, July 11, 1990; 64 FR 56453, Oct. 20, 1999; 67 FR 9587, Mar. 4, 2002; 70 FR 14985, Mar. 24, 2005]

Appendix B: MATLAB Proprietary Code

Model without fouling

```
function [go] = go();

M = [1 0 0 0 0 0 0;
    0 1 0 0 0 0 0;
    0 0 0 0 0 0 0;
    0 0 0 0 0 0 0;
    0 0 0 0 0 0 0;
    0 0 0 0 0 0 0;
    0 0 0 0 0 0 0];
options=odeset('Mass',M,'MassSingular','yes','MStateDependence','none');

% Membrane constants
mu=10;                          % Solution viscosity (g/m s)
P_tm=100;                       % Transmembrane pressure (mmHg)
Lp=10E-8;                       % Hydraulic permeability (m/s mmHg)
sigma=1;                        % Osmotic reflection coefficient
diff=10E-8;                     % Solute diffusivity in solvent (m^2/s)
PhiKC=0.01;                     % Theta constant
PhiKD=0.02;                     % Theta constant
L=0.001;                        % Length of membrane (m)
Ac=0.005;                       % Cross-sectional area of membrane (m^2)
kc=2.33*mu^(1/6)*diff^(1/3);    % Mass transfer coefficient (m/s)

Vr0=5*10^(-6);                  % Initial retentate volume (m^3)
Cr0=10;                         % Initial retentate concentration (mol/m^3)

z0 = [0.0001; 0.5; 0.02; 0.023; 1];   % fmincon initial guess
optimfval=optimset('Algorithm','interior-point','Display','off');        %
suppress fsolve output
[z,zval]=fmincon(@IC,z0,[],[],[],[],[0 0 0 0 0 ],[Inf Inf 1 1
Inf],[],optimfval);

    function [Q] = IC(g)
        % Solves a system of equations to find appropriate initial
        % conditions for the DAE system.

        q=[Lp*(P_tm-sigma*g(5))-g(1);
            (PhiKC*g(1)*L)/(PhiKD*diff)-g(2);
            PhiKC/(1-(1-PhiKC)*exp(-g(2)))-g(3);
            (g(3)*exp(g(1)/kc))/(1-g(3)+g(3)*exp(g(1)/kc))-g(4);
            23.487*exp(0.0116*((Cr0*g(4)/g(3))-(Cr0*g(4))))-g(5)];

        Q=abs(norm(q));
    end

[t,R]=ode15s(@test_membrane,[0 153],[Vr0 Cr0 z(1) z(2) z(3) z(4)
z(5)],options);

    function [fR] = test_membrane(t, R)
        % 3/19/2011
```

```
        % solution vector
        fR = zeros(7,1);

        % ----------------------------------------
        % differential equations
        % ----------------------------------------
        % Volume (m^3) IC 0.001-0.005 L or 10^(-6)-5*10^(-6) m^3
        fR(1)=-Ac*R(3);

        % Cr (g/m^3 solution) IC 84-448 g/L or 84000-448000 g/m^3
        fR(2)=(1/R(1))*(-(R(3)*R(6)*R(2)*Ac)-(R(2)*fR(1)));

        % Velocity (m/s)
        fR(3)=Lp*(P_tm-sigma*R(7))-R(3);

        % Peclet number (dimensionless)
        fR(4)=(PhiKC*R(3)*L)/(PhiKD*diff)-R(4);

        % Theta (dimensionless) IC 0-1
        %fR(5)=0.98-R(5);
        fR(5)=PhiKC/(1-(1-PhiKC)*exp(-R(4)))-R(5);

        % Theta prime (dimensionless) IC 0-1... theta prime > theta
        %fR(6)=0.99-R(6);
        fR(6)=(R(5)*exp(R(3)/kc))/(1-R(5)+R(5)*exp(R(3)/kc))-R(6);

        % Osmotic pressure (mm Hg) IC 48-3840 mmHg
        fR(7)=23.487*exp(0.0116*((R(2)*R(6)/R(5))-(R(2)*R(6))))-R(7);
    end

subplot(3,4,1)
plot(t,R(:,1))
title('Vr v. t')
subplot(3,4,2)
plot(t,R(:,2))
title('Cr v. t')
subplot(3,4,3)
plot(t,R(:,3))
title('vf v. t')
subplot(3,4,4)
plot(t,R(:,4))
title('Pe v. t')
subplot(3,4,5)
plot(t,R(:,5))
title('theta v. t')
subplot(3,4,6)
plot(t,R(:,6))
title('theta prime v. t')
subplot(3,4,7)
plot(t,R(:,7))
title('osmotic p v. t')
subplot(3,4,8)
plot(t,R(:,2).*R(:,6))
title('Cf v. t')
```

```
subplot(3,4,9)
plot(t,R(:,6).*R(:,2)./R(:,5))
title('Cr,u v. t')
subplot(3,4,10)
plot(t,R(:,2).*R(:,1))
title('mAb mass (retentate) v. t')
subplot(3,4,11)
plot(t,R(:,2)-R(:,6).*R(:,2))
title('Cr-Cf')
subplot(3,4,12)
plot(t, R(:,2).*R(:,6).*(Vr0-R(:,1)))
title('mAb mass (filtrate) v. t')

end
```

Model with fouling

```
function [go] = go();
% Change inputted phi values in go.m (line 44) and in test_membrane.m
% (lines 10-11) when comparing simulated annealing results.
M = [1 0 0 0 0 0 0 0 0;
     0 1 0 0 0 0 0 0 0;
     0 0 0 0 0 0 0 0 0;
     0 0 0 0 0 0 0 0 0;
     0 0 0 0 0 0 0 0 0;
     0 0 0 0 0 0 0 0 0;
     0 0 0 0 0 0 0 0 0;
     0 0 0 0 0 0 0 1 0;
     0 0 0 0 0 0 0 0 0];
options=odeset('Mass',M,'MassSingular','yes','MStateDependence','none');

z0 = [0.0001; 0.5; 0.02; 0.023; 1; 0.01];   % fsolve initial guess
optimfval=optimset('Algorithm','interior-point','Display','off');
[z,zval]=fmincon(@IC,z0,[],[],[],[],[0 0 0 0 0 0],...
    [Inf Inf 1 1 Inf Inf],[],optimfval);

Vr0=1*10^(-3);                  % Initial retentate volume (m^3)
Cr0=1;                          % Initial retentate concentration (mol/m^3)
Vf0=0;                          % Initial filtrate volume (m^3)

    function [Q] = IC(g)
        % Solves a system of equations to find appropriate initial
        % conditions for the DAE system.
        Vr0=1*10^(-3);              % Initial retentate volume (m^3)
        Cr0=1;                      % Initial retentate concentration (mol/m^3)
        Vf0=0;                      % Initial filtrate volume (m^3)

        mu=10;                      % Solution viscosity (g/m s)
        diff=10^(-8);               % Solute diffusivity in solvent (m^2/s)
        L=0.0001;                       % Length of membrane (m)
        kc=2.33*mu^(1/6)*diff^(1/3);    % Mass transfer coefficient (m/s)

        Ka=3.36*10^(-4);            % Fouling model coefficient (s^-1)
        Kc=5.03*10^(6);             % Fouling model coefficient (s/m^2)

        P_tm=100;                   % Transmembrane pressure (mmHg)
        Lp0=0.0001;                 % Initial hydraulic permeability (m/s mmHg)
        sigma=1;                    % Osmotic reflection coefficient
        delPi0=23.97;               % Initial osmotic pressure (mmHg)
        Ac=0.005;                   % Cross-sectional area of membrane (m^2)

        phiGuess=[0.01 0.02];

        J0=Ac*Lp0*(P_tm-sigma*delPi0);    % Initial flux (m/s)

        q=[g(6)*(P_tm-sigma*g(5))-g(1);
            (phiGuess(1)*g(1)*L)/(phiGuess(2)*diff)-g(2);
            phiGuess(1)/(1-(1-phiGuess(1))*exp(-g(2)))-g(3);
            (g(3)*exp(g(1)/kc))/(1-g(3)+g(3)*exp(g(1)/kc))-g(4);
```

```
            23.487*exp(0.0116*((Cr0*g(4)/g(3))-(Cr0*g(4))))-g(5);
            ((((1-Ka*5E-8)^(-4))+Kc*J0*Vf0)^(-1))*J0/(P_tm-sigma*g(5))-g(6)];

        Q=abs(norm(q));
    end

[t,R]=ode15s(@test_membrane,[0:.5:2200],[Vr0 Cr0 z(1) z(2) z(3) z(4) z(5) Vf0
z(6)],options);

subplot(4,4,1)
plot(t,R(:,1)/100*5)
title('Vr (m^3)')
subplot(4,4,2)
plot(t,R(:,2))
title('Cr (g/m^3)')
subplot(4,4,3)
plot(t,R(:,3)/1000)
title('vf or J (m/s)')
subplot(4,4,4)
plot(t,R(:,4))
title('Pe')
subplot(4,4,5)
plot(t,R(:,5))
title('theta')
subplot(4,4,6)
plot(t,R(:,6))
title('theta prime')
subplot(4,4,7)
plot(t,R(:,7))
title('osmotic p (mm Hg)')
subplot(4,4,8)
plot(t,R(:,2).*R(:,6))
title('Cf (g/m^3)')
subplot(4,4,9)
plot(t,R(:,6)./R(:,5).*R(:,2))
title('Cr,u (g/m^3)')
subplot(4,4,10)
plot(t,R(:,8))
title('Vf (m^3)')
subplot(4,4,11)
plot(t,R(:,9)/1000)
title('Lp (m/s mm Hg)')
subplot(4,4,12)
plot(t,R(:,1).*R(:,2)/20)
title('Mass, retentate (g)')          % ignores Cr,u
subplot(4,4,13)
plot(t,R(:,2).*R(:,6).*R(:,8))
title('Mass, filtrate (g)')
subplot(4,4,14)
plot(t,R(:,6)./R(:,5).*R(:,2)-R(:,2).*R(:,6));
title('Cru-Cf (g/m^3)')
end


function [fR] = test_membrane(t, R)
% solution vector
```

```
fR = zeros(9,1);

PhiKC=0.01;                         % Theta constant
PhiKD=0.02;                         % Theta constant

% constants
mu=10;                              % Solution viscosity (g/m s)
diff=10^(-8);                       % Solute diffusivity in solvent (m^2/s)
L=0.0001;                           % Length of membrane (m)
kc=2.33*mu^(1/6)*diff^(1/3);        % Mass transfer coefficient (m/s)

Ka=3.36*10^(-4);                    % Fouling model coefficient (s^-1)
Kc=5.03*10^(6);                     % Fouling model coefficient (s/m^2)

P_tm=100;                           % Transmembrane pressure (mmHg)
Lp0=0.0001;                         % Initial hydraulic permeability (m/s mmHg)
sigma=1;                            % Osmotic reflection coefficient
delPi0=23.97;                       % Initial osmotic pressure (mmHg)
Ac=0.005;                           % Cross-sectional area of membrane (m^2)

J0=Ac*Lp0*(P_tm-sigma*delPi0);

% ----------------------------------------
% differential equations
% ----------------------------------------
% Volume (m^3) IC 0.001-0.005 L or 10^(-6)-5*10^(-6) m^3
fR(1)=-Ac*R(3);

% Cr (g/m^3 solution) IC 84-448 g/L or 84000-448000 g/m^3
fR(2)=(1/R(1))*(-(R(3)*R(6)*R(2)*Ac)-(R(2)*fR(1)));

% Throughput volume (m^3) IC 0
fR(8)=Ac*R(3);

% ----------------------------------------
% algebraic constraints
% ----------------------------------------
% Velocity/flux (m/s)
fR(3)=R(9)*(P_tm-sigma*R(7))-R(3);

% Peclet number (dimensionless)
fR(4)=(PhiKC*R(3)*L)/(PhiKD*diff)-R(4);

% Theta (dimensionless) IC 0-1
fR(5)=0.98-R(5);
%fR(5)=PhiKC/(1-(1-PhiKC)*exp(-R(4)))-R(5);

% Theta prime (dimensionless) IC 0-1... theta prime > theta
fR(6)=0.99-R(6);
%fR(6)=(R(5)*exp(R(3)/kc))/(1-R(5)+R(5)*exp(R(3)/kc))-R(6);

% Osmotic pressure (mm Hg) IC 48-3840 mmHg
fR(7)=23.487*exp(0.0116*((R(2)*R(6)/R(5))-(R(2)*R(6))))-R(7);
```

```
% Hydraulic permeability (m/s mm Hg)
%fR(9)=4.96873411768589e-05-R(9);
fR(9)=((((1-Ka*t)^(-4))+(Kc*J0*R(8)))^(-1))*J0/(P_tm-sigma*R(7))-R(9);

end
```

Complete model with SA

```
function [results] = go(data, phi)
% 1. import experimental data, stored in Excel sheet
% 2. run results.m, then go to test_membrane.m and change the PhiKc guess to
results(1), and the PhiKd guess to results(2)
% 3. run compare(data,results) to view side-by-side comparison of SA-based
graph and data graph.

M =[1 0 0 0 0 0 0 0 0;
    0 1 0 0 0 0 0 0 0;
    0 0 0 0 0 0 0 0 0;
    0 0 0 0 0 0 0 0 0;
    0 0 0 0 0 0 0 0 0;
    0 0 0 0 0 0 0 0 0;
    0 0 0 0 0 0 0 0 0;
    0 0 0 0 0 0 0 1 0;
    0 0 0 0 0 0 0 0 0];
options_ode=odeset('Mass',M,'MassSingular','yes','MStateDependence','none','S
tats','off');

%-------------------------
% Membrane constants
%-------------------------
mu=10;                          % Solution viscosity (g/m s)
diff=10^(-8);                   % Solute diffusivity in solvent (m^2/s)
L=0.0001;                       % Length of membrane (m)
kc=2.33*mu^(1/6)*diff^(1/3);    % Mass transfer coefficient (m/s)

Ka=3.36*10^(-4);                % Fouling model coefficient (s^-1)
Kc=5.03*10^(6);                 % Fouling model coefficient (s/m^2)

P_tm=100;                       % Transmembrane pressure (mmHg)
Lp0=0.01;                       % Initial hydraulic permeability (m/s mmHg)
sigma=1;                        % Osmotic reflection coefficient
delPi0=23.97;                   % Initial osmotic pressure (mmHg)
Ac=0.005;                       % Cross-sectional area of membrane (m^2)

J0=Ac*Lp0*(P_tm-sigma*delPi0);  % Initial flux (m/s)

Vr0=1*10^(-3);                  % Initial retentate volume (m^3)
Cr0=1;                          % Initial retentate concentration (mol/m^3)
Vf0=0;                          % Initial filtrate volume (m^3)

z0 = [0.0001; 0.5; 0.02; 0.023; 1; 0.01];   % fsolve initial guess
optimfval=optimset('Algorithm','interior-point','Display','off');

[results,fval]=runFit();              % run simulated annealing

% once the optimization is stopped, store in results vector so that
% compare.m is easy to use
[z,zval]=fmincon(@IC,z0,[],[],[],[],[0 0 0 0 0 0],[Inf Inf 1 1 Inf
Inf],[],optimfval);
results(1,3:8)=z(1:6);
```

```
function [x,fval,time] = runFit()
    % Runs simulated annealing.

    x0 = [phi(1) phi(2)];    % Start iterating from the guess given
    lb = [0 0];              % No nonzero phiKc, phiKd
    ub = [1 1];

    options_sim =
        saoptimset('Display','iter','TemperatureFcn',@temperatureexp,...
        'DisplayInterval',1,'PlotFcns',{@saplotf,@saplotbestf,...
        @saplotstopping,@saplotbestx},'MaxFunEvals',Inf,...
        'ObjectiveLimit',1E-10,'InitialTemperature',1,...
        'ReannealInterval',100);

    [x,fval]=simulannealbnd(@runModel,x0,lb,ub,options_sim);
        % finds the minimum value of error in runModel
end

function [error] = runModel(phiGuess)
    % Uses fsolve to calculate initial DAE guesses and then solves the
    % ODE with those guesses.

    % calculate DAE guesses
    [z,zval]=fmincon(@IC,z0,[],[],[],[],[0 0 0 0 0 0],...
        [Inf Inf 1 1 Inf Inf],[],optimfval);

    function [Q] = IC(g)
        % Solves a system of equations to find appropriate initial
        % conditions for the DAE system.

        q=[g(6)*(P_tm-sigma*g(5))-g(1);
            (phiGuess(1)*g(1)*L)/(phiGuess(2)*diff)-g(2);
            phiGuess(1)/(1-(1-phiGuess(1))*exp(-g(2)))-g(3);
            (g(3)*exp(g(1)/kc))/(1-g(3)+g(3)*exp(g(1)/kc))-g(4);
            23.487*exp(0.0116*((Cr0*g(4)/g(3))-(Cr0*g(4))))-g(5);
        ((((1-Ka*5E-8)^(-4))+Kc*J0*Vf0)^(-1))*J0/(P_tm-sigma*g(5))-g(6)];

        Q=abs(norm(q));
    end

    function [fR] = oderesults(t, R)
        % Stores all ODEs and algebraic equations of the actual model.

        % solution vector
        fR = zeros(9,1);

        % these two values change after each iteration and must be
        % reassigned in oderesults
        PhiKC=phiGuess(1);                  % Theta constant
        PhiKD=phiGuess(2);                  % Theta constant

        % ----------------------------------------
        % differential equations
```

```
            % ----------------------------------------
            % Volume (m^3) IC 0.001-0.005 L or 10^(-6)-5*10^(-6) m^3
            fR(1)=-Ac*R(3);

            % Cr (g/m^3 solution) IC 84-448 g/L or 84000-448000 g/m^3
            fR(2)=(1/R(1))*(-(R(3)*R(6)*R(2)*Ac)-(R(2)*fR(1)));

            % Throughput volume (m^3) IC 0
            fR(8)=Ac*R(3);

            % ----------------------------------------
            % algebraic constraints
            % ----------------------------------------
            % Velocity/flux (m/s)
            fR(3)=R(9)*(P_tm-sigma*R(7))-R(3);

            % Peclet number (dimensionless)
            fR(4)=(PhiKC*R(3)*L)/(PhiKD*diff)-R(4);

            % Theta (dimensionless) IC 0-1
            fR(5)=PhiKC/(1-(1-PhiKC)*exp(-R(4)))-R(5);

            % Theta prime (dimensionless) IC 0-1... theta prime > theta
            fR(6)=(R(5)*exp(R(3)/kc))/(1-R(5)+R(5)*exp(R(3)/kc))-R(6);

            % Osmotic pressure (mm Hg) IC 48-3840 mmHg
            fR(7)=23.487*exp(0.0116*((R(2)*R(6)/R(5))-(R(2)*R(6))))-R(7);

            % Hydraulic permeability (m/s mm Hg)
      fR(9)=((((1-Ka*t)^(-4))+(Kc*J0*R(8)))^(-1))*J0/(P_tm-sigma*R(7))-R(9);
        end

        try
     % the time span in ode15s must be consistent with the imported data.
            [t,R]=ode15s(@oderesults,[0:0.5:560],[Vr0 Cr0 z(1) z(2) z(3) z(4)
z(5) Vf0 z(6)],options_ode); %#ok<ASGLU>

            % given the inputted phiKc, phiKd guess, temp stores the
            % calculated results' deviation from experimental data
            temp(:,1)=data(:,2)-R(:,5);
            temp(:,2)=data(:,3)-R(:,6);

            error=norm(temp);

        catch
            error=100;                  % if the PhiKc, PhiKd guess results
        end                             % in inconsistent y0, discard results

    end

    function [Q] = IC(g)
        % Solves a system of equations to find appropriate initial
        % conditions for the DAE system.
```

```
        q=[g(6)*(P_tm-sigma*g(5))-g(1);
            (results(1)*g(1)*L)/(results(2)*diff)-g(2);
            results(1)/(1-(1-results(1))*exp(-g(2)))-g(3);
            (g(3)*exp(g(1)/kc))/(1-g(3)+g(3)*exp(g(1)/kc))-g(4);
            23.487*exp(0.0116*((Cr0*g(4)/g(3))-(Cr0*g(4))))-g(5);
            ((((1-Ka*5E-8)^(-4))+Kc*J0*Vf0)^(-1))*J0/(P_tm-sigma*g(5))-g(6)];

        Q=abs(norm(q));
    end

end
```

FilterTec™ Plus

3-Filter Testing Station

- *Simultaneously Compare 3 Filters*
- *Filterability Studies & Vmax Determination*
- *Evaluate Filter Combinations*
- *Monitor/Control Pressure, Feed Rate, Collection Rate, etc.*
- *Automatic Documentation to Spreadsheet*
- *Built-In Alarms for Walk-Away Operation*
- *Compatible with All Manufacturers' Filters*

3-Filter Testing Station

i n t e l l i g e n t b i o p r o c e s s i n g s y s t e m s

SciLog®
Intelligent Bioprocessing Systems

www.scilog.com Ph: (800)955-1993

FilterTec™ Plus

3-Filter Testing Station

Parallel Testing

Save time and improve efficiency in Filterability Studies & Vmax Determinations. The FilterTec™ Plus testing station gives you the flexibility to evaluate three filters simultaneously. Plus, you'll have the freedom to test filter combinations on your schedule. This allows you to test any combination of filters from the same or different manufacturers.

Save Money with Real-time Monitoring

Improve your lab's productivity and efficiency. With FilterTec™ Plus be assured that your tests will maintain a constant rate or pressure without supervision. FilterTec™ Plus has five operational modes and six user-definable alarms that allow you to work on other projects while doing filter tests.

- R/P Stat Mode: Constant Rate/Constant Pressure Filtration with six user-definable alarms.
- P Stat Mode: Constant Pressure Filtration with six user-definable alarms.
- R/P Step-Scan Mode: Automated, programmable, continuous changing of pump rate or pressure with time.

Save Time with Automated Documentation

Don't waste time manually documenting filtration information. SciDoc interface software is sent to you ready to use for real-time verification and documentation of filtration parameters. Automatic documentation allows for easy comparison of filters, and you'll be able to quickly present your data findings.

- SciDoc interface software with custom macros for Excel® for data compilation.
- Complete process analysis with graphing of data.
- Real-time verification and documentation of process parameters.

FilterTec™ Plus is shipped to you complete, ready to use as a 3-Filter Testing Station. This Station consists of 3 balances with cables, the Serial-3 Balance Interface box, and a stand and clamp set for holding your 3 filters over the balances. An optional 6-way Rotary Valve is available and is controlled by the operational modes.

You can test one, two, or three filters simultaneously.

This system has several different parallel or serial configurations.

The first of the more common configurations uses one head to provide solution through a manifold to 3 filters while monitoring or controlling the pressure with each filter emptying into its own container on its own balance.

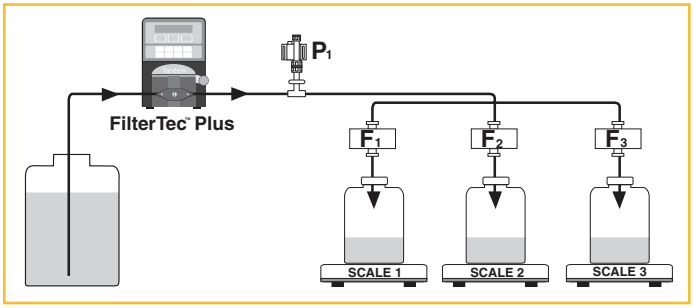

A constant pressure can be easily maintained, and the collection rates achieved will be based upon the dynamics of the filter. If the filters are the same, the Feed Rate will be roughly spit into thirds.

The second common configuration utilizes 3 pump heads, 3 sets of tubing, all 3 sensors and balances, with everything running in parallel.

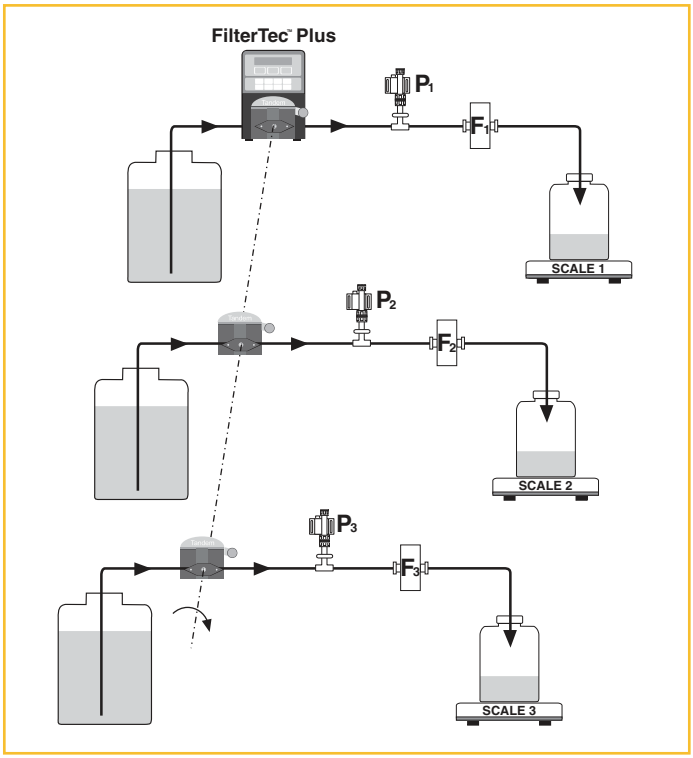

This setup puts the control of the feed rate in the hands of channel 1 with channels 2 and 3 being similar, but not always identical. To minimize differences, use tubing from the same manufacturer and lot whenever possible.

Also, while only one of the 3 sensors will be used for control, each sensor and balance will provide independent alarms based on the system's settings. When in Constant Pressure Mode, the source sensor's channel is controlled, and the other channels again will be similar but not identical.

SciLog, Inc. 8845 South Greenview Drive, Suite 4, Middleton, WI 53562 Ph: (800)955-1993 Fx: (608) 824-0509 www.scilog.com

PHARMA REFRACTOMETER FOR IN-LINE CONCENTRATION MEASUREMENT

K-PATENTS
PROCESS INSTRUMENTS

K-PATENTS PHARMA REFRACTOMETER PR-23-AC

SB:PR-23/Pharma

TYPICAL APPLICATIONS

PHARMACEUTICAL CHEMICALS
Acetylsalicylic acid, Calcium gluconate, Glycerophosphates, Chloral hydrate, Saccharin, Antihistamines, Tranquilizers, Antifilarials, Diethyl carbamazine citrate, Antidiabetics and more.

ACTIVE PHARMACEUTICAL INGREDIENTS
Actives, Excipients, Intermediates, Raw material, Fine chemicals, and Bulk chemicals.

ANTIBIOTICS
Penicillin, Streptomycin, Tetracyclines, Chloramphenicol, and Antifungals.

BLOOD PRODUCTS
Blood, Plasma, Serum, Infusion liquids, Sodium chloride, and Glucose.

PROTEINS
Proteins and Protein buffer solutions

SYNTHETIC DRUGS
Sulfa drugs, Antituberculosis drugs, Antileprotic drugs, Analgesics, Anesthetics, and Antimalarials.

VITAMINS
Ascorbid acid, Ca-arabonate, Riboflavin, Vitamin-B, Vitamin-C Sodium Pantonate. and more.

SYNTHETIC HORMONES

SYRUPS
Concentrated aqueous solutions of sucrose.

DRUGS OF VEGETABLE ORIGIN
Quinine, Strychnine and Brucine, Emetine, and Digitalis Glycosides, and Herbal extracts.

VACCINES AND SERA

SURGICAL SUTURES
Glue for human tissue.

ACIDS, BASES AND SOLVENTS

REGULATORY COMPLIANCE

Food and Drug Administration's (FDA's) regulations require documented act of demonstrating that a specific procedure, process, and activity will consistently lead to the expected results. This is called validation.

K-Patents Process Refractometer PR-23 is ideal real-time instrument that meets the pharmaceutical industry standards and guidelines including PAT, GMP, CIP/SIP, 21 CFR Part 11 and validation. The ability to understand and continuously control parameters such as Refractive Index n_D contributes significantly to the development of effective drugs and efficient manufacturing processes.

K-Patents Pharma Refractometer PR-23-AC fulfills the pharmaceutical drug production regulations for process wetted part materials, sealing, and surface roughnesses. No animal originated media are used in the machining and polishing processes.

K-Patents refractometers are designed, manufactured and serviced under ISO 9001 quality system and procedures that guarantee the accuracy and repeatability of the measurement results. Each sensor is provided with a calibration certificate comparing a set of standard liquids to the actual sensor output. Therefore, the calibration and accuracy can be routinely verified with the traceable standard refractive index liquids.

Validation often includes the qualification of systems and equipment. It is a requirement for Good Manufacturing Practices (GMPs) and other regulatory requirements.

K-Patents provides a qualification procedure and equipment that help the user to prove the suitability of the refractometer for its designated function. This includes a set up for tests with refractometer in a laboratory or in a pilot process in making small quantities of the drug.

EQUIPMENT QUALIFICATION

These steps are common for a K-Patents Pharma Refractometer PR-23-AC qualification process:

1A. LAB TEST WITH STATIC SAMPLE

Laboratory test for manual sampling in a laboratory cuvette consisting of an agitator with stirrer and connections for thermostat controlled water.

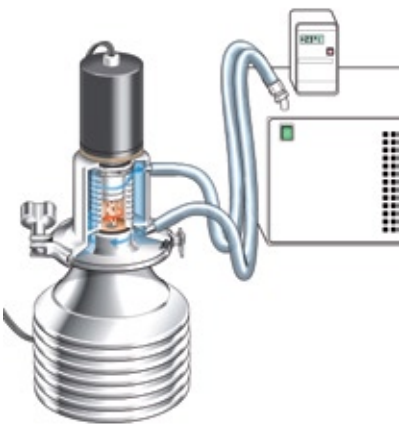

1B. LAB TEST WITH CONTINUOUS SAMPLE

Laboratory test for continuous sampling in a laboratory cuvette consisting of connections for a sample inlet and outlet and for thermostat controlled water.

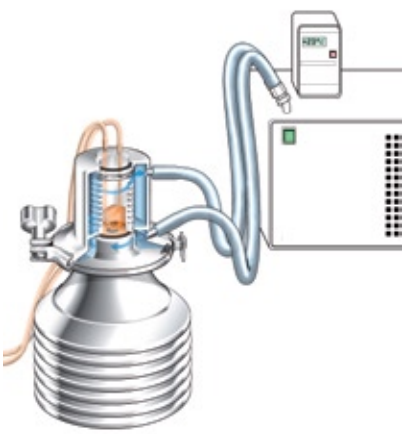

2. TEST IN PILOT SCALE

Installation in a pilot process using a pharma mini flow cell.

3. INSTALLATION AT FULL PRODUCTION SCALE

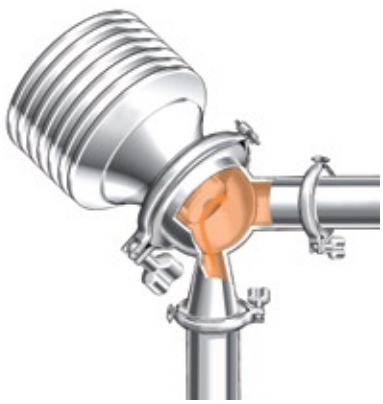

DRUG FORMULATION

Step one of the equipment qualification process is also an applicable procedure for creating proprietary chemical curves for different drug recipies on the user's own manufacturing facility. This makes the drug formulation and validation easier in considerably less time.

DIGITAL MEASUREMENT PRINCIPLE

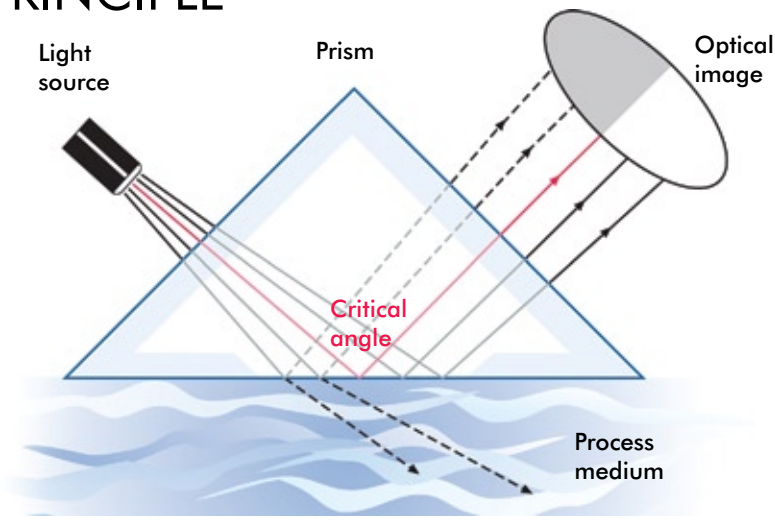

The light source sends light against the interface between a prism and the process solution, where the rays meet the surface at different angles.

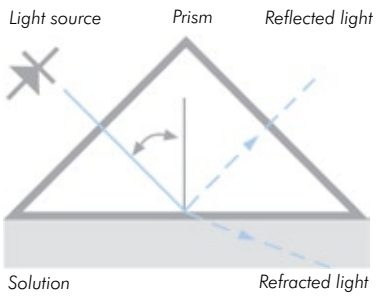

Depending on the angle, some rays are totally reflected. And, some rays are only partially reflected, most of the light is refracted into the process solution.

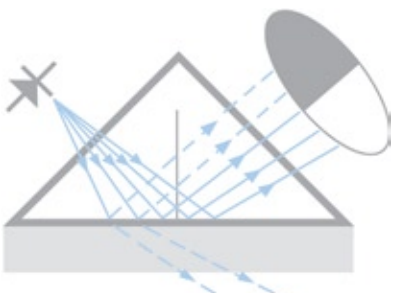

Thus an optical image with a dark sector and a light sector is created.

The angle corresponding to the shadow line is called the Critical Angle of Total Reflection. The Critical Angle is a function of the refractive index and therefore the concentration of the solution.

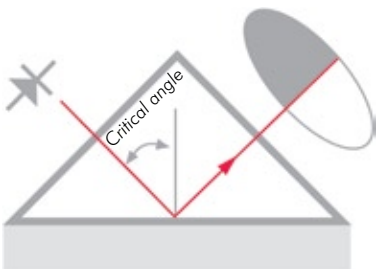

A digital CCD-camera detects the optical image and the shadow line. The camera transforms the optical image point-by-point to an electrical signal. The exact shadow line position is located and the refractive index n_D is determined.

A built-in temperature sensor meas-ures the temperature T on the interface of the process liquid. The indicating transmitter converts the refractive index n_D and temperature T to concentration units.

The diagnostics program ensures that the measurement is reliable.

FDA 21 CFR PART 11 ADHERENCE

The K-Patents Refractometer includes an Ethernet communication solution. Together with the user's own procedural and administrative user controls it facilitates electronic data records for FDA 21 CFR Part 11 adherence. The transmitter uses the UDP/IP protocol to communicate over the Ethernet to any type of computer. This eliminates human error and allows for refractometer generated measurement and diagnostic data capture for storage, analysis and reporting.

Any computer with a standard Ethernet connection can be configured to view and download data from the sensor by using a standard web browser.

Access to the refractometer and to the refractometer generated data can be restricted to authorized personnel only using a password protection.

DESIGN

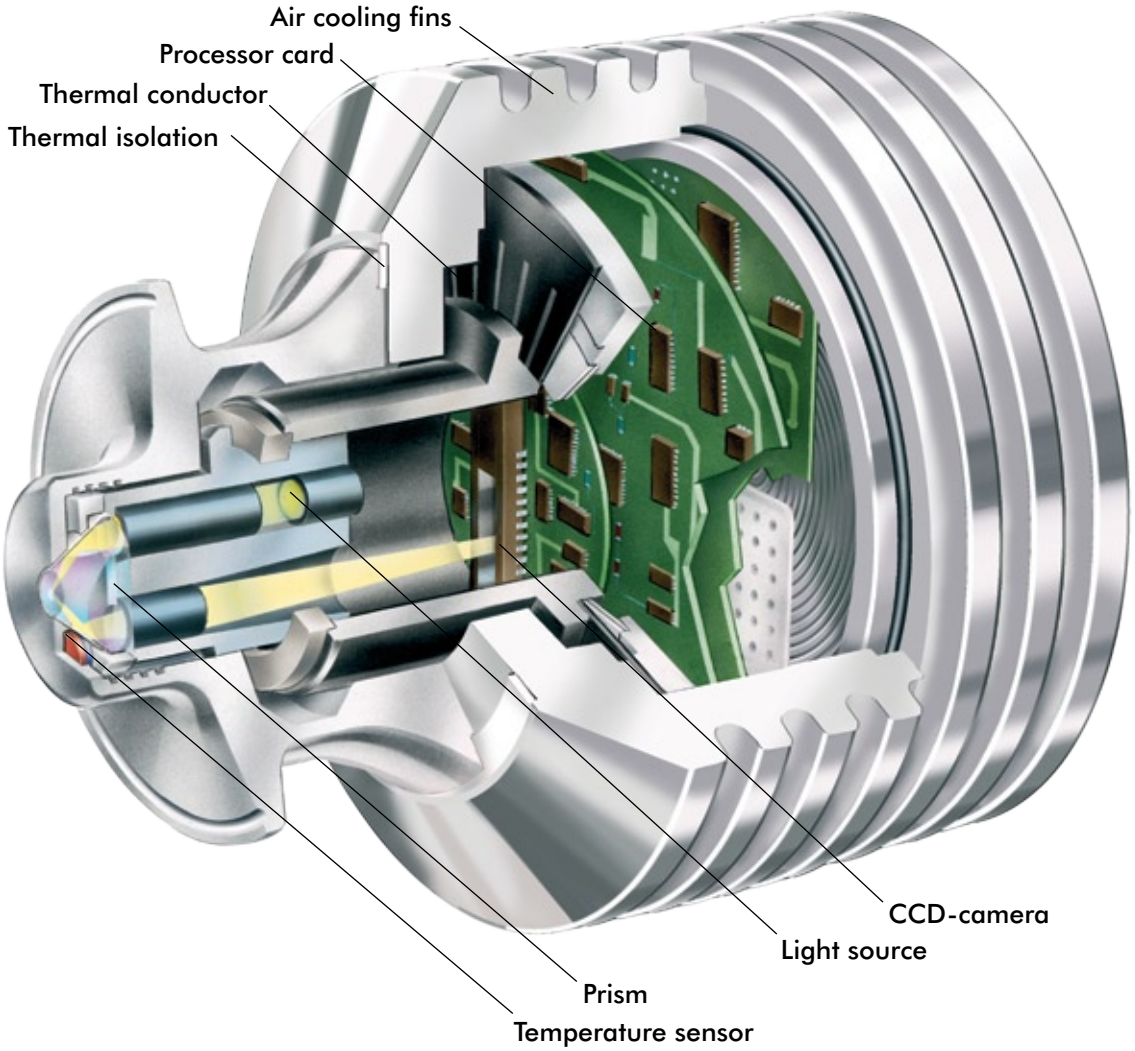

CORE-Optics

All measuring components (light source, prism, temperature sensor and CCD-camera) are in one solid CORE-optics module.

The patented CORE-optics is mechanically isolated from the influence of external forces and vibrations. The CORE-optics contains no mechanical adjustments.

(US Patent No. 6067151)

SPECIFICATIONS

Compact sensor PR-23-AC:

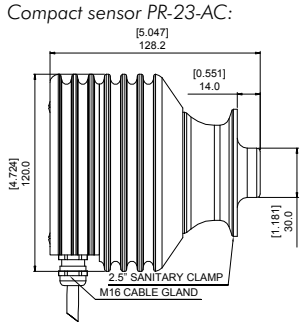

Laboratory test cuvette LTC for off-line laboratory testing:

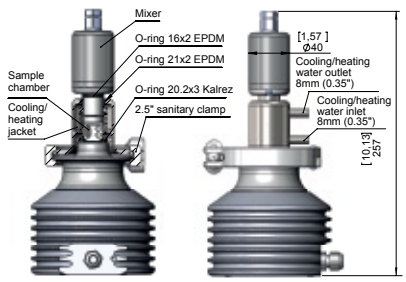

Mini flow cell PMFC for low volume pilot processes:

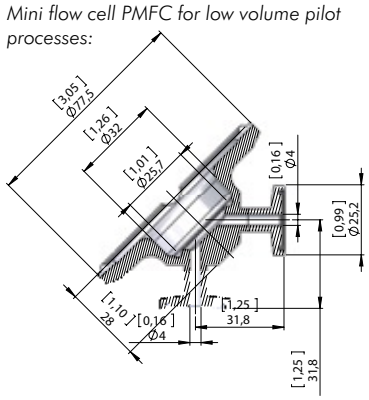

Indicating transmitter DTR in stainless steel enclosure:

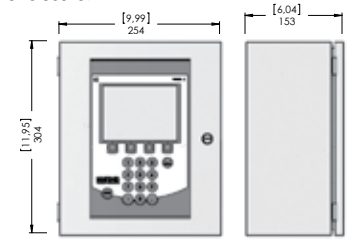

Refractive Index range:	*Standard: Full range, n_D = 1.3200...1.5300 (corresponds to 0...100 % b.w.)*
Accuracy:	*Refractive index n_D ±0.0002 (corresponds typically to ± 0.1% by weight)* *Repeatability n_D ±0.0001 (corresponds typically to ±0.05% by weight)*
Speed of response:	*1 s undamped, damping time selectable up to 5 min*
Calibration:	*With Cargille standard R.I. liquids over full range of n_D 1.3200...1.5300*
CORE-Optics:	*No mechanical adjustments (US Patent No. US6067151)*
Digital measurement:	*3648 pixel CCD element*
Light source:	*Light emitting diode (LED), 589 nm wavelength, sodium D-line*
Temperature sensor:	*Built-in Pt-1000, linearization according to IEC 751*
Temperature compensation:	*Automatic, digital compensation*
Instrument verification:	*According to ISO 9000 quality system: NIST traceable with standard R.I. liquids and Transmitter's menu guided procedure and report for printing*
Ambient temperature:	*Sensor: max. 45°C (113°F), min. -20°C (-4°F)* *Indicating transmitter: max. 50°C (122°F), min. 0°C (32°F)*
SENSOR PR-23-AC:	
Process connection:	*Sanitary 3A-clamp 2.5"*
Process temperature:	*-20°C...130°C (-4°F...266°F)*
Surface roughness, option:	*Ra 0.4µm (15µ inch)*
Process wetted parts, standard:	*AISI 316L stainless steel, prism spinel, prism gaskets PTFE (teflon), EPDM*
Sensor protection class:	*IP67, Nema 4X*
Sensor weight:	*2 kg (4.4 lbs)*
Laboratory test cuvette LTC for off-line laboratory testing:	*AISI 316 L stainless steel laboratory test cuvette for manual and static sampling. Contains an agitator with PTFE (teflon) stirrer, and connections for sample inlet and outlet, and 1/4" tube connections for thermostat controlled water.*
Pharma mini flow cell PMFC:	*For in-line testing of low volume samples in pilot conditions, process connection Sanitary 3A-clamp 1,5", electropolished wetted parts material with surface roughness of Ra 0.4µm (15µ inch)*
INDICATING TRANSMITTER DTR:	
Display:	*320x240 pixel graphical LCD with LED backlight*
Keypad:	*18 membrane keys*
Current output:	*Two independent current outputs, 4-20 mA, max. load 1000 Ohm, galvanic isolation 1500 VDC or AC (peak), hold function during prism wash*
Ethernet connection:	*10/100 Mbit/s, data acquisition over UDP/IP Protocol with K-Patents data logging software*
Power:	*AC input 100-240 VAC/50-60 Hz, optional 24 VDC, 30 VA*
Alarms/Wash relays:	*Two built-in signal relays, max. 250 V/3 A*
Sensor connectivity:	*One or two sensors can be connected to the DTR. Sensors independent of each other: own parameter sets and usable in different applications. Two current outputs configurable independently to indicate process concentration or temperature of either sensor.*
Transmitter protection class:	*Enclosure IP66, Nema 4X*
Enclosure material:	*Standard: Polycarbonate, optional: AISI 304 stainless steel*
Indicating transmitter weight:	*4.5 kg (10 lbs)*
INTERCONNECTING CABLE:	*IEC 61158-2 compliant two-wire cable*
Interconnecting cable length:	*Standard 10 m (33 ft), max. 200 m (660 ft)*

ORDERING INFORMATION:

- *Sensor type and flow cell option(s)*
- *Desired scale*
- *Properties of process solution*
- *Process temperature range*
- *Surface roughness*
- *Process pipe size*
- *Process flow rate*
- *Supply voltage and frequency*
- *Material certificates*
- *Options*

K-PATENTS OY
P.O. BOX 77
ELANNONTIE 5
FI-01511 VANTAA, FINLAND
PHONE: INT.+358-207-291 570
FAX: INT.+358-207-291 577
INFO@KPATENTS.COM
WWW.KPATENTS.COM

K-PATENTS, INC.
1804 CENTRE POINT CIRCLE, SUITE 106
NAPERVILLE, IL 60563
U.S.A.
PHONE: (630) 955 1545
FAX: (630) 955 1585
INFO@KPATENTS-USA.COM
WWW.KPATENTS.COM

Appendix D: Pro Forma for Scenario Analyses

Year	2012	2013	2014	2015	2016	2017	2018	2019
Income Statement								
Revenue	$ -	$ 6,937,500	$ 13,875,000	$ 20,812,500	$ 27,750,000	$ 27,750,000	$ 27,750,000	$ 27,750,000
Cost of Sales	$ (688,638)	$ (496,914)	$ (494,520)	$ (494,520)	$ (494,520)	$ (494,520)	$ (494,520)	$ (494,520)
Operating Costs, SG&A	$ (1,935,800)	$ (3,154,550)	$ (4,403,300)	$ (5,652,050)	$ (5,652,050)	$ (5,652,050)	$ (5,652,050)	$ (5,652,050)
Depreciation	$ -	$ (39,480)	$ (63,646)	$ (38,666)	$ (23,200)	$ (23,016)	$ (11,646)	$ (138)
Pre-Tax Income	$ (2,624,438)	$ 3,246,557	$ 8,913,534	$ 14,627,264	$ 21,580,230	$ 21,580,414	$ 21,591,784	$ 21,603,292
Taxes (40%)	$ 1,049,775	$ (1,298,623)	$ (3,565,414)	$ (5,850,905)	$ (8,632,092)	$ (8,632,166)	$ (8,636,714)	$ (8,641,317)
Net Income								
Cash Flow Statement								
Cash from Operating Activities								
Plus: Depreciation	$ -	$ 39,480	$ 63,646	$ 38,666	$ 23,200	$ 23,016	$ 11,646	$ 138
WC Change								
(+)/- A/R	$ -	$ (570,205)	$ (570,205)	$ (570,205)	$ (570,205)	$ -	$ -	$ -
(+)/- Inventory	$ (135)	$ (270)	$ -	$ -	$ -	$ -	$ -	$ -
(+)/- A/P	$ 40,241	$ -	$ -	$ -	$ -	$ -	$ -	$ -
(+)/- C/R	$ (171,763)	$ 7,500	$ -	$ -	$ -	$ -	$ -	$ -
Total WC Change	$ (131,656)	$ (562,975)	$ (570,205)	$ (570,205)	$ (570,205)	$ -	$ -	$ -
Cash From Investing Activities								
(Purchase)/Selling of Equipment	$ (197,398)	$ (2,394)	$ -	$ -	$ -	$ -	$ -	$ -
Cash From Financing Activities								
Issuance of Common Stock	$ 970,341	$ 1,000,000	$ -	$ -	$ -	$ -	$ -	$ -
Free Cash Flow	$ (933,376)	$ 2,422,044	$ 4,841,561	$ 8,244,819	$ 12,401,133	$ 12,971,264	$ 12,966,716	$ 12,962,113
% Design Capacity	0%	25%	50%	75%	100%	100%	100%	100%
	Investment				*Divided Free Cash Flows*			
RSCH Stage Investors (39.3% Equity)	$ (970,341)	$ (933,376)	$ 951,370	$ 1,901,748	$ 3,238,535	$ 4,871,120	$ 5,095,065	$ 5,093,279
Sales Stage Investors (60.7% Equity)	$ (1,000,000)	$ -	$ 1,470,674	$ 2,939,814	$ 5,006,284	$ 7,530,013	$ 7,876,199	$ 7,873,438
NPV at 25%	$ 25,516,587							
NPV at 30%	$ 18,507,527							
RSCH Stage MIRR	44%							
Sales Stage MIRR	62%							

R1 Q1 C1 G2

Year	2012	2013	2014	2015	2016	2017	2018	2019
Income Statement								
Revenue	$ -	$ 6,937,500	$ 13,875,000	$ 20,812,500	$ 27,750,000	$ 27,750,000	$ 27,750,000	$ 27,750,000
Cost of Sales	$ (688,638)	$ (496,914)	$ (494,520)	$ (494,520)	$ (494,520)	$ (494,520)	$ (494,520)	$ (494,520)
Operating Costs, SG&A	$ (1,935,800)	$ (3,154,550)	$ (4,403,300)	$ (5,652,050)	$ (5,652,050)	$ (5,652,050)	$ (5,652,050)	$ (5,652,050)
Depreciation	$ -	$ (39,480)	$ (63,646)	$ (38,666)	$ (23,200)	$ (23,016)	$ (11,646)	$ (138)
Pre-Tax Income	$ (2,624,438)	$ 3,246,557	$ 8,913,534	$ 14,627,264	$ 21,580,230	$ 21,580,414	$ 21,591,784	$ 21,603,292
Taxes (40%)	$ 1,049,775	$ (1,298,623)	$ (3,565,414)	$ (5,850,905)	$ (8,632,092)	$ (8,632,166)	$ (8,636,714)	$ (8,641,317)
Net Income								
Cash Flow Statement								
Cash from Operating Activities								
Plus: Depreciation	$ -	$ 39,480	$ 63,646	$ 38,666	$ 23,200	$ 23,016	$ 11,646	$ 138
WC Change								
(+)/- A/R	$ -	$ (570,205)	$ (570,205)	$ (570,205)	$ (570,205)	$ -	$ -	$ -
(+)/- Inventory	$ (135)	$ (270)	$ -	$ -	$ -	$ -	$ -	$ -
(+)/- A/P	$ 40,241	$ -	$ -	$ -	$ -	$ -	$ -	$ -
(+)/- C/R	$ (171,763)	$ 7,500	$ -	$ -	$ -	$ -	$ -	$ -
Total WC Change	$ (131,656)	$ (562,975)	$ (570,205)	$ (570,205)	$ (570,205)	$ -	$ -	$ -
Cash From Investing Activities								
(Purchase)/Selling of Equipment	$ (197,398)	$ (2,394)	$ -	$ -	$ -	$ -	$ -	$ -
Cash From Financing Activities								
Issuance of Common Stock	$ 970,341	$ 1,000,000	$ -	$ -	$ -	$ -	$ -	$ -
Free Cash Flow	$ (933,376)	$ 2,422,044	$ 4,841,561	$ 8,244,819	$ 12,401,133	$ 12,971,264	$ 12,966,716	$ 12,962,113
% Design Capacity	0%	25%	50%	75%	100%	100%	100%	100%
	Investment				*Divided Free Cash Flows*			
RSCH Stage Investors (39.3% Equity)	$ (970,341)	$ (933,376)	$ 951,370	$ 1,901,748	$ 3,238,535	$ 4,871,120	$ 5,095,065	$ 5,093,279
Sales Stage Investors (60.7% Equity)	$ (1,000,000)	$ -	$ 1,470,674	$ 2,939,814	$ 5,006,284	$ 7,530,013	$ 7,876,199	$ 7,873,438
NPV at 25%	$ 24,330,397							
NPV at 30%	$ 17,919,001							
RSCH Stage MIRR	43%							
Sales Stage MIRR	61%							

R1 Q1 C2 G1

Year	2012	2013	2014	2015	2016	2017	2018	2019
Income Statement								
Revenue	$ -	$ 6,937,500	$ 13,875,000	$ 20,812,500	$ 27,750,000	$ 27,750,000	$ 27,750,000	$ 13,875,000
Cost of Sales	$ (688,638)	$ (496,914)	$ (494,520)	$ (494,520)	$ (494,520)	$ (494,520)	$ (494,520)	$ (494,520)
Operating Costs, SG&A	$ (1,935,800)	$ (3,154,550)	$ (4,403,300)	$ (5,652,050)	$ (5,652,050)	$ (5,652,050)	$ (5,652,050)	$ (5,652,050)
Depreciation	$ -	$ (39,480)	$ (63,646)	$ (38,666)	$ (23,200)	$ (23,016)	$ (11,646)	$ (138)
Pre-Tax Income	$ (2,624,438)	$ 3,246,557	$ 8,913,534	$ 14,627,264	$ 21,580,230	$ 21,580,414	$ 21,591,784	$ 7,728,292
Taxes (40%)	$ 1,049,775	$ (1,298,623)	$ (3,565,414)	$ (5,850,905)	$ (8,632,092)	$ (8,632,166)	$ (8,636,714)	$ (3,091,317)
Net Income								
Cash Flow Statement								
Cash from Operating Activities								
Plus: Depreciation	$ -	$ 39,480	$ 63,646	$ 38,666	$ 23,200	$ 23,016	$ 11,646	$ 138
WC Change								
(+)/- A/R	$ -	$ (570,205)	$ (570,205)	$ (570,205)	$ (570,205)	$ -	$ -	$ -
(+)/- Inventory	$ (135)	$ (270)	$ -	$ -	$ -	$ -	$ -	$ -
(+)/- A/P	$ 40,241	$ -	$ -	$ -	$ -	$ -	$ -	$ -
(+)/- C/R	$ (171,763)	$ 7,500	$ -	$ -	$ -	$ -	$ -	$ -
Total WC Change	$ (131,656)	$ (562,975)	$ (570,205)	$ (570,205)	$ (570,205)	$ -	$ -	$ -
Cash From Investing Activities								
(Purchase)/Selling of Equipment	$ (197,398)	$ (2,394)	$ -	$ -	$ -	$ -	$ -	$ -
Cash From Financing Activities								
Issuance of Common Stock	$ 970,341	$ 1,000,000	$ -	$ -	$ -	$ -	$ -	$ -
Free Cash Flow	$ (933,376)	$ 2,422,044	$ 4,841,561	$ 8,244,819	$ 12,401,133	$ 12,971,264	$ 12,966,716	$ 4,637,113
% Design Capacity	0%	25%	50%	75%	100%	100%	100%	100%
	Investment				*Divided Free Cash Flows*			
RSCH Stage Investors (39.3% Equity)	$ (970,341)	$ (933,376)	$ 951,370	$ 1,901,748	$ 3,238,535	$ 4,871,120	$ 5,095,065	$ 5,093,279
Sales Stage Investors (60.7% Equity)	$ (1,000,000)	$ -	$ 1,470,674	$ 2,939,814	$ 5,006,284	$ 7,530,013	$ 7,876,199	$ 7,873,438
NPV at 25%	$ 18,888,595							
NPV at 30%	$ 14,492,171							
RSCH Stage MIRR	37%							
Sales Stage MIRR	54%							

R1 Q1 C2 G2

Year	2012	2013	2014	2015	2016	2017	2018	2019
Income Statement								
Revenue	$ -	$ 6,937,500	$ 13,875,000	$ 20,812,500	$ 27,750,000	$ 27,750,000	$ 27,750,000	$ 13,875,000
Cost of Sales	$ (688,638)	$ (496,914)	$ (494,520)	$ (494,520)	$ (494,520)	$ (494,520)	$ (494,520)	$ (494,520)
Operating Costs, SG&A	$ (1,935,800)	$ (3,154,550)	$ (4,403,300)	$ (5,652,050)	$ (5,652,050)	$ (5,652,050)	$ (5,652,050)	$ (5,652,050)
Depreciation	$ -	$ (39,480)	$ (63,646)	$ (38,666)	$ (23,200)	$ (23,016)	$ (11,646)	$ (138)
Pre-Tax Income	$ (2,624,438)	$ 3,246,557	$ 8,913,534	$ 14,627,264	$ 21,580,230	$ 21,580,414	$ 21,591,784	$ 7,728,292
Taxes (40%)	$ 1,049,775	$ (1,298,623)	$ (3,565,414)	$ (5,850,905)	$ (8,632,092)	$ (8,632,166)	$ (8,636,714)	$ (3,091,317)
Net Income								
Cash Flow Statement								
Cash from Operating Activities								
Plus: Depreciation	$ -	$ 39,480	$ 63,646	$ 38,666	$ 23,200	$ 23,016	$ 11,646	$ 138
WC Change								
(+)/- A/R	$ -	$ (570,205)	$ (570,205)	$ (570,205)	$ (570,205)	$ -	$ -	$ -
(+)/- Inventory	$ (135)	$ (270)	$ -	$ -	$ -	$ -	$ -	$ -
(+)/- A/P	$ 40,241	$ -	$ -	$ -	$ -	$ -	$ -	$ -
(+)/- C/R	$ (171,763)	$ 7,500	$ -	$ -	$ -	$ -	$ -	$ -
Total WC Change	$ (131,656)	$ (562,975)	$ (570,205)	$ (570,205)	$ (570,205)	$ -	$ -	$ -
Cash From Investing Activities								
(Purchase)/Selling of Equipment	$ (197,398)	$ (2,394)	$ -	$ -	$ -	$ -	$ -	$ -
Cash From Financing Activities								
Issuance of Common Stock	$ 970,341	$ 1,000,000	$ -	$ -	$ -	$ -	$ -	$ -
Free Cash Flow	$ (933,376)	$ 2,422,044	$ 4,841,561	$ 8,244,819	$ 12,401,133	$ 12,971,264	$ 12,966,716	$ 4,637,113
% Design Capacity	0%	25%	50%	75%	100%	100%	100%	100%
	Investment				*Divided Free Cash Flows*			
RSCH Stage Investors (39.3% Equity)	$ (970,341)	$ (933,376)	$ 951,370	$ 1,901,748	$ 3,238,535	$ 4,871,120	$ 5,095,065	$ 5,093,279
Sales Stage Investors (60.7% Equity)	$ (1,000,000)	$ -	$ 1,470,674	$ 2,939,814	$ 5,006,284	$ 7,530,013	$ 7,876,199	$ 7,873,438
NPV at 25%	$ 18,464,244							
NPV at 30%	$ 14,281,630							
RSCH Stage MIRR	36%							
Sales Stage MIRR	53%							

R1 Q1 C3 G1

Year	2012	2013	2014	2015	2016	2017	2018	2019
Income Statement								
Revenue	$ -	$ 6,937,500	$ 13,875,000	$ 20,812,500	$ 27,750,000	$ 27,750,000	$ 27,750,000	$ -
Cost of Sales	$ (688,638)	$ (496,914)	$ (494,520)	$ (494,520)	$ (494,520)	$ (494,520)	$ (494,520)	$ (494,520)
Operating Costs, SG&A	$ (1,935,800)	$ (3,154,550)	$ (4,403,300)	$ (5,652,050)	$ (5,652,050)	$ (5,652,050)	$ (5,652,050)	$ (5,652,050)
Depreciation	$ -	$ (39,480)	$ (63,646)	$ (38,666)	$ (23,200)	$ (23,016)	$ (11,646)	$ (138)
Pre-Tax Income	$ (2,624,438)	$ 3,246,557	$ 8,913,534	$ 14,627,264	$ 21,580,230	$ 21,580,414	$ 21,591,784	$ (6,146,708)
Taxes (40%)	$ 1,049,775	$ (1,298,623)	$ (3,565,414)	$ (5,850,905)	$ (8,632,092)	$ (8,632,166)	$ (8,636,714)	$ 2,458,683
Net Income								
Cash Flow Statement								
Cash from Operating Activities								
Plus: Depreciation	$ -	$ 39,480	$ 63,646	$ 38,666	$ 23,200	$ 23,016	$ 11,646	$ 138
WC Change								
(+)/- A/R	$ -	$ (570,205)	$ (570,205)	$ (570,205)	$ (570,205)	$ -	$ -	$ -
(+)/- Inventory	$ (135)	$ (270)	$ -	$ -	$ -	$ -	$ -	$ -
(+)/- A/P	$ 40,241	$ -	$ -	$ -	$ -	$ -	$ -	$ -
(+)/- C/R	$ (171,763)	$ 7,500	$ -	$ -	$ -	$ -	$ -	$ -
Total WC Change	$ (131,656)	$ (562,975)	$ (570,205)	$ (570,205)	$ (570,205)	$ -	$ -	$ -
Cash From Investing Activities								
(Purchase)/Selling of Equipment	$ (197,398)	$ (2,394)	$ -	$ -	$ -	$ -	$ -	$ -
Cash From Financing Activities								
Issuance of Common Stock	$ 970,341	$ 1,000,000	$ -	$ -	$ -	$ -	$ -	$ -
Free Cash Flow	$ (933,376)	$ 2,422,044	$ 4,841,561	$ 8,244,819	$ 12,401,133	$ 12,971,264	$ 12,966,716	$ (3,687,887)
% Design Capacity	0%	25%	50%	75%	100%	100%	100%	100%
	Investment				*Divided Free Cash Flows*			
RSCH Stage Investors (39.3% Equity)	$ (970,341)	$ (933,376)	$ 951,370	$ 1,901,748	$ 3,238,535	$ 4,871,120	$ 5,095,065	$ 5,093,279
Sales Stage Investors (60.7% Equity)	$ (1,000,000)	$ -	$ 1,470,674	$ 2,939,814	$ 5,006,284	$ 7,530,013	$ 7,876,199	$ 7,873,438
NPV at 25%	$ 12,260,604							
NPV at 30%	$ 10,476,816							
RSCH Stage MIRR	12%							
Sales Stage MIRR	11%							

R1 Q1 C3 G2

Year	2012	2013	2014	2015	2016	2017	2018	2019
Income Statement								
Revenue	$ -	$ 6,937,500	$ 13,875,000	$ 20,812,500	$ 27,750,000	$ 27,750,000	$ 27,750,000	$ -
Cost of Sales	$ (688,638)	$ (496,914)	$ (494,520)	$ (494,520)	$ (494,520)	$ (494,520)	$ (494,520)	$ (494,520)
Operating Costs, SG&A	$ (1,935,800)	$ (3,154,550)	$ (4,403,300)	$ (5,652,050)	$ (5,652,050)	$ (5,652,050)	$ (5,652,050)	$ (5,652,050)
Depreciation	$ -	$ (39,480)	$ (63,646)	$ (38,666)	$ (23,200)	$ (23,016)	$ (11,646)	$ (138)
Pre-Tax Income	$ (2,624,438)	$ 3,246,557	$ 8,913,534	$ 14,627,264	$ 21,580,230	$ 21,580,414	$ 21,591,784	$ (6,146,708)
Taxes (40%)	$ 1,049,775	$ (1,298,623)	$ (3,565,414)	$ (5,850,905)	$ (8,632,092)	$ (8,632,166)	$ (8,636,714)	$ 2,458,683
Net Income								
Cash Flow Statement								
Cash from Operating Activities								
Plus: Depreciation	$ -	$ 39,480	$ 63,646	$ 38,666	$ 23,200	$ 23,016	$ 11,646	$ 138
WC Change								
(+)/- A/R	$ -	$ (570,205)	$ (570,205)	$ (570,205)	$ (570,205)	$ -	$ -	$ -
(+)/- Inventory	$ (135)	$ (270)	$ -	$ -	$ -	$ -	$ -	$ -
(+)/- A/P	$ 40,241	$ -	$ -	$ -	$ -	$ -	$ -	$ -
(+)/- C/R	$ (171,763)	$ 7,500	$ -	$ -	$ -	$ -	$ -	$ -
Total WC Change	$ (131,656)	$ (562,975)	$ (570,205)	$ (570,205)	$ (570,205)	$ -	$ -	$ -
Cash From Investing Activities								
(Purchase)/Selling of Equipment	$ (197,398)	$ (2,394)	$ -	$ -	$ -	$ -	$ -	$ -
Cash From Financing Activities								
Issuance of Common Stock	$ 970,341	$ 1,000,000	$ -	$ -	$ -	$ -	$ -	$ -
Free Cash Flow	$ (933,376)	$ 2,422,044	$ 4,841,561	$ 8,244,819	$ 12,401,133	$ 12,971,264	$ 12,966,716	$ (3,687,887)
% Design Capacity	0%	25%	50%	75%	100%	100%	100%	100%
	Investment				*Divided Free Cash Flows*			
RSCH Stage Investors (39.3% Equity)	$ (970,341)	$ (933,376)	$ 951,370	$ 1,901,748	$ 3,238,535	$ 4,871,120	$ 5,095,065	$ 5,093,279
Sales Stage Investors (60.7% Equity)	$ (1,000,000)	$ -	$ 1,470,674	$ 2,939,814	$ 5,006,284	$ 7,530,013	$ 7,876,199	$ 7,873,438
NPV at 25%	$ 12,598,090							
NPV at 30%	$ 10,644,259							
RSCH Stage MIRR	13%							
Sales Stage MIRR	12%							

R1 Q2 C1 G1

Year	2012	2013	2014	2015	2016	2017	2018	2019
Income Statement								
Revenue	$ -	$ 5,100,000	$ 10,200,000	$ 15,300,000	$ 20,400,000	$ 20,400,000	$ 20,400,000	$ 20,400,000
Cost of Sales	$ (688,638)	$ (496,914)	$ (494,520)	$ (494,520)	$ (494,520)	$ (494,520)	$ (494,520)	$ (494,520)
Operating Costs, SG&A	$ (1,605,050)	$ (2,493,050)	$ (3,411,050)	$ (4,329,050)	$ (4,329,050)	$ (4,329,050)	$ (4,329,050)	$ (4,329,050)
Depreciation	$ -	$ (39,480)	$ (63,646)	$ (38,666)	$ (23,200)	$ (23,016)	$ (11,646)	$ (138)
Pre-Tax Income	$ (2,293,688)	$ 2,070,557	$ 6,230,784	$ 10,437,764	$ 15,553,230	$ 15,553,414	$ 15,564,784	$ 15,576,292
Taxes (40%)	$ 917,475	$ (828,223)	$ (2,492,314)	$ (4,175,105)	$ (6,221,292)	$ (6,221,366)	$ (6,225,914)	$ (6,230,517)
Net Income								
Cash Flow Statement								
Cash from Operating Activities								
Plus: Depreciation	$ -	$ 39,480	$ 63,646	$ 38,666	$ 23,200	$ 23,016	$ 11,646	$ 138
WC Change								
(+)/- A/R	$ -	$ (419,178)	$ (419,178)	$ (419,178)	$ (419,178)	$ -	$ -	$ -
(+)/- Inventory	$ (135)	$ (270)	$ -	$ -	$ -	$ -	$ -	$ -
(+)/- A/P	$ 40,241	$ -	$ -	$ -	$ -	$ -	$ -	$ -
(+)/- C/R	$ (171,763)	$ 7,500	$ -	$ -	$ -	$ -	$ -	$ -
Total WC Change	$ (131,656)	$ (411,948)	$ (419,178)	$ (419,178)	$ (419,178)	$ -	$ -	$ -
Cash From Investing Activities								
(Purchase)/Selling of Equipment	$ (197,398)	$ (2,394)	$ -	$ -	$ -	$ -	$ -	$ -
Cash From Financing Activities								
Issuance of Common Stock	$ 970,341	$ 1,000,000	$ -	$ -	$ -	$ -	$ -	$ -
Free Cash Flow	$ (734,926)	$ 1,867,472	$ 3,382,938	$ 5,882,147	$ 8,935,960	$ 9,355,064	$ 9,350,516	$ 9,345,913
% Design Capacity	0%	25%	50%	75%	100%	100%	100%	100%
	Investment				*Divided Free Cash Flows*			
RSCH Stage Investors (39.3% Equity)	$ (970,341)	$ (734,926)	$ 733,536	$ 1,328,806	$ 2,310,486	$ 3,510,012	$ 3,674,635	$ 3,672,849
Sales Stage Investors (60.7% Equity)	$ (1,000,000)	$ -	$ 1,133,936	$ 2,054,133	$ 3,571,661	$ 5,425,947	$ 5,680,429	$ 5,677,668
NPV at 25%	$ 17,858,534							
NPV at 30%	$ 12,817,578							
RSCH Stage MIRR	41%							
Sales Stage MIRR	56%							

R1 Q2 C1 G2

Year	2012	2013	2014	2015	2016	2017	2018	2019
Income Statement								
Revenue	$ -	$ 5,100,000	$ 10,200,000	$ 15,300,000	$ 20,400,000	$ 20,400,000	$ 20,400,000	$ 20,400,000
Cost of Sales	$ (688,638)	$ (496,914)	$ (494,520)	$ (494,520)	$ (494,520)	$ (494,520)	$ (494,520)	$ (494,520)
Operating Costs, SG&A	$ (1,605,050)	$ (2,493,050)	$ (3,411,050)	$ (4,329,050)	$ (4,329,050)	$ (4,329,050)	$ (4,329,050)	$ (4,329,050)
Depreciation	$ -	$ (39,480)	$ (63,646)	$ (38,666)	$ (23,200)	$ (23,016)	$ (11,646)	$ (138)
Pre-Tax Income	$ (2,293,688)	$ 2,070,557	$ 6,230,784	$ 10,437,764	$ 15,553,230	$ 15,553,414	$ 15,564,784	$ 15,576,292
Taxes (40%)	$ 917,475	$ (828,223)	$ (2,492,314)	$ (4,175,105)	$ (6,221,292)	$ (6,221,366)	$ (6,225,914)	$ (6,230,517)
Net Income								
Cash Flow Statement								
Cash from Operating Activities								
Plus: Depreciation	$ -	$ 39,480	$ 63,646	$ 38,666	$ 23,200	$ 23,016	$ 11,646	$ 138
WC Change								
(+)/- A/R	$ -	$ (419,178)	$ (419,178)	$ (419,178)	$ (419,178)	$ -	$ -	$ -
(+)/- Inventory	$ (135)	$ (270)	$ -	$ -	$ -	$ -	$ -	$ -
(+)/- A/P	$ 40,241	$ -	$ -	$ -	$ -	$ -	$ -	$ -
(+)/- C/R	$ (171,763)	$ 7,500	$ -	$ -	$ -	$ -	$ -	$ -
Total WC Change	$ (131,656)	$ (411,948)	$ (419,178)	$ (419,178)	$ (419,178)	$ -	$ -	$ -
Cash From Investing Activities								
(Purchase)/Selling of Equipment	$ (197,398)	$ (2,394)	$ -	$ -	$ -	$ -	$ -	$ -
Cash From Financing Activities								
Issuance of Common Stock	$ 970,341	$ 1,000,000	$ -	$ -	$ -	$ -	$ -	$ -
Free Cash Flow	$ (734,926)	$ 1,867,472	$ 3,382,938	$ 5,882,147	$ 8,935,960	$ 9,355,064	$ 9,350,516	$ 9,345,913
% Design Capacity	0%	25%	50%	75%	100%	100%	100%	100%
	Investment				*Divided Free Cash Flows*			
RSCH Stage Investors (39.3% Equity)	$ (970,341)	$ (734,926)	$ 733,536	$ 1,328,806	$ 2,310,486	$ 3,510,012	$ 3,674,635	$ 3,672,849
Sales Stage Investors (60.7% Equity)	$ (1,000,000)	$ -	$ 1,133,936	$ 2,054,133	$ 3,571,661	$ 5,425,947	$ 5,680,429	$ 5,677,668
NPV at 25%	$ 17,003,270							
NPV at 30%	$ 12,393,241							
RSCH Stage MIRR	40%							
Sales Stage MIRR	55%							

R1 Q2 C2 G1

Year	2012	2013	2014	2015	2016	2017	2018	2019
Income Statement								
Revenue	$ -	$ 5,100,000	$ 10,200,000	$ 15,300,000	$ 20,400,000	$ 20,400,000	$ 20,400,000	$ 10,200,000
Cost of Sales	$ (688,638)	$ (496,914)	$ (494,520)	$ (494,520)	$ (494,520)	$ (494,520)	$ (494,520)	$ (494,520)
Operating Costs, SG&A	$ (1,605,050)	$ (2,493,050)	$ (3,411,050)	$ (4,329,050)	$ (4,329,050)	$ (4,329,050)	$ (4,329,050)	$ (4,329,050)
Depreciation	$ -	$ (39,480)	$ (63,646)	$ (38,666)	$ (23,200)	$ (23,016)	$ (11,646)	$ (138)
Pre-Tax Income	$ (2,293,688)	$ 2,070,557	$ 6,230,784	$ 10,437,764	$ 15,553,230	$ 15,553,414	$ 15,564,784	$ 5,376,292
Taxes (40%)	$ 917,475	$ (828,223)	$ (2,492,314)	$ (4,175,105)	$ (6,221,292)	$ (6,221,366)	$ (6,225,914)	$ (2,150,517)
Net Income								
Cash Flow Statement								
Cash from Operating Activities								
Plus: Depreciation	$ -	$ 39,480	$ 63,646	$ 38,666	$ 23,200	$ 23,016	$ 11,646	$ 138
WC Change								
(+)/- A/R	$ -	$ (419,178)	$ (419,178)	$ (419,178)	$ (419,178)	$ -	$ -	$ -
(+)/- Inventory	$ (135)	$ (270)	$ -	$ -	$ -	$ -	$ -	$ -
(+)/- A/P	$ 40,241	$ -	$ -	$ -	$ -	$ -	$ -	$ -
(+)/- C/R	$ (171,763)	$ 7,500	$ -	$ -	$ -	$ -	$ -	$ -
Total WC Change	$ (131,656)	$ (411,948)	$ (419,178)	$ (419,178)	$ (419,178)	$ -	$ -	$ -
Cash From Investing Activities								
(Purchase)/Selling of Equipment	$ (197,398)	$ (2,394)	$ -	$ -	$ -	$ -	$ -	$ -
Cash From Financing Activities								
Issuance of Common Stock	$ 970,341	$ 1,000,000	$ -	$ -	$ -	$ -	$ -	$ -
Free Cash Flow	$ (734,926)	$ 1,867,472	$ 3,382,938	$ 5,882,147	$ 8,935,960	$ 9,355,064	$ 9,350,516	$ 3,225,913
% Design Capacity	0%	25%	50%	75%	100%	100%	100%	100%
	Investment				*Divided Free Cash Flows*			
RSCH Stage Investors (39.3% Equity)	$ (970,341)	$ (734,926)	$ 733,536	$ 1,328,806	$ 2,310,486	$ 3,510,012	$ 3,674,635	$ 3,672,849
Sales Stage Investors (60.7% Equity)	$ (1,000,000)	$ -	$ 1,133,936	$ 2,054,133	$ 3,571,661	$ 5,425,947	$ 5,680,429	$ 5,677,668
NPV at 25%	$ 12,986,064							
NPV at 30%	$ 9,865,749							
RSCH Stage MIRR	34%							
Sales Stage MIRR	48%							

R1 Q2 C2 G2

Year	2012	2013	2014	2015	2016	2017	2018	2019
Income Statement								
Revenue	$ -	$ 5,100,000	$ 10,200,000	$ 15,300,000	$ 20,400,000	$ 20,400,000	$ 20,400,000	$ 10,200,000
Cost of Sales	$ (688,638)	$ (496,914)	$ (494,520)	$ (494,520)	$ (494,520)	$ (494,520)	$ (494,520)	$ (494,520)
Operating Costs, SG&A	$ (1,605,050)	$ (2,493,050)	$ (3,411,050)	$ (4,329,050)	$ (4,329,050)	$ (4,329,050)	$ (4,329,050)	$ (4,329,050)
Depreciation	$ -	$ (39,480)	$ (63,646)	$ (38,666)	$ (23,200)	$ (23,016)	$ (11,646)	$ (138)
Pre-Tax Income	$ (2,293,688)	$ 2,070,557	$ 6,230,784	$ 10,437,764	$ 15,553,230	$ 15,553,414	$ 15,564,784	$ 5,376,292
Taxes (40%)	$ 917,475	$ (828,223)	$ (2,492,314)	$ (4,175,105)	$ (6,221,292)	$ (6,221,366)	$ (6,225,914)	$ (2,150,517)
Net Income								
Cash Flow Statement								
Cash from Operating Activities								
Plus: Depreciation	$ -	$ 39,480	$ 63,646	$ 38,666	$ 23,200	$ 23,016	$ 11,646	$ 138
WC Change								
(+)/- A/R	$ -	$ (419,178)	$ (419,178)	$ (419,178)	$ (419,178)	$ -	$ -	$ -
(+)/- Inventory	$ (135)	$ (270)	$ -	$ -	$ -	$ -	$ -	$ -
(+)/- A/P	$ 40,241	$ -	$ -	$ -	$ -	$ -	$ -	$ -
(+)/- C/R	$ (171,763)	$ 7,500	$ -	$ -	$ -	$ -	$ -	$ -
Total WC Change	$ (131,656)	$ (411,948)	$ (419,178)	$ (419,178)	$ (419,178)	$ -	$ -	$ -
Cash From Investing Activities								
(Purchase)/Selling of Equipment	$ (197,398)	$ (2,394)	$ -	$ -	$ -	$ -	$ -	$ -
Cash From Financing Activities								
Issuance of Common Stock	$ 970,341	$ 1,000,000	$ -	$ -	$ -	$ -	$ -	$ -
Free Cash Flow	$ (734,926)	$ 1,867,472	$ 3,382,938	$ 5,882,147	$ 8,935,960	$ 9,355,064	$ 9,350,516	$ 3,225,913
% Design Capacity	0%	25%	50%	75%	100%	100%	100%	100%
	Investment				*Divided Free Cash Flows*			
RSCH Stage Investors (39.3% Equity)	$ (970,341)	$ (734,926)	$ 733,536	$ 1,328,806	$ 2,310,486	$ 3,510,012	$ 3,674,635	$ 3,672,849
Sales Stage Investors (60.7% Equity)	$ (1,000,000)	$ -	$ 1,133,936	$ 2,054,133	$ 3,571,661	$ 5,425,947	$ 5,680,429	$ 5,677,668
NPV at 25%	$ 12,690,854							
NPV at 30%	$ 9,719,281							
RSCH Stage MIRR	33%							
Sales Stage MIRR	48%							

R1 Q2 C3 G1

Year	2012	2013	2014	2015	2016	2017	2018	2019
Income Statement								
Revenue	$ -	$ 5,100,000	$ 10,200,000	$ 15,300,000	$ 20,400,000	$ 20,400,000	$ 20,400,000	$ -
Cost of Sales	$ (688,638)	$ (496,914)	$ (494,520)	$ (494,520)	$ (494,520)	$ (494,520)	$ (494,520)	$ (494,520)
Operating Costs, SG&A	$ (1,605,050)	$ (2,493,050)	$ (3,411,050)	$ (4,329,050)	$ (4,329,050)	$ (4,329,050)	$ (4,329,050)	$ (4,329,050)
Depreciation	$ -	$ (39,480)	$ (63,646)	$ (38,666)	$ (23,200)	$ (23,016)	$ (11,646)	$ (138)
Pre-Tax Income	$ (2,293,688)	$ 2,070,557	$ 6,230,784	$ 10,437,764	$ 15,553,230	$ 15,553,414	$ 15,564,784	$ (4,823,708)
Taxes (40%)	$ 917,475	$ (828,223)	$ (2,492,314)	$ (4,175,105)	$ (6,221,292)	$ (6,221,366)	$ (6,225,914)	$ 1,929,483
Net Income								
Cash Flow Statement								
Cash from Operating Activities								
Plus: Depreciation	$ -	$ 39,480	$ 63,646	$ 38,666	$ 23,200	$ 23,016	$ 11,646	$ 138
WC Change								
(+)/- A/R	$ -	$ (419,178)	$ (419,178)	$ (419,178)	$ (419,178)	$ -	$ -	$ -
(+)/- Inventory	$ (135)	$ (270)	$ -	$ -	$ -	$ -	$ -	$ -
(+)/- A/P	$ 40,241	$ -	$ -	$ -	$ -	$ -	$ -	$ -
(+)/- C/R	$ (171,763)	$ 7,500	$ -	$ -	$ -	$ -	$ -	$ -
Total WC Change	$ (131,656)	$ (411,948)	$ (419,178)	$ (419,178)	$ (419,178)	$ -	$ -	$ -
Cash From Investing Activities								
(Purchase)/Selling of Equipment	$ (197,398)	$ (2,394)	$ -	$ -	$ -	$ -	$ -	$ -
Cash From Financing Activities								
Issuance of Common Stock	$ 970,341	$ 1,000,000	$ -	$ -	$ -	$ -	$ -	$ -
Free Cash Flow	$ (734,926)	$ 1,867,472	$ 3,382,938	$ 5,882,147	$ 8,935,960	$ 9,355,064	$ 9,350,516	$ (2,894,087)
% Design Capacity	0%	25%	50%	75%	100%	100%	100%	100%
	Investment				*Divided Free Cash Flows*			
RSCH Stage Investors (39.3% Equity)	$ (970,341)	$ (734,926)	$ 733,536	$ 1,328,806	$ 2,310,486	$ 3,510,012	$ 3,674,635	$ 3,672,849
Sales Stage Investors (60.7% Equity)	$ (1,000,000)	$ -	$ 1,133,936	$ 2,054,133	$ 3,571,661	$ 5,425,947	$ 5,680,429	$ 5,677,668
NPV at 25%	$ 8,113,595							
NPV at 30%	$ 6,913,920							
RSCH Stage MIRR	10%							
Sales Stage MIRR	9%							

R1 Q2 C3 G2

Year	2012	2013	2014	2015	2016	2017	2018	2019
Income Statement								
Revenue	$ -	$ 5,100,000	$ 10,200,000	$ 15,300,000	$ 20,400,000	$ 20,400,000	$ 20,400,000	$ -
Cost of Sales	$ (688,638)	$ (496,914)	$ (494,520)	$ (494,520)	$ (494,520)	$ (494,520)	$ (494,520)	$ (494,520)
Operating Costs, SG&A	$ (1,605,050)	$ (2,493,050)	$ (3,411,050)	$ (4,329,050)	$ (4,329,050)	$ (4,329,050)	$ (4,329,050)	$ (4,329,050)
Depreciation	$ -	$ (39,480)	$ (63,646)	$ (38,666)	$ (23,200)	$ (23,016)	$ (11,646)	$ (138)
Pre-Tax Income	$ (2,293,688)	$ 2,070,557	$ 6,230,784	$ 10,437,764	$ 15,553,230	$ 15,553,414	$ 15,564,784	$ (4,823,708)
Taxes (40%)	$ 917,475	$ (828,223)	$ (2,492,314)	$ (4,175,105)	$ (6,221,292)	$ (6,221,366)	$ (6,225,914)	$ 1,929,483
Net Income								
Cash Flow Statement								
Cash from Operating Activities								
Plus: Depreciation	$ -	$ 39,480	$ 63,646	$ 38,666	$ 23,200	$ 23,016	$ 11,646	$ 138
WC Change								
(+)/- A/R	$ -	$ (419,178)	$ (419,178)	$ (419,178)	$ (419,178)	$ -	$ -	$ -
(+)/- Inventory	$ (135)	$ (270)	$ -	$ -	$ -	$ -	$ -	$ -
(+)/- A/P	$ 40,241	$ -	$ -	$ -	$ -	$ -	$ -	$ -
(+)/- C/R	$ (171,763)	$ 7,500	$ -	$ -	$ -	$ -	$ -	$ -
Total WC Change	$ (131,656)	$ (411,948)	$ (419,178)	$ (419,178)	$ (419,178)	$ -	$ -	$ -
Cash From Investing Activities								
(Purchase)/Selling of Equipment	$ (197,398)	$ (2,394)	$ -	$ -	$ -	$ -	$ -	$ -
Cash From Financing Activities								
Issuance of Common Stock	$ 970,341	$ 1,000,000	$ -	$ -	$ -	$ -	$ -	$ -
Free Cash Flow	$ (734,926)	$ 1,867,472	$ 3,382,938	$ 5,882,147	$ 8,935,960	$ 9,355,064	$ 9,350,516	$ (2,894,087)
% Design Capacity	0%	25%	50%	75%	100%	100%	100%	100%
	Investment				*Divided Free Cash Flows*			
RSCH Stage Investors (39.3% Equity)	$ (970,341)	$ (734,926)	$ 733,536	$ 1,328,806	$ 2,310,486	$ 3,510,012	$ 3,674,635	$ 3,672,849
Sales Stage Investors (60.7% Equity)	$ (1,000,000)	$ -	$ 1,133,936	$ 2,054,133	$ 3,571,661	$ 5,425,947	$ 5,680,429	$ 5,677,668
NPV at 25%	$ 8,378,439							
NPV at 30%	$ 7,045,322							
RSCH Stage MIRR	11%							
Sales Stage MIRR	11%							

R1 Q3 C1 G1

Year	2012	2013	2014	2015	2016	2017	2018	2019
Income Statement								
Revenue	$ -	$ 3,787,500	$ 7,575,000	$ 11,362,500	$ 15,150,000	$ 15,150,000	$ 15,150,000	$ 15,150,000
Cost of Sales	$ (688,638)	$ (496,914)	$ (494,520)	$ (494,520)	$ (494,520)	$ (494,520)	$ (494,520)	$ (494,520)
Operating Costs, SG&A	$ (1,368,800)	$ (2,020,550)	$ (2,702,300)	$ (3,384,050)	$ (3,384,050)	$ (3,384,050)	$ (3,384,050)	$ (3,384,050)
Depreciation	$ -	$ (39,480)	$ (63,646)	$ (38,666)	$ (23,200)	$ (23,016)	$ (11,646)	$ (138)
Pre-Tax Income	$ (2,057,438)	$ 1,230,557	$ 4,314,534	$ 7,445,264	$ 11,248,230	$ 11,248,414	$ 11,259,784	$ 11,271,292
Taxes (40%)	$ 822,975	$ (492,223)	$ (1,725,814)	$ (2,978,105)	$ (4,499,292)	$ (4,499,366)	$ (4,503,914)	$ (4,508,517)
Net Income								
Cash Flow Statement								
Cash from Operating Activities								
Plus: Depreciation	$ -	$ 39,480	$ 63,646	$ 38,666	$ 23,200	$ 23,016	$ 11,646	$ 138
WC Change								
(+)/- A/R	$ -	$ (311,301)	$ (311,301)	$ (311,301)	$ (311,301)	$ -	$ -	$ -
(+)/- Inventory	$ (135)	$ (270)	$ -	$ -	$ -	$ -	$ -	$ -
(+)/- A/P	$ 40,241	$ -	$ -	$ -	$ -	$ -	$ -	$ -
(+)/- C/R	$ (171,763)	$ 7,500	$ -	$ -	$ -	$ -	$ -	$ -
Total WC Change	$ (131,656)	$ (304,071)	$ (311,301)	$ (311,301)	$ (311,301)	$ -	$ -	$ -
Cash From Investing Activities								
(Purchase)/Selling of Equipment	$ (197,398)	$ (2,394)	$ -	$ -	$ -	$ -	$ -	$ -
Cash From Financing Activities								
Issuance of Common Stock	$ 970,341	$ 1,000,000	$ -	$ -	$ -	$ -	$ -	$ -
Free Cash Flow	$ (593,176)	$ 1,471,349	$ 2,341,065	$ 4,194,523	$ 6,460,837	$ 6,772,064	$ 6,767,516	$ 6,762,913
% Design Capacity	0%	25%	50%	75%	100%	100%	100%	100%
	Investment				*Divided Free Cash Flows*			
RSCH Stage Investors (39.3% Equity)	$ (970,341)	$ (593,176)	$ 577,940	$ 919,562	$ 1,647,593	$ 2,537,793	$ 2,660,042	$ 2,658,256
Sales Stage Investors (60.7% Equity)	$ (1,000,000)	$ -	$ 893,408	$ 1,421,503	$ 2,546,930	$ 3,923,044	$ 4,112,022	$ 4,109,261
NPV at 25%	$ 12,388,496							
NPV at 30%	$ 8,753,329							
RSCH Stage MIRR	37%							
Sales Stage MIRR	51%							

R1 Q3 C1 G2

Year	2012	2013	2014	2015	2016	2017	2018	2019
Income Statement								
Revenue	$ -	$ 3,787,500	$ 7,575,000	$ 11,362,500	$ 15,150,000	$ 15,150,000	$ 15,150,000	$ 15,150,000
Cost of Sales	$ (688,638)	$ (496,914)	$ (494,520)	$ (494,520)	$ (494,520)	$ (494,520)	$ (494,520)	$ (494,520)
Operating Costs, SG&A	$ (1,368,800)	$ (2,020,550)	$ (2,702,300)	$ (3,384,050)	$ (3,384,050)	$ (3,384,050)	$ (3,384,050)	$ (3,384,050)
Depreciation	$ -	$ (39,480)	$ (63,646)	$ (38,666)	$ (23,200)	$ (23,016)	$ (11,646)	$ (138)
Pre-Tax Income	$ (2,057,438)	$ 1,230,557	$ 4,314,534	$ 7,445,264	$ 11,248,230	$ 11,248,414	$ 11,259,784	$ 11,271,292
Taxes (40%)	$ 822,975	$ (492,223)	$ (1,725,814)	$ (2,978,105)	$ (4,499,292)	$ (4,499,366)	$ (4,503,914)	$ (4,508,517)
Net Income								
Cash Flow Statement								
Cash from Operating Activities								
Plus: Depreciation	$ -	$ 39,480	$ 63,646	$ 38,666	$ 23,200	$ 23,016	$ 11,646	$ 138
WC Change								
(+)/- A/R	$ -	$ (311,301)	$ (311,301)	$ (311,301)	$ (311,301)	$ -	$ -	$ -
(+)/- Inventory	$ (135)	$ (270)	$ -	$ -	$ -	$ -	$ -	$ -
(+)/- A/P	$ 40,241	$ -	$ -	$ -	$ -	$ -	$ -	$ -
(+)/- C/R	$ (171,763)	$ 7,500	$ -	$ -	$ -	$ -	$ -	$ -
Total WC Change	$ (131,656)	$ (304,071)	$ (311,301)	$ (311,301)	$ (311,301)	$ -	$ -	$ -
Cash From Investing Activities								
(Purchase)/Selling of Equipment	$ (197,398)	$ (2,394)	$ -	$ -	$ -	$ -	$ -	$ -
Cash From Financing Activities								
Issuance of Common Stock	$ 970,341	$ 1,000,000	$ -	$ -	$ -	$ -	$ -	$ -
Free Cash Flow	$ (593,176)	$ 1,471,349	$ 2,341,065	$ 4,194,523	$ 6,460,837	$ 6,772,064	$ 6,767,516	$ 6,762,913
% Design Capacity	0%	25%	50%	75%	100%	100%	100%	100%
	Investment				*Divided Free Cash Flows*			
RSCH Stage Investors (39.3% Equity)	$ (970,341)	$ (593,176)	$ 577,940	$ 919,562	$ 1,647,593	$ 2,537,793	$ 2,660,042	$ 2,658,256
Sales Stage Investors (60.7% Equity)	$ (1,000,000)	$ -	$ 893,408	$ 1,421,503	$ 2,546,930	$ 3,923,044	$ 4,112,022	$ 4,109,261
NPV at 25%	$ 11,769,608							
NPV at 30%	$ 8,446,269							
RSCH Stage MIRR	36%							
Sales Stage MIRR	50%							

R1 Q3 C2 G1

Year	2012	2013	2014	2015	2016	2017	2018	2019
Income Statement								
Revenue	$ -	$ 3,787,500	$ 7,575,000	$ 11,362,500	$ 15,150,000	$ 15,150,000	$ 15,150,000	$ 7,575,000
Cost of Sales	$ (688,638)	$ (496,914)	$ (494,520)	$ (494,520)	$ (494,520)	$ (494,520)	$ (494,520)	$ (494,520)
Operating Costs, SG&A	$ (1,368,800)	$ (2,020,550)	$ (2,702,300)	$ (3,384,050)	$ (3,384,050)	$ (3,384,050)	$ (3,384,050)	$ (3,384,050)
Depreciation	$ -	$ (39,480)	$ (63,646)	$ (38,666)	$ (23,200)	$ (23,016)	$ (11,646)	$ (138)
Pre-Tax Income	$ (2,057,438)	$ 1,230,557	$ 4,314,534	$ 7,445,264	$ 11,248,230	$ 11,248,414	$ 11,259,784	$ 3,696,292
Taxes (40%)	$ 822,975	$ (492,223)	$ (1,725,814)	$ (2,978,105)	$ (4,499,292)	$ (4,499,366)	$ (4,503,914)	$ (1,478,517)
Net Income								
Cash Flow Statement								
Cash from Operating Activities								
Plus: Depreciation	$ -	$ 39,480	$ 63,646	$ 38,666	$ 23,200	$ 23,016	$ 11,646	$ 138
WC Change								
(+)/- A/R	$ -	$ (311,301)	$ (311,301)	$ (311,301)	$ (311,301)	$ -	$ -	$ -
(+)/- Inventory	$ (135)	$ (270)	$ -	$ -	$ -	$ -	$ -	$ -
(+)/- A/P	$ 40,241	$ -	$ -	$ -	$ -	$ -	$ -	$ -
(+)/- C/R	$ (171,763)	$ 7,500	$ -	$ -	$ -	$ -	$ -	$ -
Total WC Change	$ (131,656)	$ (304,071)	$ (311,301)	$ (311,301)	$ (311,301)	$ -	$ -	$ -
Cash From Investing Activities								
(Purchase)/Selling of Equipment	$ (197,398)	$ (2,394)	$ -	$ -	$ -	$ -	$ -	$ -
Cash From Financing Activities								
Issuance of Common Stock	$ 970,341	$ 1,000,000	$ -	$ -	$ -	$ -	$ -	$ -
Free Cash Flow	$ (593,176)	$ 1,471,349	$ 2,341,065	$ 4,194,523	$ 6,460,837	$ 6,772,064	$ 6,767,516	$ 2,217,913
% Design Capacity	0%	25%	50%	75%	100%	100%	100%	100%
	Investment				*Divided Free Cash Flows*			
RSCH Stage Investors (39.3% Equity)	$ (970,341)	$ (593,176)	$ 577,940	$ 919,562	$ 1,647,593	$ 2,537,793	$ 2,660,042	$ 2,658,256
Sales Stage Investors (60.7% Equity)	$ (1,000,000)	$ -	$ 893,408	$ 1,421,503	$ 2,546,930	$ 3,923,044	$ 4,112,022	$ 4,109,261
NPV at 25%	$ 8,769,971							
NPV at 30%	$ 6,561,162							
RSCH Stage MIRR	30%							
Sales Stage MIRR	43%							

R1 Q3 C2 G2

Year	2012	2013	2014	2015	2016	2017	2018	2019
Income Statement								
Revenue	$ -	$ 3,787,500	$ 7,575,000	$ 11,362,500	$ 15,150,000	$ 15,150,000	$ 15,150,000	$ 7,575,000
Cost of Sales	$ (688,638)	$ (496,914)	$ (494,520)	$ (494,520)	$ (494,520)	$ (494,520)	$ (494,520)	$ (494,520)
Operating Costs, SG&A	$ (1,368,800)	$ (2,020,550)	$ (2,702,300)	$ (3,384,050)	$ (3,384,050)	$ (3,384,050)	$ (3,384,050)	$ (3,384,050)
Depreciation	$ -	$ (39,480)	$ (63,646)	$ (38,666)	$ (23,200)	$ (23,016)	$ (11,646)	$ (138)
Pre-Tax Income	$ (2,057,438)	$ 1,230,557	$ 4,314,534	$ 7,445,264	$ 11,248,230	$ 11,248,414	$ 11,259,784	$ 3,696,292
Taxes (40%)	$ 822,975	$ (492,223)	$ (1,725,814)	$ (2,978,105)	$ (4,499,292)	$ (4,499,366)	$ (4,503,914)	$ (1,478,517)
Net Income								
Cash Flow Statement								
Cash from Operating Activities								
Plus: Depreciation	$ -	$ 39,480	$ 63,646	$ 38,666	$ 23,200	$ 23,016	$ 11,646	$ 138
WC Change								
(+)/- A/R	$ -	$ (311,301)	$ (311,301)	$ (311,301)	$ (311,301)	$ -	$ -	$ -
(+)/- Inventory	$ (135)	$ (270)	$ -	$ -	$ -	$ -	$ -	$ -
(+)/- A/P	$ 40,241	$ -	$ -	$ -	$ -	$ -	$ -	$ -
(+)/- C/R	$ (171,763)	$ 7,500	$ -	$ -	$ -	$ -	$ -	$ -
Total WC Change	$ (131,656)	$ (304,071)	$ (311,301)	$ (311,301)	$ (311,301)	$ -	$ -	$ -
Cash From Investing Activities								
(Purchase)/Selling of Equipment	$ (197,398)	$ (2,394)	$ -	$ -	$ -	$ -	$ -	$ -
Cash From Financing Activities								
Issuance of Common Stock	$ 970,341	$ 1,000,000	$ -	$ -	$ -	$ -	$ -	$ -
Free Cash Flow	$ (593,176)	$ 1,471,349	$ 2,341,065	$ 4,194,523	$ 6,460,837	$ 6,772,064	$ 6,767,516	$ 2,217,913
% Design Capacity	0%	25%	50%	75%	100%	100%	100%	100%
	Investment				*Divided Free Cash Flows*			
RSCH Stage Investors (39.3% Equity)	$ (970,341)	$ (593,176)	$ 577,940	$ 919,562	$ 1,647,593	$ 2,537,793	$ 2,660,042	$ 2,658,256
Sales Stage Investors (60.7% Equity)	$ (1,000,000)	$ -	$ 893,408	$ 1,421,503	$ 2,546,930	$ 3,923,044	$ 4,112,022	$ 4,109,261
NPV at 25%	$ 8,567,005							
NPV at 30%	$ 6,460,461							
RSCH Stage MIRR	29%							
Sales Stage MIRR	42%							

R1 Q3 C3 G1

Year	2012	2013	2014	2015	2016	2017	2018	2019
Income Statement								
Revenue	$ -	$ 3,787,500	$ 7,575,000	$ 11,362,500	$ 15,150,000	$ 15,150,000	$ 15,150,000	$ -
Cost of Sales	$ (688,638)	$ (496,914)	$ (494,520)	$ (494,520)	$ (494,520)	$ (494,520)	$ (494,520)	$ (494,520)
Operating Costs, SG&A	$ (1,368,800)	$ (2,020,550)	$ (2,702,300)	$ (3,384,050)	$ (3,384,050)	$ (3,384,050)	$ (3,384,050)	$ (3,384,050)
Depreciation	$ -	$ (39,480)	$ (63,646)	$ (38,666)	$ (23,200)	$ (23,016)	$ (11,646)	$ (138)
Pre-Tax Income	$ (2,057,438)	$ 1,230,557	$ 4,314,534	$ 7,445,264	$ 11,248,230	$ 11,248,414	$ 11,259,784	$ (3,878,708)
Taxes (40%)	$ 822,975	$ (492,223)	$ (1,725,814)	$ (2,978,105)	$ (4,499,292)	$ (4,499,366)	$ (4,503,914)	$ 1,551,483
Net Income								
Cash Flow Statement								
Cash from Operating Activities								
Plus: Depreciation	$ -	$ 39,480	$ 63,646	$ 38,666	$ 23,200	$ 23,016	$ 11,646	$ 138
WC Change								
(+)/- A/R	$ -	$ (311,301)	$ (311,301)	$ (311,301)	$ (311,301)	$ -	$ -	$ -
(+)/- Inventory	$ (135)	$ (270)	$ -	$ -	$ -	$ -	$ -	$ -
(+)/- A/P	$ 40,241	$ -	$ -	$ -	$ -	$ -	$ -	$ -
(+)/- C/R	$ (171,763)	$ 7,500	$ -	$ -	$ -	$ -	$ -	$ -
Total WC Change	$ (131,656)	$ (304,071)	$ (311,301)	$ (311,301)	$ (311,301)	$ -	$ -	$ -
Cash From Investing Activities								
(Purchase)/Selling of Equipment	$ (197,398)	$ (2,394)	$ -	$ -	$ -	$ -	$ -	$ -
Cash From Financing Activities								
Issuance of Common Stock	$ 970,341	$ 1,000,000	$ -	$ -	$ -	$ -	$ -	$ -
Free Cash Flow	$ (593,176)	$ 1,471,349	$ 2,341,065	$ 4,194,523	$ 6,460,837	$ 6,772,064	$ 6,767,516	$ (2,327,087)
% Design Capacity	0%	25%	50%	75%	100%	100%	100%	100%
	Investment				*Divided Free Cash Flows*			
RSCH Stage Investors (39.3% Equity)	$ (970,341)	$ (593,176)	$ 577,940	$ 919,562	$ 1,647,593	$ 2,537,793	$ 2,660,042	$ 2,658,256
Sales Stage Investors (60.7% Equity)	$ (1,000,000)	$ -	$ 893,408	$ 1,421,503	$ 2,546,930	$ 3,923,044	$ 4,112,022	$ 4,109,261
NPV at 25%	$ 5,151,446							
NPV at 30%	$ 4,368,995							
RSCH Stage MIRR	8%							
Sales Stage MIRR	8%							

R1 Q3 C3 G2

Year	2012	2013	2014	2015	2016	2017	2018	2019
Income Statement								
Revenue	$ -	$ 3,787,500	$ 7,575,000	$ 11,362,500	$ 15,150,000	$ 15,150,000	$ 15,150,000	$ -
Cost of Sales	$ (688,638)	$ (496,914)	$ (494,520)	$ (494,520)	$ (494,520)	$ (494,520)	$ (494,520)	$ (494,520)
Operating Costs, SG&A	$ (1,368,800)	$ (2,020,550)	$ (2,702,300)	$ (3,384,050)	$ (3,384,050)	$ (3,384,050)	$ (3,384,050)	$ (3,384,050)
Depreciation	$ -	$ (39,480)	$ (63,646)	$ (38,666)	$ (23,200)	$ (23,016)	$ (11,646)	$ (138)
Pre-Tax Income	$ (2,057,438)	$ 1,230,557	$ 4,314,534	$ 7,445,264	$ 11,248,230	$ 11,248,414	$ 11,259,784	$ (3,878,708)
Taxes (40%)	$ 822,975	$ (492,223)	$ (1,725,814)	$ (2,978,105)	$ (4,499,292)	$ (4,499,366)	$ (4,503,914)	$ 1,551,483
Net Income								
Cash Flow Statement								
Cash from Operating Activities								
Plus: Depreciation	$ -	$ 39,480	$ 63,646	$ 38,666	$ 23,200	$ 23,016	$ 11,646	$ 138
WC Change								
(+)/- A/R	$ -	$ (311,301)	$ (311,301)	$ (311,301)	$ (311,301)	$ -	$ -	$ -
(+)/- Inventory	$ (135)	$ (270)	$ -	$ -	$ -	$ -	$ -	$ -
(+)/- A/P	$ 40,241	$ -	$ -	$ -	$ -	$ -	$ -	$ -
(+)/- C/R	$ (171,763)	$ 7,500	$ -	$ -	$ -	$ -	$ -	$ -
Total WC Change	$ (131,656)	$ (304,071)	$ (311,301)	$ (311,301)	$ (311,301)	$ -	$ -	$ -
Cash From Investing Activities								
(Purchase)/Selling of Equipment	$ (197,398)	$ (2,394)	$ -	$ -	$ -	$ -	$ -	$ -
Cash From Financing Activities								
Issuance of Common Stock	$ 970,341	$ 1,000,000	$ -	$ -	$ -	$ -	$ -	$ -
Free Cash Flow	$ (593,176)	$ 1,471,349	$ 2,341,065	$ 4,194,523	$ 6,460,837	$ 6,772,064	$ 6,767,516	$ (2,327,087)
% Design Capacity	0%	25%	50%	75%	100%	100%	100%	100%
	Investment				*Divided Free Cash Flows*			
RSCH Stage Investors (39.3% Equity)	$ (970,341)	$ (593,176)	$ 577,940	$ 919,562	$ 1,647,593	$ 2,537,793	$ 2,660,042	$ 2,658,256
Sales Stage Investors (60.7% Equity)	$ (1,000,000)	$ -	$ 893,408	$ 1,421,503	$ 2,546,930	$ 3,923,044	$ 4,112,022	$ 4,109,261
NPV at 25%	$ 5,364,402							
NPV at 30%	$ 4,474,653							
RSCH Stage MIRR	9%							
Sales Stage MIRR	9%							

R2 Q1 C1 G1

Year	2012	2013	2014	2015	2016	2017	2018	2019
Income Statement								
Revenue	$ -	$ -	$ 6,937,500	$ 13,875,000	$ 20,812,500	$ 27,750,000	$ 27,750,000	$ 27,750,000
Cost of Sales	$ (688,638)	$ (496,914)	$ (494,520)	$ (494,520)	$ (494,520)	$ (494,520)	$ (494,520)	$ (494,520)
Operating Costs, SG&A	$ (687,050)	$ (1,905,800)	$ (3,154,550)	$ (4,403,300)	$ (4,403,300)	$ (4,403,300)	$ (4,403,300)	$ (4,403,300)
Depreciation	$ -	$ (39,480)	$ (63,646)	$ (38,666)	$ (23,200)	$ (23,016)	$ (11,646)	$ -
Pre-Tax Income	$ (1,375,688)	$ (2,442,193)	$ 3,224,784	$ 8,938,514	$ 15,891,480	$ 22,829,164	$ 22,840,534	$ 22,852,180
Taxes (40%)	$ 550,275	$ 976,877	$ (1,289,914)	$ (3,575,405)	$ (6,356,592)	$ (9,131,666)	$ (9,136,214)	$ (9,140,872)
Net Income								
Cash Flow Statement								
Cash from Operating Activities								
Plus: Depreciation	$ -	$ 39,480	$ 63,646	$ 38,666	$ 23,200	$ 23,016	$ 11,646	$ -
WC Change								
(+)/- A/R	$ -	$ -	$ (570,205)	$ (570,205)	$ (570,205)	$ (570,205)	$ -	$ -
(+)/- Inventory	$ (135)	$ (270)	$ -	$ -	$ -	$ -	$ -	$ -
(+)/- A/P	$ 40,241	$ -	$ -	$ -	$ -	$ -	$ -	$ -
(+)/- C/R	$ (171,763)	$ 7,500	$ -	$ -	$ -	$ -	$ -	$ -
Total WC Change	$ (131,656)	$ 7,230	$ (570,205)	$ (570,205)	$ (570,205)	$ (570,205)	$ -	$ -
Cash From Investing Activities								
(Purchase)/Selling of Equipment	$ (197,398)	$ (2,394)	$ -	$ -	$ -	$ -	$ -	$ -
Cash From Financing Activities								
Issuance of Common Stock	$ 970,341	$ -	$ 1,000,000	$ -	$ -	$ -	$ -	$ -
Free Cash Flow	$ (184,126)	$ (1,421,000)	$ 2,428,311	$ 4,831,569	$ 8,987,883	$ 13,150,309	$ 13,715,966	$ 13,711,308
% Design Capacity	0%	25%	50%	75%	100%	100%	100%	0%
	Investment				*Divided Free Cash Flows*			
RSCH Stage Investors (39.3% Equity)	$ (970,341)	$ (184,126)	$ (1,421,000)	$ 731,689	$ 1,455,830	$ 2,708,195	$ 3,962,401	$ 4,132,843
Sales Stage Investors (60.7% Equity)	$ (1,000,000)	$ -	$ -	$ 1,696,622	$ 3,375,739	$ 6,279,688	$ 9,187,908	$ 9,583,124
NPV at 25%	$ 20,764,974							
NPV at 30%	$ 14,215,614							
RSCH Stage MIRR	35%							
Sales Stage MIRR	64%							

R2 Q1 C1 G2

Year	2012	2013	2014	2015	2016	2017	2018	2019
Income Statement								
Revenue	$ -	$ -	$ 6,937,500	$ 13,875,000	$ 20,812,500	$ 27,750,000	$ 27,750,000	$ 27,750,000
Cost of Sales	$ (688,638)	$ (496,914)	$ (494,520)	$ (494,520)	$ (494,520)	$ (494,520)	$ (494,520)	$ (494,520)
Operating Costs, SG&A	$ (687,050)	$ (1,905,800)	$ (3,154,550)	$ (4,403,300)	$ (4,403,300)	$ (4,403,300)	$ (4,403,300)	$ (4,403,300)
Depreciation	$ -	$ (39,480)	$ (63,646)	$ (38,666)	$ (23,200)	$ (23,016)	$ (11,646)	$ -
Pre-Tax Income	$ (1,375,688)	$ (2,442,193)	$ 3,224,784	$ 8,938,514	$ 15,891,480	$ 22,829,164	$ 22,840,534	$ 22,852,180
Taxes (40%)	$ 550,275	$ 976,877	$ (1,289,914)	$ (3,575,405)	$ (6,356,592)	$ (9,131,666)	$ (9,136,214)	$ (9,140,872)
Net Income								
Cash Flow Statement								
Cash from Operating Activities								
Plus: Depreciation	$ -	$ 39,480	$ 63,646	$ 38,666	$ 23,200	$ 23,016	$ 11,646	$ -
WC Change								
(+)/- A/R	$ -	$ -	$ (570,205)	$ (570,205)	$ (570,205)	$ (570,205)	$ -	$ -
(+)/- Inventory	$ (135)	$ (270)	$ -	$ -	$ -	$ -	$ -	$ -
(+)/- A/P	$ 40,241	$ -	$ -	$ -	$ -	$ -	$ -	$ -
(+)/- C/R	$ (171,763)	$ 7,500	$ -	$ -	$ -	$ -	$ -	$ -
Total WC Change	$ (131,656)	$ 7,230	$ (570,205)	$ (570,205)	$ (570,205)	$ (570,205)	$ -	$ -
Cash From Investing Activities								
(Purchase)/Selling of Equipment	$ (197,398)	$ (2,394)	$ -	$ -	$ -	$ -	$ -	$ -
Cash From Financing Activities								
Issuance of Common Stock	$ 970,341	$ -	$ 1,000,000	$ -	$ -	$ -	$ -	$ -
Free Cash Flow	$ (184,126)	$ (1,421,000)	$ 2,428,311	$ 4,831,569	$ 8,987,883	$ 13,150,309	$ 13,715,966	$ 13,711,308
% Design Capacity	0%	25%	50%	75%	100%	100%	100%	0%
	Investment				*Divided Free Cash Flows*			
RSCH Stage Investors (39.3% Equity)	$ (970,341)	$ (184,126)	$ (1,421,000)	$ 731,689	$ 1,455,830	$ 2,708,195	$ 3,962,401	$ 4,132,843
Sales Stage Investors (60.7% Equity)	$ (1,000,000)	$ -	$ -	$ 1,696,622	$ 3,375,739	$ 6,279,688	$ 9,187,908	$ 9,583,124
NPV at 25%	$ 19,510,223							
NPV at 30%	$ 13,593,073							
RSCH Stage MIRR	34%							
Sales Stage MIRR	62%							

R2 Q1 C2 G1

Year	2012	2013	2014	2015	2016	2017	2018	2019
Income Statement								
Revenue	$ -	$ -	$ 6,937,500	$ 13,875,000	$ 20,812,500	$ 27,750,000	$ 27,750,000	$ 13,875,000
Cost of Sales	$ (688,638)	$ (496,914)	$ (494,520)	$ (494,520)	$ (494,520)	$ (494,520)	$ (494,520)	$ (494,520)
Operating Costs, SG&A	$ (687,050)	$ (1,905,800)	$ (3,154,550)	$ (4,403,300)	$ (4,403,300)	$ (4,403,300)	$ (4,403,300)	$ (4,403,300)
Depreciation	$ -	$ (39,480)	$ (63,646)	$ (38,666)	$ (23,200)	$ (23,016)	$ (11,646)	$ -
Pre-Tax Income	$ (1,375,688)	$ (2,442,193)	$ 3,224,784	$ 8,938,514	$ 15,891,480	$ 22,829,164	$ 22,840,534	$ 8,977,180
Taxes (40%)	$ 550,275	$ 976,877	$ (1,289,914)	$ (3,575,405)	$ (6,356,592)	$ (9,131,666)	$ (9,136,214)	$ (3,590,872)
Net Income								
Cash Flow Statement								
Cash from Operating Activities								
Plus: Depreciation	$ -	$ 39,480	$ 63,646	$ 38,666	$ 23,200	$ 23,016	$ 11,646	$ -
WC Change								
(+)/- A/R	$ -	$ -	$ (570,205)	$ (570,205)	$ (570,205)	$ (570,205)	$ -	$ -
(+)/- Inventory	$ (135)	$ (270)	$ -	$ -	$ -	$ -	$ -	$ -
(+)/- A/P	$ 40,241	$ -	$ -	$ -	$ -	$ -	$ -	$ -
(+)/- C/R	$ (171,763)	$ 7,500	$ -	$ -	$ -	$ -	$ -	$ -
Total WC Change	$ (131,656)	$ 7,230	$ (570,205)	$ (570,205)	$ (570,205)	$ (570,205)	$ -	$ -
Cash From Investing Activities								
(Purchase)/Selling of Equipment	$ (197,398)	$ (2,394)	$ -	$ -	$ -	$ -	$ -	$ -
Cash From Financing Activities								
Issuance of Common Stock	$ 970,341	$ -	$ 1,000,000	$ -	$ -	$ -	$ -	$ -
Free Cash Flow	$ (184,126)	$ (1,421,000)	$ 2,428,311	$ 4,831,569	$ 8,987,883	$ 13,150,309	$ 13,715,966	$ 5,386,308
% Design Capacity	0%	25%	50%	75%	100%	100%	100%	0%
	Investment				*Divided Free Cash Flows*			
RSCH Stage Investors (39.3% Equity)	$ (970,341)	$ (184,126)	$ (1,421,000)	$ 731,689	$ 1,455,830	$ 2,708,195	$ 3,962,401	$ 4,132,843
Sales Stage Investors (60.7% Equity)	$ (1,000,000)	$ -	$ -	$ 1,696,622	$ 3,375,739	$ 6,279,688	$ 9,187,908	$ 9,583,124
NPV at 25%	$ 14,136,982							
NPV at 30%	$ 10,200,259							
RSCH Stage MIRR	28%							
Sales Stage MIRR	55%							

R2 Q1 C2 G2

Year	2012	2013	2014	2015	2016	2017	2018	2019
Income Statement								
Revenue	$ -	$ -	$ 6,937,500	$ 13,875,000	$ 20,812,500	$ 27,750,000	$ 27,750,000	$ 13,875,000
Cost of Sales	$ (688,638)	$ (496,914)	$ (494,520)	$ (494,520)	$ (494,520)	$ (494,520)	$ (494,520)	$ (494,520)
Operating Costs, SG&A	$ (687,050)	$ (1,905,800)	$ (3,154,550)	$ (4,403,300)	$ (4,403,300)	$ (4,403,300)	$ (4,403,300)	$ (4,403,300)
Depreciation	$ -	$ (39,480)	$ (63,646)	$ (38,666)	$ (23,200)	$ (23,016)	$ (11,646)	$ -
Pre-Tax Income	$ (1,375,688)	$ (2,442,193)	$ 3,224,784	$ 8,938,514	$ 15,891,480	$ 22,829,164	$ 22,840,534	$ 8,977,180
Taxes (40%)	$ 550,275	$ 976,877	$ (1,289,914)	$ (3,575,405)	$ (6,356,592)	$ (9,131,666)	$ (9,136,214)	$ (3,590,872)
Net Income								
Cash Flow Statement								
Cash from Operating Activities								
Plus: Depreciation	$ -	$ 39,480	$ 63,646	$ 38,666	$ 23,200	$ 23,016	$ 11,646	$ -
WC Change								
(+)/- A/R	$ -	$ -	$ (570,205)	$ (570,205)	$ (570,205)	$ (570,205)	$ -	$ -
(+)/- Inventory	$ (135)	$ (270)	$ -	$ -	$ -	$ -	$ -	$ -
(+)/- A/P	$ 40,241	$ -	$ -	$ -	$ -	$ -	$ -	$ -
(+)/- C/R	$ (171,763)	$ 7,500	$ -	$ -	$ -	$ -	$ -	$ -
Total WC Change	$ (131,656)	$ 7,230	$ (570,205)	$ (570,205)	$ (570,205)	$ (570,205)	$ -	$ -
Cash From Investing Activities								
(Purchase)/Selling of Equipment	$ (197,398)	$ (2,394)	$ -	$ -	$ -	$ -	$ -	$ -
Cash From Financing Activities								
Issuance of Common Stock	$ 970,341	$ -	$ 1,000,000	$ -	$ -	$ -	$ -	$ -
Free Cash Flow	$ (184,126)	$ (1,421,000)	$ 2,428,311	$ 4,831,569	$ 8,987,883	$ 13,150,309	$ 13,715,966	$ 5,386,308
% Design Capacity	0%	25%	50%	75%	100%	100%	100%	0%
	Investment				*Divided Free Cash Flows*			
RSCH Stage Investors (39.3% Equity)	$ (970,341)	$ (184,126)	$ (1,421,000)	$ 731,689	$ 1,455,830	$ 2,708,195	$ 3,962,401	$ 4,132,843
Sales Stage Investors (60.7% Equity)	$ (1,000,000)	$ -	$ -	$ 1,696,622	$ 3,375,739	$ 6,279,688	$ 9,187,908	$ 9,583,124
NPV at 25%	$ 13,644,070							
NPV at 30%	$ 9,955,702							
RSCH Stage MIRR	27%							
Sales Stage MIRR	54%							

R2 Q1 C3 G1

Year	2012	2013	2014	2015	2016	2017	2018	2019
Income Statement								
Revenue	$ -	$ -	$ 6,937,500	$ 13,875,000	$ 20,812,500	$ 27,750,000	$ 27,750,000	$ -
Cost of Sales	$ (688,638)	$ (496,914)	$ (494,520)	$ (494,520)	$ (494,520)	$ (494,520)	$ (494,520)	$ (494,520)
Operating Costs, SG&A	$ (687,050)	$ (1,905,800)	$ (3,154,550)	$ (4,403,300)	$ (4,403,300)	$ (4,403,300)	$ (4,403,300)	$ (4,403,300)
Depreciation	$ -	$ (39,480)	$ (63,646)	$ (38,666)	$ (23,200)	$ (23,016)	$ (11,646)	$ -
Pre-Tax Income	$ (1,375,688)	$ (2,442,193)	$ 3,224,784	$ 8,938,514	$ 15,891,480	$ 22,829,164	$ 22,840,534	$ (4,897,820)
Taxes (40%)	$ 550,275	$ 976,877	$ (1,289,914)	$ (3,575,405)	$ (6,356,592)	$ (9,131,666)	$ (9,136,214)	$ 1,959,128
Net Income								
Cash Flow Statement								
Cash from Operating Activities								
Plus: Depreciation	$ -	$ 39,480	$ 63,646	$ 38,666	$ 23,200	$ 23,016	$ 11,646	$ -
WC Change								
(+)/- A/R	$ -	$ -	$ (570,205)	$ (570,205)	$ (570,205)	$ (570,205)	$ -	$ -
(+)/- Inventory	$ (135)	$ (270)	$ -	$ -	$ -	$ -	$ -	$ -
(+)/- A/P	$ 40,241	$ -	$ -	$ -	$ -	$ -	$ -	$ -
(+)/- C/R	$ (171,763)	$ 7,500	$ -	$ -	$ -	$ -	$ -	$ -
Total WC Change	$ (131,656)	$ 7,230	$ (570,205)	$ (570,205)	$ (570,205)	$ (570,205)	$ -	$ -
Cash From Investing Activities								
(Purchase)/Selling of Equipment	$ (197,398)	$ (2,394)	$ -	$ -	$ -	$ -	$ -	$ -
Cash From Financing Activities								
Issuance of Common Stock	$ 970,341	$ -	$ 1,000,000	$ -	$ -	$ -	$ -	$ -
Free Cash Flow	$ (184,126)	$ (1,421,000)	$ 2,428,311	$ 4,831,569	$ 8,987,883	$ 13,150,309	$ 13,715,966	$ (2,938,692)
% Design Capacity	0%	25%	50%	75%	100%	100%	100%	0%
	Investment			*Divided Free Cash Flows*				
RSCH Stage Investors (39.3% Equity)	$ (970,341)	$ (184,126)	$ (1,421,000)	$ 731,689	$ 1,455,830	$ 2,708,195	$ 3,962,401	$ 4,132,843
Sales Stage Investors (60.7% Equity)	$ (1,000,000)	$ -	$ -	$ 1,696,622	$ 3,375,739	$ 6,279,688	$ 9,187,908	$ 9,583,124
NPV at 25%	$ 7,508,990							
NPV at 30%	$ 6,184,903							
RSCH Stage MIRR	9%							
Sales Stage MIRR	11%							

R2 Q1 C3 G2

Year	2012	2013	2014	2015	2016	2017	2018	2019
Income Statement								
Revenue	$ -	$ -	$ 6,937,500	$ 13,875,000	$ 20,812,500	$ 27,750,000	$ 27,750,000	$ -
Cost of Sales	$ (688,638)	$ (496,914)	$ (494,520)	$ (494,520)	$ (494,520)	$ (494,520)	$ (494,520)	$ (494,520)
Operating Costs, SG&A	$ (687,050)	$ (1,905,800)	$ (3,154,550)	$ (4,403,300)	$ (4,403,300)	$ (4,403,300)	$ (4,403,300)	$ (4,403,300)
Depreciation	$ -	$ (39,480)	$ (63,646)	$ (38,666)	$ (23,200)	$ (23,016)	$ (11,646)	$ -
Pre-Tax Income	$ (1,375,688)	$ (2,442,193)	$ 3,224,784	$ 8,938,514	$ 15,891,480	$ 22,829,164	$ 22,840,534	$ (4,897,820)
Taxes (40%)	$ 550,275	$ 976,877	$ (1,289,914)	$ (3,575,405)	$ (6,356,592)	$ (9,131,666)	$ (9,136,214)	$ 1,959,128
Net Income								
Cash Flow Statement								
Cash from Operating Activities								
Plus: Depreciation	$ -	$ 39,480	$ 63,646	$ 38,666	$ 23,200	$ 23,016	$ 11,646	$ -
WC Change								
(+)/- A/R	$ -	$ -	$ (570,205)	$ (570,205)	$ (570,205)	$ (570,205)	$ -	$ -
(+)/- Inventory	$ (135)	$ (270)	$ -	$ -	$ -	$ -	$ -	$ -
(+)/- A/P	$ 40,241	$ -	$ -	$ -	$ -	$ -	$ -	$ -
(+)/- C/R	$ (171,763)	$ 7,500	$ -	$ -	$ -	$ -	$ -	$ -
Total WC Change	$ (131,656)	$ 7,230	$ (570,205)	$ (570,205)	$ (570,205)	$ (570,205)	$ -	$ -
Cash From Investing Activities								
(Purchase)/Selling of Equipment	$ (197,398)	$ (2,394)	$ -	$ -	$ -	$ -	$ -	$ -
Cash From Financing Activities								
Issuance of Common Stock	$ 970,341	$ -	$ 1,000,000	$ -	$ -	$ -	$ -	$ -
Free Cash Flow	$ (184,126)	$ (1,421,000)	$ 2,428,311	$ 4,831,569	$ 8,987,883	$ 13,150,309	$ 13,715,966	$ (2,938,692)
% Design Capacity	0%	25%	50%	75%	100%	100%	100%	0%
	Investment				*Divided Free Cash Flows*			
RSCH Stage Investors (39.3% Equity)	$ (970,341)	$ (184,126)	$ (1,421,000)	$ 731,689	$ 1,455,830	$ 2,708,195	$ 3,962,401	$ 4,132,843
Sales Stage Investors (60.7% Equity)	$ (1,000,000)	$ -	$ -	$ 1,696,622	$ 3,375,739	$ 6,279,688	$ 9,187,908	$ 9,583,124
NPV at 25%	$ 7,777,916							
NPV at 30%	$ 6,318,330							
RSCH Stage MIRR	10%							
Sales Stage MIRR	12%							

R2 Q2 C1 G1

Year	2012	2013	2014	2015	2016	2017	2018	2019
Income Statement								
Revenue	$ -	$ -	$ 5,100,000	$ 10,200,000	$ 15,300,000	$ 20,400,000	$ 20,400,000	$ 20,400,000
Cost of Sales	$ (688,638)	$ (496,914)	$ (494,520)	$ (494,520)	$ (494,520)	$ (494,520)	$ (494,520)	$ (494,520)
Operating Costs, SG&A	$ (687,050)	$ (1,575,050)	$ (2,493,050)	$ (3,411,050)	$ (3,411,050)	$ (3,411,050)	$ (3,411,050)	$ (3,411,050)
Depreciation	$ -	$ (39,480)	$ (63,646)	$ (38,666)	$ (23,200)	$ (23,016)	$ (11,646)	$ -
Pre-Tax Income	$ (1,375,688)	$ (2,111,443)	$ 2,048,784	$ 6,255,764	$ 11,371,230	$ 16,471,414	$ 16,482,784	$ 16,494,430
Taxes (40%)	$ 550,275	$ 844,577	$ (819,514)	$ (2,502,305)	$ (4,548,492)	$ (6,588,566)	$ (6,593,114)	$ (6,597,772)
Net Income								
Cash Flow Statement								
Cash from Operating Activities								
Plus: Depreciation	$ -	$ 39,480	$ 63,646	$ 38,666	$ 23,200	$ 23,016	$ 11,646	$ -
WC Change								
(+)/- A/R	$ -	$ -	$ (419,178)	$ (419,178)	$ (419,178)	$ (419,178)	$ -	$ -
(+)/- Inventory	$ (135)	$ (270)	$ -	$ -	$ -	$ -	$ -	$ -
(+)/- A/P	$ 40,241	$ -	$ -	$ -	$ -	$ -	$ -	$ -
(+)/- C/R	$ (171,763)	$ 7,500	$ -	$ -	$ -	$ -	$ -	$ -
Total WC Change	$ (131,656)	$ 7,230	$ (419,178)	$ (419,178)	$ (419,178)	$ (419,178)	$ -	$ -
Cash From Investing Activities								
(Purchase)/Selling of Equipment	$ (197,398)	$ (2,394)	$ -	$ -	$ -	$ -	$ -	$ -
Cash From Financing Activities								
Issuance of Common Stock	$ 970,341	$ -	$ 1,000,000	$ -	$ -	$ -	$ -	$ -
Free Cash Flow	$ (184,126)	$ (1,222,550)	$ 1,873,738	$ 3,372,947	$ 6,426,760	$ 9,486,686	$ 9,901,316	$ 9,896,658
% Design Capacity	0%	25%	50%	75%	100%	100%	100%	0%
	Investment				*Divided Free Cash Flows*			
RSCH Stage Investors (39.3% Equity)	$ (970,341)	$ (184,126)	$ (1,222,550)	$ 564,588	$ 1,016,323	$ 1,936,487	$ 2,858,492	$ 2,983,427
Sales Stage Investors (60.7% Equity)	$ (1,000,000)	$ -	$ -	$ 1,309,151	$ 2,356,623	$ 4,490,273	$ 6,628,194	$ 6,917,889
NPV at 25%	$ 14,373,920							
NPV at 30%	$ 9,673,285							
RSCH Stage MIRR	31%							
Sales Stage MIRR	58%							

R2 Q2 C1 G2

Year	2012	2013	2014	2015	2016	2017	2018	2019
Income Statement								
Revenue	$ -	$ -	$ 5,100,000	$ 10,200,000	$ 15,300,000	$ 20,400,000	$ 20,400,000	$ 20,400,000
Cost of Sales	$ (688,638)	$ (496,914)	$ (494,520)	$ (494,520)	$ (494,520)	$ (494,520)	$ (494,520)	$ (494,520)
Operating Costs, SG&A	$ (687,050)	$ (1,575,050)	$ (2,493,050)	$ (3,411,050)	$ (3,411,050)	$ (3,411,050)	$ (3,411,050)	$ (3,411,050)
Depreciation	$ -	$ (39,480)	$ (63,646)	$ (38,666)	$ (23,200)	$ (23,016)	$ (11,646)	$ -
Pre-Tax Income	$ (1,375,688)	$ (2,111,443)	$ 2,048,784	$ 6,255,764	$ 11,371,230	$ 16,471,414	$ 16,482,784	$ 16,494,430
Taxes (40%)	$ 550,275	$ 844,577	$ (819,514)	$ (2,502,305)	$ (4,548,492)	$ (6,588,566)	$ (6,593,114)	$ (6,597,772)
Net Income								
Cash Flow Statement								
Cash from Operating Activities								
Plus: Depreciation	$ -	$ 39,480	$ 63,646	$ 38,666	$ 23,200	$ 23,016	$ 11,646	$ -
WC Change								
(+)/- A/R	$ -	$ -	$ (419,178)	$ (419,178)	$ (419,178)	$ (419,178)	$ -	$ -
(+)/- Inventory	$ (135)	$ (270)	$ -	$ -	$ -	$ -	$ -	$ -
(+)/- A/P	$ 40,241	$ -	$ -	$ -	$ -	$ -	$ -	$ -
(+)/- C/R	$ (171,763)	$ 7,500	$ -	$ -	$ -	$ -	$ -	$ -
Total WC Change	$ (131,656)	$ 7,230	$ (419,178)	$ (419,178)	$ (419,178)	$ (419,178)	$ -	$ -
Cash From Investing Activities								
(Purchase)/Selling of Equipment	$ (197,398)	$ (2,394)	$ -	$ -	$ -	$ -	$ -	$ -
Cash From Financing Activities								
Issuance of Common Stock	$ 970,341	$ -	$ 1,000,000	$ -	$ -	$ -	$ -	$ -
Free Cash Flow	$ (184,126)	$ (1,222,550)	$ 1,873,738	$ 3,372,947	$ 6,426,760	$ 9,486,686	$ 9,901,316	$ 9,896,658
% Design Capacity	0%	25%	50%	75%	100%	100%	100%	0%
	Investment				*Divided Free Cash Flows*			
RSCH Stage Investors (39.3% Equity)	$ (970,341)	$ (184,126)	$ (1,222,550)	$ 564,588	$ 1,016,323	$ 1,936,487	$ 2,858,492	$ 2,983,427
Sales Stage Investors (60.7% Equity)	$ (1,000,000)	$ -	$ -	$ 1,309,151	$ 2,356,623	$ 4,490,273	$ 6,628,194	$ 6,917,889
NPV at 25%	$ 13,468,256							
NPV at 30%	$ 9,223,942							
RSCH Stage MIRR	30%							
Sales Stage MIRR	56%							

R2 Q2 C2 G1

Year	2012	2013	2014	2015	2016	2017	2018	2019
Income Statement								
Revenue	$ -	$ -	$ 5,100,000	$ 10,200,000	$ 15,300,000	$ 20,400,000	$ 20,400,000	$ 10,200,000
Cost of Sales	$ (688,638)	$ (496,914)	$ (494,520)	$ (494,520)	$ (494,520)	$ (494,520)	$ (494,520)	$ (494,520)
Operating Costs, SG&A	$ (687,050)	$ (1,575,050)	$ (2,493,050)	$ (3,411,050)	$ (3,411,050)	$ (3,411,050)	$ (3,411,050)	$ (3,411,050)
Depreciation	$ -	$ (39,480)	$ (63,646)	$ (38,666)	$ (23,200)	$ (23,016)	$ (11,646)	$ -
Pre-Tax Income	$ (1,375,688)	$ (2,111,443)	$ 2,048,784	$ 6,255,764	$ 11,371,230	$ 16,471,414	$ 16,482,784	$ 6,294,430
Taxes (40%)	$ 550,275	$ 844,577	$ (819,514)	$ (2,502,305)	$ (4,548,492)	$ (6,588,566)	$ (6,593,114)	$ (2,517,772)
Net Income								
Cash Flow Statement								
Cash from Operating Activities								
Plus: Depreciation	$ -	$ 39,480	$ 63,646	$ 38,666	$ 23,200	$ 23,016	$ 11,646	$ -
WC Change								
(+)/- A/R	$ -	$ -	$ (419,178)	$ (419,178)	$ (419,178)	$ (419,178)	$ -	$ -
(+)/- Inventory	$ (135)	$ (270)	$ -	$ -	$ -	$ -	$ -	$ -
(+)/- A/P	$ 40,241	$ -	$ -	$ -	$ -	$ -	$ -	$ -
(+)/- C/R	$ (171,763)	$ 7,500	$ -	$ -	$ -	$ -	$ -	$ -
Total WC Change	$ (131,656)	$ 7,230	$ (419,178)	$ (419,178)	$ (419,178)	$ (419,178)	$ -	$ -
Cash From Investing Activities								
(Purchase)/Selling of Equipment	$ (197,398)	$ (2,394)	$ -	$ -	$ -	$ -	$ -	$ -
Cash From Financing Activities								
Issuance of Common Stock	$ 970,341	$ -	$ 1,000,000	$ -	$ -	$ -	$ -	$ -
Free Cash Flow	$ (184,126)	$ (1,222,550)	$ 1,873,738	$ 3,372,947	$ 6,426,760	$ 9,486,686	$ 9,901,316	$ 3,776,658
% Design Capacity	0%	25%	50%	75%	100%	100%	100%	0%
	Investment				*Divided Free Cash Flows*			
RSCH Stage Investors (39.3% Equity)	$ (970,341)	$ (184,126)	$ (1,222,550)	$ 564,588	$ 1,016,323	$ 1,936,487	$ 2,858,492	$ 2,983,427
Sales Stage Investors (60.7% Equity)	$ (1,000,000)	$ -	$ -	$ 1,309,151	$ 2,356,623	$ 4,490,273	$ 6,628,194	$ 6,917,889
NPV at 25%	$ 9,501,450							
NPV at 30%	$ 6,721,457							
RSCH Stage MIRR	24%							
Sales Stage MIRR	49%							

R2 Q2 C2 G1

Year	2012	2013	2014	2015	2016	2017	2018	2019
Income Statement								
Revenue	$ -	$ -	$ 5,100,000	$ 10,200,000	$ 15,300,000	$ 20,400,000	$ 20,400,000	$ 10,200,000
Cost of Sales	$ (688,638)	$ (496,914)	$ (494,520)	$ (494,520)	$ (494,520)	$ (494,520)	$ (494,520)	$ (494,520)
Operating Costs, SG&A	$ (687,050)	$ (1,575,050)	$ (2,493,050)	$ (3,411,050)	$ (3,411,050)	$ (3,411,050)	$ (3,411,050)	$ (3,411,050)
Depreciation	$ -	$ (39,480)	$ (63,646)	$ (38,666)	$ (23,200)	$ (23,016)	$ (11,646)	$ -
Pre-Tax Income	$ (1,375,688)	$ (2,111,443)	$ 2,048,784	$ 6,255,764	$ 11,371,230	$ 16,471,414	$ 16,482,784	$ 6,294,430
Taxes (40%)	$ 550,275	$ 844,577	$ (819,514)	$ (2,502,305)	$ (4,548,492)	$ (6,588,566)	$ (6,593,114)	$ (2,517,772)
Net Income								
Cash Flow Statement								
Cash from Operating Activities								
Plus: Depreciation	$ -	$ 39,480	$ 63,646	$ 38,666	$ 23,200	$ 23,016	$ 11,646	$ -
WC Change								
(+)/- A/R	$ -	$ -	$ (419,178)	$ (419,178)	$ (419,178)	$ (419,178)	$ -	$ -
(+)/- Inventory	$ (135)	$ (270)	$ -	$ -	$ -	$ -	$ -	$ -
(+)/- A/P	$ 40,241	$ -	$ -	$ -	$ -	$ -	$ -	$ -
(+)/- C/R	$ (171,763)	$ 7,500	$ -	$ -	$ -	$ -	$ -	$ -
Total WC Change	$ (131,656)	$ 7,230	$ (419,178)	$ (419,178)	$ (419,178)	$ (419,178)	$ -	$ -
Cash From Investing Activities								
(Purchase)/Selling of Equipment	$ (197,398)	$ (2,394)	$ -	$ -	$ -	$ -	$ -	$ -
Cash From Financing Activities								
Issuance of Common Stock	$ 970,341	$ -	$ 1,000,000	$ -	$ -	$ -	$ -	$ -
Free Cash Flow	$ (184,126)	$ (1,222,550)	$ 1,873,738	$ 3,372,947	$ 6,426,760	$ 9,486,686	$ 9,901,316	$ 3,776,658
% Design Capacity	0%	25%	50%	75%	100%	100%	100%	0%
	Investment				*Divided Free Cash Flows*			
RSCH Stage Investors (39.3% Equity)	$ (970,341)	$ (184,126)	$ (1,222,550)	$ 564,588	$ 1,016,323	$ 1,936,487	$ 2,858,492	$ 2,983,427
Sales Stage Investors (60.7% Equity)	$ (1,000,000)	$ -	$ -	$ 1,309,151	$ 2,356,623	$ 4,490,273	$ 6,628,194	$ 6,917,889
NPV at 25%	$ 9,155,840							
NPV at 30%	$ 6,549,983							
RSCH Stage MIRR	23%							
Sales Stage MIRR	48%							

R2 Q2 C3 G1

Year	2012	2013	2014	2015	2016	2017	2018	2019
Income Statement								
Revenue	$ -	$ -	$ 5,100,000	$ 10,200,000	$ 15,300,000	$ 20,400,000	$ 20,400,000	$ -
Cost of Sales	$ (688,638)	$ (496,914)	$ (494,520)	$ (494,520)	$ (494,520)	$ (494,520)	$ (494,520)	$ (494,520)
Operating Costs, SG&A	$ (687,050)	$ (1,575,050)	$ (2,493,050)	$ (3,411,050)	$ (3,411,050)	$ (3,411,050)	$ (3,411,050)	$ (3,411,050)
Depreciation	$ -	$ (39,480)	$ (63,646)	$ (38,666)	$ (23,200)	$ (23,016)	$ (11,646)	$ -
Pre-Tax Income	$ (1,375,688)	$ (2,111,443)	$ 2,048,784	$ 6,255,764	$ 11,371,230	$ 16,471,414	$ 16,482,784	$ (3,905,570)
Taxes (40%)	$ 550,275	$ 844,577	$ (819,514)	$ (2,502,305)	$ (4,548,492)	$ (6,588,566)	$ (6,593,114)	$ 1,562,228
Net Income								
Cash Flow Statement								
Cash from Operating Activities								
Plus: Depreciation	$ -	$ 39,480	$ 63,646	$ 38,666	$ 23,200	$ 23,016	$ 11,646	$ -
WC Change								
(+)/- A/R	$ -	$ -	$ (419,178)	$ (419,178)	$ (419,178)	$ (419,178)	$ -	$ -
(+)/- Inventory	$ (135)	$ (270)	$ -	$ -	$ -	$ -	$ -	$ -
(+)/- A/P	$ 40,241	$ -	$ -	$ -	$ -	$ -	$ -	$ -
(+)/- C/R	$ (171,763)	$ 7,500	$ -	$ -	$ -	$ -	$ -	$ -
Total WC Change	$ (131,656)	$ 7,230	$ (419,178)	$ (419,178)	$ (419,178)	$ (419,178)	$ -	$ -
Cash From Investing Activities								
(Purchase)/Selling of Equipment	$ (197,398)	$ (2,394)	$ -	$ -	$ -	$ -	$ -	$ -
Cash From Financing Activities								
Issuance of Common Stock	$ 970,341	$ -	$ 1,000,000	$ -	$ -	$ -	$ -	$ -
Free Cash Flow	$ (184,126)	$ (1,222,550)	$ 1,873,738	$ 3,372,947	$ 6,426,760	$ 9,486,686	$ 9,901,316	$ (2,343,342)
% Design Capacity	0%	25%	50%	75%	100%	100%	100%	0%
	Investment				*Divided Free Cash Flows*			
RSCH Stage Investors (39.3% Equity)	$ (970,341)	$ (184,126)	$ (1,222,550)	$ 564,588	$ 1,016,323	$ 1,936,487	$ 2,858,492	$ 2,983,427
Sales Stage Investors (60.7% Equity)	$ (1,000,000)	$ -	$ -	$ 1,309,151	$ 2,356,623	$ 4,490,273	$ 6,628,194	$ 6,917,889
NPV at 25%	$ 4,628,981							
NPV at 30%	$ 3,769,628							
RSCH Stage MIRR	7%							
Sales Stage MIRR	9%							

R2 Q2 C3 G2

Year	2012	2013	2014	2015	2016	2017	2018	2019
Income Statement								
Revenue	$ -	$ -	$ 5,100,000	$ 10,200,000	$ 15,300,000	$ 20,400,000	$ 20,400,000	$ -
Cost of Sales	$ (688,638)	$ (496,914)	$ (494,520)	$ (494,520)	$ (494,520)	$ (494,520)	$ (494,520)	$ (494,520)
Operating Costs, SG&A	$ (687,050)	$ (1,575,050)	$ (2,493,050)	$ (3,411,050)	$ (3,411,050)	$ (3,411,050)	$ (3,411,050)	$ (3,411,050)
Depreciation	$ -	$ (39,480)	$ (63,646)	$ (38,666)	$ (23,200)	$ (23,016)	$ (11,646)	$ -
Pre-Tax Income	$ (1,375,688)	$ (2,111,443)	$ 2,048,784	$ 6,255,764	$ 11,371,230	$ 16,471,414	$ 16,482,784	$ (3,905,570)
Taxes (40%)	$ 550,275	$ 844,577	$ (819,514)	$ (2,502,305)	$ (4,548,492)	$ (6,588,566)	$ (6,593,114)	$ 1,562,228
Net Income								
Cash Flow Statement								
Cash from Operating Activities								
Plus: Depreciation	$ -	$ 39,480	$ 63,646	$ 38,666	$ 23,200	$ 23,016	$ 11,646	$ -
WC Change								
(+)/- A/R	$ -	$ -	$ (419,178)	$ (419,178)	$ (419,178)	$ (419,178)	$ -	$ -
(+)/- Inventory	$ (135)	$ (270)	$ -	$ -	$ -	$ -	$ -	$ -
(+)/- A/P	$ 40,241	$ -	$ -	$ -	$ -	$ -	$ -	$ -
(+)/- C/R	$ (171,763)	$ 7,500	$ -	$ -	$ -	$ -	$ -	$ -
Total WC Change	$ (131,656)	$ 7,230	$ (419,178)	$ (419,178)	$ (419,178)	$ (419,178)	$ -	$ -
Cash From Investing Activities								
(Purchase)/Selling of Equipment	$ (197,398)	$ (2,394)	$ -	$ -	$ -	$ -	$ -	$ -
Cash From Financing Activities								
Issuance of Common Stock	$ 970,341	$ -	$ 1,000,000	$ -	$ -	$ -	$ -	$ -
Free Cash Flow	$ (184,126)	$ (1,222,550)	$ 1,873,738	$ 3,372,947	$ 6,426,760	$ 9,486,686	$ 9,901,316	$ (2,343,342)
% Design Capacity	0%	25%	50%	75%	100%	100%	100%	0%
	Investment				*Divided Free Cash Flows*			
RSCH Stage Investors (39.3% Equity)	$ (970,341)	$ (184,126)	$ (1,222,550)	$ 564,588	$ 1,016,323	$ 1,936,487	$ 2,858,492	$ 2,983,427
Sales Stage Investors (60.7% Equity)	$ (1,000,000)	$ -	$ -	$ 1,309,151	$ 2,356,623	$ 4,490,273	$ 6,628,194	$ 6,917,889
NPV at 25%	$ 4,843,425							
NPV at 30%	$ 3,876,024							
RSCH Stage MIRR	8%							
Sales Stage MIRR	11%							

R2 Q3 C1 G1

Year	2012	2013	2014	2015	2016	2017	2018	2019
Income Statement								
Revenue	$ -	$ -	$ 3,787,500	$ 7,575,000	$ 11,362,500	$ 15,150,000	$ 15,150,000	$ 15,150,000
Cost of Sales	$ (688,638)	$ (496,914)	$ (494,520)	$ (494,520)	$ (494,520)	$ (494,520)	$ (494,520)	$ (494,520)
Operating Costs, SG&A	$ (687,050)	$ (1,338,800)	$ (2,020,550)	$ (2,702,300)	$ (2,702,300)	$ (2,702,300)	$ (2,702,300)	$ (2,702,300)
Depreciation	$ -	$ (39,480)	$ (63,646)	$ (38,666)	$ (23,200)	$ (23,016)	$ (11,646)	$ -
Pre-Tax Income	$ (1,375,688)	$ (1,875,193)	$ 1,208,784	$ 4,339,514	$ 8,142,480	$ 11,930,164	$ 11,941,534	$ 11,953,180
Taxes (40%)	$ 550,275	$ 750,077	$ (483,514)	$ (1,735,805)	$ (3,256,992)	$ (4,772,066)	$ (4,776,614)	$ (4,781,272)
Net Income								
Cash Flow Statement								
Cash from Operating Activities								
Plus: Depreciation	$ -	$ 39,480	$ 63,646	$ 38,666	$ 23,200	$ 23,016	$ 11,646	$ -
WC Change								
(+)/- A/R	$ -	$ -	$ (311,301)	$ (311,301)	$ (311,301)	$ (311,301)	$ -	$ -
(+)/- Inventory	$ (135)	$ (270)	$ -	$ -	$ -	$ -	$ -	$ -
(+)/- A/P	$ 40,241	$ -	$ -	$ -	$ -	$ -	$ -	$ -
(+)/- C/R	$ (171,763)	$ 7,500	$ -	$ -	$ -	$ -	$ -	$ -
Total WC Change	$ (131,656)	$ 7,230	$ (311,301)	$ (311,301)	$ (311,301)	$ (311,301)	$ -	$ -
Cash From Investing Activities								
(Purchase)/Selling of Equipment	$ (197,398)	$ (2,394)	$ -	$ -	$ -	$ -	$ -	$ -
Cash From Financing Activities								
Issuance of Common Stock	$ 970,341	$ -	$ 1,000,000	$ -	$ -	$ -	$ -	$ -
Free Cash Flow	$ (184,126)	$ (1,080,800)	$ 1,477,615	$ 2,331,073	$ 4,597,387	$ 6,869,813	$ 7,176,566	$ 7,171,908
% Design Capacity	0%	25%	50%	75%	100%	100%	100%	0%
	Investment				*Divided Free Cash Flows*			
RSCH Stage Investors (39.3% Equity)	$ (970,341)	$ (184,126)	$ (1,080,800)	$ 445,229	$ 702,390	$ 1,385,267	$ 2,069,986	$ 2,162,416
Sales Stage Investors (60.7% Equity)	$ (1,000,000)	$ -	$ -	$ 1,032,386	$ 1,628,683	$ 3,212,120	$ 4,799,827	$ 5,014,151
NPV at 25%	$ 9,808,882							
NPV at 30%	$ 6,428,765							
RSCH Stage MIRR	27%							
Sales Stage MIRR	52%							

R2 Q3 C1 G2

Year	2012	2013	2014	2015	2016	2017	2018	2019
Income Statement								
Revenue	$ -	$ -	$ 3,787,500	$ 7,575,000	$ 11,362,500	$ 15,150,000	$ 15,150,000	$ 15,150,000
Cost of Sales	$ (688,638)	$ (496,914)	$ (494,520)	$ (494,520)	$ (494,520)	$ (494,520)	$ (494,520)	$ (494,520)
Operating Costs, SG&A	$ (687,050)	$ (1,338,800)	$ (2,020,550)	$ (2,702,300)	$ (2,702,300)	$ (2,702,300)	$ (2,702,300)	$ (2,702,300)
Depreciation	$ -	$ (39,480)	$ (63,646)	$ (38,666)	$ (23,200)	$ (23,016)	$ (11,646)	$ -
Pre-Tax Income	$ (1,375,688)	$ (1,875,193)	$ 1,208,784	$ 4,339,514	$ 8,142,480	$ 11,930,164	$ 11,941,534	$ 11,953,180
Taxes (40%)	$ 550,275	$ 750,077	$ (483,514)	$ (1,735,805)	$ (3,256,992)	$ (4,772,066)	$ (4,776,614)	$ (4,781,272)
Net Income								
Cash Flow Statement								
Cash from Operating Activities								
Plus: Depreciation	$ -	$ 39,480	$ 63,646	$ 38,666	$ 23,200	$ 23,016	$ 11,646	$ -
WC Change								
(+)/- A/R	$ -	$ -	$ (311,301)	$ (311,301)	$ (311,301)	$ (311,301)	$ -	$ -
(+)/- Inventory	$ (135)	$ (270)	$ -	$ -	$ -	$ -	$ -	$ -
(+)/- A/P	$ 40,241	$ -	$ -	$ -	$ -	$ -	$ -	$ -
(+)/- C/R	$ (171,763)	$ 7,500	$ -	$ -	$ -	$ -	$ -	$ -
Total WC Change	$ (131,656)	$ 7,230	$ (311,301)	$ (311,301)	$ (311,301)	$ (311,301)	$ -	$ -
Cash From Investing Activities								
(Purchase)/Selling of Equipment	$ (197,398)	$ (2,394)	$ -	$ -	$ -	$ -	$ -	$ -
Cash From Financing Activities								
Issuance of Common Stock	$ 970,341	$ -	$ 1,000,000	$ -	$ -	$ -	$ -	$ -
Free Cash Flow	$ (184,126)	$ (1,080,800)	$ 1,477,615	$ 2,331,073	$ 4,597,387	$ 6,869,813	$ 7,176,566	$ 7,171,908
% Design Capacity	0%	25%	50%	75%	100%	100%	100%	0%
	Investment				*Divided Free Cash Flows*			
RSCH Stage Investors (39.3% Equity)	$ (970,341)	$ (184,126)	$ (1,080,800)	$ 445,229	$ 702,390	$ 1,385,267	$ 2,069,986	$ 2,162,416
Sales Stage Investors (60.7% Equity)	$ (1,000,000)	$ -	$ -	$ 1,032,386	$ 1,628,683	$ 3,212,120	$ 4,799,827	$ 5,014,151
NPV at 25%	$ 9,152,565							
NPV at 30%	$ 6,103,135							
RSCH Stage MIRR	26%							
Sales Stage MIRR	51%							

R2 Q3 C2 G1

Year	2012	2013	2014	2015	2016	2017	2018	2019
Income Statement								
Revenue	$ -	$ -	$ 3,787,500	$ 7,575,000	$ 11,362,500	$ 15,150,000	$ 15,150,000	$ 7,575,000
Cost of Sales	$ (688,638)	$ (496,914)	$ (494,520)	$ (494,520)	$ (494,520)	$ (494,520)	$ (494,520)	$ (494,520)
Operating Costs, SG&A	$ (687,050)	$ (1,338,800)	$ (2,020,550)	$ (2,702,300)	$ (2,702,300)	$ (2,702,300)	$ (2,702,300)	$ (2,702,300)
Depreciation	$ -	$ (39,480)	$ (63,646)	$ (38,666)	$ (23,200)	$ (23,016)	$ (11,646)	$ -
Pre-Tax Income	$ (1,375,688)	$ (1,875,193)	$ 1,208,784	$ 4,339,514	$ 8,142,480	$ 11,930,164	$ 11,941,534	$ 4,378,180
Taxes (40%)	$ 550,275	$ 750,077	$ (483,514)	$ (1,735,805)	$ (3,256,992)	$ (4,772,066)	$ (4,776,614)	$ (1,751,272)
Net Income								
Cash Flow Statement								
Cash from Operating Activities								
Plus: Depreciation	$ -	$ 39,480	$ 63,646	$ 38,666	$ 23,200	$ 23,016	$ 11,646	$ -
WC Change								
(+)/- A/R	$ -	$ -	$ (311,301)	$ (311,301)	$ (311,301)	$ (311,301)	$ -	$ -
(+)/- Inventory	$ (135)	$ (270)	$ -	$ -	$ -	$ -	$ -	$ -
(+)/- A/P	$ 40,241	$ -	$ -	$ -	$ -	$ -	$ -	$ -
(+)/- C/R	$ (171,763)	$ 7,500	$ -	$ -	$ -	$ -	$ -	$ -
Total WC Change	$ (131,656)	$ 7,230	$ (311,301)	$ (311,301)	$ (311,301)	$ (311,301)	$ -	$ -
Cash From Investing Activities								
(Purchase)/Selling of Equipment	$ (197,398)	$ (2,394)	$ -	$ -	$ -	$ -	$ -	$ -
Cash From Financing Activities								
Issuance of Common Stock	$ 970,341	$ -	$ 1,000,000	$ -	$ -	$ -	$ -	$ -
Free Cash Flow	$ (184,126)	$ (1,080,800)	$ 1,477,615	$ 2,331,073	$ 4,597,387	$ 6,869,813	$ 7,176,566	$ 2,626,908
% Design Capacity	0%	25%	50%	75%	100%	100%	100%	0%
	Investment				*Divided Free Cash Flows*			
RSCH Stage Investors (39.3% Equity)	$ (970,341)	$ (184,126)	$ (1,080,800)	$ 445,229	$ 702,390	$ 1,385,267	$ 2,069,986	$ 2,162,416
Sales Stage Investors (60.7% Equity)	$ (1,000,000)	$ -	$ -	$ 1,032,386	$ 1,628,683	$ 3,212,120	$ 4,799,827	$ 5,014,151
NPV at 25%	$ 6,190,356							
NPV at 30%	$ 4,236,598							
RSCH Stage MIRR	20%							
Sales Stage MIRR	44%							

R2 Q3 C2 G2

Year	2012	2013	2014	2015	2016	2017	2018	2019
Income Statement								
Revenue	$ -	$ -	$ 3,787,500	$ 7,575,000	$ 11,362,500	$ 15,150,000	$ 15,150,000	$ 7,575,000
Cost of Sales	$ (688,638)	$ (496,914)	$ (494,520)	$ (494,520)	$ (494,520)	$ (494,520)	$ (494,520)	$ (494,520)
Operating Costs, SG&A	$ (687,050)	$ (1,338,800)	$ (2,020,550)	$ (2,702,300)	$ (2,702,300)	$ (2,702,300)	$ (2,702,300)	$ (2,702,300)
Depreciation	$ -	$ (39,480)	$ (63,646)	$ (38,666)	$ (23,200)	$ (23,016)	$ (11,646)	$ -
Pre-Tax Income	$ (1,375,688)	$ (1,875,193)	$ 1,208,784	$ 4,339,514	$ 8,142,480	$ 11,930,164	$ 11,941,534	$ 4,378,180
Taxes (40%)	$ 550,275	$ 750,077	$ (483,514)	$ (1,735,805)	$ (3,256,992)	$ (4,772,066)	$ (4,776,614)	$ (1,751,272)
Net Income								
Cash Flow Statement								
Cash from Operating Activities								
Plus: Depreciation	$ -	$ 39,480	$ 63,646	$ 38,666	$ 23,200	$ 23,016	$ 11,646	$ -
WC Change								
(+)/- A/R	$ -	$ -	$ (311,301)	$ (311,301)	$ (311,301)	$ (311,301)	$ -	$ -
(+)/- Inventory	$ (135)	$ (270)	$ -	$ -	$ -	$ -	$ -	$ -
(+)/- A/P	$ 40,241	$ -	$ -	$ -	$ -	$ -	$ -	$ -
(+)/- C/R	$ (171,763)	$ 7,500	$ -	$ -	$ -	$ -	$ -	$ -
Total WC Change	$ (131,656)	$ 7,230	$ (311,301)	$ (311,301)	$ (311,301)	$ (311,301)	$ -	$ -
Cash From Investing Activities								
(Purchase)/Selling of Equipment	$ (197,398)	$ (2,394)	$ -	$ -	$ -	$ -	$ -	$ -
Cash From Financing Activities								
Issuance of Common Stock	$ 970,341	$ -	$ 1,000,000	$ -	$ -	$ -	$ -	$ -
Free Cash Flow	$ (184,126)	$ (1,080,800)	$ 1,477,615	$ 2,331,073	$ 4,597,387	$ 6,869,813	$ 7,176,566	$ 2,626,908
% Design Capacity	0%	25%	50%	75%	100%	100%	100%	0%
	Investment				*Divided Free Cash Flows*			
RSCH Stage Investors (39.3% Equity)	$ (970,341)	$ (184,126)	$ (1,080,800)	$ 445,229	$ 702,390	$ 1,385,267	$ 2,069,986	$ 2,162,416
Sales Stage Investors (60.7% Equity)	$ (1,000,000)	$ -	$ -	$ 1,032,386	$ 1,628,683	$ 3,212,120	$ 4,799,827	$ 5,014,151
NPV at 25%	$ 5,949,963							
NPV at 30%	$ 4,117,327							
RSCH Stage MIRR	20%							
Sales Stage MIRR	43%							

R2 Q3 C3 G1

Year	2012	2013	2014	2015	2016	2017	2018	2019
Income Statement								
Revenue	$ -	$ -	$ 3,787,500	$ 7,575,000	$ 11,362,500	$ 15,150,000	$ 15,150,000	$ -
Cost of Sales	$ (688,638)	$ (496,914)	$ (494,520)	$ (494,520)	$ (494,520)	$ (494,520)	$ (494,520)	$ (494,520)
Operating Costs, SG&A	$ (687,050)	$ (1,338,800)	$ (2,020,550)	$ (2,702,300)	$ (2,702,300)	$ (2,702,300)	$ (2,702,300)	$ (2,702,300)
Depreciation	$ -	$ (39,480)	$ (63,646)	$ (38,666)	$ (23,200)	$ (23,016)	$ (11,646)	$ -
Pre-Tax Income	$ (1,375,688)	$ (1,875,193)	$ 1,208,784	$ 4,339,514	$ 8,142,480	$ 11,930,164	$ 11,941,534	$ (3,196,820)
Taxes (40%)	$ 550,275	$ 750,077	$ (483,514)	$ (1,735,805)	$ (3,256,992)	$ (4,772,066)	$ (4,776,614)	$ 1,278,728
Net Income								
Cash Flow Statement								
Cash from Operating Activities								
Plus: Depreciation	$ -	$ 39,480	$ 63,646	$ 38,666	$ 23,200	$ 23,016	$ 11,646	$ -
WC Change								
(+)/- A/R	$ -	$ -	$ (311,301)	$ (311,301)	$ (311,301)	$ (311,301)	$ -	$ -
(+)/- Inventory	$ (135)	$ (270)	$ -	$ -	$ -	$ -	$ -	$ -
(+)/- A/P	$ 40,241	$ -	$ -	$ -	$ -	$ -	$ -	$ -
(+)/- C/R	$ (171,763)	$ 7,500	$ -	$ -	$ -	$ -	$ -	$ -
Total WC Change	$ (131,656)	$ 7,230	$ (311,301)	$ (311,301)	$ (311,301)	$ (311,301)	$ -	$ -
Cash From Investing Activities								
(Purchase)/Selling of Equipment	$ (197,398)	$ (2,394)	$ -	$ -	$ -	$ -	$ -	$ -
Cash From Financing Activities								
Issuance of Common Stock	$ 970,341	$ -	$ 1,000,000	$ -	$ -	$ -	$ -	$ -
Free Cash Flow	$ (184,126)	$ (1,080,800)	$ 1,477,615	$ 2,331,073	$ 4,597,387	$ 6,869,813	$ 7,176,566	$ (1,918,092)
% Design Capacity	0%	25%	50%	75%	100%	100%	100%	0%
	Investment				*Divided Free Cash Flows*			
RSCH Stage Investors (39.3% Equity)	$ (970,341)	$ (184,126)	$ (1,080,800)	$ 445,229	$ 702,390	$ 1,385,267	$ 2,069,986	$ 2,162,416
Sales Stage Investors (60.7% Equity)	$ (1,000,000)	$ -	$ -	$ 1,032,386	$ 1,628,683	$ 3,212,120	$ 4,799,827	$ 5,014,151
NPV at 25%	$ 2,571,831							
NPV at 30%	$ 2,044,431							
RSCH Stage MIRR	4%							
Sales Stage MIRR	7%							

R2 Q3 C3 G2

Year	2012	2013	2014	2015	2016	2017	2018	2019
Income Statement								
Revenue	$ -	$ -	$ 3,787,500	$ 7,575,000	$ 11,362,500	$ 15,150,000	$ 15,150,000	$ -
Cost of Sales	$ (688,638)	$ (496,914)	$ (494,520)	$ (494,520)	$ (494,520)	$ (494,520)	$ (494,520)	$ (494,520)
Operating Costs, SG&A	$ (687,050)	$ (1,338,800)	$ (2,020,550)	$ (2,702,300)	$ (2,702,300)	$ (2,702,300)	$ (2,702,300)	$ (2,702,300)
Depreciation	$ -	$ (39,480)	$ (63,646)	$ (38,666)	$ (23,200)	$ (23,016)	$ (11,646)	$ -
Pre-Tax Income	$ (1,375,688)	$ (1,875,193)	$ 1,208,784	$ 4,339,514	$ 8,142,480	$ 11,930,164	$ 11,941,534	$ (3,196,820)
Taxes (40%)	$ 550,275	$ 750,077	$ (483,514)	$ (1,735,805)	$ (3,256,992)	$ (4,772,066)	$ (4,776,614)	$ 1,278,728
Net Income								
Cash Flow Statement								
Cash from Operating Activities								
Plus: Depreciation	$ -	$ 39,480	$ 63,646	$ 38,666	$ 23,200	$ 23,016	$ 11,646	$ -
WC Change								
(+)/- A/R	$ -	$ -	$ (311,301)	$ (311,301)	$ (311,301)	$ (311,301)	$ -	$ -
(+)/- Inventory	$ (135)	$ (270)	$ -	$ -	$ -	$ -	$ -	$ -
(+)/- A/P	$ 40,241	$ -	$ -	$ -	$ -	$ -	$ -	$ -
(+)/- C/R	$ (171,763)	$ 7,500	$ -	$ -	$ -	$ -	$ -	$ -
Total WC Change	$ (131,656)	$ 7,230	$ (311,301)	$ (311,301)	$ (311,301)	$ (311,301)	$ -	$ -
Cash From Investing Activities								
(Purchase)/Selling of Equipment	$ (197,398)	$ (2,394)	$ -	$ -	$ -	$ -	$ -	$ -
Cash From Financing Activities								
Issuance of Common Stock	$ 970,341	$ -	$ 1,000,000	$ -	$ -	$ -	$ -	$ -
Free Cash Flow	$ (184,126)	$ (1,080,800)	$ 1,477,615	$ 2,331,073	$ 4,597,387	$ 6,869,813	$ 7,176,566	$ (1,918,092)
% Design Capacity	0%	25%	50%	75%	100%	100%	100%	0%
	Investment				*Divided Free Cash Flows*			
RSCH Stage Investors (39.3% Equity)	$ (970,341)	$ (184,126)	$ (1,080,800)	$ 445,229	$ 702,390	$ 1,385,267	$ 2,069,986	$ 2,162,416
Sales Stage Investors (60.7% Equity)	$ (1,000,000)	$ -	$ -	$ 1,032,386	$ 1,628,683	$ 3,212,120	$ 4,799,827	$ 5,014,151
NPV at 25%	$ 2,747,360							
NPV at 30%	$ 2,131,519							
RSCH Stage MIRR	5%							
Sales Stage MIRR	9%							

Sources Cited

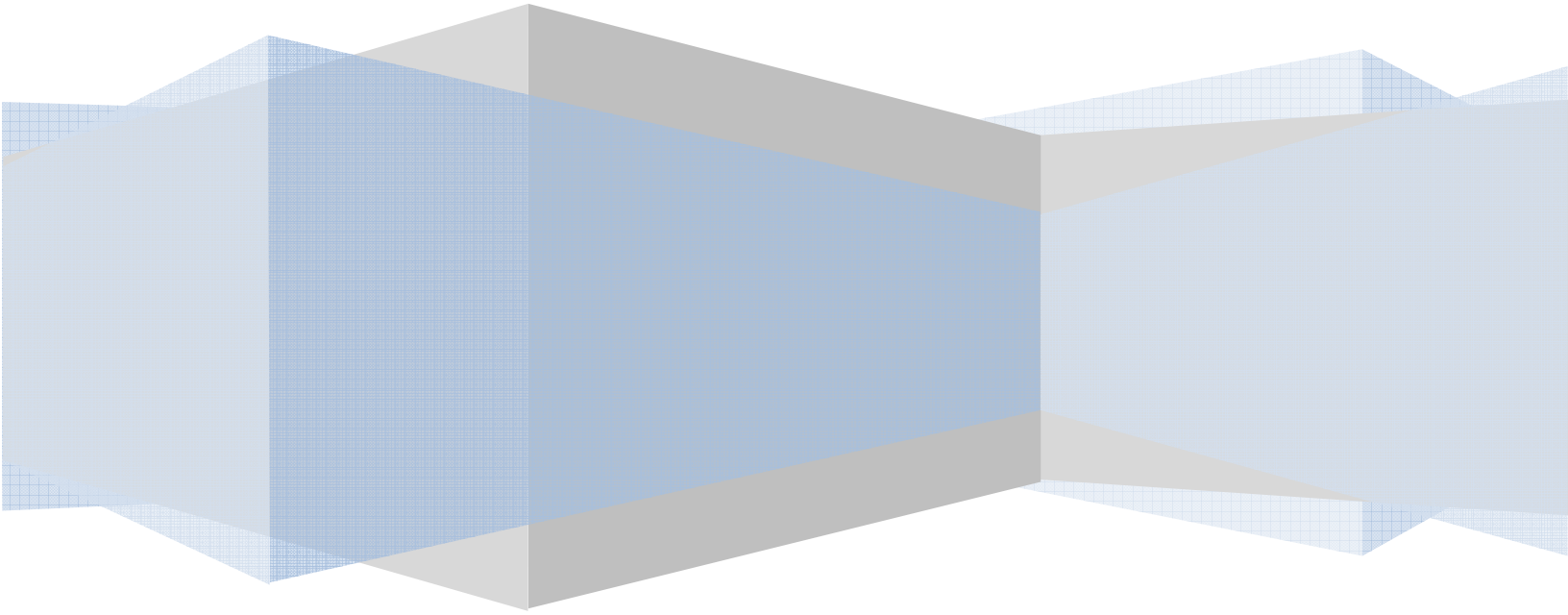

Chapter 1

1-1 Chaffkin, Andrew, Melissa Headberg, Louise Jacobovitz, and Matthew Louie. *Biopharmaceutical Process-Contract Development Organization: Startup. Chemical and Biomolecular Engineering Senior Design Report.* University of Pennsylvania, 2010. Web. 25 Mar. 2011.

1-2 Millipore, https://www.millipore.com/bibliography.nsf/dda0cb48c91c0fb6852567430063b5d6/98fdf6f24f215bc685256ca9006c2a25/$FILE/MILLIPORE%20PTE.pdf

Chapter 3

3-1. Ersoy, Oguz. "High Throughput Monoclonal Antibody Purification." Innovations in Pharmaceutical Biotechnology: 84-88. IPT Online UK. Innovations in Pharmaceutical Technology. Web. <http://www.iptonline.com/articles/public/IPT_17_2005_p84_88x.pdf>.

3-2. "Monoclonal Antibodies Approved by the FDA for Therapeutic Use." Actip.org. Animal Cell Technology Industrial Platform, Feb. 2011. Web. 12 Apr. 2011. <http://www.actip.org/pages/monoclonal_antibodiestable.html>.

3-3. Farid, S. "Process Economics of Industrial Monoclonal Antibody Manufacture." Journal of Chromatography B 848.1 (2007): 8-18. ScienceDirect. Web. <http://www.sciencedirect.com/>.

3-4. "Advantages of Plants to Produce Therapeutic Proteins." Bio.org. Biotechnology Industry Organization, Mar. 2002. Web. 12 Apr. 2011. <http://www.bio.org/healthcare/pmp/factsheet3.asp?p=yes>.

3-5. Kumar, Amir, Jerold Martin, and Ralf Kuriyel. "Scale Up of Direct Flow Membrane Filters." Pall.com. Pall Life Sciences, 2010. Web. <http://www.pall.com/pdf/10-3545_PDA_2010_Kuriyel_POS.pdf>.

3-6. Rajniak, P., S. Tsinontides, D. Pham, W. Hunke, S. Reynolds, and R. Chern. "Sterilizing Filtration—Principles and Practice for Successful Scale-up to Manufacturing." Journal of Membrane Science 325.1 (2008): 223-37. ScienceDirect. Web. <http://www.sciencedirect.com/>.

3-7. SciLog Bioprocessing Systems. Filter Size Determination Using the “Vmax” Method with the FilterTec. SciLog Bioprocessing Systems. Scilog.com. 28 Dec. 2005. Web. <http://www.scilog.com/pdf/products/lab/filtertec-plus-direct-flow-filtration-normal-flow-filtration/application-notes/AN3002_FilterTec_Vmax_Filter_Determinations_122805.pdf>.

3-8. Schick, Karl. Significant Increases (35%) in Dead End Filtration Throughput Using Non-traditional Liquid Handling Procedures. Publication. SciLog Bioprocessing Systems, 27 Dec. 2005. Web. <http://www.scilog.com/pdf/products/lab/filtertec-plus-direct-flow-filtration-normal-flow-filtration/application-notes/AN3001_FilterTec_Enhanced_Filtration_Yields_Paper_122705.pdf>.

3-9. "FilterTec Plus Multi-Filter Capacity Testing." Scilog.com. SciLog Bioprocessing Systems. Web. <http://www.scilog.com/products/lab/filtertec-plus-multi-filter-capacity-testing-normal-flow-filtration-system>.

3-10. SciLog Bioprocessing Systems. FilterTec Plus 3-Filter Testing Station. SciLog Bioprocessing Systems. Scilog.com. Web.

<http://www.scilog.com/pdf/products/lab/filtertec-plus-direct-flow-filtration-normal-flow-filtration/a4-sized/FilterTec_Plus_Brochure.pdf>.
3-11. Filter Sizing Methods for Normal Flow Filtration Applications. Tech. Millipore Corporation, 2000. Web.<http://www.millipore.com/publications.nsf/a73664f9f981af8c852569b9005b4eee/3f2260dcc7f1b79585256a8b003800ed/$FILE/AN1512EN00.pdf>.
3-12. Vmax Filtration System Optimization. Tech. Millipore Corporation, Dec. 1999. Web. <http://www.millipore.com/publications.nsf/a73664f9f981af8c852569b9005b4eee/c1407d0f84125a8285256ae9004267ba/$FILE/vb010.pdf>.

Chapter 4

4-1 Tarleton, E. S., and Richard J. Wakeman. *Dictionary of Filtration and Separation*. Exeter, UK: Filtration Solutions, 2008. Print.
4-2 Royce, Jonathan T. "Practical Application of the Cake-Complete, Pore-Plugging Model for Sizing Normal Flow Filters." *PDA Journal of Pharmaceutical Science and Technology*(2009). Print.
4-3 Tarleton.
4-4 "MUSCOD-II." *IWR: Home*. Prof Dr. H.c. Hans Georg Bock. Web. 03 Apr. 2011. <http://www.iwr.uni-heidelberg.de/~agbock/RESEARCH/muscod.php>.
4-5 Pregler, Bill. "Cross-Flow Filtration Gaining Adherents Among Wineries." *Q-Filter*. 15 Jan. 2006. Web. 04 Apr. 2011. <http://www.qfilter.com/Resource.aspx/DocumentDetail/29>..
4-6 *Deen*, *W. M. 1987*. Hindered transport of large molecules in liquid-filled pores. *AIChE* J. 33,. 1409-1425.
4-7 Bolton, Glen R., William M. Deen, and Barbara S. Daniels. "Assessment of the Charge Selectivity of Glomerular Basement Membrane Using Ficoll Sulfate." *Renal Physiology* (1998). Print.
4-8 Bolton GR, Boesch AW, Lazzara MJ: *The effects of flow rate on membrane capacity: Development and application of adsorptive membrane fouling models*. J Memb Sci 279: 625-634, 2006.
4-9 Vilker, Vincent L. "The Osmotic Pressure of Concentrated Protein Solutions: Effect of Concentration and Ph in Saline Solutions of Bovine Serum Albumin." *Journal of Colloid and Interface Science* 79.2 (1981): 548-66. Print.
4-10 Pujar, Narahari S., and Andrew L. Zydney. "Electrostatic Effects on Protein Partitioning in Size-exclusion Chromatography and Membrane Ultrafiltration." *Journal of Chromatography*796.2 (1998): 229-38. Print.
4-11 Rohani, M. M., and A. L. Zydney. "Role of Electrostatic Interactions during Protein Ultrafiltration."*Adv Colloid Interface Sci* (2010). Print.
4-12 Bhalla, Gaurav. *Osmotic Reflection Coefficient*. MIT, May 2009. Web. 03 Apr. 2011. <http://web.mit.edu/cheme/news/seminars-09/Bhalla%20Guarav_5_5_09.pdf>.
4-13 "Biomax Membrane Properties and Applications." *Membrane Product Sheets*. Biomax. Web. 03 Apr. 2011.
4-14 "Millipore Membrane Properties and Applications." *Membrane Product Sheets*. Millipore. Web. 03 Apr. 2011.

Chapter 5

5-1. Buchwald, Peter. "FEM-based Oxygen Consumption and Cell Viability Models for Avascular Pancreatic Islets." Theoretical Biology and Medical Modelling 6.1 (2009): 5. PubMed. National Center for Biotechnology Information, 16 Apr. 2009. Web. <http://www.ncbi.nlm.nih.gov/pubmed/19371422>.

5-2. Yadav, Sandeep, Steven J. Shire, and Devendra Kalonia. "Factors Affecting the Viscosity in High Concentration Solutions of Different Monoclonal Antibodies." Journal of Pharmaceutical Sciences 99.12. Wiley Online Library. Wiley, 10 May 2010. Web. 15 Apr. 2011. <Factors Affecting the Viscosity in High Concentration Solutions of Different Monoclonal Antibodies>.

5-3. Chapter 4 Membrane Equipment. PPT.

5-4. "OptiSep Filters." SmartFlow Technologies. Web. 15 Apr. 2011. www.smartflow-tech.com

5-5. COMSOL Multiphysics. Separation through Dialysis. Model Documentation. COMSOL. Web. <http://www.comsol.com/showroom/documentation/model/258/>.

Chapter 7

7-1 Strickland, Debbie. *Guide to Biotechnology.* Rep. Ed. Roxanna Guilford-Blake. Biotechnology Industry Organization (BIO), 2008.

7-2 Ibid.

7-3 Ibid.

7-4 Ibid.

7-5 Pharmaceutical Research and Manufacturers of America, Pharmaceutical Industry Profile 2010 (Washington, DC: PhRMA, March 2010).

7-6 Strickland.

7-7 Ibid.

7-8 "Biosimilars Forecast to Reach $10 Billion by 2017." *PharmaLive* 16 Sept. 2010. Web. <http://www.pharmalive.com/subscriptions/news.cfm?nid=729859>.

7-9 *Pharmaceutical Industry Profile.* Publication. International Trade Administration, 2010. <http://trade.gov>.

7-10 "Pharmaceuticals and Biotech." *Wetfeet.com*. Web. 25 Mar. 2011. <http://www.wetfeet.com/Careers-and-Industries/Industries/Pharmaceuticals-and-Biotech.aspx>.

7-11 Strickland.

7-12 DeArment, Alaric. "Biosimilars Development Continues Emergence." *Drugstorenews.com.* 15 Nov. 2010. Web. 25 Mar. 2011.

7-13 *Outlook 2010.* Rep. Boston, MA: Tufts University Center for the Study of Drug Development, 2010.

7-14 Chaffkin, Andrew, Melissa Headberg, Louise Jacobovitz, and Matthew Louie. *Biopharmaceutical Process-Contract Development Organization: Startup. Chemical and Biomolecular Engineering Senior Design Report.* University of Pennsylvania, 2010. Web. 25 Mar. 2011.

7-15 Ibid.

7-16 PhRMA.

7-17 Ibid.
7-18 Amato, Stephanie, Alan Futran, Kevin Krebs, Brian Recchione. *The Synthseq Approach to Personal Genotyping*. *Chemical and Biomolecular Engineering Engineering Senior Design Report.* University of Pennsylvania, 2010. Web. 25 Mar. 2011.
7-19 Ibid.
7-20 Ibid.
7-21 Ibid.
7-22 "Daily Treasury Yield Curve Rates." *Treasury.gov.* 1 Apr. 2011. Web. 4 Apr. 2011.
7-23 "Prime Loan Interest Rate Forecast." *Forecast.org.* 1 Apr. 2011. Web. 4 Apr. 2011.